Karlsruher Institut für Technologie

Chemical Engineering of Plants for Salt Tolerance

Zur Erlangung des akademischen Grades eines

DOKTORS DER NATURWISSENSCHAFTEN

(Dr. rer. nat.)

von der KIT-Fakultät für Chemie und Biowissenschaften

des Karlsruher Instituts für Technologie (KIT)-Universitätsbereich

genehmigte

DISSERTATION

von

M.Sc. Kinfemichael Geressu ASFAW

aus

Huruta, Äthiopien

KIT-Dekan: Prof. Dr. Manfred Wilhelm

Referent: Prof. Dr. Peter Nick

Korreferent: Prof. Dr. Ute Schepers

Tag der mündlichen Prüfung: 05.02.2020

Die vorliegende Dissertation wurde im Zeitraum von Juli 2015 bis Januar 2020 am Botanischen Institut, Lehrstuhl für Molekulare Zellbiologie des Karlsruher Instituts für Technologie (KIT), angefertig.

Hiermit erkläre ich, dass die vorliegende Dissertation, von der Benutzung der angegebenen Hilfsmittel abgesehen, von mir selbständig verfasst wurde. Alle Stellen, die ihrem Wortlaut oder Inhalt gemäß aus anderen Arbeiten entnommen sind, wurden durch Angabe der Quelle kenntlich gamacht. Diese Dissertation liegt in gleicher oder ähnlicher Form keiner anderen Prüfungsbehörde vor.

Wesentliche Teile dieser Dissertation wurden bereits in der Fachzeitschrift Nature Scientific Reports veröffentlicht [Kinfemichael Geressu Asfaw, Qiong Liu, Jan Maisch, Stephan W. Münch, Ilona Wehl, Stefan Bräse, Ivan Bogeski, Ute Schepers & Peter Nick (2019). A Peptoid Delivers CoQ-derivative to Plant Mitochondria via Endocytosis. DOI: 10.1038/s41598-019-46182-z].

Karlsruhe, im Januar 2020

Kinfemichael Geressu ASFAW

To My Late Wife

Mrs. Tsega Alemu ASFAW

Maiden Name HAILU

(1980-2018)

Acknowledgements

First of all, I would like to thank very greatly the Almighty God, Jesus Christ for creating and keeping me alive and healthy until this very moment. Second, I would like to express my heartfelt and deepest thanks for my supervisor Prof. Dr. Peter Nick who accepted me as a PhD student, gave me the opportunity to work at Botany Institute I, Karlsruhe Institute of Technology (KIT), Karlsruhe ,and financed my entire 3 years and half work from his own project. Moreover, he conceived the original ideas of my PhD projects, and shaped and sharpen my knowledge, both through the regular group meetings and manuscript preparation for publication. Really, I have no words which are strong enough to express my gratitude to Prof. Dr. Peter Nick. Dear Professor, you are my real academic father. Third, my gratitude goes to Prof. Dr. Ute Schepers from KIT, Campus North, Institute of Functional Interfaces (IFG), who synthesized and provided us repeatedly with the construct plant PeptoQ which is one of the main pillars of this dissertation. Moreover, she wrote the plant PeptoQ synthesis scheme. Fourth, I am indebted to Dr. Qiong Liu who guided me very well at the beginning of my PhD study and established the foundation for the profound and sophisticated later tasks. Fifth, I would like to thank Rose Eghbalian who conducted SOD and CAT activities, and Mn-SOD gene expression assay, Dr. Michael Riemann who consulted and gave me suggestions at different occasions, Dr. Jan Maisch who supported me with regard to microscopy, Dr. Rohit Dhakarey who provided us with an entry clone of rice OPR7 (OsOPR7) gene, Dr. Xiaolu Xu who shared me her expertise about total RNA extraction, SQ-PCR, qRT-PCR and qRT-PCR data analysis, Dr. Christina Manz who helped me in translating the abstract of this dissertation into Deutsch (Zusammenfassung) and in designing the declarative statements (written on the front page of this dissertation) in Deutsch, Dr. Sahar Akaberi who shared me her expertise in cDNA synthesis, Dr. Elizabeth Eiche who performed cations level analysis, Prof. Dr. Bettina Hause who determined plant hormone levels, Sabine Purper who helped me in relation to cell culture and in the processing of various chemicals purchase, and Nadja Wunsch who supported me in the provision of SQ-PCR and qRT-PCR enzyme and chemicals input and in processing my primers orders. Sixth, I would like to thank all the post

docs and technical staffs both in the lab and the botanical garden. Seventh, I would like to express my gratitude to all PhD, Master and Bachelor students of our laboratory, Molekulare Zellbiologie (in the cell biology, biodiversity and plant stress group) and Allgemeine Botanik for quite joyful and friendly time we had during my entire PhD life.

Last but not least, I would like to express my gratitude and thanks to my late wife, Mrs. Tsega Alemu ASFAW (maiden name HAILU) who took care of our two sons; namely Eyob Kinfemichael GERESSU and Petros Kinfemichael GERESSU throughout my 3 years and half PhD work; even if, I am not lucky enough to have her by my side during the celebration of my PhD defense. Moreover, I would like to thank my two sons, Eyob and Petros for helping me in writing this Dissertation indirectly by reducing the house and kitchen tasks burden that awaits me everyday.

Kinfemichael Geressu ASFAW

Table of Contents

Abbreviations

AA, ascorbic acid

ABA, abscisic acid

ABC, ATP binding-cassette

AKT1, hyperpolarization-activated inward rectifying K^+ channel 1

AOX, antioxidant

APX, ascorbate peroxidase

ATAF, Arabidopsis transcription activation factor

ATP, adenosine triphosphate

AUX1, auxin influx carrier 1

BRs, brassinosteroids

BY-2, *Nicotiana tabacum* L.cv bright yellow 2

CaMV, cauliflower mosaic virus

CAT, catalase

CAX1, H^+/Ca^{2+} exchanger

CCD, charge-coupled device

CDK, cyclin-dependent kinase

cDNA, complementary deoxyribonucleic acid

CHPAA, 3-chloro-4-hydroxyphenylacetic acid

CKs, cytokinins

CME, clathrin mediated endocytosis

COI1, coronatine insensitive 1

CoQ, ubiquinone

CoQH, ubisemiquinone

$CoQH_2$, ubiquinol

CoQ10, coenzyme Q10

CoRR, colocalisation for redox regulation of gene expression

CPPs, cell penetrating peptides

CPPos, cell penetrating peptoids

CSC, cysteine synthase complex

Ct, cycle threshold

CTS1, COMATOSE

CUC, cup-shaped cotyledon

CYP20-3, cyclophilin 20-3

DF, dilution factor

DHAR, dehydroascorbate reductase

DHR 123, dihydrorhodamine 123

DIC, diisopropylcarbodiimide

DiOC6, 3-3'-dihexyloxa carbocyanine iodide

DMF, dimethylformamide

DMSO, dimethyl sulfoxide

DNA, deoxyribonucleic acid

EC, electrical conductivity

ECe, electrical conductivity of the saturated paste extract

EDTA, ethylenediaminetetraacetic acid

EF-1α, elongation factor-1α

EL, electrolyte leakage

ER, endoplasmic reticulum

ESP, exchangeable sodium percentage

ET, ethylene

ETC, electron transport chain

FAO, food and agriculture organization

Fd, ferredoxin

Fmoc, fluorenylmethyloxycarbonyl

GAL, 1-galactone-γ- lactone dehydrogenase

GFP, green fluorescent protein

GPX, guaiacol peroxidase

GR, glutathione reductase

GSH, reduced glutathione

GSTs, glutathione-s-transferases

HAK1, high affinity K+ transporter 1

HAKs, high affinity K+ transporters

HIV-1, human immunodeficiency virus 1

HKT, histidine kinase transporter

HKT1, histidine kinase transporter 1

HPLC, high-performance liquid chromatography

IAA, indole-3-acetic acid

IFG, institute of functional interfaces

IKA, ikarugamycin

JA, jasmonic acid

JA-Ile, jasmonyl-isoleucine

J**As,**	jasmonates
JAZ1,	jasmonate ZIM/tify-domain 1
JAZ2,	jasmonate ZIM/tify-domain 2
JAZ3,	jasmonate ZIM/tify-domain 3
KIT,	Karlsruhe institute of technology
Lat B,	latrunculin B
LPO,	lipid peroxidation
L25,	ribosomal protein L25
MALDI-TOF,	matrix-assisted laser desorption/ionization-time of flight
MAPKs,	mitogen-activated protein kinases
MDA,	malondialdehyde
MDHAR,	monodehydroascorbate reductase
MeJA,	methyl jasmonate
Mha,	million hectares
MI,	mitotic index
miRNA,	micro ribonucleic acid
Mn-SOD,	manganese-superoxide dismutase
MS,	mass spectrometry
MS,	murashige and skoog
mtCPPs,	mitochondrial cell penetrating peptides
mtETC,	mitochondrial electron transport chain
NAC,	NAM (for no apical meristem), ATAF (for Arabidopsis transcription activation factor), and CUC (for cup-shaped cotyledon)
NAD+,	oxidized nicotinamide adenine dinucleotide

NADPH, reduced nicotinamide adenine dinucleotide phosphate

NADP+, oxidized nicotinamide adenine dinucleotide phosphate

NAM, no apical meristem

NBT, nitroblue tetrazolium

NHX, Na^+/H^+ exchanger

NHX1, Na^+/H^+ exchanger 1

NSCCs, non-selective cation channels

OE, stably OsOPR7 overexpressor

ORGs, OPDA-responsive genes

OPC-8:0, 3-oxo-2-(2'(z)-pentenyl)-cyclopentane-1-octanoic acid

OPDA, 12-oxo-phytodienoic acid

OPR, 12-oxo-phytodienoic acid reductase

OPR7, 12-oxo-phytodienoic acid reductase 7

OsOPR7, *Oryza sativa* 12-oxo-phytodienoic acid reductase 7

PBS, phosphate-buffered saline

PCR, polymerase chain reaction

PCV, packed cell volume

pmf, proton motive force

PMS, phenazine methosulfate

PPase, inorganic pyrophosphatase/inorganic diphosphatase

PPI, potash and phosphate institute

PPQ, plant PeptoQ

PSI, photosystem I

PSII, photosystem II

PTDs, protein transduction domains

PUFAs, polyunsaturated fatty acids

PVP, polyvinylpyrrolidone

qRT-PCR, quantitative real-time polymerase chain reaction

RboHs, respiratory burst oxidase homologs

RNA, ribonucleic acid

ROS, reactive oxygen species

RT-PCR, reverse transcription polymerase chain reaction

SAT, serine acetyltransferase

SCF, Sk1-Cul1-F-Box protein

siRNA, small interfering RNA

SKOR, stellar K^+ outward rectifier

SLT1, lithium-tolerant

SOD, superoxide dismutase

SOS, salt overly sensitive

SOS1, salt overly sensitive 1

SOS2, salt overly sensitive 2

SOS3, salt overly sensitive 3

SQ-PCR, semiquantitative polymerase chain reaction

TAT, transcription trans-activating

TBA, 2-thiobarbituric acid

TFA, trifluoroacetic acid

TGA, TGA transcription factors

TIRF, total internal reflection fluorescence

TPSA, topological polar surface area

TNG, trans-Golgi network

UQ, ubiquinone

UV, ultraviolet

Wm, wortmannin

WT, wild type

XOD, xanthine oxidase

YFP, yellow fluorescent protein

Abstract

Salinity is one of the serious threats to global agriculture that threatens human food security. To tackle the problem, there were and still are quite several scientific efforts in place. Hence, in this dissertation, we used chemical and genetic engineering approaches to unravel the sophisticated knot of the problem using a Trojan peptoid called plant PeptoQ and overexpression of OsOPR7 gene in non-transformed WT tobacco BY-2 cells. First, plant PeptoQ that can be used to target a functional cargo (a rhodamine-labelled semiquinone peptoid as mimetic of coenzyme Q10) into mitochondria of tobacco BY-2 cells was characterized with regard to its cellular uptake and potential cytotoxicity. We found that the uptake is specific for mitochondria, rapid, dose-dependent, and requires both clathrin-mediated and clathrin-independent endocytosis, as well as actin filaments, while microtubules seem to be dispensable. Viability of the treated cells was not affected, and they showed better survival under salt stress, a condition that perturbs oxidative homeostasis in mitochondria. Using double labelling with appropriate fluorescent markers, we showed that targeting of this Trojan Peptoid to the mitochondria is not based on a passage through the plasma membrane (as thought hitherto), but on import via endocytotic vesicles and subsequent accumulation of the positively charged side chains at the negatively charged inner mitochondrial membrane. Second, the effects of pretreatment with plant PeptoQ and OsOPR7 overexpression, on salt stress induced detrimental effects in WT BY-2 cells were investigated. In general, both pretreatment with plant PeptoQ and overexpression of OsOPR7 in WT BY-2 cells, mitigated salt stress induced deleterious effects more or less in a similar manner. Cell expansion and cell viability were fully and partially compensated at moderate (75 mM NaCl) and high (150 mM NaCl) salt stress respectively by peptoid treatment and OsOPR7 overexpression. However, even if, the detrimental effects of salt stress on cell division (proliferation) were mitigated by both approaches, it was more sensitive as compared to cell expansion and viability. Furthermore, they significantly ameliorated doubling time, and effectively suppressed salt stress induced increase in MDA and superoxide levels in WT BY-2 cells. However, both approaches had no effect on hydrogen peroxide level. Plant PeptoQ pretreatment and OsOPR7 overexpression lead to increased SOD activity but decreased Mn-SOD transcript induction. However, they had no effect on catalase (CAT) activity. Except SOS1, NAC and OPR7 genes , other salt-related genes such as ion channels (NHX1 and SKOR), regulators for ion channels (SOS3 and SLT1) and jasmonate related gene (JAZ3) did not show strong transcript modulation in response to salinity, plant PeptoQ treatment and OsOPR7 overexpression. Similarly, even if, ionic balance was strongly perturbed by salt stress, both plant PeptoQ treatment and OsOPR7 overexpression had no mitigatory role at all. On the other hand, pretreatment of salt stressed WT and OsOPR7 overexpressor (OE) BY-2 cells with plant PeptoQ, caused increased OPDA level; however, it had no significant effect on JA-Ile level. It lead to a significant shift of the biosynthetic pathway from JA-Ile to OPDA, and this channeling of the pathway towards OPDA was significantly more accentuated for moderate salt stress (75 mM NaCl) but it faded as it proceeds to

high salt stress (150 mM NaCl). Both plant PeptoQ pretreatment and OsOPR7 overexpression conferred salt tolerance to the non-transformed WT BY-2 cells by mitigating the salt stress induced detrimental effects effectively and efficiently.

Zusammenfassung

Salinität ist eine der ernsthaften Bedrohungen für die globale Landwirtschaft und bedroht die menschliche Ernährungssicherheit. Um dieses Problem zu bewältigen, gab und gibt es zahlreiche wissenschaftliche Anstrengungen. Aus diesem Grund verwendeten wir im Rahmen dieser Dissertation chemische und gentechnische Ansätze, um das komplexe Problem mithilfe eines Trojanischen Peptoids namens plant PeptoQ und der Überexpression des OsOPR7 Gene in nicht transformierten WT Tabak BY-2 Zellen zu entschlüsseln. Plant PeptoQ kann verwendet werden, um eine funktionelle Fracht (ein Rhodamin-markiertes Semichinon-Peptoid, welches das Coenzym Q10 imitiert) in die Mitochondrien von Tabak BY-2 Zellen zu schleusen und wurde zunächst hinsichtlich der zellulären Aufnahme und der potenziellen Zytotoxizität charakterisiert. Wir fanden heraus, dass die Aufnahme spezifisch für Mitochondrien ist, schnell und dosisabhängig erfolgt und sowohl eine Clathrin-vermittelte als auch eine Clathrin-unabhängige Endozytose sowie Aktinfilamente benötigt, während Mikrotubuli verzichtbar zu sein schienen. Die Überlebensfähigkeit der behandelten Zellen wurde nicht beeinträchtigt und sie zeigten ein besseres Überleben unter Salzstress, welcher die oxidative Homöostase in Mitochondrien stört. Durch eine Doppelmarkierung mit geeigneten Fluoreszenzmarkern, haben wir gezeigt, dass die Tatsache, dass dieses Trojanische Peptoid die Mitochondrien zum Ziel hat, nicht auf einer Passage durch die Plasmamembran beruht (wie bisher angenommen), sondern auf dem Import über endozytische Vesikel und der anschließenden Akkumulation der positiv geladenen Seitenketten an der negativ geladenen inneren Mitochondrienmembran. Anschließend wurden die Auswirkungen einer Vorbehandlung mit plant PeptoQ und einer Überexpression des OsOPR7 auf Salzstress-induzierte negative Effekte in WT BY-2 Zellen untersucht. Im Allgemeinen bewirkten sowohl die Vorbehandlung mit plant PeptoQ als auch die Überexpression des OsOPR7 in WT BY-2 Zellen auf mehr oder weniger ähnliche Weise eine Verminderung der Salzstress-induzierten schädlichen Effekte. Sowohl die Expansion als auch die Lebensfähigkeit der Zellen wurde bei mäßigem Salzstress (75 mM NaCl) vollständig und bei hohem Salzstress (150 mM NaCl) teilweise durch die Peptoidbehandlung und die OsOPR7 Überexpression kompensiert. Die Zellteilung (Proliferation) andererseits war im Vergleich zur Zellexpansion und der Lebensfähigkeit empfindlicher, obwohl auch hier beide Ansätze die Auswirkung von Salzstress minderten. Darüber hinaus verbesserten sie die Verdopplungszeit signifikant und unterdrückten wirksam den durch Salzstress verursachten Anstieg des MDA- und Superoxidgehalts in WT BY-2 Zellen.

Auf den Wasserstoffperoxidgehalt hingegen hatten die beiden Ansätze keinen Einfluss. Die Vorbehandlung mit plant PeptoQ und die Überexpression des OsOPR7 führten zu einer erhöhten SOD-Aktivität, verringerten jedoch die Induktion des Mn-SOD-Transkripts. Auf die Aktivität der Katalase (CAT) hatten die Ansätze keinen Effekt. Mit Ausnahme von SOS1, NAC und OPR7-Genen, zeigten andere salzbezogene Gene wie Ionenkanäle (NHX1 und SKOR), Regulatoren für Ionenkanäle (SOS3 und SLT1) und jasmonatbezogene Gene (JAZ3) keine starke Veränderung der Transkripte in Reaktion auf Salzgehalt, Vorbehandlung mit plant PeptoQ und Überexpression des OsOPR7. Ähnlich dazu hatten sowohl die Behandlung mit plant PeptoQ als auch die OsOPR7 Überexpression überhaupt keinen mildernden Effekt, wenn das Ionengleichgewicht stark durch Salzstress gestört wurde. Andererseits verursachte die Vorbehandlung von mit Salz belasteten WT- und OsOPR7 überexprimierten BY-2 Zellen mit plant PeptoQ einen erhöhten OPDA-Spiegel, der sich jedoch nicht signifikant auf den JA-Ile Gehalt auswirkte. Es kam zu einer signifikanten Verschiebung des Biosyntheseweges von JA-Ile zu OPDA wobei diese Kanalisierung zu OPDA bei mäßigem Salzstress (75 mM NaCl) deutlich verstärkt war, beim Übergang zu hohem Salzstress (150 mM NaCl) jedoch nachließ. Sowohl die Vorbehandlung mit plant PeptoQ als auch die Überexpression des OsOPR7 verliehen den nicht transformierten WT BY-2 Zellen Salztoleranz, indem sie die durch Salzstress verursachten schädlichen Wirkungen wirksam und effizient abschwächten.

1. Introduction

The global human population has been projected to be 9.3 billion by the year 2050 (FAO, 2009). Hence, the crop agricultural productivity needs to be boosted by 87% worldwide especially in relation to major crops like wheat, maize, soy and rice in order to feed the 2.3 billion additional people (Kromdijk and Long, 2016). However, the effort to maximize agricultural productivity has been constrained mainly by abiotic environmental factors that reduce crop yield by 71% on the global scale (Boyer, 1982). Among abiotic stress factors, soil salinity is the most threatening and devastating one (Ashraf et al., 2008). It affects plants growth, development and harvest quality indirectly, and directly through its osmotic, ionic and oxidative stresses (Zhu, 2001, Hasan et al., 2015). It causes severe reduction in crops productivity, consequently, they produce limited yield significantly below their genetic potential (Munns, 2002; Flowers, 2004). Salt-affected soils are characterized by the accumulation of a significant amount of soluble salts in the soil (Bockheim and Gennadiye, 2000) such as NaCl, Na_2SO_4, KCl, $MgCl_2$ and $NaHCO_3$ where NaCl is the most soluble and quite prevalent salt (Bie et al., 2004; Munns and Tester, 2008; Khan et al., 2012; Almeida et al., 2017). They are categorized as non-saline, slightly saline, moderately saline, strongly saline and very strongly saline soils based on the electrical conductivity (ECe) of the saturated paste extract (Table 1). Salt-affected soils do occur almost in all climatic regimes and continents (FAO, 1988) where they are widespread and prevalent in arid and semi-arid regions of the world owing to highest evapotranspiration as compared to limited annual precipitation, and intensive as well as suboptimal irrigation practices (Akhter et al., 2003; Plaut et al., 2013; Hanin et al., 2016).

Table 1: Soil salinity classes and crop growth with respect to each class. Source: FAO, 1988.

Soil Salinity Class	EC of Saturation Extract (dS/m)	Effect on Crop Plants
Non-saline	0 - 2	Salinity effects negligible
Slightly saline	2 - 4	Yields of selective crops may be restricted
Moderately saline	4 - 8	Yields of many crops are restricted
Strongly saline	8 - 16	Only tolerant crops yield satisfactorily
Very strongly saline	> 16	Only a few very tolerant crops yield satisfactorily

It has been estimated that in more than 100 countries, about 50% of the irrigated land and 20% of the cultivated agricultural land have been affected by salinization worldwide (Sairam and Tyagi, 2004; Munns, 2002; Flowers, 2004). In general, about 351.2 and 581 million hectares (Mha) of lands have been seriously affected by salinity and sodicity respectively globally which add up to 932.2 Mha (Rengasamy, 2006; Wong et al., 2006) (Table 2). Where Central America and Australasia are the least and the most salt-affected landmasses respectively in the

world. This implies that around 7% of the total land area of the world is salt-affected (Flowers, 2004; Munns, 2005; Giri et al., 2007) and about 2 million hectares and 3 hectares of land are being salt-affected on the global scale annually and each minute respectively (Kalaji and Pietkiewica, 1993; FAO, 2008; Hasan et al., 2015). Unless it is reversed by different interventions and strategies, if the current situation continues as it is, by the middle of the 21st century, about 50% of the global cultivable land will be lost due to soil salinization (Mahajan and Tuteja, 2005; Wang et al., 2007). Moreover, the problem is expected to be more accentuated as a result of global climate change. For example, reports show that by the end of the 21st century, the global temperature and Sea Level Rise (SLR) are expected to be increased from 1.4-5.8^{o}C and 1.8-5.9mm/year respectively. Consequently, the decline in freshwater resources and elevated evapotranspiration, would aggravate the salinization problem substantially on the global scale (Yano et al., 2007; Teh and Koh, 2016).

Table 2: Global distribution of saline and sodic soils. Source: Rengasamy, 2006.

Land mass	Area in million hectares [Mha]		
	Saline	Sodic	Total
Central America	**2**	**-**	**2**
North America	**6.2**	**9.6**	**15.8**
Southeast Asia	**20.0**	**-**	**20.0**
Europe	**7.8**	**22.9**	**30.7**
Africa	**53.5**	**27.0**	**80.5**
South Asia	**83.3**	**1.8**	**85.1**
South America	**69.4**	**59.6**	**129.0**
North and Central Asia	**91.6**	**120.1**	**211.7**
Australasia	**17.4**	**340.0**	**357.4**
World Total	**351.2**	**581.0**	**932.2**

1.1. Sources of soil salinity

Saline soils originate from primary (natural) and secondary (anthropogenic) sources. The primary saline soils forming causes include weathering of minerals and parent rocks (Moreira-Nordemann, 1984), coastal areas salinization by sea water intrusion (Mahajan and Tuteja, 2005; Kotera et al., 2008), rain water which bears 50mg L^{-1} NaCl, tsunamis (Munns and Tester, 2008) and lake or land surface windblown materials (Plaut et al., 2013). On the other hand, secondary (human-induced) causes of soil salinization encompass replacement of the natural deep-rooted perennial vegetation with annual crops (Manchanda and Garg, 2008), intensive agricultural cultivation (FAO, 2008) and improper irrigation management and the use of salt-rich irrigation water (Plaut et al., 2013). Secondary salinization is anticipated to increase as a result of global climate change. That is, due to

increased temperature (especially in arid and semi-arid regions) and changes in precipitation pattern (temperate and sub-tropical regions), there would be extensive demand for irrigation (Fischer et al. 2007). Thus, due to irrigation with salt-rich water (due to reduced freshwater resources and increase SLR) (Teh and Koh, 2016), significant salinization would be an inevitable consequence (Nongpiur et al., 2016) and eventually, it accentuates the existing soil salinity problem.

1.2. Types of soil salinity

Salt-affected soils are classified into two main groups, namely saline and sodic soils. Saline soils are characterized by the possession of predominantly neutral soluble salts, with an electrical conductivity (EC) of > 4dS/m at 25^{o}C, pH of < 8.2 and Na^{+} as a dominant soluble cation. And they are common and dominant in arid and semi-arid regions of the world and affect plant growth and development through the induction of water deficit and ion toxicity. On the other hand, sodic soils are widespread and common in semi-arid and sub-humid regions, and are identified by their >8.2 pH, <4dS/m EC and >15 exchangeable sodium percentage (ESP). In general, sodic (alkaline) soils affect plant growth through their detrimental effect on soil physical properties and pH (FAO, 1988). More specifically, besides their osmotic and ionic stresses, they cause the precipitation of important nutrients such as phosphates and metallic micronutrients, destruction of roots cellular structures (Li et al., 2009) and disruption of the slightly acidic pH (around 5.5) of the apoplast which is maintained actively by the plasma membrane localised proton ATPases . This apoplastic situation is essential for sustainable cell expansion growth (Haruta et al., 2010). Moreover, alkalinity is expected to impair the activity of osmotically induced calcium influx by disrupting its cotransport with proton. As a secondary effect, soil alkalinity also causes the failure of NADPH Oxidase RboH generated superoxide anions ($O_2^{\bullet -}$) dissipation due to the absence of protons as electron acceptors. In general, compared to equimolar salinity at neutral pH, alkaline sodium stress owns much serious effects on plants (Wang et al., 2011). Even if, this reality is well known, the adaptive mechanisms and the molecular signals in soil alkalinity are far from understood (Riemann et al., 2015).

1.3. Effects of soil salinity on plants

Salt stress, both salinity and sodicity, affect plant growth, development and productivity both directly and indirectly (Zhu, 2001).

1.3.1. Indirect effects of soil salinity

Salt-affected soils influence the growth and development of plants by deteriorating the nutrient cycle and the decomposition processes through their destructive role on soil physical, chemical and biological properties (Wong et al., 2005). Soil structure, which is one of the physical properties that determines the agronomic potential of the soil would be seriously affected in salt-affected soils particularly in sodic soils. That is, in sodic soils, the calcium (Ca^{2+}) and magnesium (Mg^{2+}) ions would be substituted by Na^{+} ion in the cation exchange complex, and consequently there would be clay particles dispersion. This dispersion and associated soil swelling

as well as particle slaking from aggregates, undergoes reorientation and resulted in worse soil structure, surface crusting and lower hydraulic conductivity. Consequently, germination and emergence would be inhibited due to worse aeration, water supply, soil macro-fauna movement, nutrient availability and infiltration (De Souza Silva and Fay, 2012). On the other hand, soil microorganisms (components of soil biological properties) which play crucial role in various vital processes such as oxidation, nitrogen fixation, nitrification, ammonification, nutrient transformation and decomposition of organic matter are affected by the osmotic and specific ion effects of salinity in salt-affected soils (Oren, 1999; Yan et al., 2015). Therefore, under such bad soil conditions of salt-affected soils, plants or crops yield will be extremely limited due to poor germination, emergence, growth and development.

1.3.2. Direct effects of soil salinity

Apart from its indirect effects, salinity causes severe and intricated detrimental impacts on plant growth and development at molecular, cellular and whole plant level directly through its osmotic, ionic and oxidative stresses (Zhu, 2002). Moreover, among the three direct effects, oxidative stress is the central factor which is responsible for the salinity-induced irreversible damages on plants. Hence, this dissertation will focus on this stress factor.

1.3.2.1. Osmotic Stress

Osmotic (water-deficit) effect is the impact of soil water salinity that occurs at its initial stage which is independent of the accumulation of soluble salts in the plant system (Munns, 2005; Rahnama et al., 2010). It happens due to the accumulation of salts in the root zone that creates hyperosmotic condition (low soil water potential) and consequently it precludes water uptake and induces water deficit (Pardo et al., 2000; Roy et al., 2014). In turn, the signal generated by the shortage of water would result in decline of intracellular turgor pressure and reduced cell expansion as it is conveyed from roots to shoots, probably, within minutes after the onset of the salt stress (Munns, 2005; Munns and Tester, 2008). Moreover, the same signal causes reduced stomatal conductance as it induces the biosynthesis of abscisic acid (ABA). Eventually, there would be lower photosynthetic activity, biomass production and the subsequent yield loss as a direct result of lower stomatal conductance (Munns, 2005; Munns and tester, 2008; Roy et al., 2014; Almeida et al., 2017). In general, salinity causes adverse effects in plants at the cellular level (Hasegawa et al., 2000; Munns, 2005; Munns and Tester, 2008).

1.3.2.2. Ionic Stress

During the second phase of salt stress, when salt concentration especially that of sodium (Na^+) increased in the soil water solution, it creates quite negative membrane potential inside the plasma membrane of root cells. This in turn, causes the net influx of Na^+ passively while its efflux became energetically expensive and active (Maathuis et al., 2014). The Non-Selective Cation Channels (NSCCs) play a pivotal role in the passive transport of Na^+ into the root cells (Blumwald et al., 2000; Kronzucker and Britto, 2011). Besides, the entrance of Na^+ into

root cells via symplast flow (through the cytoplasm), it also joins the xylem stream by passing through the cell wall and the intercellular spaces (apoplastic flow) (Yeo et al., 1987; Kronzucker and Britto, 2011). The passively uptaken Na^+ ions by the root cells would be transported to the shoots by bulk flow through xylem (Almeida et al., 2017). Then the excessively uptaken ions specifically Na^+ and/or Cl^- would be significantly accumulated in the cytosol particularly in that of the older leaves (Abogadallah, 2010; Roy et al., 2014). This toxic level accumulation of Na^+ and/or Cl^- would cause the leakage of electrolytes (due to its toxic effects on the plasma membrane), early leaf senescence and tissue necrosis especially in older leaves. Moreover, its toxicity would interfere with different metabolic processes in the cytosol and impair them. Consequently, the rate of biochemical and physiological activities would be reduced (Ahmad et al., 2014, Hashem et al., 2014; Roy et al., 2014; Almeida et al., 2017). This is mainly due to the deleterious effect of salt stress (particularly that of NaCl) in causing ion imbalance in plant cells (Munns and Tester, 2008). The net influx and accumulation of Na^+ in the cytosol, leads to ion imbalance, especially that of potassium (K^+) in several ways. Increased cytosolic Na^+ influx caused membrane depolarization which is followed by elevated K^+ efflux and in turn, it resulted in reduced K^+/Na^+ ratio and K^+ starvation (Tomemori et al., 2002; Cakmak, 2005; Sun et al., 2009; Adams and Shin, 2014). Moreover, through inhibition of K^+ transporters like HAK5 (carrier-type HUP/HAK/KT transport) (Nieves-Cordones et al., 2010) and AKT1 (hyperpolarization-activated inward rectifying K^+ channel) (Hirsch et al., 1998; Fuchs et al., 2005), it significantly impairs the uptake of K^+ by root cells (Almeida et al., 2017). On the other hand, Na^+ competes with K^+ for the major binding sites in protein synthesis, ribosome function, enzymatic reactions, and generally the key metabolic processes in the cytoplasm due to its physicochemical property similarity with K^+ (PPI, 1998). Potassium (K^+) ion imbalance and starvation, would eventually lead to limited plant growth and development (Cakmak, 2005). This is because K^+ as being one of the essential macronutrients, it plays key roles in regulation of cytosolic pH homeostasis and membrane potential, turgor generation, osmotic adjustment, enzyme activation, maintaining electroneutrality and protein activities (PPI, 1998; Zheng et al., 2008; Barragan et al., 2012). Since these enzymatic and metabolic activities are mediated by potassium K^+, it cannot be mimicked and compensated by Na^+ or other cations, hence, it would lead to limited and impaired plant growth (Cakmak, 2005).

1.3.2.3. Oxidative stress

The concerted effect of salinity induced osmotic and ionic stresses would lead to the generation and high-level accumulation of reactive oxygen species (ROS) beyond the plants scavenging capacity by affecting photosynthetic function, impairing the plants antioxidant defense machinery, inducing hormones imbalance and disruption of plants aerobic metabolism (Chaves and Oliveira, 2004; Hu et al., 2012, 2015). Specifically, it leads to the over reduction of the electron carrier systems such as ubiquinone (UQ) pool following the disruption of the tough coupling between ATP synthesis and electron transport chain (ETC), and subsequently, it causes significant generation of reactive oxygen species (ROS) (Rhoads et al., 2006; Blokhina and Fagerstedt, 2010). Thus, the intracellular high-level accumulation of ROS and/or the disruption of the cellular reduction-oxidation

(redox) system would lead to the severe and complicated state of salinity induced disaster to plant cells, oxidative stress (Moradas-Ferreira et al., 1996; Teixeira de Mattos and Neijssel, 1997). The detrimental impacts of ROS on plant cells include damage on proteins, nucleic acids (DNA and RNA), cell membrane lipids and the subsequent electrolyte leakage (EL) and senescence (Huang et al., 2014). Furthermore, unlike the osmotic water loss (where it is widely reversed when precipitation adequately compensated the increased evaporative demand which is caused by increased temperature), oxidative stress is irreversible and the central factor that accounts for the permanent salinity-induced damages in plants.

1.3.2.3.1. What are ROS?

Reactive oxygen species (ROS) are the byproducts of different metabolic pathways such as aerobic respiration that would take place in various subcellular compartments like mitochondria, chloroplasts and peroxisomes (Del Rio et al., 2006; Das and Roychoudhury, 2014; Halliwell, 2006; Navrot et al., 2007). ROS generation has been taking place from the time, oxygen (O_2) evolving photosynthetic organisms have introduced O_2 into the reducing earth´s atmosphere (Halliwell, 2006). Several reports show that from the entire oxygen consumed by plant tissues, only about 1-2% is used for ROS generation (Bhattachrjee, 2005; Das and Roychoudhury, 2014). Both oxygen free radicals and some nonradical oxygen derivatives are included in the term reactive oxygen species (ROS). When one considers, the term reactive alone, it may also refer reactive chlorine, nitrogen and bromine species (Halliwell, 2006). ROS encompass superoxide radical ($O_2^{\bullet -}$), hydrogen peroxide (H_2O_2), hydroxyl radical ($OH^{\bullet}$), singlet oxygen ($^1O_2$), hydroperoxyl radical ($HO_2^{\bullet}$), alkoxy radical ($RO^{\bullet}$) and peroxy radical ($ROO^{\bullet}$) (Mittler, 2002; Apel and Hirt, 2004; Mahajan and Tuteja, 2005; Tuteja, 2007). Even if, ROS are continuously produced as byproducts of various metabolic pathways and processes, they do not cause cellular damage to plant cells. This is because, under normal condition, there is a balance between ROS generation and detoxification. That is, under steady state conditions, the level of ROS is regulated by enzymatic and non-enzymatic antioxidative scavenging defense systems (Foyer and Noctor, 2005). However, they become quite dangerous and damaging molecules when the delicate balance between ROS generation and scavenging is perturbed by various biotic and abiotic environmental stress factors such as pathogen attacks, air pollution, herbicides, nutrient deficiency, extremes of temperature, heavy metals, salinity, UV radiation and drought. Thus, disturbance of the equilibrium between production and detoxification of ROS (Fig. 1), will lead to a sudden boost in the intracellular ROS level and remarkable accumulation (Bhattachrjee, 2005). Consequently, they cause damage to lipids, carbohydrates, proteins and nucleic acids due to their toxic and quite reactive nature (Mittler, 2002; Apel and Hirt, 2004; Mahajan and Tuteja, 2005; Tuteja, 2007).

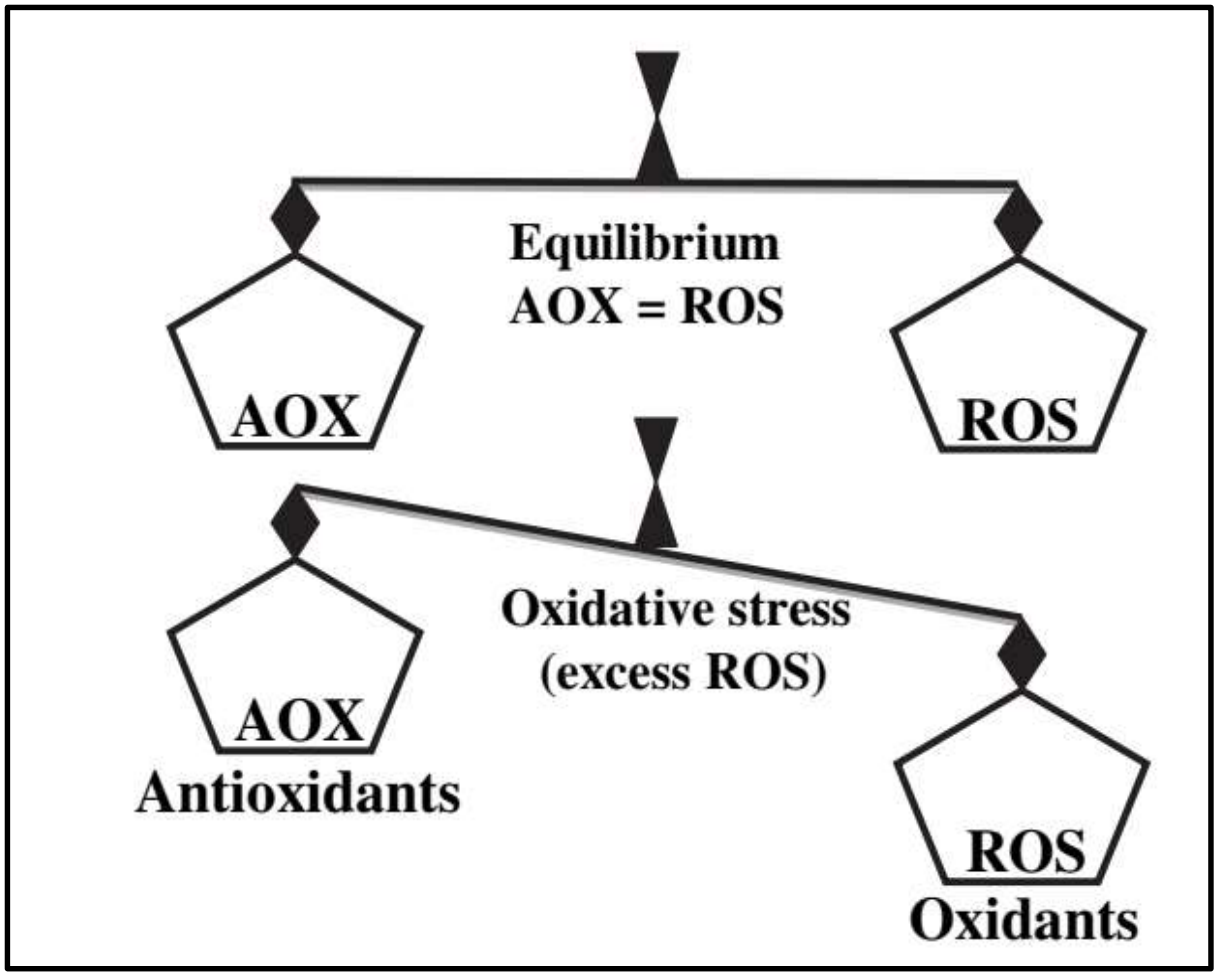

Figure 1: Equilibrium between antioxidants (AOX) and oxidants (ROS). Image source: Gill and Tuteja, 2010.

1.3.2.3.2. ROS generation in mitochondria: just one example

ROS are generated at different cellular locations both during normal and stressful conditions (Fig. 2). Chloroplasts, peroxisomes, mitochondria, endoplasmic reticulum (ER), plasma membranes and the cell wall are the cellular structures where ROS production takes place (Choudhury et al., 2013). With regard to ROS production in the mitochondrion, its ETC (mtETC) plays the pivotal role, particularly complex I and Complex III (Moller et al., 2007; Noctor et al., 2007). Reports show that ROS (specifically H_2O_2) generation in mitochondrion, used up 1-5% of its entire O_2 consumption. Even if, mitochondria produce ROS under normal conditions, its level will be remarkably elevated when the delicate balance between ATP synthesis and mtETC is perturbed by environmental stresses (e.g. drought and salinity) (Pastore et al., 2007; Blokhina and Fagerstadt, 2010). Such perturbed mitochondrial metabolism leads to the leakage of electrons and over reduction of electron carriers such as NADH Dehydrogenase (Complex I), and as a result, in its flavoprotein region, it produces $O_2^{\bullet -}$. Moreover, the process is intensified by further over reduction of Complex I as electrons flow from Complex III back to Complex I (Turrens, 2003). On the course of ROS generation by mitochondria, the Mn-SOD and the APX

convert the generated $O_2^{\bullet-}$ into H_2O_2 (Sharma et al., 2012). On the other hand, mitochondrial matrix localized enzymes such as 1-Galactone-γ-lactone dehydrogenase (GAL) contributes for ROS generation by supplying mtETC with electrons and creating over reduced condition which ends up in $O_2^{\bullet-}$ generation. Likewise, the enzyme aconitase involved in the direct generation of ROS (Rasmousson et al., 2008). Under dark conditions, mitochondrion is the chief producer of ROS. On the other hand, in the presence of light, plastids are the major sites of ROS generation along with peroxisomes (Choudhury et al., 2013) and they are the dominant contributors of salinity-induced oxidative stress in the upper plant organs. However, in this dissertation, we set aside plastids and instead, focused substantially on mitochondria. This is because of the fact that mitochondria are the major source of ROS generation in roots under stressful conditions such as salt stress (Rhoads et al., 2006). And roots are the regulators of salt acquisition and translocation (Jung and McCouch, 2013) and they are plant structures (organs) where the performance of plants under salt stress is decided in the first place.

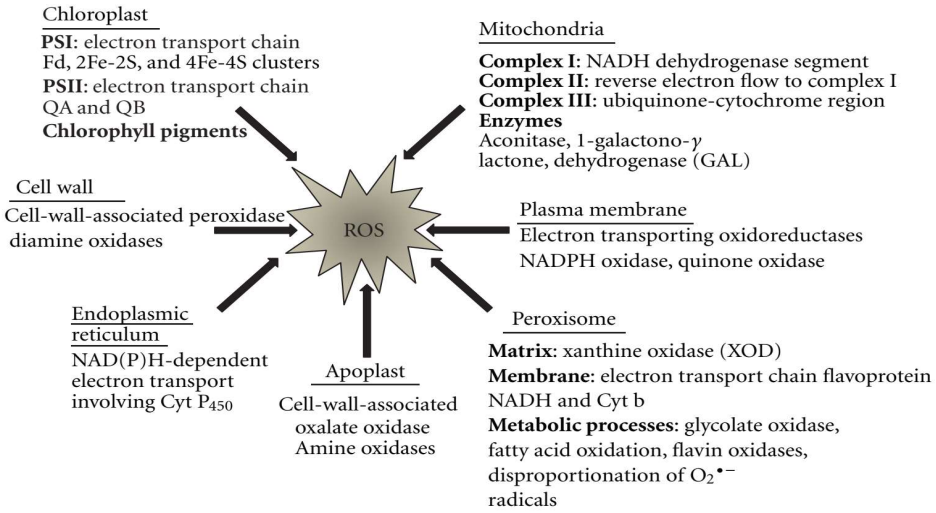

Figure 2: Reactive oxygen species (ROS) generation sites in plants. Image source: Sharma et al., 2012.

1.3.2.3.3. Factors that induce ROS generation

There are different environmental factors that induce ROS generation in plants such as pathogen attack, heavy metals, chilling, salinity, drought, herbicides and atmospheric pollutants (Fig. 3) (Mittler, 2002; Mittler et al., 2004, Karuppanapandian and Manoharan, 2008). For example, in plants, heavy metals like Hg^{2+} cause the accumulation of ROS either by interfering with the metabolic activities of ROS producing organelles and compartments or by inhibiting the function of antioxidative enzymes (Overmyer et al., 2003; Mittler et al., 2004; Karuppanapandian and Manoharan, 2008; Karuppanapandian et al., 2009). The generated less toxic ROS such as H_2O_2 will be then converted into the highly reactive $OH^{\bullet}$ free radical by Haber-Weiss/ Fenton reaction in the presence of transition metals such as Cu^{2+} and Fe^{2+} (Karuppanapandian et al., 2011).

Drought and salinity are further treated below as two examples of important abiotic environmental factors that trigger ROS generation. During drought stress, abscisic acid (ABA) attempts to mitigate the associated water loss through stomatal closure. This leads to minimized available CO_2 for photosynthetic activities, which in turn, reduces Calvin Cycle mediated regeneration of $NADP^+$. Consequently, the photosynthetic ETC will be overreduced and eventually, ROS such as $O_2^{\bullet-}$ will be generated by leakage of electrons to O_2 through Mehler reaction. Then the generated $O_2^{\bullet-}$ will be converted to highly toxic free radicals via series of chain reactions (Karuppanapandian et al., 2011; Sharma et al., 2012). On the other hand, salt stress causes excessive generation of ROS such as $O_2^{\bullet-}$, H_2O_2, $^1O_2$ and $OH^{\bullet}$ through its osmotic and specific ion effects (Hernandez et al., 2000). The osmotic effect leads to overproduction of ROS via overreduction of photosynthetic ETC, exposure of the photosynthetic machinery to high level of excitation energy and stimulated photorespiration. This is a result of photosynthetic activity (CO_2 fixation) inhibition due to quite limited CO_2 availability which has been emanated from stomatal closure. On the other hand, the specific ion effect caused elevated ROS generation by inducing various metabolic pathways like photorespiration and by disabling the ETC in subcellular structure such as mitochondria and chloroplasts (Sharma et al., 2012).

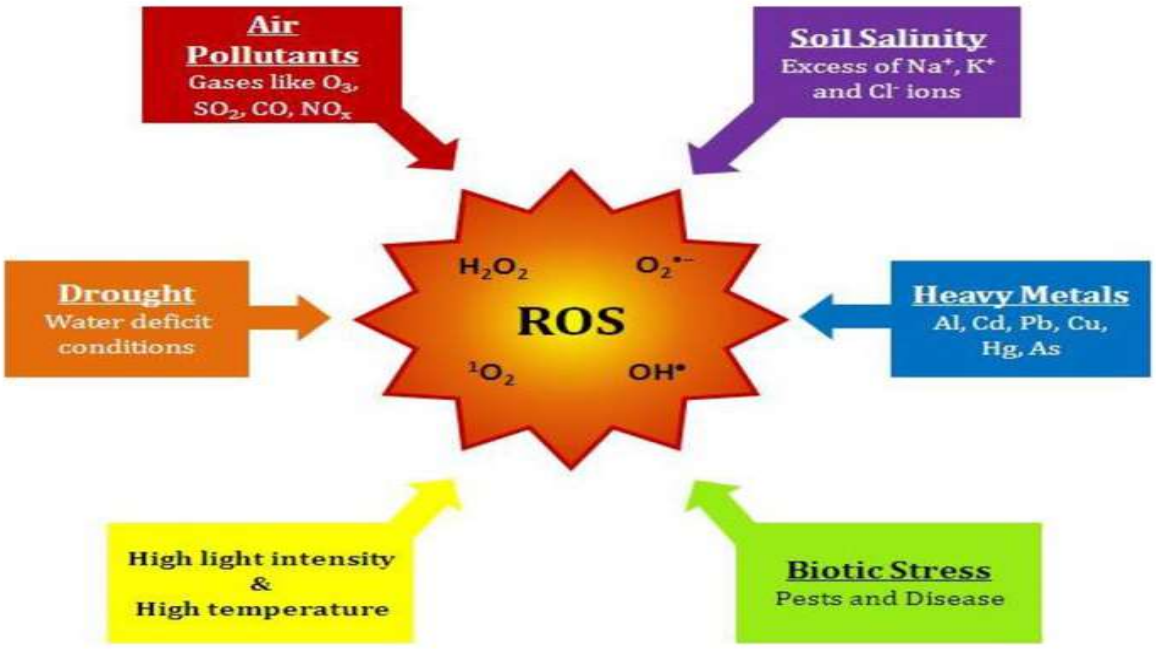

Figure 3: The different factors that trigger reactive oxygen species (ROS) generation. Image source: Das and Roychoudhury, 2014.

1.3.2.3.4. ROS have dual functions

During the stress response of plant cells, ROS can play a dual role, in that, they take part in signalling cascade and act as second messengers at low/moderate concentration, but they damage biomolecules at higher

concentration (Miller et al., 2008; Miller et al., 2010). Reactive oxygen species (ROS) play a pivotal role in intracellular signalling, specifically as second messengers at low or moderate concentration (Sharma et al., 2012). This is due to the fact that ROS are equipped with all the important characteristics that a signalling molecule should have, such as being generated rapidly and efficiently whenever needed, and discarded swiftly and successfully in the absence of quest for them (Neil et al., 2003). ROS participate in the signalling cascades by interacting chemically with target proteins that cause protein modification, and specific atoms like sulphur (S) and iron (Fe) (Nathan, 2003). The different ROS, namely $O_2^{\bullet-}$, H_2O_2, $^1O_2$ and $OH^{\bullet}$ have different capability in their function as intracellular signalling molecules. For example, $O_2^{\bullet-}$ due to its inability to pass across membranes (because of its negative charge) and instability (due to SOD mediated and spontaneous dismutation to H_2O_2), it is considered as poor signalling molecule (Sharma et al., 2012). On the other hand, H_2O_2 is quite efficient and ideal signalling molecule due to its stability, selective reactivity and ability to diffuse through membranes easily (D´Autreaux and Toledano, 2007; Paulsen and Carroll, 2010; Sharma et al., 2012). Furthermore, the same ROS type generated in different subcellular compartments plays quite distinct signalling role (Sharma et al., 2012). For instance, H_2O_2 produced in the chloroplast, functions in triggering the biosynthetic genes and transcription factors that take part in the generation of secondary messengers whereas H_2O_2 produced in peroxisomes deals with the activation of transcripts that involve in protein repair (Sewelam et al., 2014).

During early signalling events, within minutes after abiotic or biotic environmental stimuli application, ROS are generated along with activation of mitogen-activated protein kinases (MAPKs) and ions flux across the plasma membrane (Benschop et al., 2007; Finka et al., 2012). Environmental stress induced influx of Ca^{2+} results in increased cytosolic Ca^{2+} level which activates respiratory burst oxidase homolog (RboH) both directly and indirectly (through stimulation of series of events that trigger calcium-dependent protein kinases that activate RboHs by phosphorylation) (Mittler et al., 2011; Dubiella et al., 2013; Gilroy et al., 2014). The ROS generated by the activated RboHs shall be detected by the nearby cells, and as a result, further calcium influx will be triggered, and their own RboHs shall be activated by the increased Ca^{2+} level. This signalling process will lead to systemic response to abiotic and/or biotic stresses by its auto-propagation from cell to cell throughout the whole plant (Choudhury et al., 2017). ROS also play signalling role through their effect on the cellular redox balance or homeostasis (Mittler, 2017). For example, variation in ROS concentration causes change in the cellular redox balance that will be sensed and translated into quite different signals by various pathways which end in the generation of adaptive responses by directing the cells in question to do so (Foyer and Noctor, 2005). Moreover, the signalling role of ROS is manifested indirectly through the detection of products of ROS damaged cells (Evans et al., 2005) or sensing variation in cellular redox potential (Price et al., 1994).

Even if, ROS at low/moderate concentration act as second messengers and actively participate in intracellular signalling cascades; at higher concentration, they cause oxidative damage that ends up in cell death through the

destruction of important biomolecules particularly lipids, proteins and DNA (Fig. 5) (Choudhury et al., 2013; Das and Roychoudhury, 2014). In plant cells, when the controlled and sustainable ROS production through lipid peroxidation (LPO) exceeds the optimum level under the influence of environmental cues, it becomes quite damaging. It affects membrane phospholipids by attacking the glycerol-fatty acid ester linkage and the carbon-atoms double bond. Moreover, among the most important components of plasma membrane, ROS specifically target the polyunsaturated fatty acids (PUFAs) such as linolenic acid and linoleic acid. Even if, other ROS members are also participating in LPO, the hydroxyl radical is the most serious and damaging one. This is because it has a potential to maximize and exacerbate the oxidative damage to lipids, proteins and DNA by inducing series of cyclic chain reactions. Thus, ROS affect different cellular and biochemical activities through LPO such as deactivation of membrane-localized enzymes, ion-channels and membrane receptors and making the plasma membrane non-selective and leaky through the augmentation of its fluidity (Das and Roychoudhury, 2014). LPO occurs in three consecutive and interconnected steps such as initiation, propagation and termination. During initiation step, free radicals such as $O_2^{\bullet -}$ and $OH^{\bullet}$ are generated by energizing molecular oxygen. The generated ROS, specifically, $OH^{\bullet}$ leads to the production of PUFA alkyl radical ($PUFA^{\bullet}$) by interacting with methylene groups of PUFA (Smirnoff, 2000). At propagation step, the peroxyl radical ($PUFA\text{-}OO^{\bullet}$) generated as a result of interaction of $PUFA^{\bullet}$ with O_2, will extract hydrogen atom from the neighboring PUFA side chains and induces the LPO propagation process. Consequently, lipid epoxides, hydro-peroxide, aldehydes, and alkoxyl radicals are generated. Eventually, the various lipid derived radicals generated in the entire process will interact with one another and terminate the process by the formation of lipid dimers (Fig. 4) (Bhattacharjee, 2005; Das and Roychoudhury, 2014).

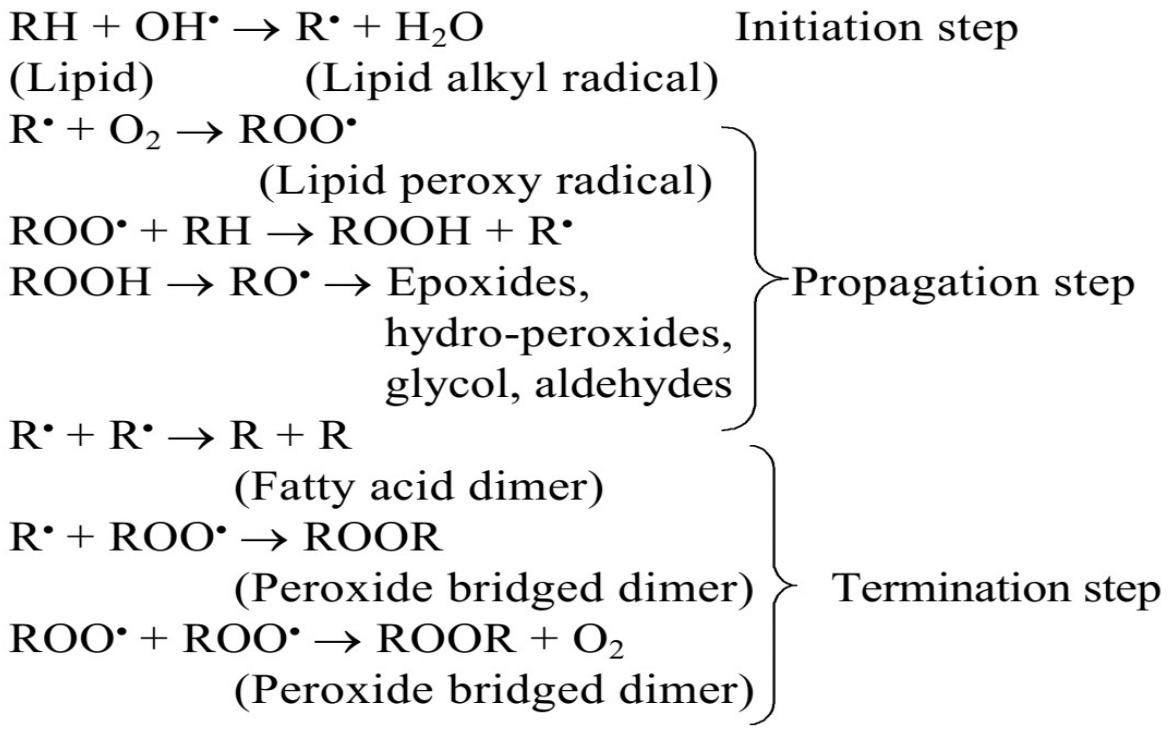

Figure 4: The three consecutive and interconnected lipid peroxidation (LPO) steps. ´R´ represents the polyunsaturated fatty acid (PUFA). Image source: Bhattacharjee, 2005.

The environmental stress induced and LPO aggravated ROS, oxidize proteins through direct or indirect chemical modifications (Das and Roychoudhury, 2014). Direct proteins chemical modifications such as glutathionylation, disulfide bond formation, nitrosylation and carboxylation cause the specific protein in question to carry out a different function. On the other hand, proteins are modified indirectly through their interaction with the LPO products. Those amino acids containing thiol groups as well as sulfur are the hotspots for ROS attack. In general, amino acids respond differently to the ROS assault. Amino acids such as tryptophan (Trp), threonine (Thr), arginine (Arg), lysine (Lys) and proline (Pro) will be made quite fertile targets for proteolytic degradation after being altered by site specific modification which is orchestrated by the increased ROS concentration. Overall, ROS attack proteins through enzyme inactivation, amino acids modification, peptide chain breakage and increased proteolytic degradation (Moller et al., 2007; Das and Roychoudhury, 2014).

ROS attack DNA through nucleotide nitrogenous base modification, deoxyribose sugar residue oxidation, removal of a nucleotide, DNA strand breakage and protein-DNA crosslinking (Das and Roychoudhury, 2014). The hydroxyl radical, $OH^{\bullet}$ interacts with the purine and pyrimidine double bonds and also assaults the deoxyribose sugar backbone by abstracting the H-atom (Halliwell, 2006). Furthermore, the removal of H-atom from the Carbon-4 of the deoxyribose sugar will lead to DNA single strand breakage via the formation of deoxyribose radical (Evans et al., 2004). In general, both chloroplastic and mitochondrial DNA are the hotspots for ROS attack

unlike the nuclear DNA. This is because of their close subcellular localization to the ROS generating apparatus and the absence of histone mediated protection (Das and Roychoudhury, 2014).

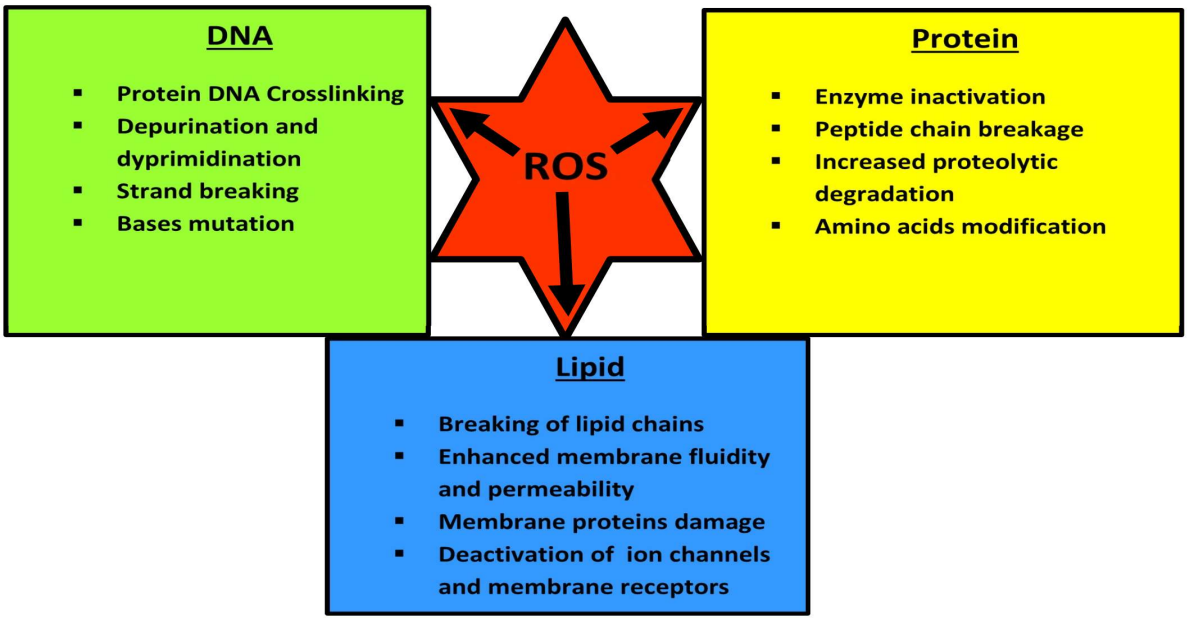

Figure 5: Effects of ROS on biomolecules such as DNA, protein and lipid. Image source: Das and Roychoudhury, 2014.

1.4. Plants response to salt stress

In plants response to salt stress, the stress needs to be perceived and sensed by receptors such as ion channels, histidine kinase, G-protein-coupled receptors, receptor like kinase and so on at the membrane level before the signal is transduced into the nucleus via secondary messengers (Tuteja, 2007).

1.4.1. Sensing salt stress

In order to cope up with the destructive effects of salt stress, plants need to perceive and sense both osmotic and ionic (Na^+/Cl^-) stresses at the cellular and whole plant level. Even if, the exact mechanisms of sensing these two stresses have not been well elucidated (Almeida et al., 2017), they are sensed by trans-membrane proteins situated on the surface of plasma membrane or enzymes localized in the cytosol. The sodium ion (Na^+) which is the key component of salinity induced ionic stress, could be sensed extracellularly (by a membrane receptor) and/or intracellularly (by Na^+-sensitive cytosolic enzymes or membrane proteins) (Zhu, 2003). Moreover, the Na^+/H^+ antiporter, salt overly sensitive 1 (SOS1) is also considered as both Na^+ sensor and transporter (Shi et al., 2000; Zhu, 2003).

1.4.2. Salt stress signaling network: Ca^{2+}/SOS cascade-just one example

Plants have very complex salinity stress signalling pathways that involve multiple components such as Ca^{2+}, salt overly sensitive (SOS) pathway, reactive oxygen species (ROS), mitogen-activated protein kinases (MAPKs), phytohormones [e.g. abscisic acid (ABA) and jasmonic acid (JA)] and nitric oxide (Tuteja, 2007; Che-Othman et

al., 2017). However, here, we shall consider only Ca^{2+}/salt overly sensitive (SOS) signalling cascade (Fig. 6) which is among the earliest signalling pathways being triggered by salt stress (Roy et al., 2014). Ca^{2+} initiates signal transduction pathways vis-à-vis salt tolerance after being released from the apoplastic space (extracellular source) and also from different intracellular compartments as a result of increased Na^+ ions concentration under salt stress (Knight et al., 1997). The elevated cytosolic Ca^{2+} level is sensed by salt overly sensitive 3 (SOS3), and consequently, the latter would be activated and interacted with salt overly sensitive 2 (SOS2) protein kinase. The generated SOS3-SOS2 complex activates the vacuolar H^+-ATPase and PPase and helps the establishment of a robust electrochemical proton gradient across the tonoplast where other important downstream processes depend on (Dietz et al., 2001). Then using the generated proton motive force (pmf), SOS3-SOS2 complex participates in the pumping of Na^+ and Ca^{2+} into the vacuole by stimulating the vacuolar Na^+/H^+ exchanger (NHX) and H^+/Ca^{2+} exchanger (CAX1) respectively. Furthermore, it triggers the exclusion of Na^+ out of the cytosol by activating the plasma membrane localized Na^+/H^+ antiporter or salt overly sensitive 1 (SOS1) (Qiu et al., 2003, 2004; Tuteja, 2007).

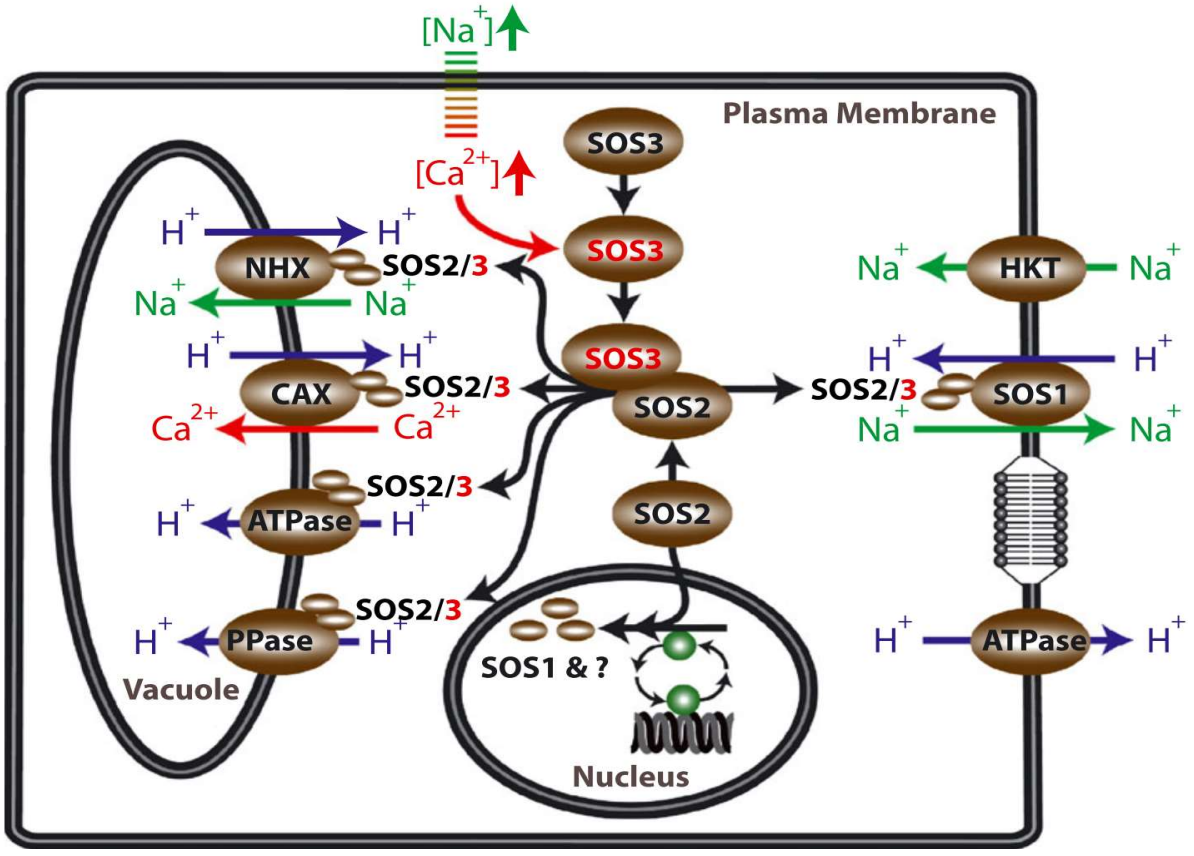

Figure 6: The Ca^{2+}/ salt overly sensitive (SOS) signaling cascade. SOS1, SOS2 and SOS3 (salt overly sensitive 1, 2 and 3), CAX= H^+/Ca^{2+} exchanger (antiporter), ATPase= Vacuolar type and plasma membrane localized ATPase, PPase = Proton-pumping pyrophosphatase, NHX= Vacuolar Na^+/H^+ exchanger (antiporter), HKT= Low affinity sodium transporter and SOS= salt overly sensitive. Image source: Che-Othman et al., 2017.

1.5. Plant hormones and salt stress

Through several years of co-existence, plants have developed various mechanisms to cope up with the detrimental effects of salinity (Ismail et al., 2012). These mechanisms are dependent on multiple and various factors; however, phytohormones are considered the most important endogenous substances that modulate the sophisticated molecular and physiological responses of plants under abiotic stresses in general (Velitchkova and Fedina, 1998; Sreenivasulu et al., 2012; Golldack et al., 2014; Fahad et al., 2015). They include cytokinins (CKs), abscisic acid (ABA), auxin (IAA), brassinosteroids (BRs), salicylic acid (SA), ethylene (ET) and jasmonates (JAs) (Balbi and Devoto, 2007; Wani et al., 2016). Jasmonic acid (JA), its derivatives such as methyl jasmonate (MeJA), jasmonyl-isoleucine (JA-Ile) and its biological active precursor 12-oxo-phytodenoic acid (OPDA), collectively referred as jasmonates (JAs) are crucial signaling molecules that regulate a broad spectrum of plant physiology and actively participate in plant responses to multitude biotic and abiotic stresses (Wasternack, 2007; Browse, 2009; Avanci et al., 2010; Hazman et al., 2015; Samota et al., 2017). They have great potential to mitigate cascades of threatening environmental stresses (Dar et al., 2015) such as Uv irradiation (Demkura et al., 2010), drought (Seo et al., 2011), salinity (Pauwels et al., 2009). Moreover, their role in drought and salinity tolerance (reviewed in Riemann et al.,2015), temperature stress tolerance (reviewed in Sharma and Laxmi, 2016), salinity, drought, heat and cold stress tolerance (reviewed in Samota et al., 2017), and biotic and abiotic stress tolerance in general (reviewed in Avanci et al., 2010; Ahmad et al., 2016).

1.5.1. Role of jasmonates (JAs) in plant salt tolerance

Jasmonates (JAs) play a positive role in the abiotic and biotic stress tolerance of plants. Studies showed that exogenous application of both JA (Kang et al., 2005; Ismail et al., 2012) and MeJA (Yoon et al., 2009; Del Amor and Cuadra-Crespo, 2011) conferred salt tolerance in plants. Moreover, overexpression of the transcription factor, OsbHLH148 which is one component of jasmonate signaling pathway resulted in drought tolerance of rice (Seo et al., 2011) and similarly, the constitutive expression of TaAOC1 gene imparted salt tolerance in bread wheat by elevating JA level (Zhao et al., 2014). Moreover, overexpression of OsOPR7 in Arabidopsis opr3 mutant rescued seed germination failure and restored male sterility (Tani et al., 2008). Exogenous application of MeJA and OPDA (only partially) rescued coleoptile growth JA-deficient mutant *hebiba* of rice under red-light irradiation (Riemann et al., 2003) and JA conferred resistance to blast fungus in rice (Riemann et al., 2013). On the other hand, pretreatment of salt stressed barely with JA resulted in improved salt tolerance (Walia et al., 2007). Recently, Zhang et al. (2017) reported that increased JA level was responsible for salt tolerance in sweet potato. On the contrary, jasmonates (JAs) are negative regulators of abiotic stress tolerance of plants such as salinity (Toda et al., 2013; Hazman et al., 2015), drought (Harb et al., 2010; Dhakarey et al., 2017) and both drought and salinity (Ye et al., 2009). And it negatively regulated IAA-induced coleoptile growth (Ueda et al., 1994).

1.6. Plants salt stress tolerance mechanisms

Plants respond to soil salinity stress through compatible solutes accumulation (osmotic stress tolerance), ion homeostasis (ionic stress tolerance) and antioxidative defense (oxidative stress tolerance) (Munns and Tester, 2008; Gupta and Huang, 2014).

1.6.1. Compatible solutes accumulation: osmotic stress tolerance mechanism

Plants mitigate the detrimental effects of salinity induced osmotic stress (water deficit) through the synthesis and accumulation of compatible solutes in the cytosol and/or sequestration of Na^+ and/or Ca^{2+} in the vacuole (Ashrafijou et al., 2010; Nabati et al., 2011; Abbasi et al., 2016). These compatible solutes (osmolytes) include proline, glycine betaine, free amino acids, sugars, quaternary ammonium compounds and polyols (Ashraf and Foolad, 2007; Hoque et al., 2007; Abbasi et al., 2016). Cells maintain the concentration of compatible osmolytes either by synthesis coupled with degradation or irreversible synthesis. Due to their high cytosolic concentration, the compatible solutes create hypotonic condition that causes the continuous entry of water into the cell. Thus, by doing so, they maintain the osmotic balance and protect cellular structures (Bohnert et al., 1995; Hasegawa et al., 2000; Gupta and Huang, 2014; Abbasi et al., 2016). Apart from taking part in turgor pressure maintenance, compatible solutes protect and stabilize membranes, proteins, protein complexes and enzymes from dehydration (water deficit) and ionically orchestrated damage, and also act as reactive oxygen species scavengers (Gadallah, 1999; Ashraf and Foolad, 2007; Hoque et al., 2008; Gupta and Huang, 2014; Muchate et al., 2016). While they carry out these important cellular functions, they do not interfere with cellular metabolisms as well as enzyme activities even at elevated concentration. This emanates from their polar, uncharged and water solubility nature (Ashrafijou et al., 2010; Nabati et al., 2011; Gupta and Huang, 2014).

1.6.2. Ion homeostasis: ionic stress tolerance mechanism

Under high soil salinity conditions, the root cells cytosol would be flooded with Na^+ ions that enter through selective/non-selective transporters or cation channels (Chinnusamy et al., 2005). The increased soil solution Na^+ concentration causes plasma membrane depolarization and subsequent K^+ leakage. Moreover, since both Na^+ and K^+ make use of similar transport mechanism, the former may better compete with the latter, and result in low cytoplasmic K^+ concentration. Nevertheless, for normal and optimal cellular activities, cells should maintain low cytosolic Na^+ concentration ($\leq$ 1mM) and high K^+ level (~100mM) (Munns and Tester, 2008; Gupta and Huang, 2014). Plants protect themselves from the deleterious effects of excess Na^+ ions by pumping them into the vacuole, sequestering in older leaves and/or excluding them out of the cytosol (Zhu, 2003). They transport the excess cytosolic Na^+ into the vacuole by means of vacuolar Na^+/H^+ antiporter and vacuolar Na^+/H^+ exchanger (NHX). Both transporters are energized by the electrochemical potential gradient generated by H^+-pumps such as H^+-ATPase (V-ATPase) and vacuolar pyrophosphatase (V-PPase) (Wang et al., 2001; Zhu, 2002; Mahajan et al., 2006). Furthermore, the excessive entry of Na^+ into root cells cytosol is blocked by a low-affinity Na^+ ion transporter, the histidine kinase transporter (HKT) (Platten et al., 2006; Tuteja, 2007). On the other hand,

the plasma membrane Na^+/H^+ antiporter plays a pivotal role in ion homeostasis by excluding Na^+ ions out of the cytosol (Na^+ efflux). This antiporter depends on the SALT OVERLY SENSITIVE (SOS) stress signaling pathway (Hasegawa et al., 2000) that consists of three important proteins, namely, SOS1, SOS2 and SOS3 (Gupta and Huang, 2014). The SOS stress signaling commences when Ca^{2+} is being released from both extracellular and intracellular sources as a result of increased Na^+ concentration. The released Ca^{2+} binds with SOS3 protein (Ca^{2+} sensor) and then the SOS3 liberates the SOS2 protein from its self-inhibition by interacting with it and forming SOS3-SOS2 complex. The generated complex phosphorylates the plasma membrane localized SOS1 (PM-Na^+/H^+ antiporter), and eventually, the SOS1 is activated and pumps Na^+ effectively out of the cytosol (Mahajan et al., 2006; Martinez-Atienza et al., 2007; Gupta and Huang, 2014).

1.6.3. Antioxidative defense: oxidative stress tolerance mechanism

Plants have developed a sophisticated enzymatic and non-enzymatic antioxidative defense system to scavenge the reactive oxygen species (ROS) generated owing to salinity induced oxidative stress (Muchate et al., 2016). Ascorbate peroxidase, glutathione reductase, superoxide dismutase, catalase, glutathione peroxidase, monodehydroascorbate reductase, dehydroascorbate reductase, glutathione-S-transferase and guaiacol peroxidase form the enzymatic antioxidative defense system. On the other hand, the non-enzymatic ROS scavenging system is composed of carotinoids, glutathione, phenolic compounds, ascorbic acid, non-protein amino acids, alkaloids and alpha tocopherols (Gill and Tuteja, 2010).

1.6.3.1. Enzymatic antioxidative defense system

The enzymatic antioxidative defense system is localized in various subcellular structures and includes catalase (CAT), superoxide dismutase (SOD), ascorbate peroxidase (APX), dehydroascorbate reductase (DHAR), monodehydroascorbate reductase (MDHAR), guaiacol peroxidase (GPX) and glutathione reductase (GR) (Karuppanapandian et al., 2011; Das and Roychoudhury, 2014).

1.6.3.1.1. Catalase (CAT)

CAT (E.C 1.11.1.6) is a tetrameric heme contacting enzyme which is predominantly localized in the peroxisomes where there is high rate of H_2O_2 generation (Mittler, 2002). Moreover, irrespective of the absence of significant antioxidative activity, it can also be found in other subcellular compartments such as chloroplasts, cytosol and the mitochondria (Mhamdi et al., 2010). During stressful conditions, there would be high rate of catabolism so as to meet the huge energy demand. Consequently, a great deal of H_2O_2 would be released as a by-product of the catabolic process. Thus, the main role of CAT is the dismutation of the produced H_2O_2 into H_2O and O_2 with quite greater turnover rate ($6x10^6$ molecules of H_2O_2 to H_2O and O_2 min^{-1}). However, with respect to the organic peroxides (R-O-O-R), CAT has low specificity (Das and Roychoudhury, 2014).

$$H_2O_2 \longrightarrow H_2O + (1/2)\ O_2$$

1.6.3.1.2. Superoxide Dismutase (SOD)

SOD (E.C. 1.15.1.1) is among the family of metalloenzymes, and it occurs in all aerobic organisms. Based on the specific metal cofactor to which it binds, there are three isozyme forms of SOD. These are Cu/Mn-SOD (localized in chloroplasts, cytosol and peroxisomes), Mn-SOD (localized in mitochondria) and Fe-SOD (localized in chloroplasts) (Mittler, 2002). SODs catalyze the disproportionation of $O_2^{\bullet -}$ into O_2 and H_2O_2. Thereby, they impede the occurrence of the Haber-Wess reaction which generated the highly toxic and lethal free radical, $OH^{\bullet}$ (Das and Roychoudhury, 2014).

$$O_2^{\bullet -} + O_2^{\bullet -} + 2H^+ \longrightarrow 2H_2O_2 + O_2$$

1.6.3.1.3. Ascorbate peroxidae (APX)

APX (E.C. 1.1.11.1) carries out the disproportionation of H_2O_2 to H_2O and dehydroascorbate (DHA) in the chloroplast and cytosol by making use of ascorbic acid (AA) as reducing agent. APX is the main component of ascorbate glutathione (ASC-GSH) cycle and it detoxifies H_2O_2 quite efficiently during environmental stressful condition due to the fact that it has higher affinity to H_2O_2 than CAT (Asada, 2000; Das and Roychoudhury, 2014). Studies show that the overexpression of the cytosolic APXs in Arabidopsis plants imparted salinity stress tolerance as compared to the wild-type counter parts (Lu et al., 2007).

$$H_2O_2 + AA \longrightarrow 2H_2O + DHA$$

1.6.3.1.4. Monodehydroascorbate reductase (MDHAR)

MDHAR (E.C. 1.6.5.4) deals with maintaining the cellular ascorbic acid (AA) pool by regenerating it using the NADPH as reducing agent from a transient monodehydroascorbate (MDHA). It performs this AA regeneration activity in the peroxisomes and mitochondria where CAT scavenges H_2O_2 and oxidizes AA (Del Rio et al., 2002; Mittler, 2002). There are mitochondria, chloroplast, peroxisomes, cytosol and glyoxysomes localized isozymes of MDHAR (Das and Roychoudhury, 2014).

$$MDHA + NADPH \longrightarrow AA + NADP^+$$

1.6.3.1.5. Dehydroascorbate reductase (DHAR)

DHAR (E.C. 1.8.5.1) it catalyzed the regeneration of one of the major antioxidants in plants, ascorbic acid (AA), where using the reduced glutathione (GSH) as an electron acceptor, it reduces dehydroascorbate (DHA) to AA (Eltayeb et al., 2007; Karuppanapandian et al., 2011). Thus, it greatly contributes in maintaining the redox state of plant cells by regulating both symplastic and apoplastic AA pool size (Chen and Gallie, 2006). In both

Arabidopsis and Tobacco plants, the overexpression of DHAR resulted in a better environmental stress tolerance (Chen and Gallie, 2006; Eltayeb et al., 2007).

$$DHA + 2GSH \longrightarrow AA + GSSG$$

1.6.3.1.6. Glutathione reductase (GR)

GR (E.C. 1.6.4.2) is a crucial enzyme localized in the mitochondria and cytosol to a certain extent and predominantly in chloroplasts, and it takes part in the regeneration of ascorbic acid (AA). It regenerates AA from MDHA and DHA using reduced glutathione (GSH) which is resulted from the NADPH mediated reduction of glutathione disulphide (GSSG) (Noctor and Foyer, 1998; Das and Roychoudhury, 2014). Moreover, GR maintains a high cellular GSH/GSSG ratio by catalyzing the NADPH-dependent disulphide bond formation (Noctor and Foyer, 1998; Asada, 2000). Studies depicted that in pea (Hernandez et al., 2001) and French bean (*Phaseolus vulgaris*) (Negesh and Devaraj, 2008), increased GR activity and a subsequent accumulation of GSH, resulted in abiotic stress tolerance (Karrupanapandian et al., 2011).

$$GSSG + NADPH \longrightarrow 2GSH + NADP^{+}$$

1.6.3.1.7. Guaiacol peroxidase (GPX)

GPX (E.C. 1.11.1.7) is a ´stress enzyme´ which removes excess H_2O_2 produced both under normal and stressful conditions by oxidizing certain substances and making use of the former free radical in the process (Karrupanapandian et al., 2011; Das and Roychoudhury, 2014). Aromatic compounds such as guaiacol and pyragallol are preferred electron donors of GPX in oxidizing ascorbate. GPXs function in the cell wall, vacuole, cytosol and extracellular space in the consumption and subsequent removal of H_2O_2 using both its extra- and intracellular forms (Asada, 2000; Jebara et al., 2005; Karrupanapandian et al., 2011). Under salinity stress, the GPX activity has been increased in common bean (*Phaseolus vulgaris*) (Jebara et al., 2005).

$$H_2O_2 + GSH \longrightarrow H_2O + GSSG$$

1.6.3.2. Non-enzymatic antioxidative defense system

The non-enzymatic antioxidative defense system that take part in protecting cellular components from antioxidative stress-induced damage include, ascorbic acid (AA), α-tocopherols, carotenoids, reduced glutathione (GSH), flavonoids, phenolic compounds and the amino acid, proline (Das and Roychoudhury, 2014).

1.6.3.2.1. Ascorbic acid (AA)

AA is well characterized, the most abundant and the main ROS-scavenging antioxidant compound in the aqueous phase that donates electrons to various enzymatic and non-enzymatic reactions (Horemans et al.,

2000; Smirnoff, 2000; Das and Roychoudhury, 2014). Through APX mediated reaction, it can reduce H_2O_2 to H_2O, and also directly detoxify $O_2^{\bullet -}$, $OH^{\bullet}$ and $^1O_2$ (Noctor and Foyer, 1998). In chloroplasts, it dissipates the excess energy by acting as a cofactor for Violoxanthin de-epoxidase and protects and preserves the activities of enzymes that have metal cofactors (Smirnoff, 2000).

1.6.3.2.2. Reduced glutathione (GSH)

GSH is a tripeptide (γ-glutamyl-cysteinyl-glycine) occurs in chloroplasts, endoplasmic reticulum (ER), mitochondria, cytosol, vacuoles, apoplast and peroxisomes with multitude functions (Noctor and Foyer, 1998; Das and Roychoudhury, 2014). Due to its elevated reducing potential that emanates from the central cysteine residue being equipped with nucleophilic character, it detoxifies H_2O_2 and gets rid of $OH^{\bullet}$, $O_2^{\bullet -}$ and $^1O_2$ non-enzymatically. Furthermore, it reduces different biomolecules in the presence of organic free radicals or ROS, and generates GSSG as a byproduct, consequently, protects them from oxidative damage. On the other hand, it maintains the GSH cellular pool through AA regeneration and production of GSSG. As result, it enables to regulate the cellular redox environment through the maintenance of redox equilibrium in different cellular structures by the former along with the latter (Noctor and Foyer, 1998; Halliwell, 2006; Karuppanapandian et al., 2011).

1.6.3.2.3. α-Tocopherol (α-TOC)

The α-TOCs are among lipophilic antioxidants that are components of biological membranes and protect them from oxidative damage by scavenging lipid radicals as well as ROS (Holländer-Czytko et al., 2005). The TOCs occur only in plants green tissues as they are produced only by photosynthetic organisms. Even if, there are four isomers (α-. β-, γ- and δ-) of TOCs, it is the α-tocopherol which is equipped with a great deal of antioxidant capability. TOCs protect both the structure and activity of PSII by reacting with O_2 and quenching the associated excess energy. Moreover, α-tocopherol, interacts with the products of the polyunsaturated fatty acid (PUFA) oxidation such as $RO^{\bullet}$, $ROO^{\bullet}$ and RO* at the membrane-water boundary. Thereby, they break and prevent chain propagation step during lipid peroxidation (LPO). In this interaction, α-tocopherol reduces the lipid radicals, and in the process, it will be changed into α-tocopherol radical ($TOH^{\bullet}$). Eventually, the latter will be converted into its reduced form and recycled by interacting with AA, GSH or other antioxidants (Igamberdiev et al., 2004). On the other hand, membrane structures are immune from the destructive effect of tocopherols by the complexation of TOCs with lysophospholipids and free fatty acids (Karuppanapandian et al., 2011). In plants under different abiotic stressful situations, elevated level of α-TOCs has been reported (Lendford and Niyogi, 2005).

1.6.3.2.4. Carotenoids (CARs)

CARS are lipophilic antioxidants that belong to plants light harvesting machinery (antennae molecules) that transfer the light energy to chlorophyll molecules after absorbing it at 450-570nm wavelength range. Thus, they act as accessory light harvesting pigments in chloroplasts. Nevertheless, their prominent function is the protection of photosystems (PSI and PSII) mainly from oxidative damage. Thus, they play antioxidative role. They carry out this feat by directly quenching ^{3}Chl* or excited chlorophyll (Chl*) and avoids $^1O_2$ generation as a result, detoxify $^1O_2$ and generating heat as a byproduct, dissipating excess excitation energy via the xanthophyll cycle, and halting chain reaction by reacting with LPO products (Collins, 2001; Karuppanapandian et al., 2011; Das and Roychoudhury, 2014). Since CARs are proximate to chlorophyll, energy is transferred from chlorophyll to them during ^{3}Chl* quenching. Consequently, CARs are the competitive inhibitors of $^1O_2$ generation (Collins, 2001).

1.6.3.2.5. Flavonoids

Flavonoids are common in plants and there are four different types based on their structure. These are anthocyanins, flavones, isoflavones and flavonols (Das and Roychoudhury, 2014). Flavonoids alleviate the oxidatively damaged outer chloroplastic membrane by scavenging $^1O_2$ (Agati et al., 2012). Moreover, they protect the photosynthetic machinery assaulted by excess excitation energy, and as a result, they act as secondary ROS scavengers in plants (Fini et al., 2011).

1.6.3.2.6. Phenolics

Phenolic compounds are secondary metabolites that include tannins, lignin and hydroxycinnamate esters. Due to their chain-breaking (through stabilization and delocalization of unpaired electrons) and Fenton reaction terminating (via transition metal ions chelating) function, phenolics play crucial antioxidative role in plants. Moreover, they halt lipid peroxidation by restricting the diffusion of free radicals through reduced membrane fluidity as a result of lipid packing order modification (Arora et al., 2002; Blokhina et al., 2003; Karuppanapandian et al., 2011). Furthermore, they take part in ROS detoxification (Winkel-Shirley, 2002).

1.6.3.2.7. Proline

The osmolyte proline is a non-enzymatic antioxidant that neutralizes the detrimental effects of various ROS. It counteracts LPO induced damages as well as removes $^1O_2$ and $OH^\bullet$ efficiently (Das and Roychoudhury, 2014). Studies show that either due to elevated generation or minimized cellular degradation, proline level has increased under stressful environmental conditions (Verbruggen and Hermans, 2008).

1.7. Soil salinization and the fate of crop production

Since soil salinity is accentuating from time to time due climate change driven elevated irrigation practice with salt-rich water, there should be appropriate measures to circumvent the problem. There have been several attempts to tackle the problem by producing salt tolerant crop cultivars besides the efforts through physical and chemical approaches. In general, two biological approaches have been used in generating salt tolerant crop cultivars (from salt tolerant wild relatives and halophytes) such as breeding and genetic engineering. In this effort, the newly developed approaches like genome engineering are used along with the traditional approaches instead of replacing them (Nongpiur et al., 2016). So far, several transgenic plants have been developed by overexpressing the Na^+/H^+ antiporter genes particularly the vacuolar antiporters (Khan, 2011). For example, transgenic *Brassica* plants that overexpressed AtNHX1(Zhang et al., 2001) and transgenic tobacco plants that overexpressed BnNHX1 genes (Wang et al., 2004) were produced and they showed improved growth under 200mM NaCl as compared to the respective wild types. However, most of the attempts so far are on the level of downstream response, there are only very few examples addressing the problem at the signaling level. Thus, in this dissertation, to understand, how oxidative stress is sensed and compensated in root cells, we used a cellular model wild type (WT) tobacco plant [*Nicotiana tabacum* L. cv Bright Yellow-2 (BY-2)]. We tried to impart salt tolerance to wild type tobacco BY-2 suspension cultured cells using genetic engineering (by overexpressing OPR7 gene from rice) and chemical engineering (by treating the WT BY-2 cells with a trojan peptoid called plant PeptoQ prior to the onset of salt stress). Both the OsOPR7-GFP gene [that we used to generate the OsOPR7 overexpressor (OE) BY-2 cells] and the peptoid which is a semiquinone mimetic of coenzyme Q10 called plant PeptoQ (that we used to engineer redox balance in the mitochondria) are discussed in detail below.

1.8. Attempts to confer salt tolerance to wild-type (WT) tobacco BY-2 cells

In this study, it has been attempted to impart salt tolerance to tobacco BY-2 cells in two ways: First, a cell penetrating peptoid called plant PeptoQ (with a mitochondria-targeting motif and a semiquinone mimetic of coenzyme Q10) was used to target mitochondria and confer improved resilience to salt stress. Second, the OsOPR7 gene that encodes for the OPR7 enzyme which converts OPDA to JA was overexpressed in wild type tobacco BY-2 cells, and consequently, the overexpressor became resistant to the detrimental effects of salt stress. Therefore, the peptoid, plant PeptoQ pretreatment and OsOPR7 overexpression in WT BY-2 cells are the two important tools used to confer salt tolerance to BY-2 cells and also, they dictate the whole story of this dissertation. The detailed background information in relation to these two tools has been explained below.

1.8.1. Mitochondrial targeting

When fairly general small molecules such as ROS can evoke quite different cellular responses depending on their subcellular localization (for instance, apoplast versus mitochondria), it might be this subcellular localization that confers specificity. To experimentally address the hypothesis that the information conveyed by a given molecule

depends on the spatial coordinates of this molecule would require that the accumulation of ROS can be controlled differentially depending on the respective intracellular region. Although, it is possible to modulate steady-state levels of ROS by scavenging enzymes such as superoxide dismutase (SOD) or catalase (CAT) as well as by non-enzymatic antioxidants such as ascorbate or tocopherols (Karuppanapandian et al., 2011), this modulation is global, acting on the entire cell in the first place. To scavenge ROS in specific sites of the cell (for instance, in the mitochondria), leaving their accumulation in other sites of the cell (for instance, in the apoplast) untouched, is a task that is more challenging. Genetic engineering, as such, is a scalar approach and cannot be used in a straightforward manner to address spatial patterns of signals (although it would be possible, in principle, to achieve this goal by expression of scavenging enzymes under control of appropriate signal peptides). To modulate steady-state levels of ROS by targeting antioxidants to a specific target site within the cell, would be more straightforward. However, such a strategy based on chemical engineering would require molecular vehicles that can pass membrane barriers and carry their functional cargo to the site of interest.

To this effect, there are cell penetrating peptides (CPPs) or protein transduction domains (PTDs) that can carry functional cargoes and pass across the plasma membrane (Rolland, 2006; Wagstaff and Jans, 2006). In mammalian system, proteins, plasmids, peptides, nucleic acids, siRNA, liposomes and nanoparticles have been effectively delivered (Jarver and Langel, 2006; Torchilin, 2007). In plants, even though, reports on their application are quite sporadic (Chugh et al., 2009), their uptake by protoplasts derived from tobacco suspension cell and triticale mesophyll protoplasts has been achieved (Mäe et al., 2005; Chugh and Eudes, 2008). Organelle-specific delivery systems, particularly, mitochondria-specific delivery of bioactive cargos have got due attention in recent years (Cerrato et al.,2016). As a result, peptides that target mitochondria, Szeto-Schiler (SS) with strong antioxidant capacity (in reducing intracellular ROS) and impeding cell death (at low concentration) have been introduced (Zhao et al., 2003, 2004; Szeto, 2006). More recently, mitochondrial cell-penetrating peptides (mtCPPs) with much more improved antioxidant properties and greater cellular entry without any sort of toxicity (even at higher concentration) and in the absence of mitochondrial membrane potential ($\Delta\psi m$) and ATP generation perturbances have been synthesized (Cerrato et al., 2015). Although these cationic CPPs are effective in vitro, their bioavailability is limited in vivo due to hydrolysis by proteases (Nam et al., 2018). Thus, peptidomimetics such as peptoids could serve as excellent alternative due to their high stability in vivo (Eggenberger et al., 2009). Unlike CPPs, the side chain in peptoids (oligo-N-alkylglycines) is linked to the amide nitrogen instead of α carbon (Simon et al., 1992; Olivos et al., 2002). Consequently, they are suitable in delivering cargoes of interest into animal (Nam et al., 2018) and plant (Eggenberger et al., 2009) cells. Mitochondrial targeting peptoids with extremely rapid and efficient mitochondrial localization with minimal negative effects have come into play recently (Nam et al., 2018). Generally, despite the fact that cell penetrating peptoids (CPPos) have been successfully synthesized and applied as effective, water soluble and nontoxic molecular vehicles (Simon et al., 1992), there are no scientific reports vis-à-vis the consequence of their interaction with the host cell.

1.8.1.1. Cell-Penetrating peptides (CPPs)

Cell penetrating peptides (CPPs) or protein transduction domains (PTDs) are short peptide sequences that often contain at most 30 amino acids (Singh et al., 2018). The idea of CPPs came into play 30 years ago, following the discovery of the transcription trans-activating (TAT) from HIV-1 (Frankel and Pabo, 1988; Green and Loewenstein, 1988), homeodomain of the protein antennapedia from fruit fly (*Drosophila melanogaster*) (Joliot et al., 1991) and VP22, an herpes virus protein (Elliot and O´Hare, 1997) which were able to enter cells, and even to the cell nucleus passing through the cell membrane. Since then the number of different varieties of CPPs being identified increased sharply and the field of CPPs developed accordingly (Cerrato et al., 2016). The CPPs are well known for their ability of penetrating the cell membrane and delivering a bioactive cargo which has much greater molecular weight as compared to theirs (Lindgren et al., 2000). Even if, there are a great variety of CPPs with respect to amino acid composition and degrees of polarity (Kauffmann et al., 2015), generally, CPPs are categorized into three main classes; namely, cationic, amphipathic and hydrophobic CPPs based on their physicochemical properties (Milletti, 2012). How and by what mechanism(s), the CPPs enter cells by passing though the cell membrane is still a point of controversy (Rothbard et al., 2005). It is underscored that the main membrane binding emanates from the electrostatic interactions between the negatively charged membrane constituents and the positively charged peptides, specifically in the case of cationic CPPs (Ziegler, 2008). Reported studies depicted that CPPs and CPP-cargo conjugates, enter the cell via direct penetration (Rydström et al., 2011), clathrin-mediated endocytosis, caveolae/lipid raft-mediated endocytosis (Arukuusk et al., 2013), clathrin/caveolae-independent endocytosis (Koren and Torchilin, 2012) and macropinocytosis (Wadia et al., 2004). The cell type, the physicochemical properties of the cargo molecule and also properties of the CPP such as length, charge distribution and so on, affect the cellular uptake mechanisms of a particular CPP and CPP-cargo conjugate (Mueller et al., 2008). Even if, CPPs are efficient in delivering bioactive cargo into cells, their in vivo application is quite limited due to the fact that they are prone to degradation by proteolytic enzymes (Nam et al., 2018).

1.8.1.2. What are cell penetrating peptoids (CPPos)?

Peptoids (N-substituted oligo-glycines) are nonnatural oligomers which were invented and came into existence in the early 1990s (Simon et al., 1992; Zuckermann et al., 1992; Udugamasooriya, 2013). They are diverse and promising class of peptidomimetic compounds (Simon et al., 1992) that are produced based on achiral peptide-based backbone by repositioning the side chain (´R´ group) from the α-carbon to the amide nitrogen (Wu et al., 2001; Webster and Cobb, 2018). The repositioning of the side chain creates two important phenomena. First, it produced a peptoid backbone with repeating tertiary amides which makes peptoids immune from any proteolytic degradation. Secondly, the location of the side chain on the amide backbone leads to the absence of stereogenic center and any hydrogen bonding. Thus, this forced peptoids to be more flexible (high degree of conformational flexibility) than their peptide counterparts (Zuckermann et al., 1992; Fowler and Blackwell, 2009; Webster and Cobb, 2018). On the other hand, unlike peptides (where only 20 side chains are possible),

peptoids can append any organic ´R´ group into their achiral backbone; consequently, they have significantly higher target bio-molecular recognition capacity compared with native peptides (Kwon and Kodadek, 2007; Astle et al., 2008). In general, the above two important parameters, equipped peptoids with unique characteristics that provide advantages over peptides. These include, protease resistance (Miller et a., 1995; Nam et al., 2018), simple, straightforward, quick and inexpensive synthesis (Horn et al., 2004; Udugamasooriya et al., 2008; Fowler and Blackwell, 2009; Simpson et al., 2009), increased cell permeability (Miller et al., 1994; Yu et al., 2005) and temperature change as well as solvent resistance (Miller et al., 1994). However, still peptoids retain basic peptides properties and do share some characteristics with peptides such as biocompatibility, high level of chemical diversity (Webster and Cobb, 2018), density of functionality and backbone polarity (Kwon and Kodadek, 2007; Astle et al., 2008).

1.8.1.2.1. Cellular uptake and subcellular localization of CPPos

Peptoids are more cell permeable than peptides. This is mainly due to their reduced hydrogen-bond donating potential (hydrogen-bonding capacity), lower lipophilicity, minimal topological polar surface area (TPSA) and a wide range of side chain composition (Tan et al., 2008). In general, the uptake efficiency and the specific cellular uptake mechanisms have not been clearly identified yet and always are under intense debate (Schröder et al., 2007). However, for effective and efficient application of peptoids as transporters and to have optimized delivery, there is an immediate need to uncover the exact mechanism(s) of cellular uptake (Rudat et al., 2010). So far, there are only limited efforts made and a few articles being published in this respect. In mammalian cells, peptoids were uptaken through endocytosis-like mechanism (Schröder et al., 2007), micropinocytosis (amino-peptoids) and direct membrane penetration (guanidinium-peptoids) (Schröder et al., 2008). On the other hand, in plant cells (tobacco BY-2 cells) peptoids were internalized by a mechanism independent of endocytosis where it involves actin filaments and microtubules (Eggenberger et al., 2009).

Studies in animal cell show that one of the major obstacles in the delivery of bioactive molecules such as peptoids is the organelle-specific or subcellular targeting (Weissig, 2005; Boddapati et al., 2008; D´Souza et al.,2008). In mammalian cells, the association of peptoids with plasma membrane, accumulation in vesicular structures and perinuclear region localization (Schröder et al., 2007) has been reported. Similarly, in the same cell types, peptoids were localized in different cellular structure based on their chemical structure, specifically the attached side chain. Thus amino-peptoids were found to be localized in the cytosol, guanidinium-peptoids were preferentially accumulated in the nucleus and nucleolus (Schröder et al., 2008, Kölmel et al., 2012) and amphipathic peptoids were characterized by mitochondrial localization (Nam et al., 2018). Nevertheless, reports on the subcellular localization of peptoids in plant cells are almost not existing.

1.8.1.3. Co-enzyme Q (CoQ)

Co-enzyme Q is a ubiquitous naturally occurring compound. Owing to its ubiquitous existence, it is also called ubiquinone (Bhagavan and Chopra, 2006). It is the product of conjugation between a hydrophobic isoprenoid

chain and a benzoquinone ring. The conjugating isoprenoid chain would have variable length based on the species in question unlike the common benzoquinone ring (Prakash et al., 2010; Varela-Lopez et al., 2015). CoQ occurs in all biological membranes at a remarkable level; however, its main location is in the inner mitochondrial membrane specifically in the hydrophobic domain of the phospholipid bilayer (Fato et al., 1985; Lopez-Lluch et al., 2010). Each animal and plant cell do possess CoQ (Trunen et al., 2004; Prakash et al., 2010). Its stability within the hydrophobic lipid bilayer is maintained by the range of variable polyisoprenyl chain length (Varela-Làpez et al., 2016). One of the conjugation partners, benzoquinone ring of CoQ manifests itself in three alternate redox states such as ubiquinol or $CoQH_2$ (the fully reduced form), ubiquinone or CoQ (the fully oxidized form) and ubisemiquinone or CoQH (the partially reduced form) (Genova and Lenaz, 2011). Moreover, the natural CoQ could occur as micellar aggregates, bound to proteins or dissolved in lipid bilayers. This ability to express itself in three physical states emanated from its high-level hydrophobicity (Varela-Làpez et al., 2016). CoQ has two main important functions, namely, mitochondrial energy coupling and acting as antioxidant (primary scavenger of free radicals). Moreover, it has less pronounced functions such as induction of gene expression, membrane stabilization, control of membrane channels and lipid solubility (Crane, 2001; Varela-López et al., 2015).

Coenzyme Q10 (CoQ10) is a CoQ with a side chain that contains 10 isoprene units. It has a chemical nomenclature of 2,3-dimethoxy-5-methyl-6-decaprenyl-1, 4-benzoquinone. CoQ10 plays a pivotal role in ATP generation through its role as a cofactor in the mitochondrial electron transport chain (ETC) (Ernster and Daller, 1995; Bhagavan and Chopra, 2006). Its hydroquinone (ubiquinol) form is capable of regenerating and recycling antioxidants such as ascorbate and tocopherols along with its strong role as a lipophilic antioxidant. Moreover, it participates also in gene expression induction and cell signaling (Crane et al., 2001; Bhagavan and Chopra, 2006). CoQ10 is present in higher plants such as tobacco and mammalian cells like humans (Suzuki et al., 1997; Takahashi et al., 2006).

1.8.1.4. Plant PeptoQ

Plant PeptoQ is a semiquinone mimetic of coenzyme Q10 (Fig. 7), which was designed as ubi-semiquinones (CoQH), representing an intermediate from reduction of ubiquinone (CoQ) into ubiquinol ($CoQH_2$). Similar to its isoprenoid-conjugated template Q10 (Ernster and Dallner, 1995), this mimetic is expected to interact with the electron transport chain at the inner mitochondrial membrane.

1.8.2. OsOPR7 overexpression

In general, 12-oxo-phytodienoic acid reductase (OPR) gene, encodes for the OPR enzyme that converts 12-OPDA to JA. Based on their substrate preference, the OPRs are categorized into two subgroups: subgroup I type (OPRIs) and subgroup II type (OPRIIs) (Schaller and Weiler, 1997; Schaller et al., 1998, 2000; Strassner et al., 1999; Tani et al., 2008). OPRIs (e.g. AtOPR1, AtOPR2, OsOPR1 and SlOPR1) preferentially reduce (-)-cis-OPDA (Strassner et al., 1999; Schaller et al., 2000; Tani et al., 2008). Nevertheless, their, in vivo substrate(s) is unknown and whether

they involve in JA biosynthesis and signaling is far from clear and an open question (Dong et al., 2013). On the other hand, OPRIIs (e.g. AtOPR3, OsOPR7 and SlOPR3) can reduce all the four OPDA isomers [(cis-(+), cis-(-), trans-(+) and trans-(-)]; however, in planta, they preferentially and largely involved in the reduction of cis-(+)-OPDA to OPC 8:0 and are thought to be involved in the biosynthesis of JA (Schaller et al., 1998). Rice OPR7 (OsOPR7) gene is involved in the biosynthesis of JA by encoding the enzyme that reduces (+)-cis-OPDA to (+)-cis-OPC-8:0. This has been further confirmed by the peroxisomal localization of OsOPR7 where the downstream reduction of OPDA in JA biosynthesis occurs (Tani et al., 2008). Therefore, the OsOPR7 gene was overexpressed in non-transformed wild-type (WT) tobacco BY-2 cells using agrobacterium mediated genetic transformation.

1.9. Scope of the study

Soil salinity is the most drastic and brutal environmental factor that threatens the global agricultural food production for human population that increases at an alarming rate. Since about 99% of crop plants are salt sensitive (glycophytes), it is mandatory to generate salt tolerant crop varieties and cultivars using the germplasm of their wild relatives and the halophytes (salt tolerant plants). Even if, much has been achieved in the investigation of the salt tolerance mechanisms of plants which is the prerequisite for generating salt tolerant varieties/cultivars, a lot has to be done yet. This is because of the fact that plant salt tolerance mechanism is multigenic and highly complex. Thus, prior to producing salt tolerant crop plants, accumulating knowledge on the salt tolerance mechanisms of plants is the must. Hence this PhD project attempts just to drip a drop onto the very giant oceanic effort of unraveling the sophisticated salt tolerance mechanisms of plants. The project consists of two sub projects where sub project I deals with the uncovering of the salt tolerance mechanisms of the wild type (WT) model plant tobacco [*Nicotiana tabacum* L. cv Bright Yellow-2 (BY-2)] by coupling it with a semiquinone mimetic of coenzyme Q10 called plant PeptoQ where it modulates and regulates intracellular ROS level in mitochondria whereas sub project II investigated the role of jasmonic acid (JA) and its derivatives, jasmonates (JAs) in the salt tolerance of crop plants by overexpressing OPR7 gene from rice (OsOPR7) in non-transformed WT tobacco BY-2 cell line.

In subproject I, the time-course and dose- response of the plant PeptoQ, its subcellular localization, cellular uptake mechanism(s) and potential cytotoxicity were investigated. Moreover, the role of plant PeptoQ in mitigating salt stress in WT BY-2 cells with respect to numerous aspects including cell proliferation, expansion and viability, ionic balance, redox homeostasis, and gene expression was investigated in detail. In subproject II, the rice (*Oryza sativa)* 12-oxo-phytodienoic acid reductase 7 (OsOPR7) gene that encodes for the enzyme OPR7 which reduces the JA intermediate precursor *cis* (+)12-OXO-PHYTODIENOIC ACID (OPDA) to JA has been overexpressed in WT tobacco BY-2 cells using agrobacterium-mediated genetic transformation, and then all the above cell growth parameters were diagnosed profoundly.

2. Materials and Methods

2.1. Cell lines and cell cultivation

Suspension cultured cells of WT tobacco (*Nicotiana tabacum* L. cv Bright Yellow-2, Nagata et al. 1992) were grown in liquid medium containing 4.3 g/L Murashige and Skoog (MS) salts (Duchefa Biochemie, The Netherlands), 30 g.L^{-1} sucrose, 200 mg.L^{-1} KH_2PO_4, 100 mg.L^{-1} (myo)-inositol, 1 mg·L^{-1} thiamine, and 0.2 mg.L^{-1} 2,4-D, pH 5.8 (Table 3). At weekly intervals, 1.5 mL of stationary cells were inoculated into a 30 mL Erlenmeyer flask with fresh medium and shaken in the dark at 26°C on a KS260 basic orbital shaker (IKA Labortechnik, Germany) at 150 rpm. Stock BY-2 calli were maintained on media solidified with agar [0.8% (w/v)] and subcultured monthly. In addition to the non-transformed WT, transgenic cell lines were used in this study and were supplemented with the respective selective agent: To visualize actin filaments, the marker cell line GF11 (Sano et al., 2005) expressing the actin-binding domain of plant fimbrin was used and cultivated in presence of hygromycin (30 mg.L^{-1}) (Table 3). To observe microtubules, the transgenic line TuB6, expressing the β-tubulin AtTUB6 from *Arabidopsis thaliana* fused to GFP driven by the Cauliflower mosaic virus (CaMV) 35S promoter (Hohenberger et al., 2011) was employed and supplemented with kanamycin (50 mg. L^{-1}) (Table 3). In order to follow the behaviour of auxin-influx carriers to suppression of endocytosis, a cell line expressing the auxin influx carrier AUX1 in fusion with YFP from *Arabidopsis thaliana* under control of an estradiol-inducible promoter (Laňková et al. 2010) was cultivated in presence of hygromycin (40 mg. L^{-1}) and induced by β-estradiol (1 µM) for 24 h at day 2 after subcultivation (Table 3). On the other hand, to investigate the role of jasmonic acid (JA) in salt tolerance of plants, the BY-2 transgenic line, expressing the 12-oxo-phytodienoic acid reductase 7 (OsOPR7) from rice (*Oryza sativa*) fused to GFP driven by the Cauliflower mosaic virus (CaMV) 35S promoter was used and cultivated in the presence of hygromycin (60 mg. L^{-1}) (Table 3). If not stated otherwise, the experiments were performed at 3 d after subcultivation.

2.2. Chemicals and fluorescent dyes

Unless specified otherwise, all the chemicals used in this study were purchased from Sigma Aldrich, Taufkirchen, Germany. Wortmannin (Wm) inhibitor of endocytosis and Ikarugamycin (IKA) inhibitor of clathrin mediated endocytosis (CME) were suspended in dimethylsulfoxide (DMSO) to get 10 and 2 mM stock solutions respectively. The actin filaments inhibitor, Latrunculin B (Lat B), the nuclear envelope/endoplasmic reticulum (ER) staining fluorescent dye, 3,3´-dihexyloxa carbocyanine iodide, $DiOC_6$ and the microtubules inhibitor, oryzalin were dissolved in DMSO to have stock solution of 10, 8.73 and 10 mM respectively. Similarly, β-estradiol which induces the expression of YFP fused auxin influx carrier, AUX1, 3-chloro-4-hydroxyphenylacetic acid (CHPAA), an auxin influx carrier AUX1 inhibitor, MitoTracker Green FM (Molecular probes), a mitochondrial staining fluorescent dye and dihydrorhodamine 123 (DHR 123) which is used in intracellular reactive oxygen species (ROS) detection were dissolved in DMSO to give stock solutions of 5, 20, 10, 1 and 10 mM respectively. Evans blue, a non-plasma membrane permeating dye 2.5% (w/v) and the SynaptoRed C2, equivalent to FM4-64

(Biotium, Germany), marker of endocytosis and vesicle trafficking (stock solution of 2 mM) were dissolved in sterilized distilled water. Furthermore, sodium chloride (NaCl) salt, which is used to induce salt stress, was dissolved in sterile distilled water in order to give moderate (75 mM NaCl) and high (150 mM NaCl) salt concentrations. The semiquinone mimetic of coenzyme Q10, plant PeptoQ [Institute of Functional Interfaces (IFG), Karlsruhe Institute of Technology (KIT), Karlsruhe, Germany] which is used to mitigate salt stress and might be used as functional molecular cargo to manipulate the oxidative balance in mitochondria to impart salt tolerance to plants was dissolved in 50 % ethanol. All treatments were accompanied by solvent controls, where the maximal concentration of solvent used in the test samples was administered and not exceeded 0.1 %.

2.3. Plant PeptoQ synthesis schemes

2.3.1. Synthesis and labelling of the plant PeptoQ 3. The plant PeptoQ 3, is the alias for a rhodamine B labeled cell penetrating peptoid, covalently connected to the ubiquinone analogue 6-(10-azidoalkyl)-benzoquinone (Fig. 7). containing an omega azidodecyl residue at position 6 instead of an isoprenyl moiety of CoQ10 1. As seen, the Quinone within the peptoid is identical as the "native" CoQ10 with exception of the isoprenoid side chain. Given that the redox properties of this type of benzoquinones are determined by the ketone groups at position 1 and 4, where the side chain has no impact on this property (Ksenzhek et al., 1982). Thus, we are convinced that plant PeptoQ endowed with the same benzoquinone head as CoQ10, is a redox active molecule and has redox properties which are comparable with those of Coenzyme Q10. Moreover, since the hydroxyl derivatives of CoQ10 owns very strong antioxidative potential (Bogeski et al., 2011; Gulaboski et al., 2013, 2016), plant PeptoQ has also remarkable antioxidative and superoxide scavenging potential.

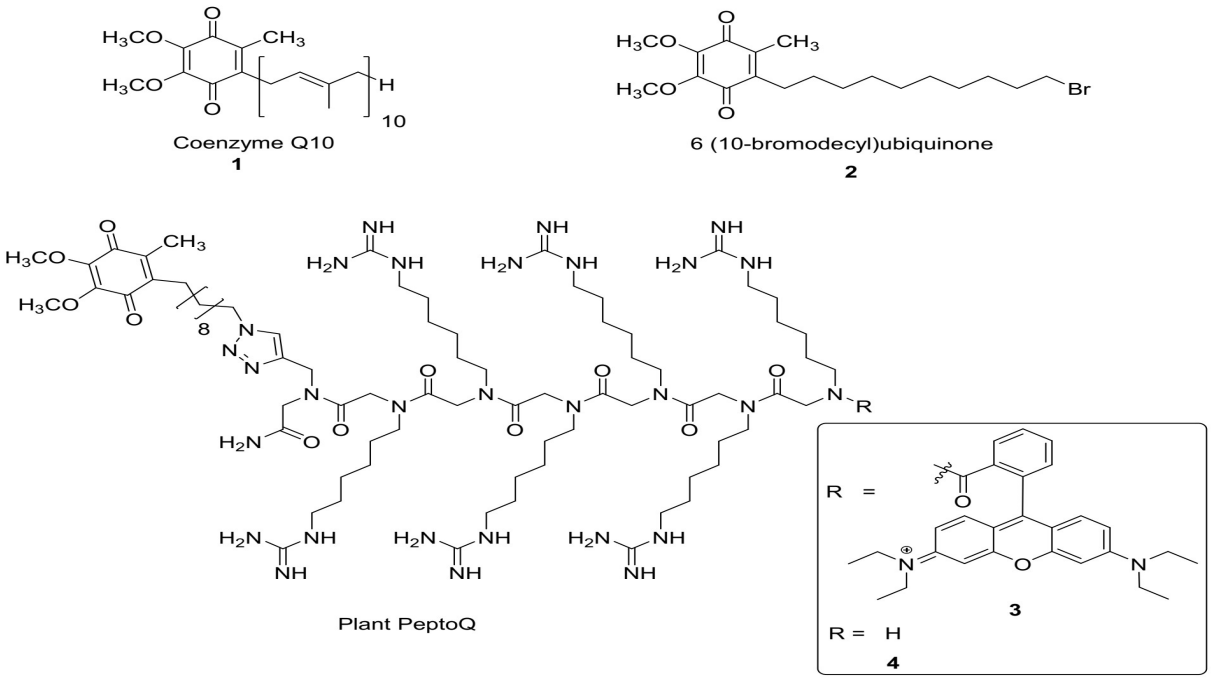

Figure 7: The chemical structures of CoQ10 **1,** the CoQ10 analogue 6-(10-bromodecyl) ubiquinone **2** and the rhodamine-labelled and unlabelled plant PeptoQ **3** and **4.** Adapted from Asfaw et al., 2019.

2.3.2. Synthesis of 2,3-dimethoxy-5-methyl-(6-(10-bromodecyl)-1,4-benzoquinone (2): 6-(10-bromodecyl) ubiquinone was synthesized according to previous reports by (Kelso et al., 2000; Yu et al., 1985). In a first step, 11-bromoundecanoic peroxide was synthesized by heating 11-bromoundecanoic acid (4.00 g, 15.1 mmol) and $SOCl_2$ (1.60 ml, 21.5 mmol) at 90°C for 15 min. Excess of $SOCl_2$ was removed by distillation under reduced pressure (15 mm Hg, 90°C) and the residue (IR,1 1799 cm^{-1}) was dissolved in diethyl ether (20 ml) and subsequently cooled to 0°C on ice. Hydrogen peroxide (30%, 1.80 ml) was added followed by dropwise addition of pyridine (1.40 ml) over 45 min. Eventually, diethyl ether (10 ml) was added and stirred for 1 h at room temperature. The product was diluted with diethyl ether (150 ml), washed with H_2O (2 × 70 ml), 1.20 M HCl (2 × 70 ml), H_2O (70 ml), 0.50 M $NaHCO_3$ (2 × 70 ml), and H_2O (70 ml). After drying over $MgSO_4$, the solvent was removed at room temperature under reduced pressure, giving crude product as a white solid (2.89 g), and processed immediately. 6-(10-Bromodecyl)-ubiquinone (**2**) was synthesized by stirring the crude product (2.89 g, 10.3 mmol), 2,3-dimethoxy-5-methyl-1,4-benzoquinone (1.01 g, 6.00 mmol), and acetic acid (60 ml) for 20 h at 100°C. After cooling to room temperature, the reaction was diluted with diethylether (600 ml), washed with H_2O (2 × 400 ml). Evaporation of the solvent under reduced pressure yielded in a reddish solid (4.31 g). Column chromatography on silica gel, eluting with CH_2Cl_2, yielded in a red oil (682 mg, 1,70 mmol, 28.32%), which was not further purified. NMR (299.9 MHz) 3.99 (s, 6H, 2x -OC**H**$_3$), 3.41 (t, *J* 5 6.8 Hz, 2H, -C**H**$_2$-Br), 2.45 (t, *J* 5 7.7 Hz, 2H, ubquinone-C**H**$_2$-), 2.02, (s, 3H, -C**H**$_3$). 1.89 (quin, *J* 5 7.4 Hz, 2H, -C**H**$_2$-CH_2-Br), 1.42–1.28 (m, 14H, -(C**H**$_2$)$_7$-) ppm; ^{13}C NMR (125.7 MHz)184.7 (**C**=O), 184.2 (**C**=O), 144.3 (2**C**, ring), 143.1 (ring), 138.7 (ring),61.2 (2x -O**C**H_3), 34.0 (-**C**H_2-), 32.8 (-**C**H_2-), 29.8 (-**C**H_2-), 29.4 (2x-**C**H_2-), 29.3 (-**C**H_2-), 28.7 (23 -**C**H_2-), 28.2 (-**C**H_2-), 26.4 (-**C**H_2-), 11.9(-**C**H_3) ppm. MALDI-TOF, matrix: DHB, m/z (%): 401 $[M]^+$

2.3.3. Solid-phase synthesis: Peptoid syntheses were performed on solid-phase following the fluorenylmethyloxycarbonyl (Fmoc)-strategy by using Boc-protecting groups for the side chains to facilitate the synthesis of the growing oligomer (Kölmel et al., 2012; Birtalan et al., 2011). Rink-amide-resin was chosen as a solid support due to its stability at ambient conditions, the ease of the first coupling step, and good cleavage conditions. Furthermore, the reaction conditions were the same for attaching the first building block to the resin and the following coupling cycles. After removal of the Fmoc group, which protected the amino-functionalized resin (with 20% piperidine in dimethylformamide (DMF)), an activated Fmoc-protected monomer was coupled to the solid phase via a peptide bond. For the microwave-assisted reactions HOBt and DIC were used as coupling reagents. The Fmoc group was removed with piperidine-solution yielding the coupled monomer for the attachment of the next building block. All reaction procedures were succeeded by repetitive washing, ending with a solvent, in which the resin was swelled to expose its reactive sites to the next reagents. The cycles of coupling and deprotection were repeated until a peptoid of the desired length was obtained.

2.3.4. Microwave-assisted synthesis of Boc-protected hexamer on a Rink amide linker (Procedure 1): The resin (AM resin LL 100-200 mesh, 0.61 mmol/g, 218 µmol, 1.00 equiv) was covered with five times of its volume of dried DMF and swelled for 30 min. After deprotection of Fmoc (3 × 5 min with 3 mL

of 20% piperidine in DMF) and thoroughly washing with DMF the acylation of the resin was done with 0.6 g bromoacetic acid (4.36 mmol, 20 equiv) and diisopropylcarbodiimide (DIC) (0.55 g, 4.36 mmol, 20 equiv) in DMF for 2 h (Fig. 8). After the reaction the resin was washed 3 × 20 min with DMF. For the coupling with propargylamine the resin was incubated with a 1 M of propargylamine in DMF overnight. Eventually the resin was washed three times with DMF and the building block *N*-(6-*tert*-butoxycarbonylamino-hexyl)-*N*-(9*H*-fluoren-9-ylmethoxycarbonyl) acetic acid (653 µmol, 3.00 equiv), HOBt (653 µmol, 3.00 equiv) and DIC (653 µmol, 3.00 equiv) were dissolved in DMF biotech grade (6.50 mL) to obtain a 0.1 M solution related to the building block. The reaction solution was added to the resin and stirred for 30 min at 60°C in a CEM microwave oven. The reaction solution was filtered, and the resin was treated a second time with freshly prepared reaction solution for 30 min at 60°C in the microwave oven (double coupling) and subsequently incubated with 3 mL of 20% piperidine in DMF (3 × 5 min) to cleave the Fmoc group. The resin was not dried after the reactions. This reaction was repeated six times to obtain the resin bound hexamer as yellowish solid.

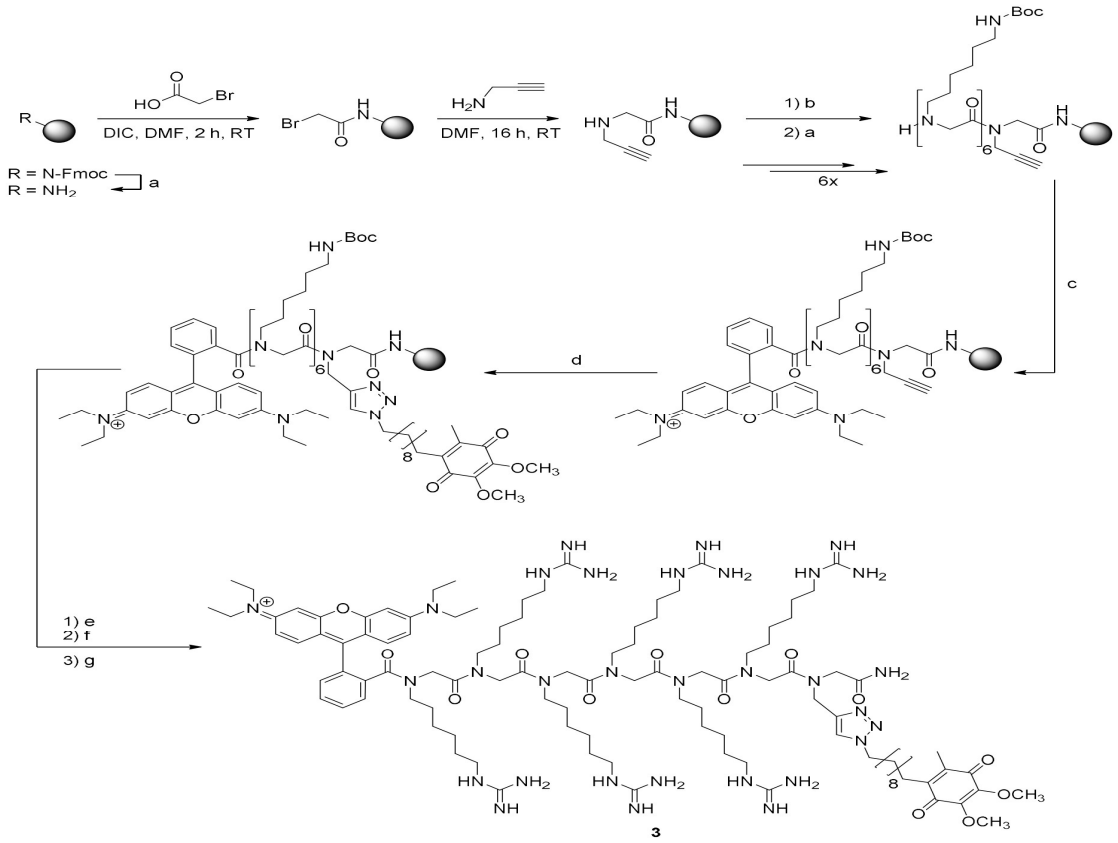

Figure 8: Synthesis scheme of the plant PeptoQ **3**. Reaction conditions: a) 20% piperidine in DMF, 3 × 5 min, RT; b) *N*-(6-*tert*-butoxycarbonylamino-hexyl)-*N*-(9*H*-fluoren-9-ylmethoxycarbonyl)acetic acid, DIC, HOBt, DMF, 30 min, 60°C microwave; c) Rhodamine B, DIC, HOBt, DMF, 30 min, 60 °C microwave; d) 6-(10-bromodecyl)-2,3-dimethoxy-5-methylcyclohexa-2,5-diene-1,4-dione, NaN_3, $CuSO_4$, sodium ascorbate, DMF, water, 2 d, RT; e) 3 M HCl in DMF, 100 min, 120 °C microwave; f) 1*H*-pyrazol-1-carboxamidine, DIPEA, DMF, 120 min, 60 °C microwave; g) TFA/dichloromethane (95:5 (v/v)), 2 h, RT. Adapted from Asfaw et al., 2019.

2.3.5. Microwave-assisted rhodamine B-labeling of the peptoid (Procedure 2): After the deprotection of Fmoc (3 × 5 min with 3 mL of 20% piperidine in DMF) and accurate washing with DMF. Rhodamine B (653 µmol, 3.00 equiv), HOBt•H_2O (653 µmol, 3.00 equiv) and DIC (653 µmol, 3.00 equiv) were dissolved in DMF biotech grade (6.50 mL) to obtain a 0.1 M solution related to the dye. The reaction solution was added to the resin of procedure 1 and stirred for 30 min at 60°C in a CEM microwave oven. The reaction solution was filtered, and the resin was treated a second time with freshly prepared reaction solution for 30 min at 60°C in the microwave oven (double coupling). The resin was not dried after the reactions.

2.3.6. 2,3-Dimethoxy-5-methyl-(6-(10-bromodecyl)-1,4-benzoquinone coupling (Procedure 3): To couple the 2,3-dimethoxy-5-methyl-(6-(10-bromodecyl)-1,4-benzoquinone via a 1,3-dipolar cycloaddion (click reaction), the resin from procedure 2 was reacted according to (Fürniss et al., 2013; Movahedi et al., 2014). In a one pot reaction with 2,3-dimethoxy-5-methyl-(6-(10-bromodecyl)-1,4-benzoquinone (131 mg, 327 µmol, 1.50 equiv) and sodium azide (327 µmol, 1.50 equiv) in DMF at room temperature. To this solution, a $CuSO_4$ solution (10 mol%) was added. Eventually, sodium ascorbate (30 mol%) and deionized water (5 vol%) was added. The temperature was then increased to 50°C and the resin was agitated for 2 d. After agitating for 2 d the reaction mixture was removed and the resin was washed thoroughly with DMF.

2.3.7. Microwave-assisted Boc-deprotection on solid phase (Procedure 4): For the deprotection of the Boc-functionalized amino groups, the resin of procedure 3 (218 µmol, 1.00 equiv) was covered with 3 mL of a 3 M hydrochloric acid in DMF solution and stirred for 100 min at 120°C in a CEM microwave oven. The resin was washed with DMF.

2.3.8. Microwave-assisted guanidinylation on solid phase (Procedure 5): After the Boc deprotection of the side-chain amines the resin from procedure 4 (218 µmol, 1.00 equiv) was covered with a solution of 1*H*-pyrazol-1-carboxamidine (1.09 mmol, 20.0 equiv), DIPEA (2.18 mmol, 40.0 equiv) and 3.20 mL of DMF. The reaction was performed in a CEM-microwave (120 min reaction time, 60°C). The resin was washed with DMF.

2.3.9. Cleavage and isolation (Procedure 6): To cleave the peptoid from solid support, a solution of 2.00 mL TFA in dichloromethane (95:5 (v/v) was added to the resin of procedure 5 and shaken for 2 h. The resin was rinsed two times with 0.5 mL methanol. Water was added to the solution and the sample was frozen and lyophilized and purified by HPLC.

2.3.10. Plant PeptoQs

Using general procedures 1, (2), 3 - 6 the product was obtained as a red solid. HPLC purification and lyophilisation yielded 15.39 mg (7.36 µmol, 3.38% over 20 steps) of Rhodamine-labeled **plant PeptoQ 3.** with a purity of >98%. MS (MALDI-TOF, matrix: DHB, m/z (%): 1993 $[M]^+$ and 18.74 mg (11.3 µmol, 5.16% over 19 steps) of non-labeled **plant PeptoQ 4** with a purity of 93 %. MS (MALDI-TOF, matrix: DHB, m/z (%): 1567 $[M]^+$.

2.3.11. HPLC purification: Preparative high performance liquid chromatography (HPLC) was performed on an *Äkta* Purifier 100 UPC equipped with a pump P-900, monitor UV-900 and UPC-900, Valve INV-907, Mixer M-925 and Valve PV-908 employing a reverse phase C18 semi-preparative column (*Macherey Nagel* VP 250/10 Nucleodur 100-5 C18ec), flow rate 1.5 mL/min, solvent A: 0.1% trifluoroacetic acid (TFA) in water, B: methanol and *Agilent* 1200 Series equipped with a diode array detector employing a reverse phase C8 semi-preparative column (Zorbax 300SB-C8 (*Agilent*), 5 µm, 9.4 mm × 250 mm), flow rate 1 mL/min, A: 0.1% TFA in water, B: 0.1% TFA in acetonitrile for purification assessment. Analytical high-performance liquid chromatography (HPLC) was performed on an *Agilent* 1100 Series equipped with a diode array detector employing a reverse phase C18 analytical column (PerfectSil Target (*MZ-Analytik),* 5 µm, 4.0 mm × 250 mm), flow rate 1 mL/min, A: 0.1% TFA in water, B: 0.1% TFA in acetonitrile for purification assessment. Analytical and preparative high-performance liquid chromatography (HPLC) was performed on a chromatographic system from Jasco (Tokyo, Japan) equipped with diode-array detector. Reverse phase C18 analytical (4.6 x 250 mm, 5 µm) or semi-preparative (10 x 250 mm, 10 µm) columns from Grace (Grace, Deerfield, IL) were employed for purity assessment and purification respectively. For chromatographic separation of the peptoids, focused gradients were run from 48% to 56% at a constant temperature of 40°C. Solvent A: 0.1% trifluoroacetic acid (TFA); B: 90% acetonitrile in 0.1% TFA. The separation of the peptoids was monitored with UV-detection in the range of 200 - 650 nm and ultraviolet (UV) spectra along with matrix-assisted laser desorption/ionization-time of flight (MALDI-TOF)-mass spectrometry (MS) to identify the product peaks. Manually collected fractions of the semi-preparative runs were freeze-dried and immediately used in the biological assays. Prior to lyophilization, fraction aliquots were directly re-injected onto the analytical column to quantify purity, which was determined by integration of the respective single peak area from the chromatograms at 218 nm.

2.4. Agrobacterium mediated transformation of WT BY-2 cells

To overexpress the rice OPR7 (OsOPR7) gene in the WT BY-2 cells, agrobacterium mediated genetic transformation was used using *Agrobacterium tumefaciens* (strain LBA4404).

2.4.1. LR reaction and selection of efficient transformation (Plasmid construction)

An entry clone of rice OPR7 (OsOPR7) gene (explained in Tani et al., 2008) was kindly provided by Dr. Rohit Dhakarey and used to construct the OsOPR7-GFP binary vector using the Gateway® LR Clonase enzyme mix kit (Invitrogen). In brief, the LR reaction mixture contained: 1-5µl (100ng) of the entry clone plasmid DNA, 1µl (100ng) of destination vector, pH7WGF2,0 (GFP, Hyg) plasmid DNA, 2µl LR reaction buffer and 2µl of the LR clonase enzyme. The reaction mixture was vortexed and spun for a while and brought to a final volume of 10µl by adding TE buffer (pH 8.0) and incubated at 25°C on a PCR cycler overnight. The following day, 2µl of proteinase K solution was added and incubated for 10 min at 37°C. To check the efficiency of transformation, selection was carried out using *Eschercia coli* DH5α strain (Table 4). About 7µl of the LR reaction product and mCherry binary vector (PTS1-mCherry) plasmid DNA were transferred into 100µl DH5α competent cells (Table

4) and incubated on ice for 30 min. The cells were heat-shocked at 42°C for 45 seconds. Then 900µl LB was added under sterile condition, mixed well and incubated for 1 and half hour at 37°C. About 150µl from each reaction mixture was plated on appropriate LB plates containing 100mg/L spectinomycin (for OsOPR7) or 50µg/mL Kanamycin (for mCherry) and spread well using glass beads. After emptying the glass beads, plates were sealed with parafilm and incubated overnight at 37°C. In each case, just one bacterial colony was touched with a tip and ejected into a glass tube containing 5ml LB with 100mg/L spectinomycin and incubate at 37°C overnight at 180rpm continuous shaking. The OsOPR7-GFP and mCherry (PTS1-mCherry) binary vectors were extracted using Roti®-Prep Plasmid MINI (Carl Roth GmbH + Co. KG, Karlsruhe, Germany). In both cases, briefly 1-3ml bacterial cell culture was harvested by centrifuging at 8,000g for 2 min. The supernatant was discarded, and the pelleted bacterial cells were resuspended in 250µl. Resuspension Buffer which contains RNase A. Bacterial cells were lysed and neutralized by adding 250µl Lysis Buffer and 350µl Neutralization Buffer respectively, and centrifuged at 15,000g at room temperature for 10 min. The supernatant was applied into spin column and centrifuged at 10,000g for 30 seconds, and the flow-through was discarded. Column washing was done by adding 750µl Washing Buffer to the spin column, centrifuged at 10,000g for 2 min, and the flow-through was discarded. The residual ethanol was removed by centrifuging the empty column at 10,000g for 30 seconds. The spin column was placed into 1.5ml microtube, 30-50µl Elution Buffer was added and incubated for 1 min at room temperature. Finally, the OsOPR7-GFP and mCherry (PTS1-mCherry) binary vectors DNA were eluted by centrifuging at 10,000g for 1 min.

2.4.2. Agrobacterium transformation (Agroinfection)

The OsOPR7-GFP and mCherry (PTS1-mCherry) binary vectors plasmid DNAs were introduced into the *A. tumefaciens* (strain LBA4404; Invitrogen Corporation, Paisley, UK) (Table 4) using an improved freeze–thaw transformation protocol (Chen et al., 1994): after thawing cells at room temperature for 10 min, 500 ng of plasmid DNA were added to competent cells and mixed gently. After shock-freezing the cells in liquid nitrogen for 1 min, they were thawed for 5 min at 37°C in a water bath. Then 900 µl of LB medium (Bertani, 1951. Duchefa, Haarlem, The Netherlands) were added and incubated shaking at 28°C for 2 h. Subsequently, cells were spun down at 8000g for 2 min and about 800–900 µl of the supernatant was removed. The pellet in the remaining volume of 100-200 µl was then resuspended and plated on solid LB medium with 100 µg/mL Spectinomycin, 300 µg/mL Streptomycin, 50 µg/mL Kanamycin and 50 µg/mL Rifampicin. Petri dishes were incubated at 28°C and colonies appeared after 2-3 days (Guan et al., 2015). A single colony of *A. tumefaciens* strain LBA4404 was inoculated into 4mL of LB medium supplemented with the appropriate antibiotics. The bacterial cultures were incubated at 28°C at 200 rpm on an orbital shaker overnight.

2.4.3. Pre-culture and co-cultivation (Plant transformation)

The overnight incubated, OsOPR7-GFP binary vector containing bacterial culture was transferred into 50 ml falcon, and centrifuged at 8,000rpm for 7 min. The supernatant was discarded, and the pellet resuspended by

adding 180 µl Paul´s Medium. Then 5 days old WT BY-2 cell culture (Table 3) was filtered three times using a sterile cell filtration device (Nalgene or similar) which contains 20 µm mesh filter and cells were mechanically damaged by pipetting up and down 15 to 17 times. About 6.5 ml of the filtered BY-2 cells were transferred to each falcon containing the binary vector bearing bacteria, and the falcons were agitated for 5 min at 100rpm to mix the bacteria with the plant cells. Aliquots (1 ml from each) of this suspension were dropped on Paul agar plates (no antibiotics) that contains sterile filter paper, incubated at 22^{o}C in darkness for 4 days. After 4 days, a single colony was taken, resuspended using distilled water and the efficiency of transformation was checked by spinning disc microscopy.

2.4.4. Elimination of agrobacterium and generation of a suspension cell line

Following successful transformation (which is confirmed by the expression of GFP), the filter papers carrying the cells were transferred onto MS agar plate containing 300µg/ml cefotaxime and 60µg/ml hygromycin, sealed with parafilm, put into a box, covered with black polyethene sheet and incubated in the culture room, in darkness for 2-3 weeks. Two weeks later, 2-3 mm diameter piece of callus was cut with sterile razor blade, put into 100ml Erlenmeyer flask containing 30ml fresh MS medium and treated with filter-sterilized antibiotics (300µg/ml cefotaxime and 60µg/ml hygromycin), the callus was broken down by pipetting the culturing medium up and down, sealed with aluminum foil and shaken in the dark at 26°C on a KS260 basic orbital shaker (IKA Labortechnik, Germany) at 150 rpm. It was subcultured every 7 days and the cefotaxime concentration reduced by 50µg/mL each week and finally stopped. However, the 60µg/mL Hygromycin treatment continued.

For transient transformation of mCherry binary vector, the BY-2 suspension cells transformed with OsOPR7-GFP were co-transformed with agrobacterium containing PTS1-mCherry plasmid. Grown on solid Paul's medium for 3 days, and then examined microscopically (without proceeding to selection step) to check the localization of OPR7 protein.

2.5. Plant materials, bacterial strains and primers

2.5.1. Plant materials: Tobacco cell cultures

Table 3: Description of tobacco BY-2 cell cultures.

Name	Genotype	Application	Source
BY-2 WT	*Nicotiana tabacum* L. cv Bright Yellow 2 (BY-2), Wild Type	Phenotyping and molecular characterization	Nagata et al., 1992
BY-2 GF11	*Nicotiana tabacum* L. cv Bright Yellow 2 (BY-2), CaMV-35S (GF11 GFP) Hygromycin	Phenotyping	Sano et al., 2005
BY-2 TuB6	*Nicotiana tabacum* L. cv Bright Yellow 2 (BY-2), CaMV-35S (TUB6 GFP) Kanamycin	Phenotyping	Hohenberger et al., 2011
BY-2 AUX1	*Nicotiana tabacum* L. cv Bright Yellow 2 (BY-2), Estradiol-inducible (AUX1-YFP) Hygromycin	Phenotyping	Lankova et al., 2010
BY-2 OsOPR7	*Nicotiana tabacum* L. cv Bright Yellow 2 (BY-2), CaMV-35S (OsOPR7 GFP) Hygromycin	Phenotyping and molecular characterization	This work

2.5.2. Bacterial strains

Table 4: Description of bacterial strains.

Name	Genotype	Application	Source
A.tumefaciens LBA4404	pAL4404, pIG121	BY-2 transformation	Invitrogen, Karlsruhe, Germany
E. coli DH5α	F-, ϕ80dlacZΔM15, Δ (lacZYA-argF) U169, recA1, endA1, gyrA96, thi-1, hsdR17, supE44, relA1	Cloning	Invitrogen, Karlsruhe, Germany

2.5.3. Primers

All the primers used in this dissertation were ordered at Sigma-Aldrich (Steinheim, Germany).

Table 5: Overview of primers used both in semiquantitative PCR (SQ-PCR) and quantitative real-time PCR (qRT-PCR).

Gene name	GenBank accession No.	Forward (5´-3´ prime)	Reverse (5´-3´ prime)
NtEF-1α	D63396	**TGAGATGCACCACGAAGCTCTTC**	**GCTGAAGCACCCATTGCTGGG**
NtL25	L18908	**GTTGCCAAGGCTGTCAAGTCAGG**	**GCACTAATACGAGGGTACTTGGGG**
NtJAZ1	AB433896	**CCAATTGCGAGACGAAATTCACTTAC**	**CCAAGCCATGCCTTATTTTCCTCATTC**
NtJAZ2	AB433897	**GCAGCACCTGCTCAACTGACC**	**GCACCACATTAGGAGGAACGCAACC**
NtJAZ3	AB433898	**GGATTCCGGTCGATTCGCCG**	**CCAAGGCTGAGATCTCCAAAGGAAC**
NtSOS1	AY383599	**GCTCAACGTACACTTCACGG**	**CCTTGCAACTTCAGCACGAC**
NtSOS3	KM658158	**CAGAAGAGTGGAAGGAGTTTGC**	**CTTCAACCTCAGAGCTCATCAC**
NtNHX1-Like	XM_016587346	**AGGATGCTACTTTCTGCGCC**	**TGGTTCCTGTTCCGTTGGAG**
NtHKT1-Like	XR_001648440	**TTCCGATACCCTGAATGGGC**	**GAGCACTACCAAAACGGCTG**
NtSKOR-Like	NM_001326274	**TTTATCCCGATGACCGGTGG**	**AAAGCTTCCTGGGCAATCCC**
OsOPR7	XM_015795324	**CCAAACGGTGCTGCACCAATATCC**	**GGTATTTCCGATGCTGCCAGGC**
NtSLT1	AF213399	**CTTGAAGCGTCGTCCTCAGA**	**CACCGTTCCTGATCCATCGT**
NtHAK1	DQ841950	**TTGGACCCAAAGAGTACCGC**	**GTCCCTCTGAGCGGATGAAT**
NtNAC	HQ413134	**TTACGCTGGAAAAGCACCCA**	**ACCCAATCGTCAAGCCTCAA**
NtMnSOD	XP_016513256	**TCGACACTAACTTTGGCTCCC**	**GTGGTTTCAATCACCAGGCG**

2.6. Plant PeptoQ cellular uptake characterization

2.6.1. Dose-response and time-course assay

If not stated otherwise, all treatments were conducted with tobacco WT BY-2 cells collected at the peak of the proliferation phase (day 3 after subcultivation). To record the dose-response relation, non-transformed WT tobacco BY-2 cells were collected at the peak of proliferation (day 3 after subcultivation) and incubated with 0.5,1, 1.5, 2, 2.5, 3, 4, 5 and 6µM of plant PeptoQ for 2 h. To measure the time-course of uptake, the same age cells were treated with 2µM rhodamine labelled plant PeptoQ and incubated for 10, 30, 60, 90, 120, 180, 240, 300 and 360 min. The procedure was repeated three times with three independent experimental series.

2.6.2. Plant PeptoQ subcellular localization assay

To pinpoint the subcellular localization of plant PeptoQ, WT BY-2 cells were treated with 2µM rhodamine labelled plant PeptoQ at day 1 to day 7 and incubated for 2 h. Then cells were washed with distilled water using custom made filter chamber. On each day, the treated and washed cells were stained with MitoTracker Green FM mitochondrial dye and incubated for 5 minutes and visualized under spinning disc microscope immediately. The procedure was repeated three times with three independent experimental series.

2.6.3. Cellular uptake mechanisms of plant PeptoQ

To find out the possible cellular uptake mechanism(s) of plant PeptoQ, 3 days old WT BY-2 cells were treated with endocytotic inhibitor, 33µM Wortmannin (Sigma–Aldrich, Taufkirchen, Germany) and 10µM Ikarugamycin (IKA) (IKA, Sigma–Aldrich, Taufkirchen, Germany), clathrin-mediated endocytosis (CME) inhibitor and incubated for 30 minutes. Then these cells were further treated with 2µM rhodamine labelled plant PeptoQ and incubated for additional 2 h. On the other hand, cells were treated with 2µM, the polystyryl dye FM4-64 and followed by 5 minutes incubation. This is used as readout for the state of endocytosis. To probe for the role of actin filaments, the actin marker cell line, GF11 was pretreated for 1 h with 10 µM of Latrunculin B (Lat B, Sigma–Aldrich, Taufkirchen, Germany), while the role of microtubules was tested by pretreatment of the microtubule-marker cell line, TuB6 with 10 µM Oryzalin over 1 h (Sigma–Aldrich, Taufkirchen, Germany). Both inhibitors were diluted from a stock solution in DMSO with the culture medium to get the final working concentration. To visualise the endoplasmic reticulum during the uptake of plant PeptoQ, cells were first incubated with 2 µM plant PeptoQ, for different time points (10, 20, 30, 40, 50, 60, 90 and 120 min), then followed by the addition of 3,3´-dihexyloxa carbocyanine iodide, $DiOC_6$ (Sigma–Aldrich, Taufkirchen, Germany), incubated for 10 min at each time point, washed thoroughly with distilled water, and finally investigated by spinning-disc microscopy. Likewise, 2µM plant PeptoQ treated cells were further treated with 0.1% v/v of MitoTracker Green (Molecular Probes) at similar time points like above to visualise mitochondria during the uptake of plant PeptoQ and to diagnose the role of endosomes in the process. The entire procedure was repeated three times with three independent experimental series.

2.6.4. Potential cytotoxicity of plant PeptoQ on WT BY-2 cells

To test for potential toxicity of plant PeptoQ (2, 4, 8, 16, 25, 40 and 50 µM) on 3 days old non-transformed WT BY-2 cells, on the one hand, and a potential functionality for the mitigation of salt-induced programmed cell death on the other, mortality was followed over time using the Evans Blue dye exclusion test (Gaff and Okong'O-Ogola, 1971) after addition of 75 mM NaCl at the time of subcultivation, either with or without supplementation of 2 µM plant PeptoQ. Mortality was followed on a daily base till day 4 after onset of the stress treatment. Mortality was determined as relative proportion of cells that after thorough washing had retained the blue dye. Each data point represents average and standard error from at least 1000 cells counted and collected from at least three independent experimental series.

2.7. Microscopy

About 0.5µL aliquots were collected and transferred into custom-made chambers (Nick et al., 2000) to eliminate the medium. Except in the case of MitoTracker staining, cells were washed thoroughly in culture medium (distilled water) and then immediately visualized under the microscope. Aliquots of 30 µl were mounted on a microscope slide, covered with a cover slip, and viewed under an AxioObserver Z1 microscope (Zeiss, Jena, Germany) that was equipped with a spinning-disc device (YOKOGAWA CSU-X1 5000) and a cooled digital CCD camera (AxioCam MRm). The signal from GFP and MitoTracker Green was activated using the 488-nm line of an Ar-Kr laser (Zeiss), while the signal from rhodamine and FM4-64 was activated through the 561-nm line of the same laser. Images were operated via the Zen 2012 (Blue edition) software platform. Mortality scores were conducted by means of an Axioskop microscope (Zeiss, Jena, Germany), equipped with a 32x long distance objective (Zeiss Neofluar, Jena, Germany), and a digital CCD camera (AxioCam MRm).

2.8. Quantitative image analysis and modelling of uptake

Uptake was quantified as described in Eggenberger et al. (2017) making use of the Image J software (http://rsb.info.nih.gov/ij/). It is important that image acquisition is standardised with respect to laser power and exposure time, which requires that automatic optimisation tools are inactivated during imaging. Fluorescence intensity in confocal sections in the cell center, was averaged over the interior of the cell and corrected against the background of a calibration area chosen from the environment of the measured cell. The regions of interest were selected using the freehand selection tool of Image J. Uptake was modelled on base of a conventional Michaelis-Menten scheme:

$$E + S \rightleftharpoons ES \rightarrow E + P$$

with E representing the binding site, S the plant PeptoQ, ES the complex driving membrane passage, and P the internalised plant PeptoQ. In case of the two-step modelling, [S] was replaced by an effective concentration $[S]_{eff}$, whereby $[S]_{eff} = [S] - cap_1$ with [S] concentration of plant PeptoQ added to the assay, and cap_1 capacity of the first binding step. Experimental data were fitted by minimising the sum of squared deviations of observed versus predicted variables over the tested concentrations of plant PeptoQ.

To quantify the association of the plant PeptoQ signal with other fluorescent markers labelling different compartments, the channels of the merged image were split, and then the individual pixel intensities of the red channel (recording the plant PeptoQ signal) were subtracted from the green channel (recording the respective fluorescent marker). Mean pixel intensity of the resulting differential image was then divided by the mean pixel intensity of the green channel for normalisation. The resulting ratio would be 0% in case that the two signals match completely, it would be 100% in case that the two signals would be completely mutually exclusive.

2.9. Cellular uptake of plant PeptoQ by real plant cell system

The rice cultivar Nipponbare (*Oryza sativa* L. ssp.*japonica* cv. Nipponbare) was used in the investigation of the cellular uptake of plant PeptoQ into real plant cell system. First, caryopses were dehusked using hand grinder, incubated the seeds in 70% ethanol for 1 min to surface sterilized, then followed by a briefly twice washing with double-distilled water. Subsequently, seeds were incubated for 30 min in a sodium hypochlorite solution that contains ~5% of active chlorine and eventually washed using sterilized double-distilled water five times (Hazman et al., 2015). Seeds were sown on plastic mesh floating on 100ml distilled water in a cubic plastic box where the embryo pointing downward. The box was covered and sealed with parafilm, further covered with black polyethylene sheet and placed inside a custom-made cardboard box and incubated for 5 days under darkness in the cell culture room. After 5 days, the germinated and well grown roots were taken, cut into three parts (root tip, elongation zone and maturation zone) using razor blade. Then each part of rice root were placed in a separate 35mm petri dish containing 4ml distilled water, treated with 2µM rhodamine B labelled plant peptoQ and incubated for 2 h. Eventually, washed three times with double-distilled water, treated with MitoTracker Green FM dye, incubated for 5 min and visualized under confocal spinning disc microscope. The procedure was repeated three times with three independent experimental series.

2.10. Measurement of packed cell volume, cell density and cell length

2.10.1. Packed cell volume (PCV)

WT BY-2 cells were treated with 0, 75 and 150 mM NaCl with and without the plant PeptoQ (2 µM) pretreatment during subcultivation. Likewise, the stably OsOPR7 overexpressor (OE) BY-2 cells were also treated with the same salt concentrations during subcultivation. Then, packed cell volume (PCV) was measured at day 7 (at stationary phase) after subcultivation and treatment (Jovanovic et al., 2010) to quantify cell growth. Aliquots of 14 ml of 0, 75 and 150 mM NaCl treated WT BY-2 suspension cells with and without plant PeptoQ pretreatment, and OE suspension cells were poured from the Erlenmeyer flasks directly into 15ml falcon tubes and kept vertically at 4^{o}C for 48 and 72 h depending on the density of the cell culture until the cells sedimented well and the supernatant became completely clear. Eventually, the PCV was read directly from the scale of the 15 ml falcon tube. The procedure was repeated three times with three independent experimental series.

2.10.2. Cell density

WT BY-2 cells were treated with 0, 75 and 150 mM NaCl during subcultivation with and without plant PeptoQ (2µM) pretreatment. Similarly, the OE transgenic BY-2 cells were also treated with 0, 75 and 150 mM NaCl during subcultivation without plant PeptoQ pretreatment. Cell counts were performed daily (from day 0 till day 4), by triplicate, with Fuchs-Rosenthal hematocytometer (0.2 mm depth) to determine the maximum cell density and doubling time (τ). Cell number was calculated using the formula: Number of Cells/mL = $\frac{\text{Total Number of Cells}}{\text{Number of squares}}$ X DF X 5,000 (Abubakar, 2016 with minor modification). On the other hand, based on the time courses for cell density and the assumption of first order kinetics: $\frac{dn}{dt} = k.n$ where n and k represent number of cells and the time constant of exponential growth respectively, we have the natural logarithm ln(n(t)) = ln(n(t=0)) + kt where the slope K could be approximated by linear regression and the natural logarithm should follow a straight line. Then, doubling time τ (= duration of the cell cycle) could be estimated from the estimated k value based on the following equation: ln (2.n(t=0)) = ln(n(t=0)) + kτ as τ = ln (2)/k. The procedure was repeated three times with three independent experimental series.

2.10.3. Cell length and cell width

For cell length and cell width measurement, WT BY-2 cells were treated with, 0, 75 and 150mM NaCl with and without plant PeptoQ (2µM) pretreatment. And also, the OE transgenic BY-2 cells were treated with the same salt concentrations during subcultivation without plant PeptoQ pretreatment. Then cells at day 3 (exponential phase) and day 7 (stationary phase) after subcultivation/treatment were imaged using an AxioImager.Z1 Apotome microscope (Zeiss, Jena, Germany) with a 20x objective by a digital image acquisition system with a cooled digital CCD camera (AxioCamMRm; Zeiss) controlled by AxioVision Software 4.8 (Zeiss). Cell width and length of the longest cell axis were measured using the AxioVision software Rel. 4.8 (Zeiss) from MosaiX images taken. For each time point, 500 cells were measured, and the procedure was repeated at least three times with three independent experimental series.

2.11. Determination of mitotic index (MI) and cell viability

2.11.1. Mitotic Index (MI)

WT tobacco BY-2 cells, treated with 0, 75 and 150 mM NaCl with and without plant PeptoQ (2µM) pretreatment, and the OE transgenic BY-2 cells treated with the same salt concentrations (without plant PeptoQ pretreatment) during subcultivation were used to measure the mitotic index (MI) in order to investigate the potential effect of salt stress on the proliferation status of BY-2 cells (Maisch and Nick, 2007). Mitotic index was recorded at 24, 48,72 and 96 h after subcultivation/ treatment. MI provides the proportion of cells in prophase, metaphase, anaphase and telophase. About 0.5mL aliquots of cell suspension were fixed in Carnoy fixative (3:1 [v/v] 96% [v/v] ethanol:glacial acetic acid) plus 0.25% Triton X-100 and nuclei were stained with 2-(4-hydroxyphenyl)-5-(4-methyl-1-piperazinyl)-2.5-bi(1Hbenzimidazole) trihydrochloride (Hoechst 33258, Sigma–Aldrich, Neu-Ulm, Germany final concentration 1µg mL-1). This is to discriminate non-mitotic (uncondensed chromatin) from

mitotic (condensed chromosomes) cells using the fluorescent dye Hoechst 33258 which intercalates into the DNA. Dividing and non-dividing cells were scored under a fluorescence microscope, AxioImager.Z1 Apotome microscope (Zeiss, Jena, Germany) with a 20x objective and digital image acquisition controlled by AxioVision Software 4.8 (Zeiss). The mitotic index was calculated as the ratio between the number of dividing cells to that of the total number of cells scored. For each time point, 1,000 cells were scored, and the procedure was repeated at least three times with three independent experimental series.

2.11.2. Cell viability

To determine cell viability, 0.5µl aliquots of 0, 75 and 150 mM NaCl treated WT BY-2 cells suspension with and without plant PeptoQ (2µM) pretreatment, and the OE transgenic BY-2 cells treated with same NaCl concentrations (without plant PeptoQ pretreatment) during subcultivation were collected at 24, 48, 72 and 96 h after subcultivation/treatment. To get rid of the medium, each sample was transferred into custom-made staining chambers (Nick et al., 2000), and then cells were stained with the vital dye Evans Blue (2.5% w/v, dissolved in distilled water) and incubated cells and dye together for 3-5 minutes (Gaff and Okong'O-Ogola, 1971). The Evans Blue was eliminated by washing three times with distilled water. In dead cells, owing to the breakdown of the plasma membrane, Evans Blue can enter cells, stain the interior of the cell blue. Thus, those cells that accumulated Evans Blue were considered dead. Cells were mounted on a slide and viewed under Axioskop microscope (Zeiss, Jena, Germany), equipped with a 32x long distance objective (Zeiss Neofluar, Jena, Germany), and a digital CCD camera (AxioCam MRm). The number of dead and alive cells was counted, and percent cell death was calculated as the ratio of the number of dead cells over the total number of scored cells. For each independent treatment, at least 3000 cells were counted in three independent experiments.

2.12. Reactive oxygen species (ROS) level assay

Reactive oxygen species (ROS) were measured both in the extracellular (apoplastic) and intracellular phases.

2.12.1. Extracellular ROS level

In the extracellular (apoplastic) phase hydrogen peroxide (H_2O_2) and superoxide ($O_2^{\bullet -}$) were measured.

2.12.1.1. Measurement of H_2O_2

The oxidative burst was determined by measuring H_2O_2 according to Bellincampi et al. (2000) in the extracellular phase. To measure extracellular H_2O_2, 4 days old cells of both WT and OE BY-2 were treated with 0, 75 and 150 mM NaCl. In brief, 1 ml cell culture from both cell lines was harvested at 1, 4 and 6 h after salt treatment by centrifugation (10 000 g, 20 sec, and 25^0C) and then H_2O_2 concentration was measured in the supernatant. An aliquot of supernatant (500 µl) was added to 500 µl assay reagent (500 µM ferrous ammonium sulphate, 50 mM H_2SO_4, 200 µM xylenol orange, 200 mM sorbitol). After 45 min incubation, the peroxide-mediated oxidation of Fe^{2+} to Fe^{3+} was determined by measuring the absorbance at 560 nm of the Fe^{3+}-xylenol orange complex (De Pinto et al., 2006). The procedure was repeated three times with three independent experimental series.

2.12.1.2. Measurement of $O_2^{\bullet-}$

The detection of $O_2^{\bullet-}$ in the extracellular phase was performed by using the nitroblue tetrazolium method (Murphy et al., 1998). To measure extracellular $O_2^{\bullet-}$, 4 days old cells of both WT and OE BY-2 were treated with 0, 75 and 150 mM NaCl. Then, 1 mL of cell culture from both cell lines was harvested by centrifugation (10,000*g*, 20s, 25°C), and $O_2^{\bullet-}$ concentration was measured in the supernatant by monitoring the reduction of nitroblue tetrazolium (100 µM) at 530 nm. The amount of $O_2^{\bullet-}$, was then calculated using ε550 nm 12.8 mM^{-1} cm^{-1} (Murphy et al., 1998). The procedure was repeated three times with three independent experimental series.

2.12.2. Intracellular ROS level

To examine the salt induced intracellular ROS production, WT BY-2 cells were treated with 0, 75 and 150 mM NaCl with and without plant PeptoQ (2µM) pretreatment (at day 3 to 4 after subcultivation) and placed under continuous shaking. Sampling was done at 10 min, 2 and 4 h after treatment by taking 200 µl of BY-2 cells, suspending them in 800µl PBS and followed by treatment with a cell-permeable fluorogenic probe reporting oxidative burst (Henderson and Chappell, 1993) dihydrorhodamine 123 (DHR 123, final concentration 10 µM), at 10 min, 2 and 4 h after treatment. After 30 min incubation, cells were washed 3 times using pre-warmed PBS at 37°C and resuspended in 1 ml PBS. Changes of the fluorescent signal were followed over time under an AxioImager Z.1 microscope (Zeiss, Jena, Germany) using the filter set 38 HE (excitation at 470 nm, beamsplitter at 495 nm, and emission at 525 nm), a 20x objective and a constant exposure time of 300 ms, and the procedure was repeated three times with three independent experimental series.

2.13. Antioxidant enzymes activity and lipid peroxidation measurement

In order to determine the antioxidant enzyme activities, 0.1g of both WT and OE BY-2 suspension cultured cells, treated with 0, 75 and 150 mM NaCl with and without plant PeptoQ (2µM) pretreatment, were vacuum-dried. Then those vacuum-dried cells were homogenized in 50 mM phosphate buffer (pH 7.0) that contains 1 mM EDTA, 1 mM polyvinylpyrolidone (PVP) and 0.05% triton X and followed by the centrifugation of the homogenate at 10,000g for 20 min at 4°C. Finally, the resulting supernatant was used for determination of antioxidant enzymes activities.

2.13.1. Catalase (CAT)

The antioxidant activity of CAT (EC.1.11.1.6) was measured on the basis of the disappearance of hydrogen peroxide (H_2O_2) (extinction coefficient of 39.4 $mM^{-1}cm^{-1}$) spectrophotometrically. The amount of enzyme needed to oxidize 1µmol of H_2O_2 per minute is considered as one unit of CAT activity (Weydert and Cullen, 2010). CAT activity was determined according to Aebi et al. (1984) protocol by combining 0.5ml enzyme extract with a 2.5ml reaction mixture that contains 0.5ml of 30mM H_2O_2 and 2ml of 100mM sodium phosphate buffer pH 6.8 that makes a final volume of 3 ml. Then spectrophotometer was used to measure the decrease in absorbance at 240nm which emanates from the depletion of hydrogen peroxide, and the procedure was repeated three times with three independent experimental series.

2.13.2. Superoxide dismutase (SOD)

The antioxidant activity of SOD (EC 1.15.1.1) was determined using the Beauchamp and Fedovich (1971) method. Briefly, a reaction mixture of 2.7ml containing, 2µM riboflavin, 13mM L-methionine, 75µM NBT and 0.05M sodium carbonate (pH 10.2) was combined with 0.3ml of the extract that adds up to a final volume of 3ml. The absorbance was recorded at 560nm using spectrophotometer, extinction coefficient of 12.8 $mM^{-1}cm^{-1}$. Units per mg of protein was used to express the specific activity of SOD. The amount of enzyme needed for the inhibition of NBT reduction by 50%, represents SOD units, and the procedure was repeated three times with three independent experimental series.

2.13.3. Lipid peroxidation

The product of lipid peroxidation, malondialdehyde (MDA), indicator of oxidative burst was measured using a reaction between MDA and 2-thiobarbituric acid (TBA) according to Hodgson and Raison (1991) with minor modification as follows: 4 days old WT BY-2 cells were treated with 0, 75 and 150 mM NaCl with and without plant PeptoQ (2µM) pretreatment, and also OE BY-2 cells were also treated with the same NaCl concentrations and samples were collected at 1 and 4 h by removing the medium using vacuum pump and about 0.1g cells were put in 2ml Eppendorf tube and frozen in liquid nitrogen. Then the combined cell fresh weight and steel bead was recorded, and cells were shock frozen again in liquid nitrogen, and then homogenized with steel beads (Tissue Lyser, Qiagen/ Retsch, Germany) in standardized manner (twice 30s at 25Hz), and frozen in liquid nitrogen. Then 1ml of sodium phosphate buffer 10mM (pH 7.4) was added to each sample, homogenized and centrifuged for 4 min at 8000g. Then 200µl of the supernatant from each treatment was added to the respective already prepared reaction mixture containing 100µl of 8.1% (w/v) Sodium Dodecyl Sulfate (SDS), 750µl of 20% (w/v) acetic acid (pH 3.5), 750µl of 0.8%(w/v) aqueous 2-thiobarbituric acid (TBA) and 200µl of Milli-Q water. For the blank, identical reaction mixture was used where the 200µl supernatant was replaced with the sodium phosphate buffer. Both reaction mixtures were mixed very well and incubated at 98°C for 1 h. Then the mixtures were cooled at room temperature and centrifuged at 8000g for 5 min and absorbance was measured at 535 nm (specific signal) and 600 nm (background). The MDA concentration in the supernatant was determined from the difference in absorption (A535 - A600nm) using a molar extinction coefficient of 155 mM^{-1} $cm^{-1}$and fresh weight (Lata et al., 2011), and the entire procedure was repeated three times with three independent experimental series.

2.14. Measurement of cellular cations content

WT BY-2 cells were treated with 0, 75 and 150 mM NaCl with and without plant PeptoQ (2µM) pretreatment, and also OE BY-2 cells were treated with the same salt concentrations at day 4 after subcultivation and incubated on a shaker at 150 rpm. Samples were collected at 1 and 3 h by removing the medium using Büchner funnel fitted vacuum pump, and then dried in an oven at 80°C for 3 days. Cells were digested according to Ippolito and Barbarick (2000) with slight modification after determining the dry weight of the samples: Digestion tubes

(Gerhardt, UK) were used to mix the dry cells of each technical and biological replicates with 5 ml of concentrated nitric acid (HNO_3) and then followed by 24 h room temperature incubation along with 6 and 24 h interval vertexing. Samples were boiled in a water bath at 105°C for 2 h, and after cooling, distilled water was added into each sample in order to obtain a final and adjusted volume of 10 ml which is vortexed accordingly. Eventually, flame atomic absorption spectrometry (AAnalyst200, Perkin Elmer) in an air-acytelene flame (Institute of Applied Geosciences, Karlsruhe Institute of Technology) was used to measure the Na^+, K^+, Ca^{2+} and Mg^{2+} contents. To prepare blank samples, 5 ml concentrated nitric acid was added into an empty digestion vessel and processed in the same way as above. Three independent technical and biological replicates were taken into consideration in calculating cations concentration with reference to the dry weights.

2.15. Molecular analysis: Gene expression

2.15.1. Total RNA extraction

Prior to total RNA extraction, 4 days old WT BY-2 with and without plant PeptoQ (2µM) pretreatment, and OE BY-2 cells (without plant PeptoQ pretreatment) were treated with 0, 75 and 150 mM NaCl. About 100 mg samples were collected using vacuum pump both from the control and the treated cells at 1 and 3 h after the onset of salt treatment, and cells were immediately shock-frozen in liquid nitrogen. Then the frozen cells were homogenized with Tissue Lyser II (Qiagen/ Retsch, Hilden, Germany) 22Hz, 2x30seconds. Total RNA was extracted using the InnuPREP plant Kit (Analytik Jena, Germany) including genomic DNA digestion with RNase-free DNAse I (Qiagen) according to the manufacturer´s instructions. The purity and integrity of the extracted total RNA was checked using both Nano-Drop 2000 and % (w/v) agarose gel electrophoresis, and the whole procedure was repeated three times with three independent experimental series.

2.15.2. Agarose gel electrophoresis

The integrity of extracted total RNA was verified using agarose gel electrophoresis. Where 1% [w/v] powdered agarose gel (Roth) was dissolved in TAE buffer [50x stock: 2 M Tris-HCl, 0.57% (v/v) acetic acid, 50 mM EDTA; pH 7.5] by heating in a microwave, and 0.5x SYBR Safe (Invitrogen, Karlsruhe, Germany) was added when the temperature lowered around 50^{o}C (it is used for detection). Total RNA samples were mixed with 5x loading dye [50% (v/v) glycerine, 0.05% (w/v) bromphenol blue, 0.05% (w/v) xylencyanol] before loading. Samples were loaded on the gel along with DNA ladder (NEB, Frankfurt, Germany) and separated by running it at 75-100 V for 30 min. Bands were visualized on a Safe Imager blue light transilluminator (Invitrogen) and photographed with a Rainbow Camera system (Hama, Monheim, Germany). Similarly, to monitor the quality of the semi-quantitative PCR (SQ-PCR) products, except the agarose gel being 1.5% (w/v), the same procedure as above was followed, and the entire procedure was repeated three times with three independent experimental series.

2.15.3. cDNA synthesis

The cDNA synthesis was carried out using total RNA as a template by means of the M-MuLV cDNA Synthesis Kit (NEB), with Oligo(dTs) (Thermo Fisher, Germany) according to the manufacturer's instructions. In brief, 1µl dNTP

(10mM), 2µl oligo (dT) 500ng (= 100µM) and 1µg total RNA were mixed together, the volume was adjusted to 16µl with RNase-free H_2O, vortexed and spin down. Then the mixture containing the total RNA sample was denatured for 5 minutes at 72°C. It was spin briefly and put promptly on ice and followed by the addition of 2µl 10X Reverse Transcriptase (RT) buffer, 1µl RNase inhibitor and 1µl M-MuLV Reverse transcriptase. Then vortexed and spin briefly, and the semiquantitative reverse transcription PCR (RT-PCR) reaction was continued at 42°C for 1 h. The enzyme was inactivated at 90°C for 10 min and hold at 12°C. The synthesized cDNA was diluted (1:10) with nuclease-free water and stored at -20°C until to be used for semiquantitative and quantitative real-time polymerase chain reactions (SQ-PCR and qRT-PCR). The procedure was repeated three times with three independent experimental series.

2.15.4. Semiquantitative PCR (SQ-PCR)

The semiquantitative PCR (SQ-PCR) was carried out as per the standard system described in (Tables 6 and 7) using the primers mentioned in (Table 5) by a conventional PCR cycler (peqLab Primus 96, Erlangen, Germany). In order to obtain the amplifications of the whole primers considered in exponential phase (which helps the clear identification of the products on the agarose gels), 30-35 cycle number has been chosen. The PCR products were processed and checked by 1.5% (w/v) agarose gel electrophoresis. A MITSUBISHI P91D screen (Invitrogen) was used to record the gel images by means of a digital image acquisition system (SafeImage, Intas, Germany). The procedure was repeated three times with three independent experimental series.

Table 6: Standard set-up for semiquantitative PCR (SQ-PCR) (20µL).

Component	Amount in µL
10X Standard Taq Reaction Buffer (TB)	2
10mM dNTPs	0.4
Taq DNA Polymerase	0.1
10µM Forward Primer	1
10µM Reverse Primer	1
Template cDNA	2
Nuclease-free water	to 20

Table 7: Cycling parameters for semiquantitative PCR (SQ-PCR).

Step	Temperature	Time
Heating up	95°C	2 min
Denaturation	94°C	30 S
Annealing	60°C	30 S
Elongation	72°C	1 min
Final Extension	68°C	5 min
Hold	10°C	∞

2.15.5. Quantitative real-time PCR (qRT-PCR)

The quantitative real-time PCR (qRT-PCR) was conducted by preparing a master mix with respect to the available genes, then split up into 61.8µl triplet mix, and eventually, mixed with 3.25µl of the respective cDNA. The entire components of the qRT-PCR mix per reaction are described in (Table 8) below. The Bio-Rad CFX Touch real-time PCR system (Bio-Rad, Munich, Germany) detection system was used to perform the qRT-PCR reaction according to the manufacturer's instructions where the following cycler conditions were applied: 95°C for 3 min, 39 cycles (95°C for 15 s and 60°C for 40 s). The primer sequences of the genes used are listed in (Table 5).

The analysis of the qRT-PCR data was carried out by $2^{-\Delta\Delta Ct}$ method (Livak and Schmittgen, 2001). First of all, the average of the three technical replicates of the cycle threshold (Ct) values of the treated, non-treated and the endogenous controls samples was calculated. Then the values of both the treated and non-treated samples were normalized by the endogenous control by calculating ΔCt values. The ΔCt of the treated and non-treated samples was calculated as (Ct gene-Ct endoControl) treated and (Ct gene-Ct endoControl) non-treated where the Ct of the endogenous control was the geometric mean of the two reference genes, ribosomal protein L25 and elongation factor-1α (EF-1α). The values normalized by the endogenous controls were also further normalized by the calibrator (non-treated) samples by calculating ΔΔCt values as (ΔCt gene) treated - (ΔCt gene) non-treated. Finally, the induction factor was calculated using the formula $2^{-\Delta\Delta Ct}$. The procedure was repeated three times with three independent experimental series.

Table 8: Standard set-up for quantitative real-time PCR (qRT-PCR) (20µL)-mix per reaction.

Component	Amount in µL
Nuclease-free H_2O	11.75
5X GoTaq buffer (NEB, Frankfurt, Germany)	4
5U/µl GoTaq Polymerase (NEB, Frankfurt, Germany)	0.1
10mM dNTPs	0.4
10µ M Forward Primer	0.4
10µM Reverse Primer	0.4
$MgCl_2$ (50mM)	1
SybrGreen	0.95
Template cDNA (1:10)	1
Final volume	**20µL**

2.16. Experimental Design and Statistical Data Analysis

A factorial experiment with randomized complete block design (RCBD) was used with two factors: tobacco cells [(WT BY-2 cells with versus without plant PeptoQ) and (WT BY-2 cells versus OsOPR7 overexpressor BY-2 cells)] and salinity (0, 75 and 150mM NaCl). All the presented data are mean values and standard errors and generated from three independent biological replicates. All data were analyzed by analysis of variance (ANOVA), LSD and Tukey HSD Post-Hoc tests using a statistical package, SPSS version 24 assuming independence, normal distribution of values and confidence interval of 95%. The significance of differences between individual samples was determined using excel based two-tailed student's t-test assuming 95% of confidence interval. Values with $*P \leq 0.05$, $**P \leq 0.01$ and $***P \leq 0.001$ are denoted as significant, highly significant, and very highly significant, respectively.

3. Results

3.1. Time-course and dose-response characterization of plant PeptoQ

Time-course and dose-response experiments were conducted to gain insight into the cellular uptake aspects of the plant PeptoQ by walled, non-transformed WT tobacco BY-2 cells. Uptake was quantified by measuring the mean fluorescence intensity of the plant PeptoQ-associated rhodamine, corrected for background intensity (Eggenberger et al., 2017), in proliferating cultures at day 3 after subcultivation (Huang et al., 2017).

3.1.1. Time-course assay of plant PeptoQ

For the time-course study, non-transformed WT BY-2 cells were incubated with 2 µM of labelled plant PeptoQ, and the rhodamine signal was followed by spinning disc confocal microscopy (Fig. 9A). The signal was rapidly increasing during the first hour of uptake and was then accumulating in vermiform structures that were interpreted as mitochondria. However, during the first hour, most of the signal this mitochondrial pattern was not developed, which can be visualized by normalising the signal amplitude for the overall lower levels at the early stages of uptake (Fig. 9B). While at 10 min after the start of incubation (the earliest time point that could be reliably observed in this time series), mostly punctate signals were seen in the peripheral cytoplasm, just adjacent to the cell membrane, and at 30 and 60 min of incubation, a reticulate signal was dominating, probably representing the endoplasmic reticulum. Only later, from 90 min of incubation, the mitochondria became evident, and the reticulate signals outside of mitochondria disappeared progressively. Also, the quantification of the signal over time revealed a non-steady nature of uptake. While the uptake was rapid during the first 20 min, it halted between 30 and 60 min, followed by a second wave of uptake became evident between 60 and 120 min. Then, beyond 120 min, no further uptake was seen (Fig. 9C). When the rate of uptake (as first derivative of the cumulative values obtained from the quantification) was plotted over time, the two waves of uptake activity became clearly evident (Fig. 9D). The first wave of uptake coincided with the reticulate distribution of the fluorescent signal, while the second wave of uptake was seen at a time, when the signal from the first wave had been mostly translocated to the mitochondria. Thus, both the cellular details as well as the quantification show that the plant PeptoQ reaches the mitochondria not in a linear process, but in a biphasic process, where in a first step a pool in the ER is filled, before the signal in a second, slower step accumulates in the mitochondria themselves.

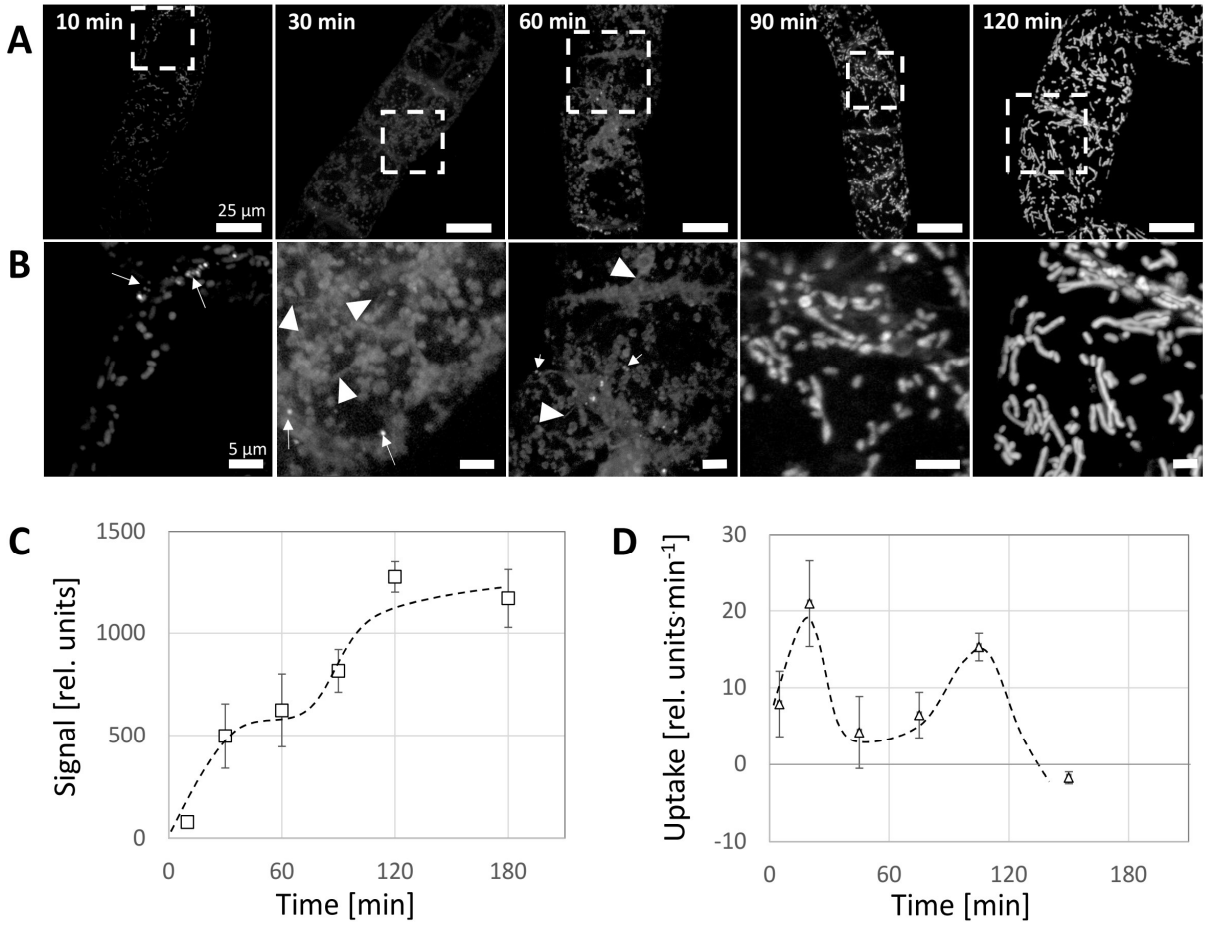

Figure 9: Time course for the uptake of plant PeptoQ into tobacco BY-2 cells. Cells were treated at day 3 after subcultivation (at the completion of the proliferation phase of the culture) with 2 µM of plant PeptoQ and followed by spinning disc confocal microscopy making use of the fluorescent signal of the conjugated rhodamine. Representative cells recorded at constant laser power and exposure time are shown in **A**, the white squares mark the region of interest magnified in **B** to show the subcellular details. White arrows indicate punctate structures that are seen in early time points which represent endoplasmic reticulum (ER) structures that have active role in the internalization process, white arrowheads indicate filamentous structures. **C** Quantification of intracellular accumulation based on the integrated intensity inside the cell corrected for background. Mean values and standard errors from three independent experiments are shown. **D** Uptake determined from the first derivative of the cumulative time course shown in **C** to show the non-steady nature of the process, where a first period of rapid uptake in the first 20 min is followed by a static period, and then the second, third and fourth waves of uptake became evident after 60, 90 and 120 min respectively. Beyond 120 min, it became saturated. This signifies that the uptake of plant PeptoQ depends on receptor(s) molecule(s). Adapted from Asfaw et al., 2019.

3.1.2. Dose-response assay of plant PeptoQ

To dissect uptake further, a dose-response study was conducted, where the BY-2 cells were incubated for 120 min (the time point, when uptake was seen to be complete in the time-course experiment) with 0.5 to 5 µM of labelled peptoid. Again, the dependency was not linear (Fig. 10A, B): for 0.5 and 1 µM, the resulting signal was not confined to mitochondria, while for higher concentrations, the mitochondrial signal clearly dominated the background in the cytoplasm. Similar to the situation at early time points seen during the uptake of 2 µM of plant PeptoQ (Fig. 9B), structures connecting patterns could be seen indicative of a situation, where the peptoids were still trapped in the ER and did not travel further (Fig. 10B, arrowheads). When a dose-response curve was constructed from a quantification of the signals, a significant increase in uptake became evident, when the concentration of the plant PeptoQ was raised from 0.5 to 2 µM. Uptake became saturated above this concentration (Fig. 10C). It has to be noted that there was a clear threshold at around 1 µM plant PeptoQ. Below this threshold, the signal was virtually absent. Michaelis-Menten based algorithm was used to model these uptake data (Fig. 10D). For the one-step model, a dissociation constant of 0.4 µM was determined by fitting observed and predicted data. However, the fit was very poor-especially, the modelling failed to reproduce the pronounced threshold seen in the data. Therefore, we changed to a two-step model, where a first uptake step saturated at 0.9 µM was followed by a second step with a dissociation constant of 0.2 µM, which fitted the observed data much more efficiently.

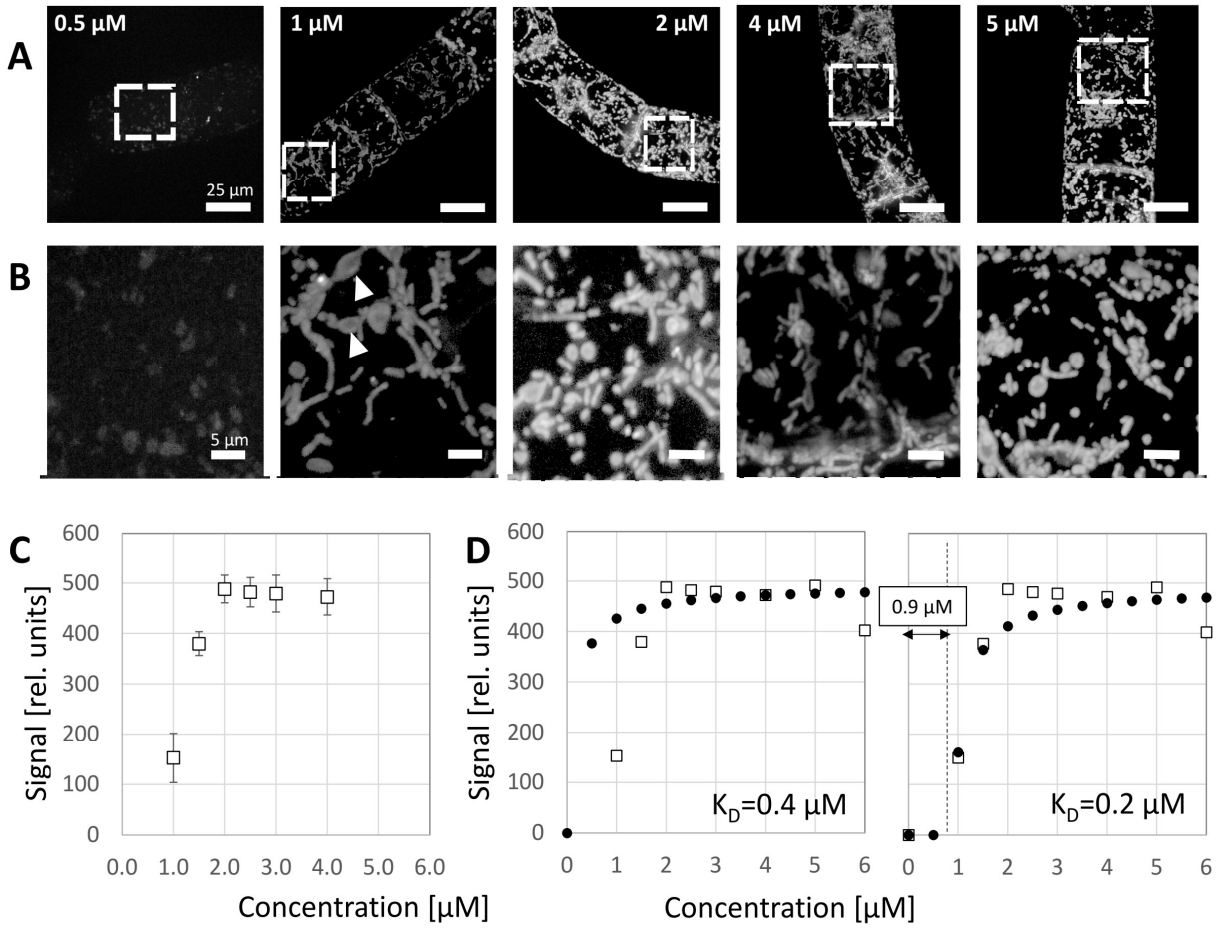

Figure 10: Dose-response for the uptake of plant PeptoQ into tobacco BY-2 cells. Cells were treated at day 3 after subcultivation (at the completion of the proliferation phase of the culture) with 0.5-5 µM of plant PeptoQ and observed by spinning disc confocal microscopy making use of the fluorescent signal of the conjugated rhodamine. Representative cells recorded at constant laser power and exposure time are shown in **A**, the white squares mark the region of interest magnified in **B** to show the subcellular details. White arrowheads indicate connective structures between mitochondria. **C** Quantification of intracellular accumulation based on the integrated intensity inside the cell corrected for background. Mean values and standard errors from three independent experiments are shown. **D** Modelling the observed values for the dose-response of uptake (white squares) by a Michaelis-Menten algorithm. In the one-stage model (left), a dissociation constant of 0.4 µM was derived from the fitting, in the two-stage model (right), a first step saturated at 0.9 µM, followed by a second step with a dissociation constant of 0.2 µM was derived. Adapted from Asfaw et al., 2019.

Therefore, the dose-response study supports the conclusion from the time-course experiments that uptake proceeds in two stages. The first stage is rapid leads to accumulation of the signal in the ER and is saturated at ~1 µM, the second stage proceeds more slowly and shows a higher affinity (K_D ~ 0.2 µM) partitions the signal from the ER to the mitochondria itself, where it accumulates to high levels.

3.2. Subcellular localisation of plant PeptoQ

In the time-course assay above, the vermiform-vesicular final pattern obtained for the labelled plant PeptoQ was interpreted as mitochondrial localisation. To test this assumption, WT BY-2 cells were treated with labelled 2 µM plant PeptoQ and incubated for 120 min, washed thoroughly, and incubated with the specific mitochondrial dye MitoTracker Green FM (1 µl/ml) for 5 min. The potential colocalisation of both signals was then assessed by spinning disc confocal microscopy using simultaneous excitation of the MitoTracker Green FM dye through the 488-nm line, and the rhodamine conjugated to the plant PeptoQ through the 561-nm line of the Ar-Kr laser. The result showed a clear colocalisation between the mitochondrial dye and the plant PeptoQ conjugated probe (Fig. 11). This tight association of the signal recording the plant PeptoQ with mitochondria was observed independently of the proliferation status and was seen both for cells from the proliferating (Figs. 11A-C) or the stationary (Figs. 11D, E) phases of the culture.

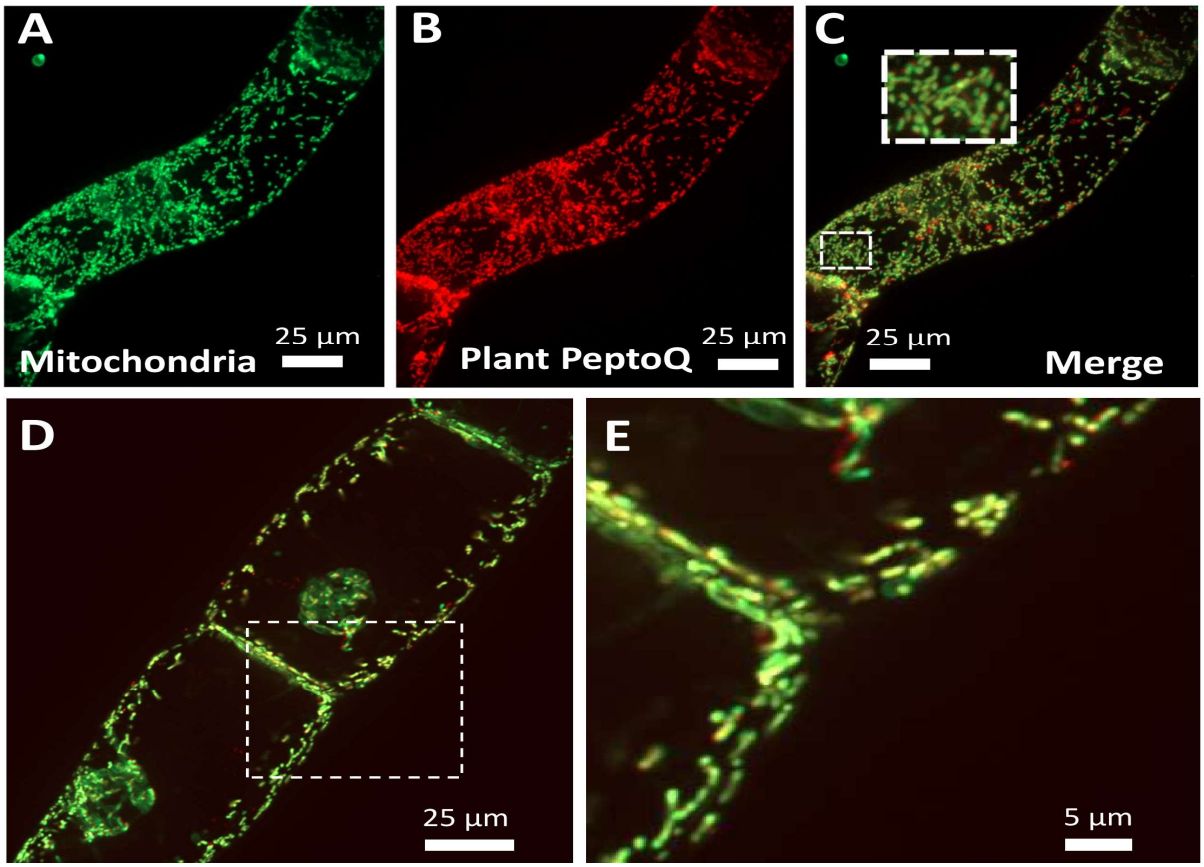

Figure 11: Mitochondrial localisation of the plant PeptoQ in tobacco BY-2 cells assessed at day 3 (**A-C**) or day 6 (**D, E**). Cells were incubated for 2 hours with 2 µM of plant PeptoQ followed by labelling with MitoTracker Green FM and then followed by spinning disc confocal microscopy making use of the fluorescent signal from MitoTracker Green FM **(A)**, and the rhodamine signal from the labelled plant PeptoQ (**B**). The merge of the two channels shown in (**C-E**) shows the close overlap of both signals. Confocal sections recorded in the mid-plane from representative cells recorded at constant laser power and exposure time are shown. Adapted from Asfaw et al., 2019.

3.3. Cellular uptake mechanisms of plant PeptoQ

In the effort to identify the possible cellular uptake mechanism(s) of plant PeptoQ into non-transformed WT BY-2 cells, endocytosis was investigated as one of the potential options. To do so, two inhibitors that are known to disrupt endocytosis were used. Such as Wortmannin (Wm) which disrupts endocytosis as a whole and Ikarugamycin (IKA) which inhibits clathrin-dependent endocytosis. First of all, the effectiveness of these drugs was verified using the fluorescent endosomal marker FM4-64 where 3 days old cells were pretreated with both drugs (33µM Wortmannin and 10µM Ikarugamycin) and incubated for 30 min, treated with 2 µM FM4-64 and incubated for 5 min. Eventually, visualized under spinning disc microscope. The FM4-64 was taken up readily in the control cells (Fig. 12D) such that numerous endosomes could be seen in trans-vacuolar strands and also around the nucleus. However, in Wortmannin (33µM) pretreated BY-2 cells, the uptake of FM4-64 was inhibited. This implies that Wortmannin blocks endocytosis effectively in our experimental set up (system). Tobacco BY-2 cells of the same stage (day 3 after subcultivation) were pretreated with Wortmannin (incubated for 30min), further treated with 2µM plant PeptoQ and incubated for additional 2 h, a time point that allows a maximum uptake (Fig. 9, Fig. 12A). Like the efficacy test with FM4-64, the cellular uptake of plant PeptoQ was blocked effectively, and the signal remained attached to the cross wall (Fig. 12B). On the other hand, Ikarugamycin was used in order to test to what extent the cellular uptake of plant PeptoQ depends on clathrin mediated endocytosis. First the efficiency of Ikarugamycin on the uptake of FM4-64 was assayed. Like the case with Wortmannin above, 3 days old WT tobacco BY-2 cells were pretreated with 10µM Ikarugamycin, incubated for 30min and followed by treatment with 2µM FM4-64 and 5min incubation. The spinning disc microscopic result showed effective internalization of the FM4-64 in the control BY-2 cells and characterized by fluorescent endosomes in trans-vacuolar strands and around the nucleus (Fig. 12D). However, such fluorescent endosomes localised in trans-vacuolar strands and around the nucleus were eliminated by pretreatment with 10µM Ikarugamycin (Fig. 12F). Instead, punctate signals were lining the membrane like beads on a string. Here, unlike the situation created by treatment with wortmannin, the signal was not confined to the cross walls (compare Fig.12E and 12F). Then 10µM Ikarugamycin pretreated (incubated for 30 min) WT tobacco BY-2 cells were treated with 2µM plant PeptoQ and incubated for 2 h. After washing three times with MS medium, cells were observed under spinning disc microscope. The result showed a punctate rhodamine B signal at the cell membrane, and predominantly at the lateral walls. The pattern observed here was the same as seen for FM4-64 (Fig. 12C). Since the cellular uptake of plant PeptoQ was effectively inhibited by Ikarugamycin pretreatment, hardly any mitochondria were detected despite the fact that the BY-2 cells were incubated with plant PeptoQ for 2 h (the time point that would allow for complete uptake).

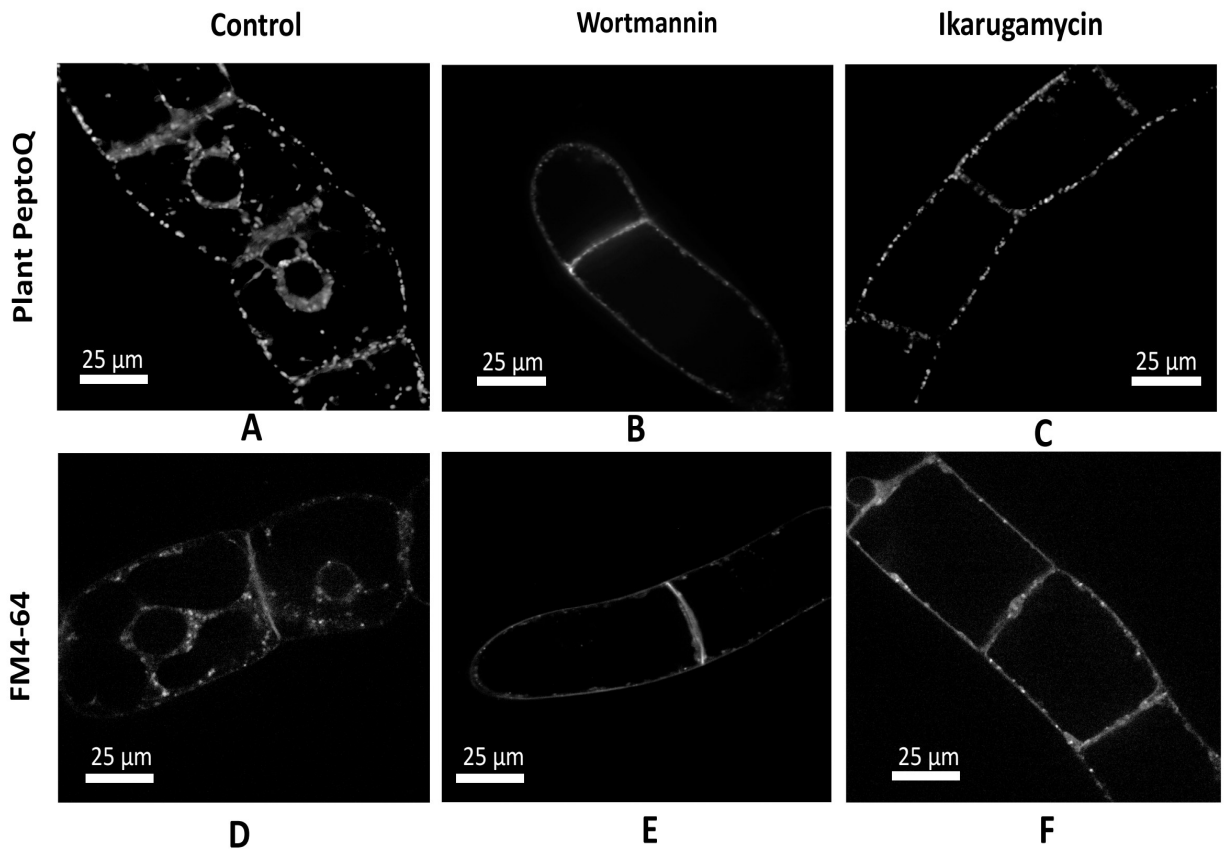

Figure 12: Inhibitors of endocytosis impair the cellular uptake of plant PeptoQ into BY-2 (**A-C**) as compared to the endosomal tracer FM4-64 **(D-F)**. Control cells **(A, D)** are shown in comparison to cells that had been pretreated for 30 min with either 33 µM Wortmannin **(B, E)** or with 10 µM Ikarugamycin **(C, F)**. Confocal sections recorded in the mid-plane from representative cells are shown. Adapted from Asfaw et al., 2019.

To test, whether the plant PeptoQ passes through endosomes, the plasma-membrane located auxin-influx carrier AUX1 was employed. A tobacco BY-2 strain expressing a fusion of AUX1 with YFP (from *Arabidopsis thaliana)* under an estradiol-driven promoter (Laňková *et al.*, 2010) was induced for expression by adding β-estradiol (1 µM) for 24 h at day 2 after subcultivation, and then treated with 2µM plant PeptoQ and followed by 2 h incubation. Upon microscopic inspection of the cell surface (Fig. 13, left-hand panel), fine punctate signals of AUX1 could be observed that were aligned like beads on a string. These strings were clustered to larger agglomerations and also, they were interspersed with larger speckles that presumably represented sites of endocytotic activity. The plant PeptoQ signal was not seen in the aligned *punctae* that probably represent the working form of the AUX1 carrier but instead in the above-mentioned speckles and agglomerations. On the other hand, the topology of uptake could be observed (Fig. 13, right-hand panel) in confocal sections of the cell center where different sized vesicular structures harbor the plant PeptoQ. The larger vesicles were localized somewhat deeper in the cytoplasm whereas the smaller ones were situated closer to the plasma membrane.

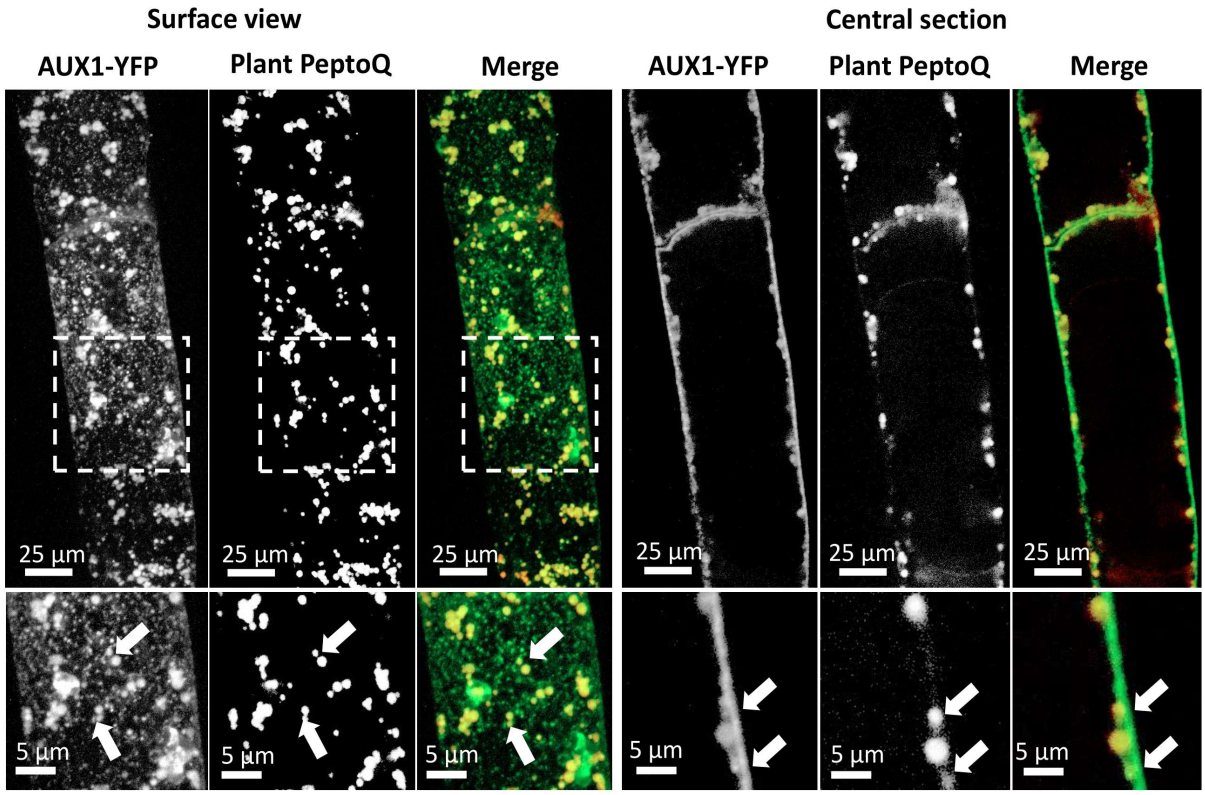

Figure 13: Colocalisation of a YFP fusion with the auxin-influx carrier AUX1 (as marker for endosomes) with the plant PeptoQ in surface view (left-hand panel) and in a central confocal section (right-hand panel). White arrows indicate vesicular structures that are labelled by both signals. Expression of AUX1-YFP was driven by an estradiol-driven promoter, which was induced 24 h prior to the experiment by β-estradiol (1 µM). Adapted from Asfaw et al., 2019.

To identify the involvement of the endoplasmic reticulum in the cellular uptake of plant PeptoQ, cells were first incubated with rhodamine B labeled 2 µM plant PeptoQ for different time points, before adding 3,3´-dihexyloxa carbocyanine iodide ($DiOC_6$), washed thoroughly with distilled water, and then investigated by spinning-disc microscopy. This cationic dye, $DiOC_6$ is labelling the ER, including the nuclear envelope, but also has a high affinity for mitochondria (Matzke and Matzke, 1986). We observed that at 10 min after addition, the rhodamine signal reporting the plant PeptoQ was tightly colocalised with a reticulate structure, probably representing the endoplasmic reticulum (Fig. 14A), especially in vicinity of the cross-walls. Individual speckle-like structures reporting both signals, probably representing mitochondria were seen as well. At later stages of uptake (Fig. 14B), the signals were more separate-while the speckles showing both the rhodamine B and the $DioC_6$ signal were now quite abundant, the reticulate network interconnecting those *bona-fide* mitochondria, was depleted from the rhodamine signal and appeared green in the channel merge. Then the degree of signal separation (Fig. 14C) was quantified over time by integrating over each individual pixel the intensity difference between the two channels divided by the average intensity of the green $DioC_6$ signal. In case of a complete overlap of both signals, this value should be 0%, while in case of complete separation, it should be 100%. At early phases of uptake, the signals for plant PeptoQ and DioC6 were tightly linked (giving a score of 25%), but during the first hour of uptake, they progressively separated, until from 60 min a plateau with a score of a bit more than 35% was reached.

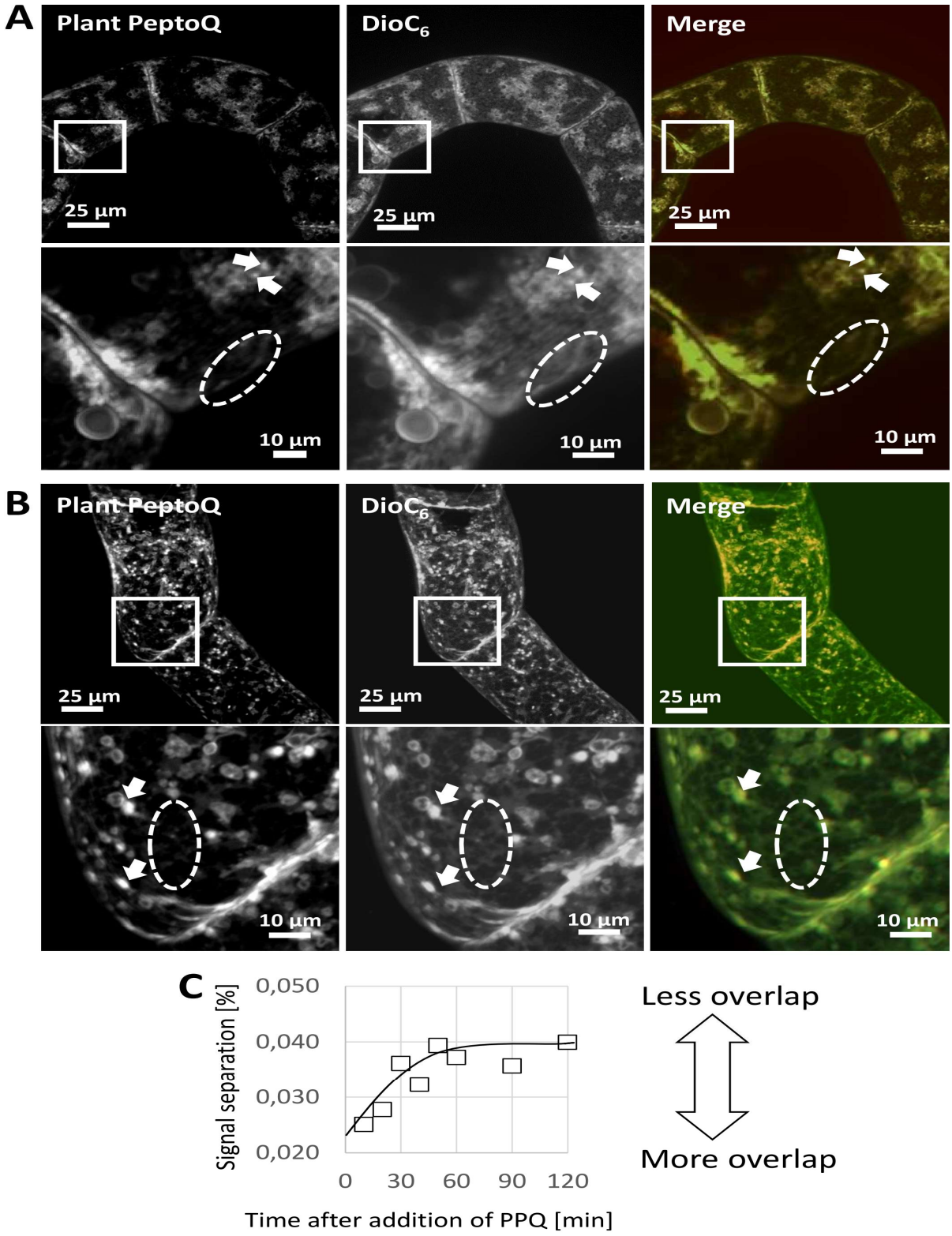

Figure 14: Dual labelling of plant PeptoQ with DioC6. Tobacco BY-2 cells collected at day 3 after subcultivation were incubated for different time intervals with 2 µM plant PeptoQ, and further labelled with 2.5 µg/ml DiOC6 immediately (incubated for 10 min) prior to observation by spinning-disc microscopy. The plant PeptoQ signal as reported by the

rhodamine reporter, and DiOC6 signal as reported by the green channel, as well as the merge of both channels is shown exemplarily for an early time point (10 min after addition of the plant PeptoQ) in **A**, and for a late time point (120 min after addition of the plant PeptoQ) in **B**. The yellow colour in the merge picture indicates overlap of both signals, bold white arrows indicate putative mitochondria, the white ellipse shows a site, where the ER is labelled, while the plant PeptoQ is only weakly detectable (indicated by the green colour in the merge). **C** Time course of separation between plant PeptoQ and DioC6 signals. Individual pixel intensities of the two signals were subtracted and normalised over the mean intensity of the DioC6 signal. Data represent mean values and standard errors. Full overlap of both signals would yield a value of 0%, complete separation of both signals would produce a value of 100%.

Similarly, to visualize mitochondria during the uptake of plant PeptoQ, 0.1% v/v of MitoTracker Green FM was added at different time intervals after treating tobacco BY-2 cells with 2 µM rhodamine B labelled plant PeptoQ. Mitotracker Green FM is a voltage sensitive dye for mitochondria, but also cross-labels the endoplasmic reticulum to a certain extent (Cruz et *al.*, 2011). At 10 min after addition of the plant PeptoQ, used as early time point, numerous speckles were labelled by Mitotracker Green FM, presumably representing mitochondria, along with reticulate structures and vesicles in-between, presumably representing the endoplasmic reticulum (Fig. 15A). In the signal merge, both structures appeared yellowish, indicative of simultaneous presence of Mitotracker Green FM and plant PeptoQ. Adjacent to the cross wall, the plant PeptoQ signal was dominating (Fig. 15A, white ellipse). When Mitotracker Green FM was added 120 min after the plant PeptoQ, the reticulate structures between mitochondria appeared mostly green, indicative of a depletion from the plant PeptoQ. Similar to the DioC6 experiment, the signal separation (Fig. 15B) was quantified and observed a similar time course, except that the curve levelled off at values that were around 10% higher as those seen for $DioC_6$, linked with a weaker labelling of the endoplasmic reticulum by Mitotracker Green FM signal as compared to $DioC_6$.Thus, both fluorescent dyes report accumulation of the plant PeptoQ in the mitochondria from an intermediate pool that is in the endoplasmic reticulum.

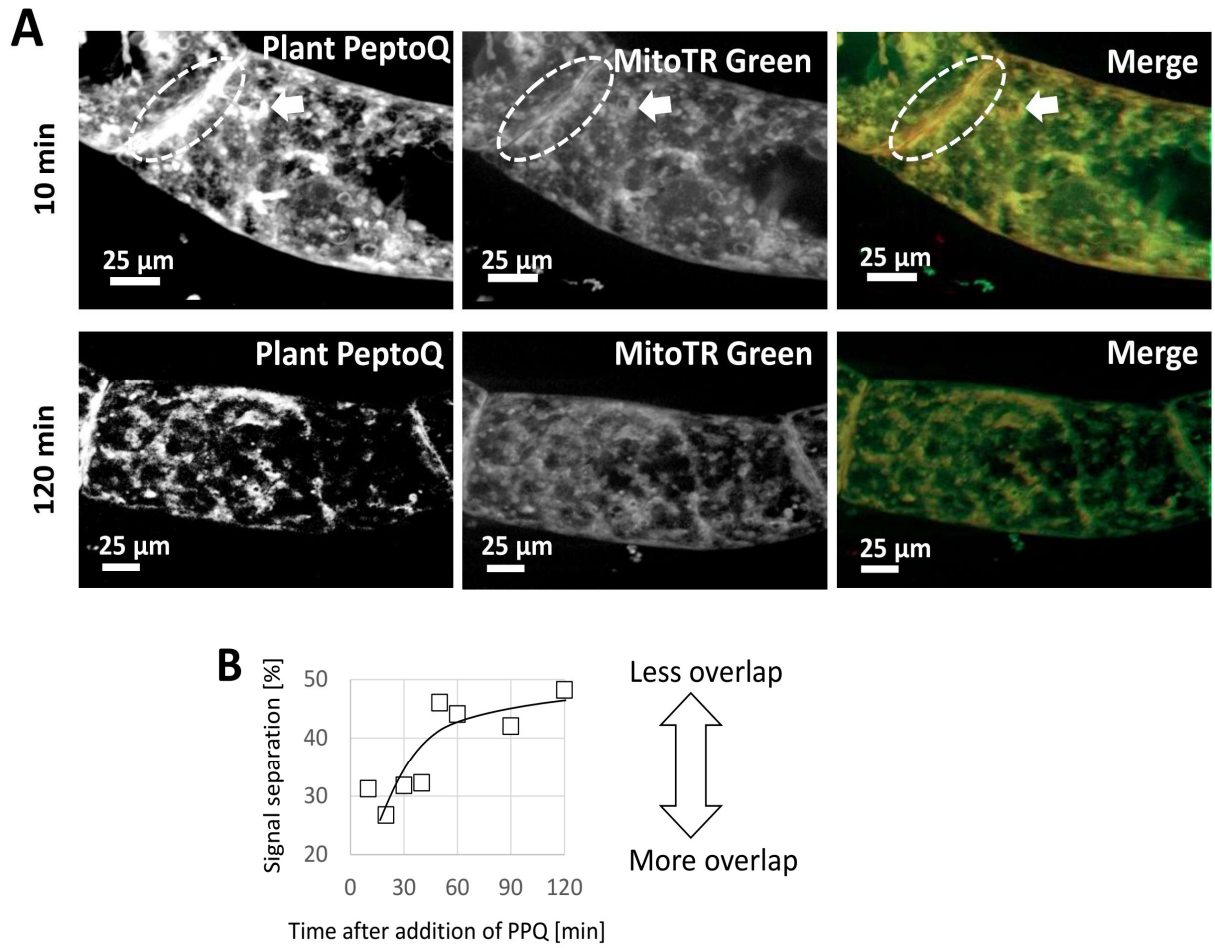

Figure 15: Dual labelling of plant PeptoQ (PPQ) with Mitotracker Green FM. Tobacco BY-2 cells collected at day 3 after subcultivation were incubated for different time intervals with 2 µM plant PeptoQ, and further labelled with 0.1 % Mitotracker Green FM, incubated for 5 min, and then visualized by spinning-disc microscopy. The plant PeptoQ signal as reported by the rhodamine reporter, and the Mitotracker Green FM signal as reported by the green channel, as well as the merge of both channels is shown exemplarily for an early (10 min after addition of the plant PeptoQ), and a late time point (120 min after addition of the plant PeptoQ). The yellow colour in the merge picture indicates overlap of both signals, bold white arrows indicate putative mitochondria, the white ellipse shows a site, where the plant PeptoQ signal is dominant in vicinity of the cross-wall, while the Mitotracker Green FM signal is weak. **B** Time course of separation between plant PeptoQ and Mitotracker Green FM signals. Individual pixel intensities of the two signals were subtracted and normalised over the mean intensity of the signal for Mitotracker Green FM. Data represent mean values and standard errors. Full overlap of both signals would yield a value of 0%, complete separation of both signals would produce a value of 100%.

3.4. The role of cytoskeleton in the cellular uptake of plant PeptoQ

The role of cytoskeleton such as actin filaments and microtubules in the cellular uptake of plant PeptoQ by the WT tobacco BY-2 cells was investigated.

3.4.1. The role of actin filaments in the cellular uptake of plant PeptoQ

The marker cell line GF11, where actin filaments are visualized by a fusion of the actin-binding domain 2 of *Arabidopsis thaliana* fimbrin with Green Fluorescent Protein (GFP) as reporter was used to investigate the role of actin filaments in the cellular uptake of the plant PeptoQ. To test whether actin is involved in the cellular uptake of plant PeptoQ, GF11 cells were pretreated with 10 µM of Latrunculin B (sufficient to completely eliminate actin filaments), a specific inhibitor that sequesters G-actin from assembly into F-actin and incubated for 1 h. The pretreated cells were further treated with 2µM plant PeptoQ for 2 h. The confocal spinning disc microscopic observation showed strong impairment of the plant PeptoQ internalization into the GF11 cells (Fig. 16D, E) characterized by the presence of only few punctate signals lining the nuclear envelope and the shift of the nuclei to the cross walls. Furthermore, at the lateral walls, there were signals lining the cell membranes which is similar to the case observed with Ikarugamycin treatments (compare Figs. 16D and 12F). Occasionally a double line could be visualized at the cross walls, that might represent the cell membranes of the two neighbouring cells (Fig. 16E, inset). In the control GF11 cells, the colocalization between the signal from the plant PeptoQ conjugated rhodamine B and GFP labelled actin filaments was assessed by spinning disc confocal microscopy (Figs. 16A-C). The actin filaments were intact, and the mitochondria were aligned along them as it is evident from the effective colocalization between the red and green fluoresces. The dual labelling revealed the mitochondria (Fig. 16C, inset, asterisks) where actin filaments were also labelled partially by the rhodamine B signal (Fig. 16B, indicated by an arrow). From the above observations, it is possible to infer that actin filaments are required for the cellular uptake and the mitochondrial localization of the plant PeptoQ.

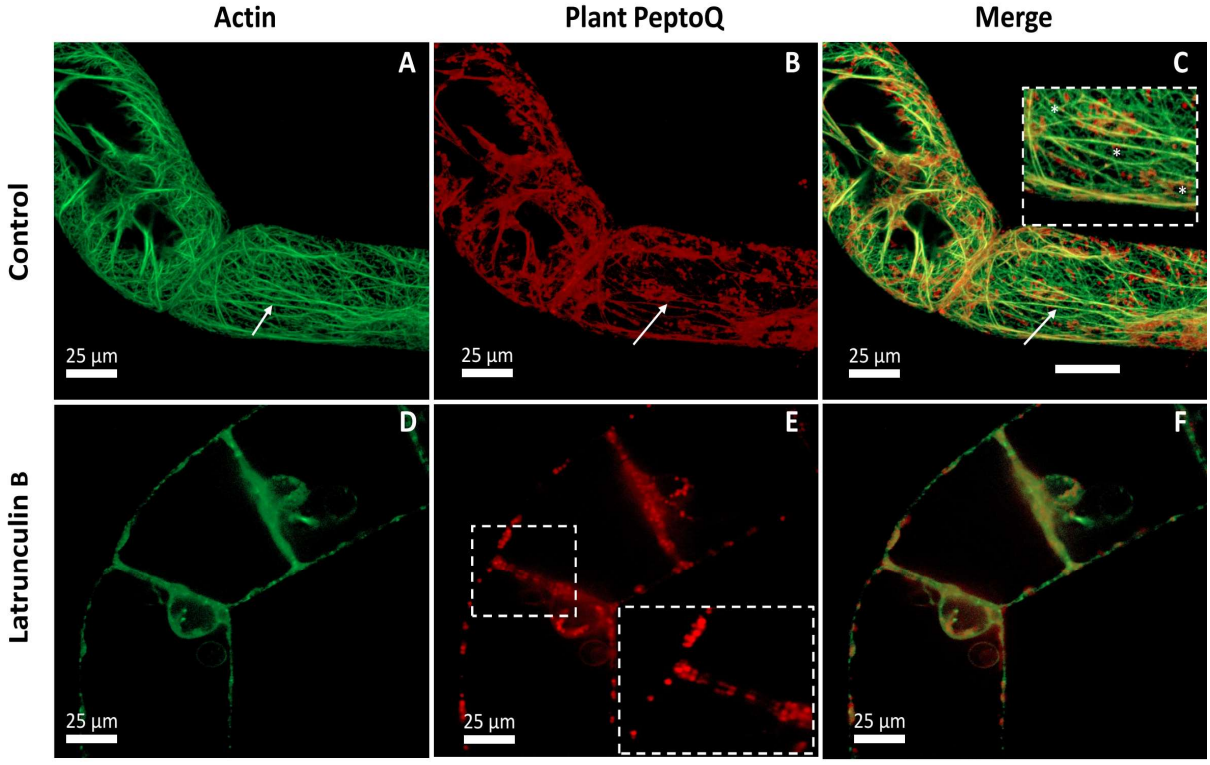

Figure 16: Uptake of plant PeptoQ depends on actin. Cells of the actin marker line GF11 (collected at day 3 after subcultivation) were incubated with 2 µM of plant PeptoQ for 2 h either without (**A-C**) or with (**D-F**) elimination of actin filaments by Latrunculin B (10 µM, 1 h). The GFP signal recording actin (**A, D**), the rhodamine signal recording the plant PeptoQ (**B, E**), and the merged signal (**C, F**) is shown in a central confocal section of representative cells. The inset in **C** highlights the association of the rhodamine-labelled mitochondria with actin filaments (asterisks), the white arrow in **A-C** the association of the rhodamine signal along actin, the inset in **E** the signals lining the two sides of the cross wall after treatment with Latrunculin B. Adapted from Asfaw et al., 2019.

3.4.2. The role of microtubules in the cellular uptake of plant PeptoQ

In analogy to actin filaments, the cell line expressing the beta-tubulin TuB6 from *Arabidopsis thaliana* fused with the Green Fluorescent Protein was used to assess the potential role of microtubules in the internalization of the plant PeptoQ. To eliminate microtubules, TuB6 cells were pretreated with 10 µM Oryzalin, a plant-specific inhibitor of microtubules, for 1 h, so as to eliminate microtubules, followed by treatment with 2 µM plant PeptoQ and with 2 h subsequent incubation. Microtubules were completely eliminated by Oryzalin pretreatment which was accompanied by more prominent fluorescent background signal (Fig. 17D). There was effective cellular uptake of plant PeptoQ irrespective of the complete elimination of microtubules by Oryzalin (Figs. 17E, F). Cortical microtubules were clearly seen against the background that might come from non-assembled tubulin heterodimers in the control which lacks pretreatment by Oryzalin (Fig. 17A). When the rhodamine B signal from the labelled plant PeptoQ was colocalized with the microtubule signal from attached GFP (Fig. 17B), at the first instance, the merged figure (Fig. 17C) looks alike the one seen for actin. However, in a profound and closer look, it could be realized that some mitochondria were colocalised with microtubules, often with a deviation orientation (Fig. 17C, white arrows in the inset). Therefore, microtubules are not involved in the cellular uptake of plant PeptoQ.

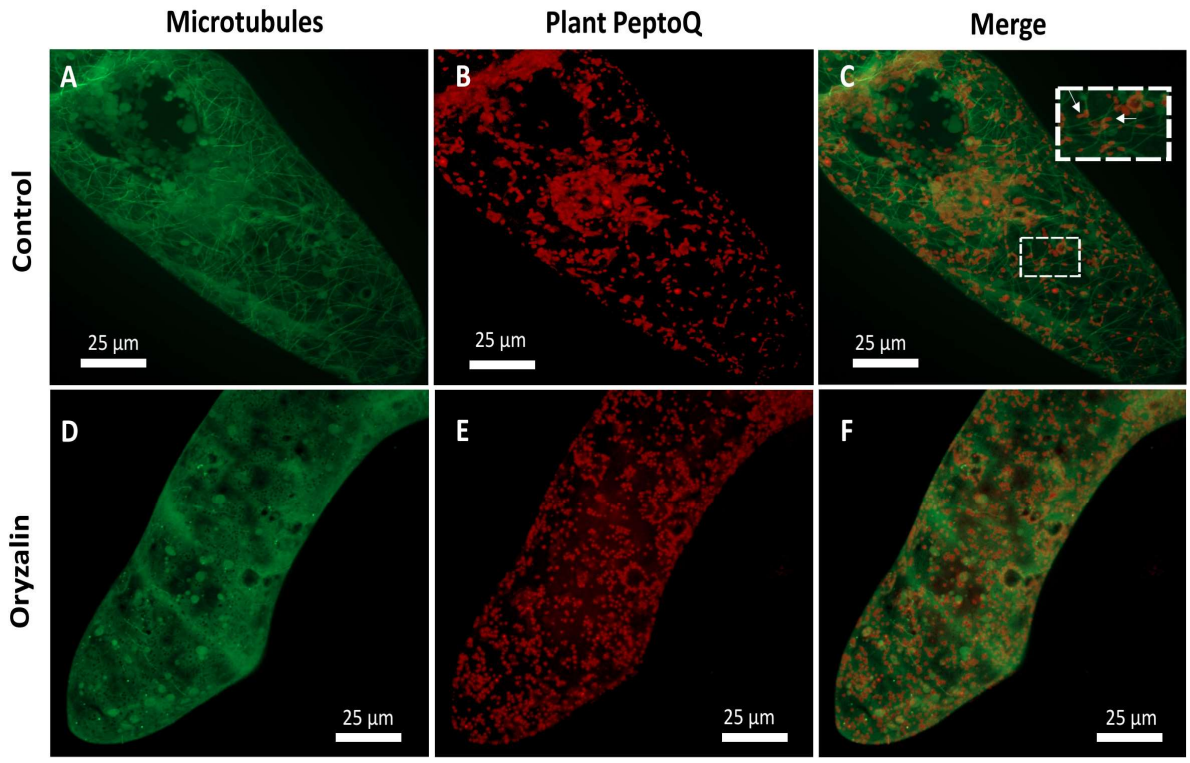

Figure 17: Uptake of plant PeptoQ does not depend on microtubules. Cells of the microtubule marker line AtTuB6 (collected at day 3 after subcultivation) were incubated with 2 µM of plant PeptoQ for 2 h either without (**A-C**) or with (**D-F**) elimination of microtubules by Oryzalin (10 µM, 1 h). The GFP signal recording tubulin (**A, D**), the rhodamine signal recording the plant PeptoQ (**B, E**), and the merged signal (**C, F**) is shown for representative cells. The inset in **C** highlights cases, where the rhodamine-labelled mitochondria deviate in their orientation from the microtubule (arrows). Adapted from Asfaw et al., 2019.

3.5. Potential cytotoxicity of plant PeptoQ

As a matter of fact, a tool for chemical manipulation should not impose toxicity on the target cell. Therefore, potential toxic effects of plant PeptoQ on WT BY-2 cells was scrutinised after loading with 2 µM plant PeptoQ for 2 h and then followed potential changes of mortality by the membrane-impermeable dye Evans Blue (2.5% w/v). It has been observed that the cells excluded the dye both in control cells as well as in cells incubated with the plant PeptoQ (Fig. 18A), cell toxicity was low (<5%) in both cases and there was no significant difference for the cells treated with the plant PeptoQ, even for prolonged cultivation for 96 h (Fig. 18B). Furthermore, the potential toxicity in response to increasing concentrations of plant PeptoQ (2, 4, 8, 16, 25, 40 and 50 µM) was followed over prolonged time (24, 48, 72, and 96 h) but any indication of increased cell toxicity could not be detected (Fig. 19). Mortality was below 5% throughout. To test whether the time frame of up to 96 h was sufficient to pick up potential programmed cell death, cell death induced by high salt stress (150 mM NaCl) was used as positive control. Here, the full level of mortality (60%) was already reached after 24 h with only minor increases during the subsequent days.

Since the plant PeptoQ was found to fully preserve the physiology of the treated cells even for prolonged incubation, in the next step, it has been asked, whether a pretreatment with plant PeptoQ could mitigate cellular damage imposed by disrupted oxidative balance in the mitochondria. Thus, moderate salt stress (75 mM NaCl) was used as stressor which induced significant toxicity, accompanied by cytosolic shrinkage, breakdown of cytoplasmic structure, and loss of membrane integrity as visualised by the penetration of Evans Blue (Fig. 18A). The mortality induced by 75 mM NaCl reached almost 50% within 24 h but dropped subsequently over the following days to around 20%, indicative of progressive adaptation and proliferation of surviving cells compensating for the initial mortality (Fig. 18B). This decrease is not caused by a resurrection of dead cells, but simply by the fact that dead cells of a suspension culture grown on the shaker, rapidly decay to debris and therefore eclipse from the sampling population, while surviving cells will proliferate. The decrease of mortality, therefore, reflects the level of adaptation and subsequent recovery. When the cells were pretreated with the plant PeptoQ prior to the salt stress, the initial mortality was much lower (from almost 50% to around 25%), and the subsequent recovery proceeded more rapidly, until 96 h after the onset of salt stress, only 7% of cells were found to be dead, which was not significantly different from cells that had not experienced any salt stress (Fig. 18B). This means that the plant PeptoQ not only did not impose any toxicity, but in addition significantly improved the survival and adaptation to salt stress. To test, whether this mitigation effect was dependent on the presence of rhodamine moiety, mortality under high salt stress (150 mM NaCl) was probed over two days (Fig. 18C). The unconjugated peptoid seemed to be slightly more effective than its rhodamine conjugate, but the difference was not significant. What was highly significant, however, was the mitigation of mortality in the peptoid treated samples.

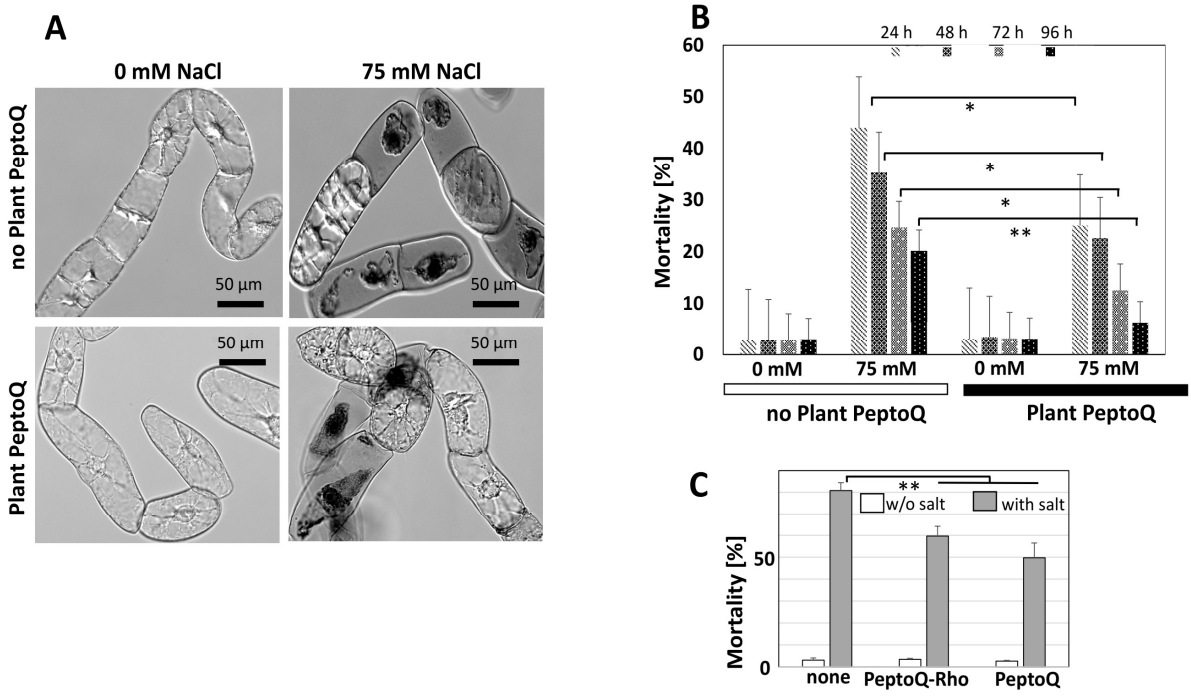

Figure 18: Plant PeptoQ does not cause any toxicity and mitigates the mortality caused by salt stress. **A** Representative cell were probed by the Evans Blue dye exclusion test. **B** Time courses of mortality. **C** Mitigation of salt-induced mortality (150 mM NaCl) by plant PeptoQ is independent of conjugation to rhodamine (PeptoQ-Rho) or absence of rhodamine moiety (PeptoQ). Data represent means and standard errors from at least three independent experimental series scoring samples of 1000 individual cells. Moderate salt stress (75 mM NaCl) was administered from 2 h after the addition of the plant PeptoQ. ** indicate differences that are significant at $P \leq 0.01$, * at $P \leq 0.05$ based on a student's t-test. Adapted from Asfaw et al., 2019.

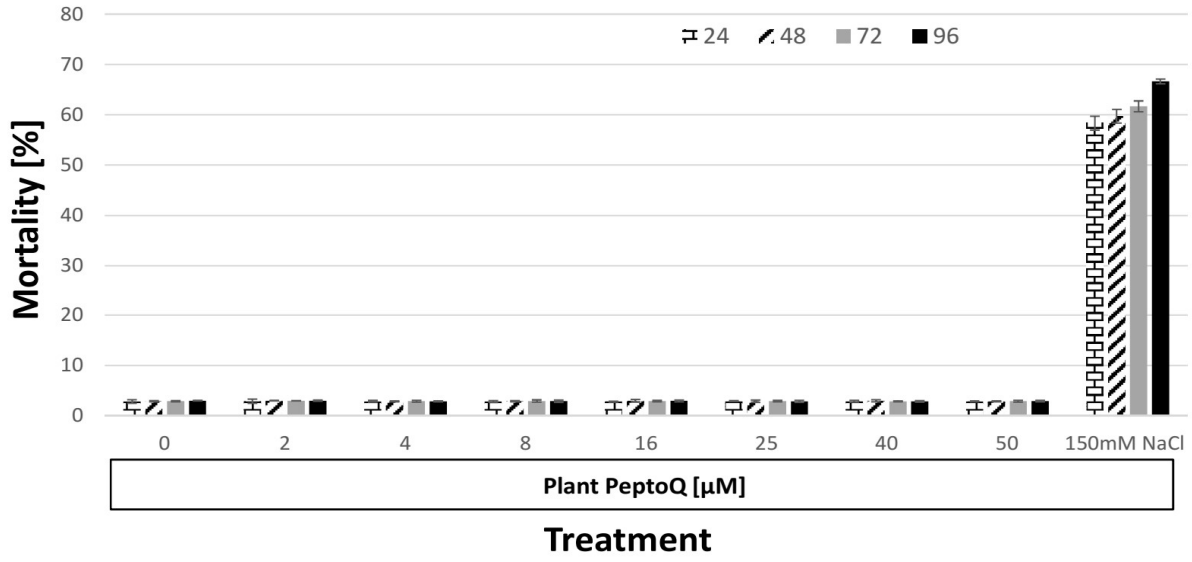

Figure 19: Effect of plant PeptoQ in different concentrations (from 0-50 µM) and salinity stress upon viability of tobacco BY-2 cells scored at different time points (24, 48, 72 & 96 h). Data represent mean and standard errors from three different biological replicates, representing a sample population of 1000 cells per replicate. Adapted from Asfaw et al., 2019.

3.6. Effect of plant PeptoQ on mitochondrial fragmentation

On the other hand, whether plant PeptoQ could suppress mitochondrial fragmentation caused by disturbed electron transport that emanates from exposure to salt stress or not was tested. At day 3 after subcultivation, WT tobacco BY-2 cells were pretreated with plant PeptoQ (incubated for 2 h), exposed to moderate salt stress (75 mM NaCl), and followed by the determination of mitochondrial area coverage at 2 and 24 h after the onset of salt stress. In the control, mitochondria were characterized by ovoid shape, and decayed into small fragments following treatment with 75 mM NaCl (Fig. 20A). However, in WT BY-2 cells that were pretreated with plant PeptoQ, the detrimental effect of salt stress was partially mitigated (Fig. 20B).

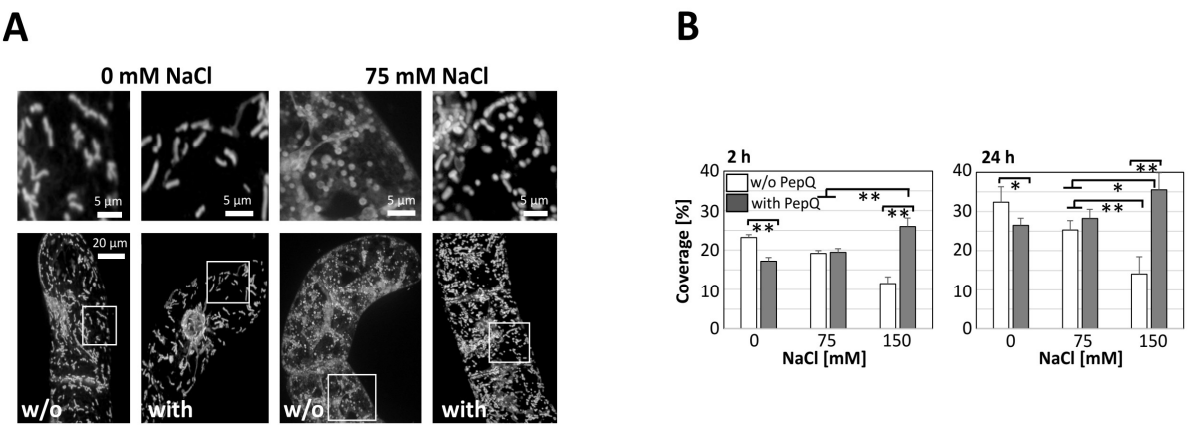

Figure 20: Effect of the plant PeptoQ on mitochondrial morphology and coverage. **A** Mitochondrial morphology in controls (0 mM NaCl) versus moderate salt stress (75 mM NaCl) in the absence (w/o), or presence (with) of plant PeptoQ (2 µM) 2 h after the onset of salt stress. The insets are given as zoom-ins in the upper row to show the differences in mitochondrial shape. **B** Mitochondrial coverage after 2 (left), or 24 h (right) of treatment with different concentrations of NaCl. Data represent mean values and standard errors of three independent experimental series. ** indicate differences significant at $P \leq 0.01$, *at $P \leq 0.05$ based on a student's t-test. Adapted from Asfaw et al., 2019.

3.7. Internalisation of plant PeptoQ into the real plant cell system

To investigate the cellular uptake of plant PeptoQ by real plant cell system, the rice cultivar Nipponbare (*Oryza sativa* L. ssp.*japonica* cv. Nipponbare) was used. Five days old germinated seeds were taken, and the roots were cut into three parts such as root tip, elongation zone and maturation zone by means of razor blade. Each root section was placed on separate 35mm petri dish, supplied with 4 ml distilled water and incubated with rhodamine B labelled plant PeptoQ for 2 h. Finally, washed with double distilled water three times, treated with 0.1% v/v of MitoTracker Green FM dye, incubated for 5 min and observed under confocal spinning disc microscope. The result showed a significant cellular uptake of plant PeptoQ both by the main root (Fig. 21 B) and the root hairs (Fig.22 B) system. Furthermore, there was remarkable and clear colocalisation between the green fluorescence from mitochondrial dye, MitoTracker Green FM and the rhodamine B signal attached to the plant PeptoQ (Fig. 21C and Fig. 22 C). The intensity of colocalisation is similar to the colocalization observed in the 6 days old tobacco BY-2 cells (compare Figs.11C, D, E, 21C and 22C.). Overall, the result implies that the plant PeptoQ could enter into the real plant cells system such as rice root and localized in the mitochondria as a final destination.

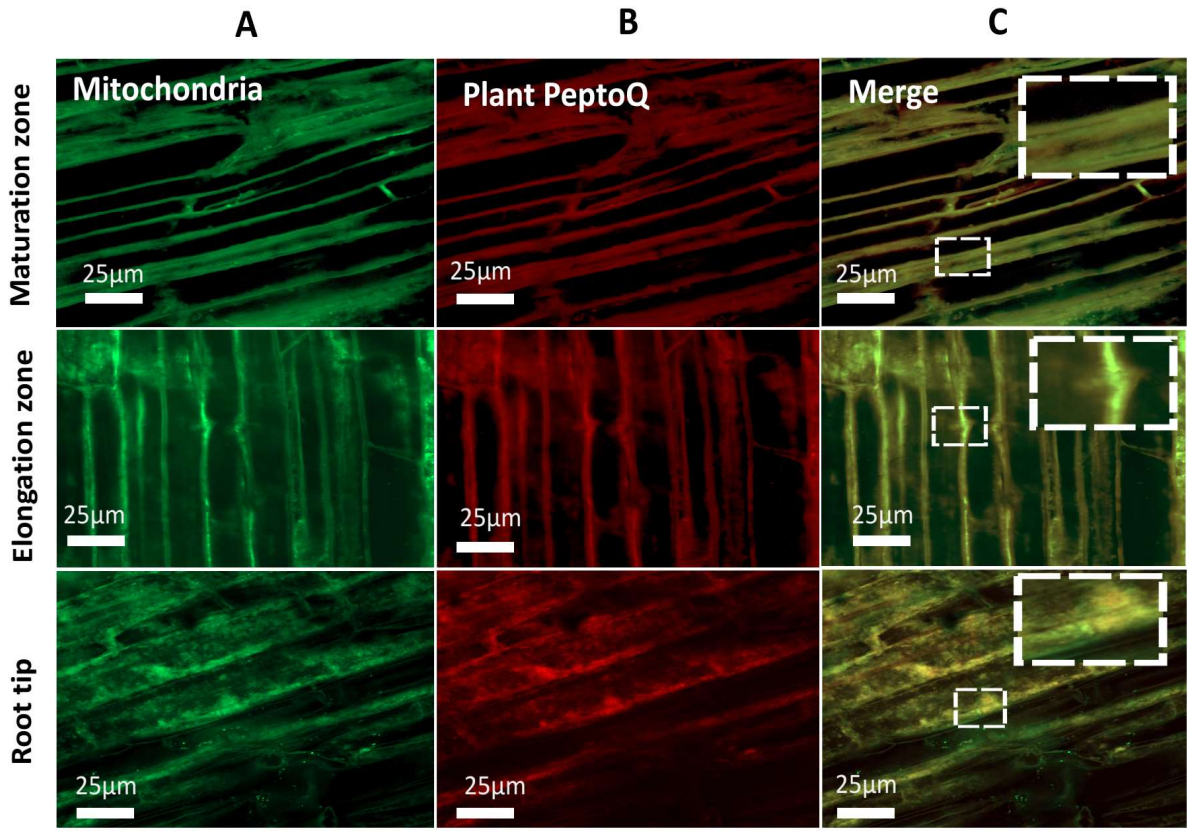

Figure 21: Cellular uptake and mitochondrial localization of the plant PeptoQ in rice root (root tip, elongation zone and maturation zone) assessed on 5 days old germinated seeds. Cells were incubated for 2 h with 2 µM plant PeptoQ followed by labelling with MitoTracker Green FM and then visualised using spinning disc confocal microscopy making use of the fluorescent signal from MitoTracker Green FM **(A)**, and the rhodamine signal from the labelled plant PeptoQ (**B**). The merge of the two channels shown in (**C**) shows the close overlap of both signals. Confocal sections recorded in the mid-plane from representative cells recorded at constant laser power and exposure time are shown.

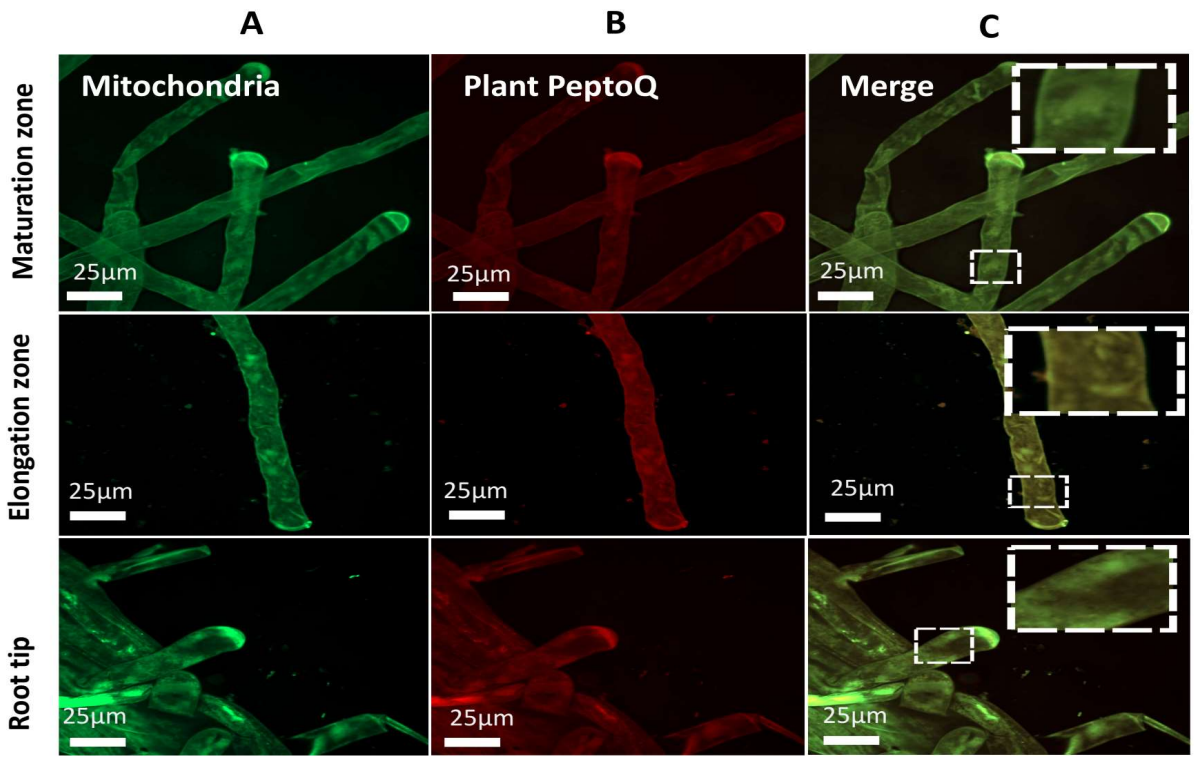

Figure 22: Cellular uptake and mitochondrial localization of the plant PeptoQ in rice root hairs (root tip, elongation zone and maturation zone) assessed on 5 days old germinated seeds. Cells were incubated for 2 h with 2 µM plant PeptoQ followed by labelling with MitoTracker Green FM and then visualised using spinning disc confocal microscopy making use of the fluorescent signal from MitoTracker Green FM **(A)**, and the rhodamine signal from the labelled plant PeptoQ (**B**). The merge of the two channels shown in (**C**) shows the close overlap of both signals. Confocal sections recorded in the mid-plane from representative cells recorded at constant laser power and exposure time are shown.

3.8. Effects of plant PeptoQ on the salt tolerance of wild type tobacco BY-2 cells

The role of plant peptoQ in mitigating salt stress-induced deleterious effects with respect to numerous aspects including cell proliferation, expansion and viability, ionic balance, redox homeostasis and gene expression was investigated profoundly.

3.8.1. Plant PeptoQ mitigates the impact of salt stress on cell growth, proliferation, expansion, and viability

3.8.1.1. Packed cell volume (PCV)

The packed cell volume (PCV), an indicator of cell growth was measured at day 7 after subcultivation. It showed significant decrease at high salt stress (150 mM NaCl) but it was not affected at moderate salt stress (75 mM NaCl) in WT BY-2 cells both with and without plant PeptoQ pretreatment (Fig. 23). In both cell samples, there

was slightly higher percentage of packed cell volume [PCV (%)] at moderate salt stress (75 mM NaCl) as compared to the control (0 mM NaCl). This implies that moderate salt stress (75 mM NaCl) stimulates cell growth to a certain extent. At both moderate (75 mM NaCl) and high (150 mM NaCl) salt stress there was no significant difference in PCV (%) between WT BY-2 cells in the presence and absence of plant PeptoQ pretreatment.

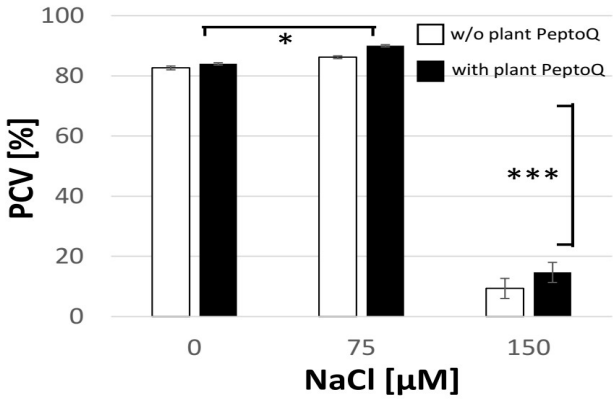

Figure. 23: Effect of plant PeptoQ on cell growth. The percent packed cell volume [PCV (%)] at the control (0 mM NaCl), moderate (75 mM NaCl) and high (150 mM NaCl) salt stress. Data represent mean values and standard errors of three independent experimental series. *** indicate differences significant at $P \leq 0.001$, *at $P \leq 0.05$ based on a student's t-test.

3.8.1.2. Cell density

Salinity caused a drastic decline in cell proliferation activity, and this decline was mitigated by pretreatment with plant PeptoQ (Fig. 24). Even for moderate salt stress (75 mM NaCl), cell density was reduced as compared to the control (Fig. 24A). This decrease was already significant (29%) at the first measured time point (24 h), and became progressively accentuated with time, with 44% inhibition at 48 h, 60% at 72 h, and 68% at 96 h. After pretreatment with plant PeptoQ, this decrease of cell density was significantly dampened (Fig. 24B). This effect was detectable already at 24 h (21% reduction as compared to 29% in the experiment without peptoid) and persisted throughout the experiment (45% reduction as compared to 68% at 96 h after the onset of salt stress). For high salt stress (150 mM NaCl), proliferation was almost completely suppressed, leaving only 8.2% (at 96 h) of the activity seen for untreated control (Fig. 24A). Here, the pretreatment with plant PeptoQ restored some of the proliferation with 14.7% (at 96 h) compared to the untreated control (Fig. 24B). From the time courses of proliferation, doubling times were estimated based on an exponential growth model (Fig. 24C). In the absence of salt stress, cell number doubled once a day independently of presence or absence of the peptoid. For moderate salt stress (75 mM NaCl), doubling increased to 39 h in the absence of the peptoid, while in presence of the peptoid, the delay was milder (30 h). For high salt stress (150 mM NaCl), doubling became virtually arrested in absence of the peptoid (with a hypothetical time of 330 h required to complete one cycle), while in presence of the peptoid, the doubling was slowed down strongly as well, but significantly less (81 h).

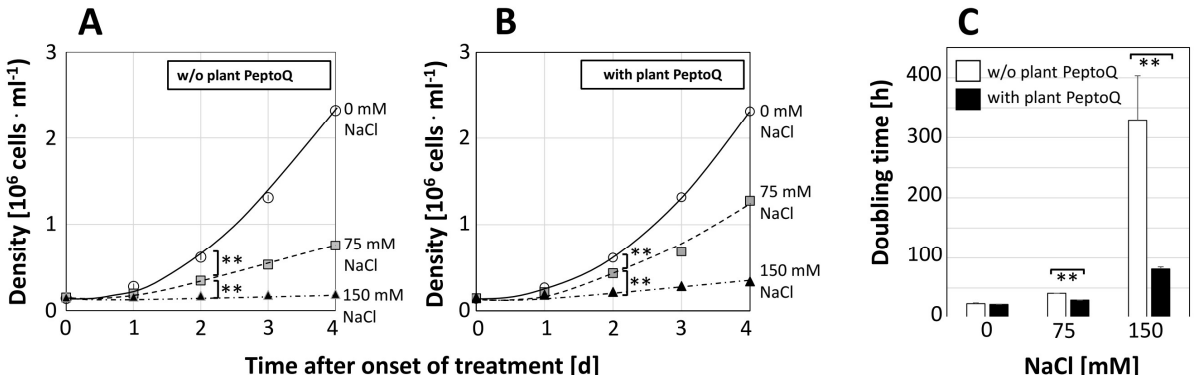

Figure 24: Effect of the plant PeptoQ on salt-induced inhibition of cell proliferation in WT tobacco BY-2 cells. Time courses of cell density in the absence of salt stress (0 mM NaCl, open circles), under moderate (75 mM NaCl, grey squares), and under high salt stress (150 mM NaCl, black triangles) without (**A**) or with (**B**) plant PeptoQ (2 µM). **C** Doubling time estimated from the time constant of exponential growth over the concentration of NaCl without (white bars) or with (black bars) plant PeptoQ (2 µM). Data represent mean values and standard errors of three independent experimental series. ** indicate differences significant at $P \leq 0.01$ based on a student's t-test.

3.8.1.3. Cell length and width

Cell length was measured at day 3 and day 7 after subcultivation when the cells enlarge their central vacuole (Fig. 25). The relative growth rate was measured through the percent in cell length change. In the absence of the peptoid, relative growth rate decreased drastically already for moderate salt stress (at 75 mM NaCl, less than 30% residual growth as compared to 0 mM NaCl). For high salt stress (150 mM NaCl), the values became even negative, meaning nothing else than that the cells shrank, presumably because the osmotic potential in the medium was more negative than that of the protoplast. In presence of the peptoid, the decline of cell expansion was clearly compensated: at 75 mM NaCl, the same growth rate was observed as in the non-stressed controls, meaning that the cells were able to fully compensate the negative osmotic potential of the medium. Even at high salt stress (150 mM NaCl), a residual expansion of around 30% was maintained (i.e. a level comparable to that seen for 75 mM NaCl in the absence of peptoid). Thus, application of plant PeptoQ fully compensated the impact of moderate salt stress (75 mM NaCl) upon cell expansion, and even for high salt stress (150 mM NaCl) allowed for a partial mitigation. As compared to the effects seen on cell proliferation under salt stress, cell expansion seemed to be more responsive to the peptoid treatment. Salt stress had no significant effect on cell width in WT BY-2 cells both in the presence and absence of plant PeptoQ pretreatment. However, cell length(L) to width(W) ratio (L: W) was significantly decreased in WT BY-2 cells both with and without plant PeptoQ pretreatment at day 3 and day 7. In the former time point, there was no significant difference in the two cell samples (Fig. 25B) but in the latter one, BY-2 cells with and without plant PeptoQ pretreatment attained significantly different L to W ratio (Fig. 25C). The Plant PeptoQ pretreated BY-2 cells displayed better L to W ratio as compared to those cells without plant PeptoQ pretreatment. Thus, this displays that the plant PeptoQ

pretreated BY-2 cells attained elongated and less broader cells as compared to BY-2 cells in the absence of plant PeptoQ pretreatment**.**

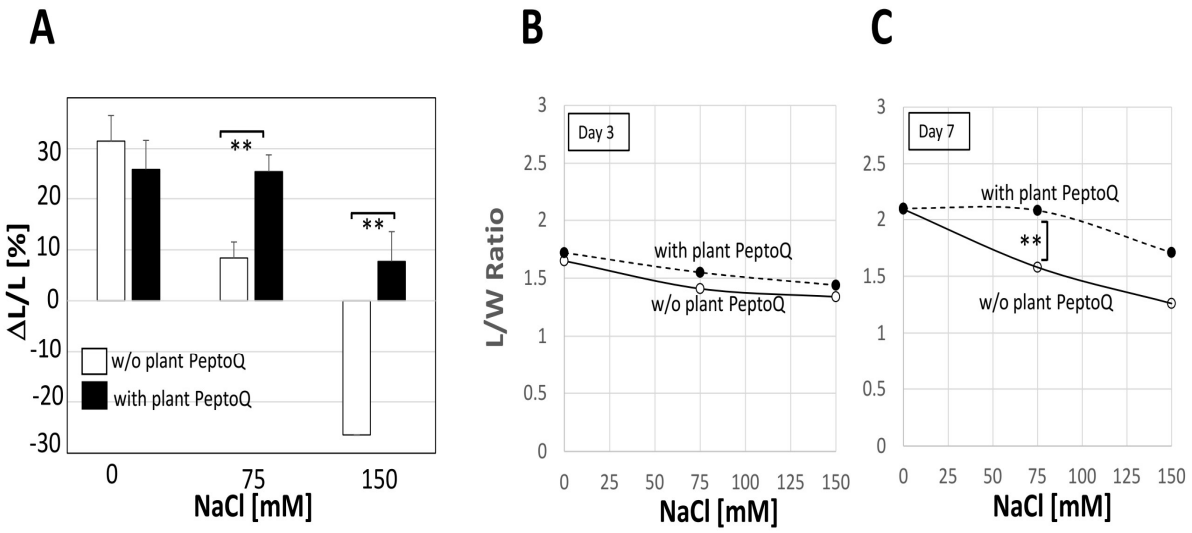

Figure 25: Effect of the plant PeptoQ on salt-induced inhibition of cell expansion in tobacco BY-2 cells. **A** relative elongation during the expansion phase (days 3 to 7 after subcultivation) in controls (0 mM NaCl), under moderate (75 mM NaCl), and under high (150 mM NaCl) salt stress. Cell length to width (L/W) ratio at day 3(**B**) and day 7(**C**) in the absence or presence of plant PeptoQ (2 µM) at the control (0mM NaCl), moderate (75 mM NaCl) and high (150 mM NaCl) salt stress. Data represent mean values and standard errors of three independent experimental series. ** indicate differences significant at $P \leq 0.01$ based on a student's t-test.

3.8.1.4. Cell viability

Arrested proliferation in response to salt stress is usually followed by cell death. Thus, cell mortality in response to salt stress over 96 h was followed using the Evans Blue Dye Exclusion assay (Fig. 26). Under moderate salt stress (75 mM NaCl, Fig.26B), in the absence of the peptoid, cell mortality first increased sharply to more than 40% at 24 h, but decreased subsequently over time to 20% (96 h), since the surviving cells continued to proliferate, while the dead cells were not able to do so. While this temporal pattern was also seen in presence of plant PeptoQ, the amplitude of the mortality response was strongly reduced: here, the peak of mortality at 24 h was only 25%, and dropped to 6% at 96 h, which means nothing else than that these cells had fully returned to the viability seen prior to salt stress. For high salt stress (150 mM NaCl, Fig. 26C), the cells were not able to recover viability, at least not during the considered time interval of 96 h. In the absence of the peptoid, about 80% of the cells had died within the first day after addition of salt, and the death toll increased further during the subsequent days reaching to more than 90% (at 96 h). While plant PeptoQ was not able to suppress this salt-induced mortality, it did significantly reduce its amplitude. Even 96 h after the onset of salt stress, still one third of the cells had remained alive (mortality was 67%).

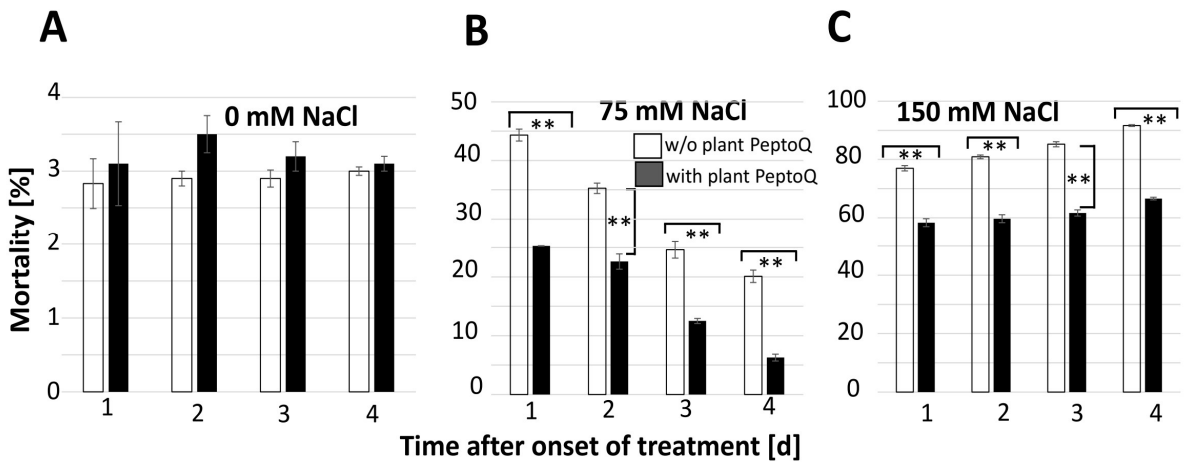

Figure 26: Effect of the plant PeptoQ on salt induced mortality in WT tobacco BY-2 cells. Time courses of mortality in absence or presence of plant PeptoQ (2 µM) at the control(**A**), moderate (**B**) and high (**C**) salt stress. Data represent mean values and standard errors of three independent experimental series. ** indicate differences significant at P ≤ 0.01 based on a student's t-test.

3.8.1.5. Mitotic Index (MI)

Mitotic index (MI) measurement started just after subcultivation and continued until 96 h (day 4). In general, MI increased at the control (0 mM NaCl), moderate (75 mM NaCl) and high (150 mM NaCl) salt stress as the incubation time increased from day 0 to day 1 (24 h). However, it decreased as the incubation time proceeds from 24 (day 1) to 96 h (day 4) both at the control and the salt stress. Moreover, the percent decline in MI, at moderate and high salt stress was more prominent in BY-2 cells without peptoid as compared to those with peptoid (Fig. 27). Thus, in BY-2 cells without peptoid, it decreased from 62% (24 h) to 46% (96 h) at moderate salt stress (Fig. 27B) but it increased from 72% (24 h) to 79 %(96h) at high salt stress (Fig. 27C) exceptionally. On the other hand, in BY-2 cells with peptoid, the percent decrease in MI, dropped from 36% (24 h) to 9% (96 h) at moderate (75mM NaCl) and from 59% (24 h) to 45% (96 h) at high (150mM NaCl) salt stress as compared to the control (Fig.27B,C). Except the fact that in BY-2 cells without plant PeptoQ pretreatment, at high salt stress (150 mM NaCl), the maximum decline in MI (compared to the control) was being at 96 h, in all the rest cases, the maximum declines in MI were registered at 24 h incubation time and high salt stress (150 mM NaCl).

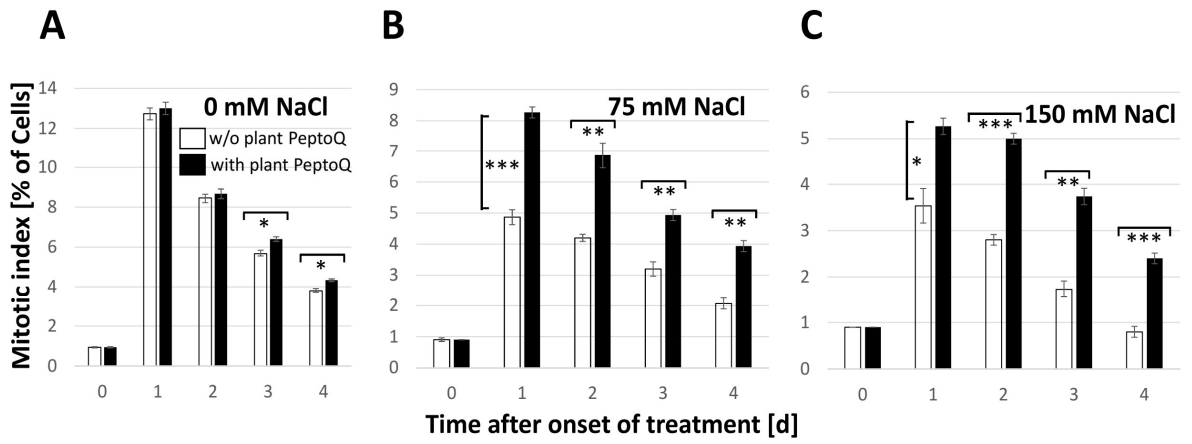

Figure 27: Effect of plant PeptoQ on mitotic index (MI). The value of MI at the control (0 mM NaCl) (**A**), moderate (75 mM NaCl) (**B**) and high (150 mM NaCl) (**C**) salt stress. Data represent mean values and standard errors of three independent experimental series. *** indicate differences significant at $P \leq 0.001$, **at $P \leq 0.01$, * at $P \leq 0.05$ based a student's t-test.

3.8.2. Plant PeptoQ improved oxidative homeostasis under salt stress

3.8.2.1. Lipid Peroxidation

The level of lipid peroxidation can be used as the readout for oxidative degradation of membranes (Heath and Packer, 1968) and measured using the product malondialdehyde (MDA) as readout. To investigate, whether plant PeptoQ can compensate the oxidative effects of salt stress on the WT tobacco BY-2 cells, cells were exposed at the onset of cell expansion (i.e. at day 4 after subcultivation) to salt stress (75 and 150 mM NaCl) either with or without plant PeptoQ pretreatment, and then sampled for MDA determination at 1 and 4 h after treatment along with a negative control not challenged by salt. MDA content increased in a dose- and time dependent manner to more than double of the salt-free control, when 150 mM NaCl were applied both at 1 and 4 h. This increase was strongly (by more than 75%) suppressed by plant PeptoQ. For 75 mM NaCl, the peptoid was even able to suppress the salt-induced increase of MDA steady-state levels completely at both time points (Fig. 28 A, B).

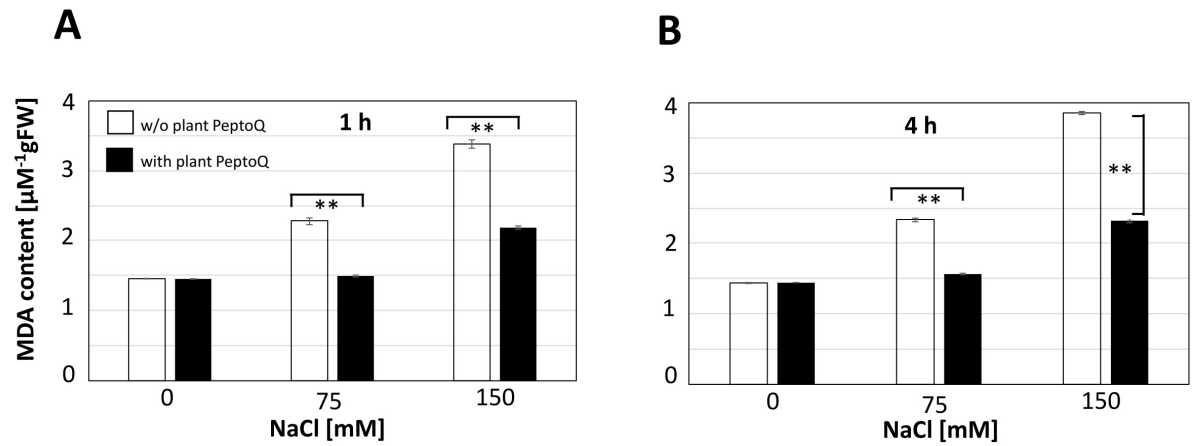

Figure 28: Effect of the plant PeptoQ on lipid peroxidation. Content of malondialdehyde (MDA) at the control (0mM NaCl), moderate (75 mM NaCl), and high (150 mM NaCl) salt stress in WT BY-2 cells without (white square) and with (black square) plant PeptoQ pretreatment at 1 (**A**) and 4 h (**B**). Data represent mean values and standard errors of three independent experimental series. ** indicate differences significant at $P \leq 0.01$ based on a student's t-test.

3.8.2.2. Intracellular Reactive Oxygen Species (ROS)

To understand the observed lipid peroxidation monitored by MDA, intracellular ROS level were investigated using the non-fluorescent dihydrorhodamine 123 (DHR 123), which is converted to the green fluorescent rhodamine 123 upon oxidation, mainly by superoxide ($O_2^{\bullet -}$). The intensity of fluorescence increased progressively, both, in a dose and a time dependent manner, in salt stressed WT BY-2 cells. However, the green fluorescence was quite significantly reduced in salt stressed BY-2 cells pretreated with plant PeptoQ, irrespective of the administered level of salinity, and incubation time (Fig. 29A). Even for high salt stress (150 mM NaCl), the suppression of ROS was almost complete. When the cells were observed at high magnification, the fluorescence was not evenly distributed across the cytoplasm, but accumulated in vesicular structures that according to size and subcellular location (e.g. preferentially near the nucleus) resembled mitochondria. The attempt to double-visualise these ROS-generating structures simultaneously with mitochondria using MitoTracker Green was not successful, because the two dyes interfered optically. The patterns seen for MDA are therefore mirrored by the patterns for intracellular ROS formation. This salt induced ROS formation is associated with particular organelles that might be mitochondria (although conclusive evidence for this statement is still lacking).

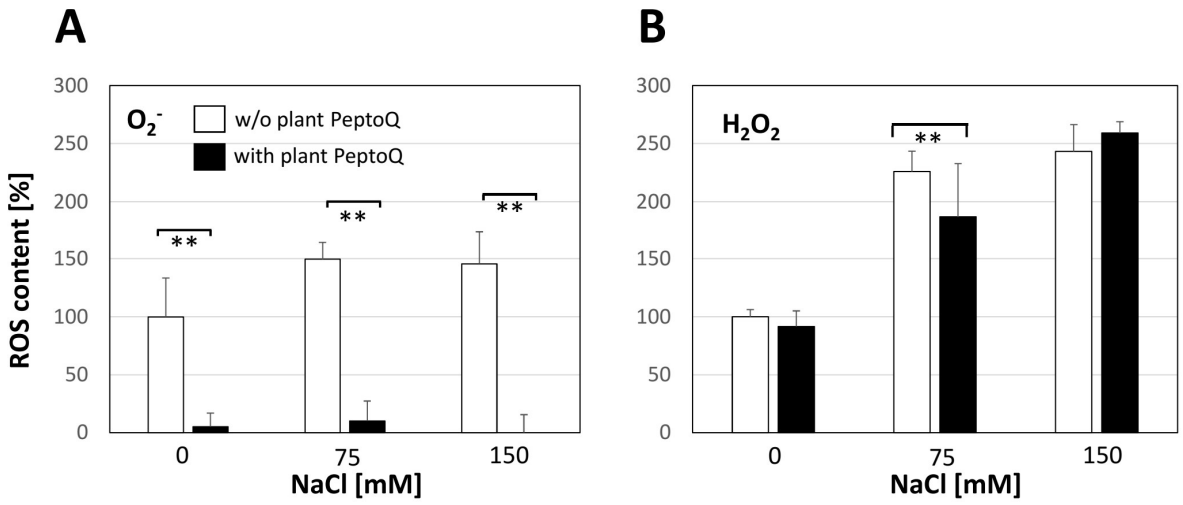

Figure 29: Effect of the plant PeptoQ on oxidative balance. Accumulation of intracellular Reactive Oxygen Species (ROS) in salt stressed WT BY-2 cells without (white square) and with (black square) plant PeptoQ pretreatment. Data represent mean values and standard errors of three independent experimental series. ** indicate differences significant at $P \leq 0.01$ based on a student's t-test.

To get further insight into intracellular levels of specific ROS species, we determined steady-state levels of superoxide (using the Nitroblue Tetrazolium Assay) and hydrogen peroxide (using Ferrous Oxidation with Xylenol Orange Assay) at 4 h after onset of salt stress. In the absence of the peptoid, the steady-state levels of superoxide increased somewhat (by 50%) as compared to the control, albeit not significantly (Fig. 29A). However, the peptoid strongly suppressed the accumulation of superoxide (by around 90%) and prevented any salt-induced increase. It should be noted that the superoxide levels were already reduced in the absence of salt. In contrast, the peptoid did not have any effect on the steady-state levels of hydrogen peroxide (Fig. 29B) that increased significantly (to around twice the resting level) under salt stress.

3.8.3. Plant PeptoQ stimulated SOD activity and expression of the mitochondrial SOD

3.8.3.1. Antioxidant enzymes activity

In order to identify the mechanisms behind the observed effects of peptoid and salt stress on the steady-state levels of intracellular ROS, the specific activities of superoxide dismutase (SOD) and catalase (CAT) were measured as central enzymatic components of intracellular oxidative homeostasis. While in absence of the peptoid, SOD activity decreased to less than a third of the control when salt stress was administered (Fig. 30A) but there was a significant increase (by 80%), when salinity was accompanied by treatment with plant PeptoQ. It should be noted that the SOD activity was not increased by the peptoid, when no salt stress was applied, which is in contrast to the superoxide levels that were strongly suppressed by the peptoid even in the absence of salt (compare Fig. 29A and 30A, black bars for 0 mM NaCl). In contrast to the effect of plant PeptoQ on SOD activity, no effect of the peptoid was seen, when catalase activities were measured (Fig. 30B), although these activities increased significantly under salt stress (around twofold).

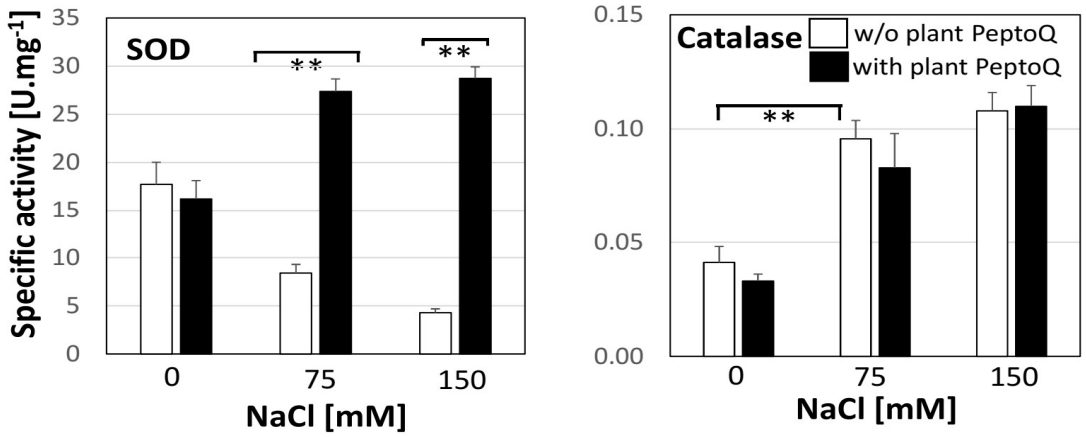

Figure 30: Effect of the plant PeptoQ on antioxidant enzyme activities. Superoxide dismutase (Mn-SOD) (**A**) and catalase (CAT) (**B**) activities in absence (white square) and presence (black square) of plant PeptoQ pretreatment. Data represent mean values and standard errors of three independent experimental series. ** indicate differences significant at $P \leq 0.01$ based on a student's t-test.

3.8.3.2. Mitochondrial SOD gene expression

Since the peptoid causes a strong and specific increase of SOD activity (Fig. 30A) while at the same time suppressing intracellular steady-state levels of superoxide (the substrate of this enzyme) (Fig. 29A), followed by a reduced lipid peroxidation under salt stress (Fig. 28A, B), the fact that whether this activity increase was linked with modulated expression of SOD gene or not was investigated. The steady-state transcript levels after 1 h (Fig. 31A), or after 3 h (Fig. 31B) either in the absence of the peptoid, or after pretreatment with 2 µM of plant PeptoQ for 2 h, was measured to ensure that the peptoid had fully accumulated in the mitochondria. To ensure comparability, the value at 1 h in absence of the peptoid was used as reference for all conditions. In the absence of plant PeptoQ, moderate salt stress (75 mM NaCl) had induced the transcript level more than 15-fold already 1 h after the addition of NaCl (Fig. 31A), while high salt stress (150 mM NaCl) was only inducing by a factor of 3. If measured at 3 h to see a later time point (Fig. 31B), also for 150 mM NaCl, the steady-state transcript level had increased to around 15-fold, and the value for 75 mM NaCl remained at the level seen after 1 h. Interestingly, the peptoid by itself (i.e. in the absence of salt stress) was inducing by around 15 and 25-fold at 1 and 3 h respectively, and this induction was suppressed almost completely under salinity (both 75 and 150 mM NaCl). This suppression was seen for both time points. The comparison with the enzymatic activity of SOD (Fig. 30A) shows that the steady-state transcript levels measured at 3 h were decreased, while the SOD activity measured at 4 h were increased in presence of plant PeptoQ. Thus, accumulation of transcripts and activity of the enzyme encoded by these transcripts, were modulated in the opposite manner.

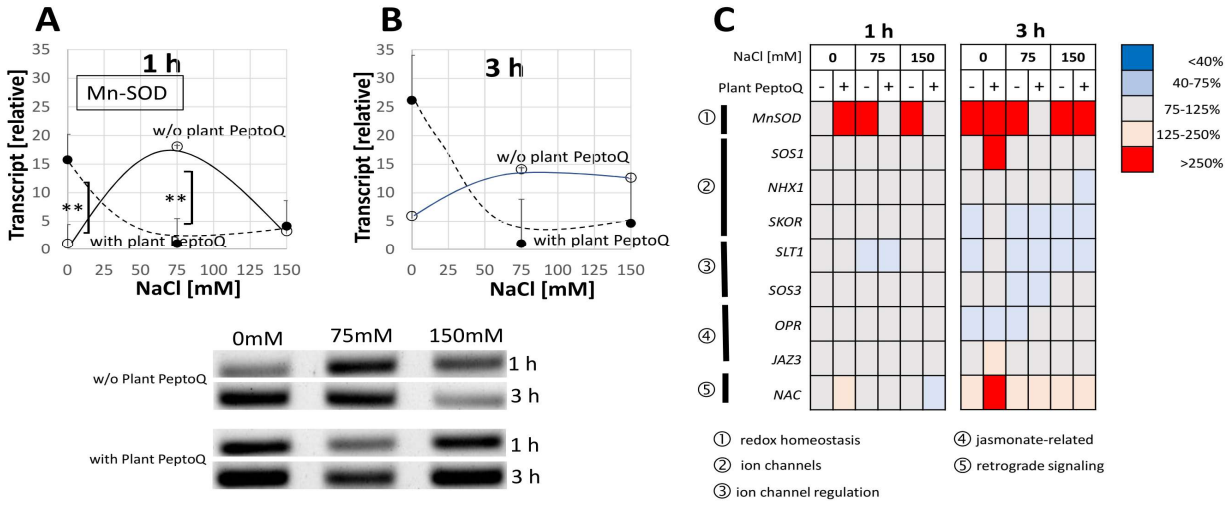

Figure 31: The relative expression of manganese superoxide dismutase (Mn-SOD), mitochondrial gene, at earlier (1) (**A**) and later (3 h) (**B**) time points in salt stressed WT BY-2 cells without (black curve) and with (broken curve) plant PeptoQ pretreatment. The expression of all the other salt-stress related genes in salt stressed BY-2 cells both with (+) and without (-) plant PeptoQ pretreatment (**C**). Agarose gel image of semiquantitative PCR (SQ-PCR) product of one representative example out of three independent experiments is shown. Data represent mean values and standard errors of three independent experimental series. ** indicate differences significant at $P \leq 0.01$ based on a student's t-test.

3.8.3.3. Other salt-related genes expression

To judge, whether these strong modulations of steady-state transcript levels were specific for Mn-SOD, or a rather general feature of salinity related gene expression, the transcripts for relevant ion channels (*SOS1* as channel extruding sodium through the plasma membrane, NHX1 as channel responsible for sequestration of sodium in the vacuole, and SKOR as channel involved in sodium-potassium homeostasis), regulators for ion channels (SOS3 as calcium-dependent regulator of SOS1, and STL1, a phosphate regulating sodium-potassium homeostasis), jasmonate-related genes (OPR as key enzyme for the peroxisomal synthesis of jasmonic acid, JAZ3 as salinity-related jasmonate-responsive regulator), and NAC as readout for retrograde signalling from mitochondria to the nucleus were measured (Fig. 32 A-H). To ensure comparability, the value at 1 h in the absence of the peptoid was used as reference for all conditions (w/o peptoid 3 h, and with peptoid 1 and 3 h). Generally, with two exceptions, the vast majority of these transcripts did not show strong modulations (Fig. 31C) neither in response to salinity, nor to the peptoid. Interestingly, the sodium extruder SOS1 showed a threefold increased level in response to the peptoid in the absence of salt stress (0 mM NaCl) at 3 h (Fig. 32A). This increase was not seen in presence of salt and it was also not seen for the earlier time point (1 h). This means that SOS1 shows a regulation pattern that was similar to that of Mn-SOD, albeit developing more slowly and also to a much lower amplitude. The other transcript that stuck out, was a tobacco homologue of AtNAC13, which for simplicity is termed NAC (Fig. 32F): By peptoid treatment, it was first significantly, by 40%, reduced, but later induced, independently of the respective concentration of NaCl. Based on a phylogeny constructed on Arabidopsis and tobacco NAC sequences, this gene seemed to be the closest homologue of ANAC013 (Fig. 33), a factor shown to be involved in retrograde signalling of oxidative disbalance (De Clercq, 2013).

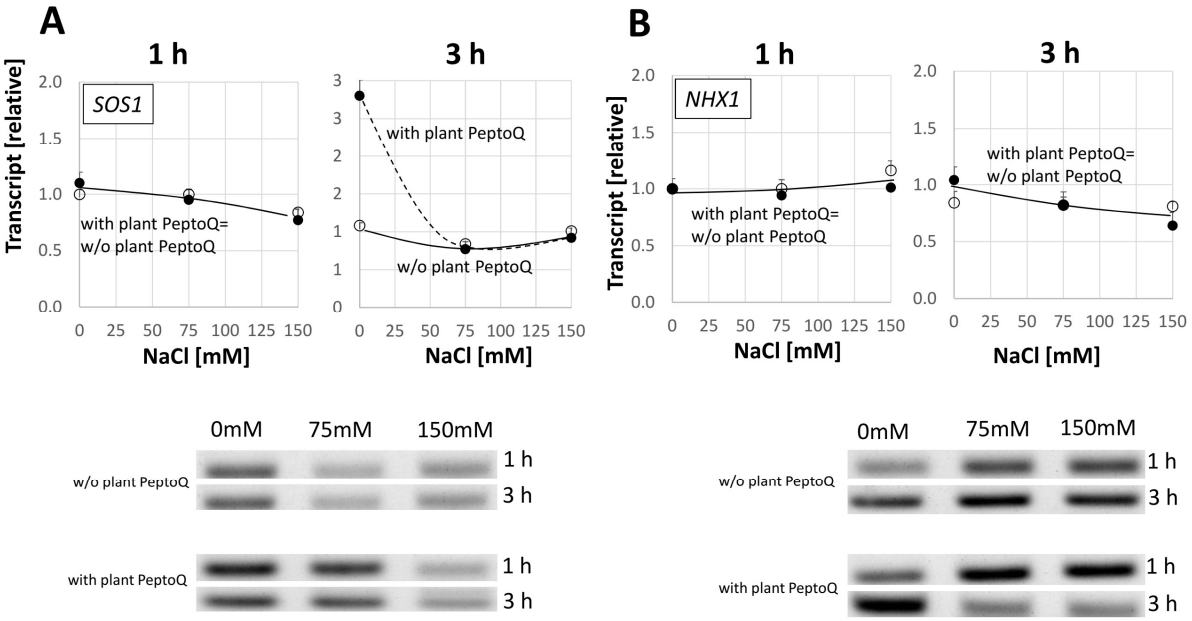

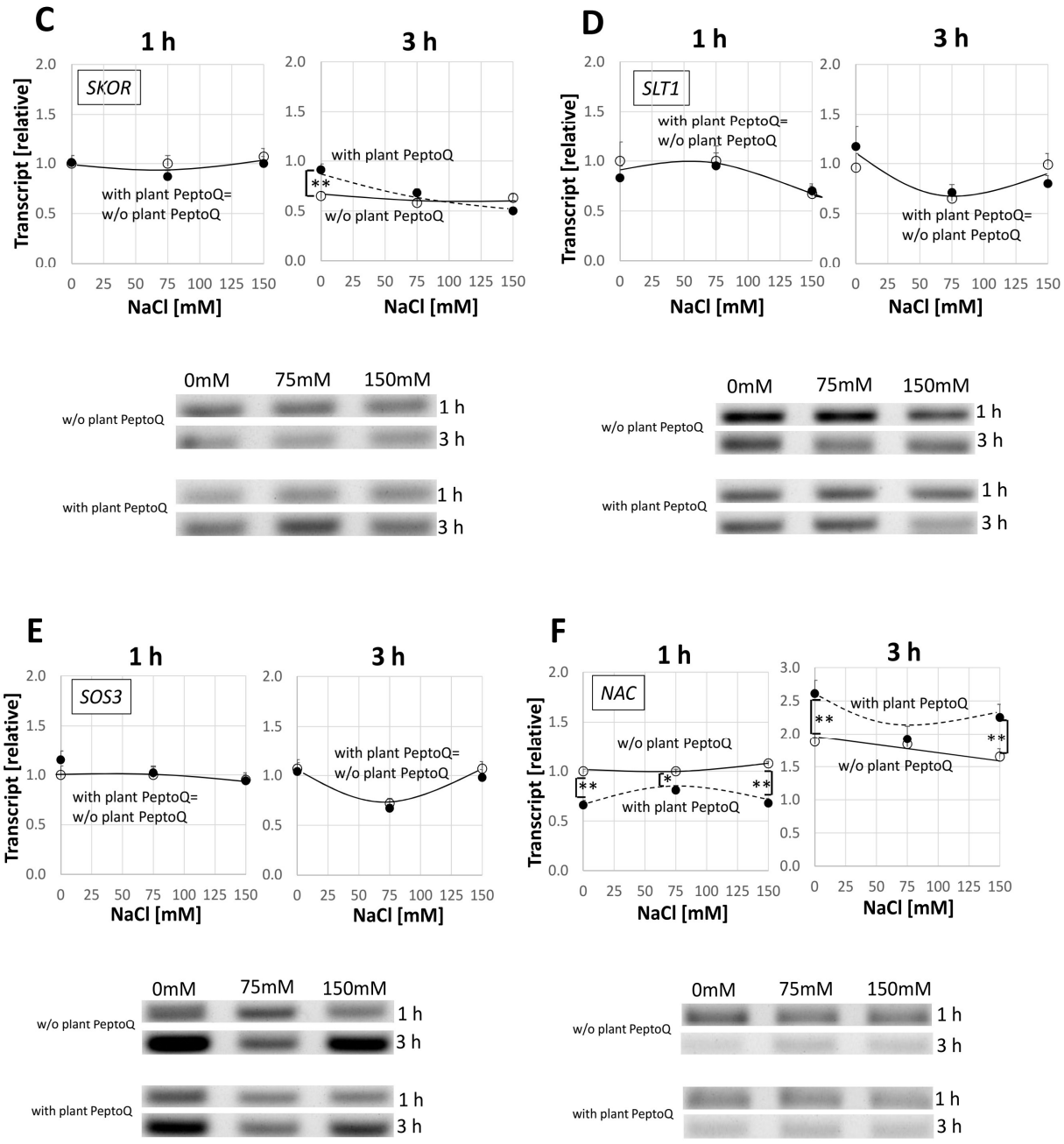
C
1 h
3 h
SKOR
Transcript [relative]
with plant PeptoQ=
w/o plant PeptoQ
with plant PeptoQ
w/o plant PeptoQ
**
NaCl [mM]
0mM
75mM
150mM
w/o plant PeptoQ
with plant PeptoQ
1 h
3 h
D
SLT1
E
SOS3
F
NAC
*

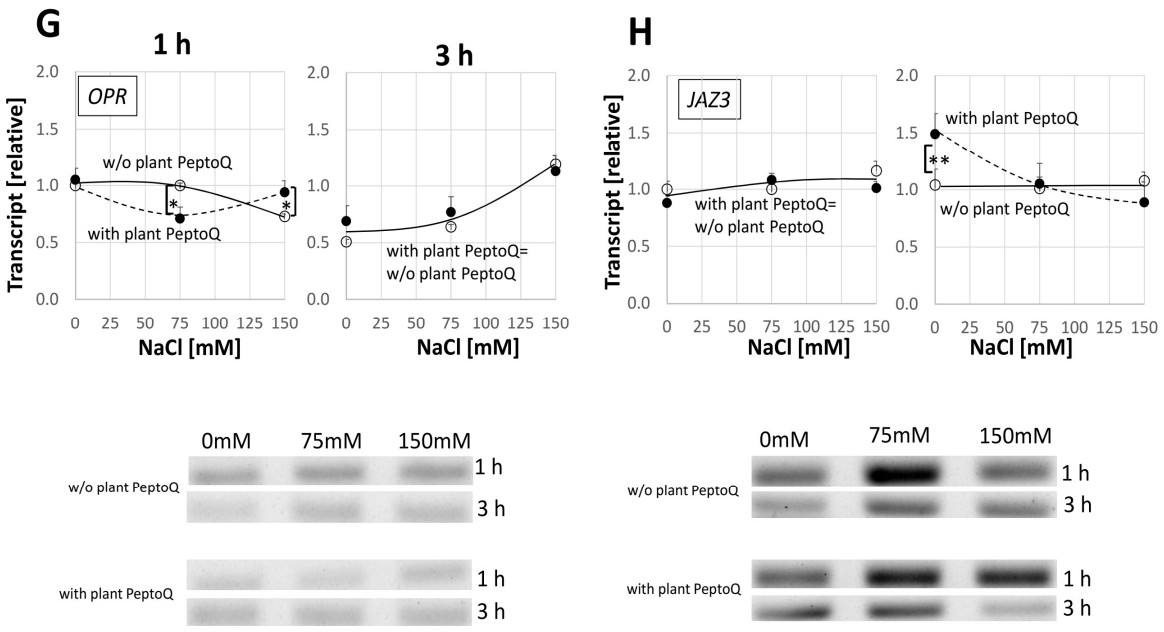

Figure 32: Expression of different salt-stress related genes. **A-H** Effect of salt stress on the expression of eight genes in WT BY-2 cells without (black curve) and with (broken curve) plant PeptoQ pretreatment. In each case, agarose gel image of semiquantitative PCR (SQ-PCR) product of one representative example out of three independent experiments is shown. Data represent mean values and standard errors of three independent experimental series. **indicate differences significant at $P \leq 0.01$, *at $P \leq 0.05$ based on a student's t-test.

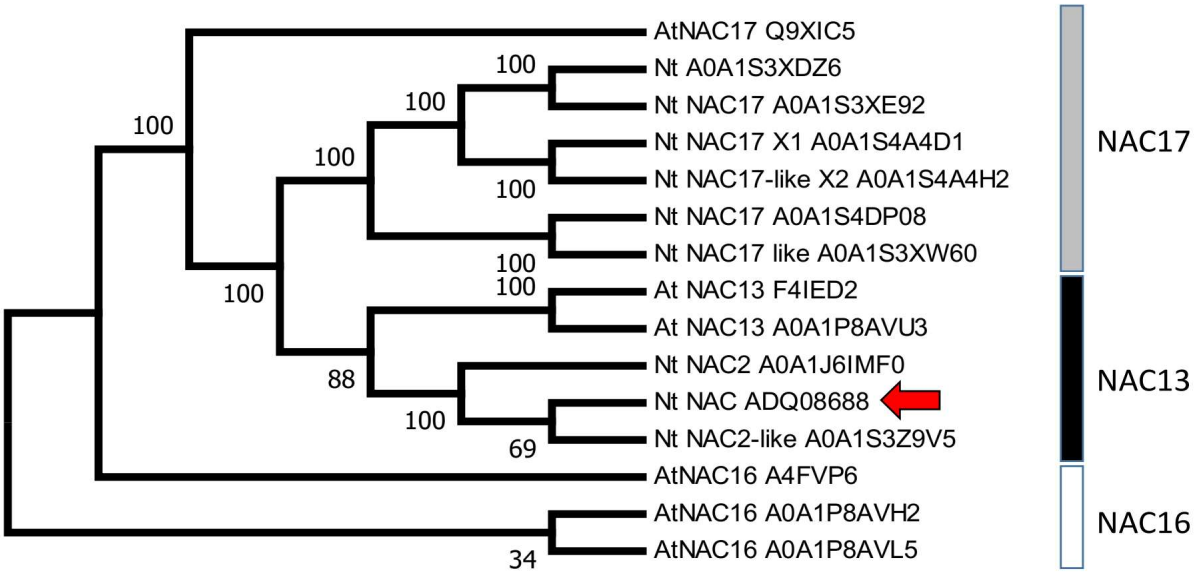

Figure 33: Neighbour-joining (NJ) phylogenetic tree that shows the close relationship of tobacco (*Nicotiana tabacum*) NtNAC gene (red arrow) to its homologue Arabidopsis (*Arabidopsis thaliana*) NAC13 (ANAC013) unlike its relationship to Arabidopsis NAC16 and NAC17.

In addition to, the genes mentioned above, additional salt-related genes; namely, JAZ1 and JAZ2 (salinity-related jasmonate-responsive regulators), and HKT1 and HAK1 (high-affinity K^+ transporters) had been investigated in preparatory studies (Fig. 34) using semiquantitative PCR (SQ-PCR) using the primers mentioned in (Table 5). However, since no significant responses were detected with respect to the expression of these genes, they were not pursued further.

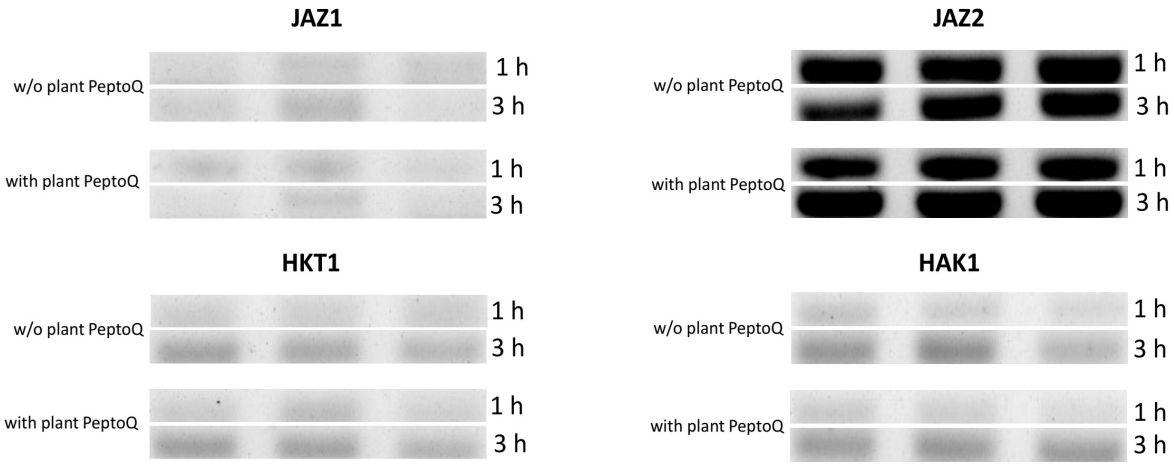

Figure 34. Agarose gel image of the semiquantitative PCR (SQ-PCR) product of four salt-related genes. In each case, one representative example out of three independent experiments is shown.

3.8.4. Plant PeptoQ does not improve ionic balance under salt stress

The damage caused by salt stress is partially due to ionic stress, such as elevated levels of sodium ions, accompanied by depletion of potassium. We determined therefore, the cellular contents for both ions after treatment with 0, 75, and 150 mM NaCl either in absence or presence of plant PeptoQ pretreatment (Fig. 35). As expected, salt stress caused a dose dependent increase in the content of sodium ions (Fig. 35A). This increase was very strong and not mitigated by the peptoid. The uptake of sodium was accompanied by a significant decrease of potassium ions (Fig. 35B). This decrease (around 30% of the initial value) was already saturated for 75 mM NaCl and was not accentuated further for high salt stress (150 mM NaCl), although sodium uptake was doubled as compared to moderate salt stress (75 mM NaCl). However, also for potassium, there was no effect of peptoid treatment. Thus, ionic balance was strongly perturbed under salt stress, and this perturbation was not mitigated by plant PeptoQ.

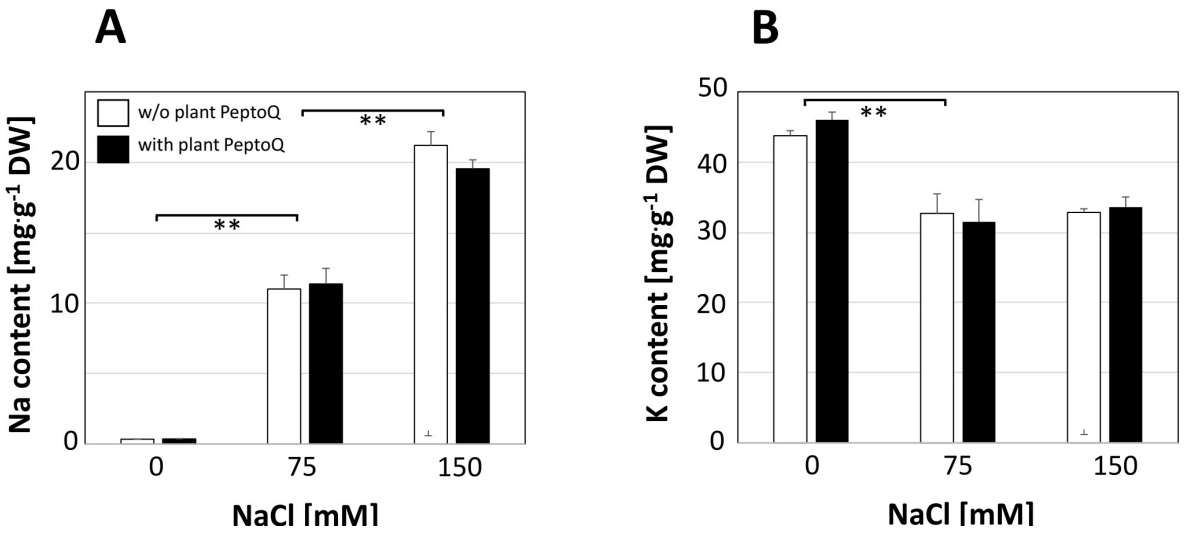

Figure 35: Effect of the plant PeptoQ on salt-induced uptake of sodium ion (**A**) and potassium ion (**B**) in non-transformed WT tobacco BY-2 cells in control (0 mM NaCl), under moderate (75 mM NaCl), and under high (150 mM NaCl) salt stress in absence (white bars) or presence (black bars) of plant PeptoQ (2 µM). Ion content is given relative to dry weight. Data represent mean values and standard errors of three independent experimental series. ** indicate differences significant at $P \leq 0.01$ based on a student's t-test.

3.8.5. Plant PeptoQ partitions jasmonate synthesis towards OPDA

Salt stress leads to activation of jasmonate synthesis and signalling, which improves adaptation, if appropriately down-modulated, but can initiate salinity-induced necrosis, if constitutively active (Ismail et al., 2014). Therefore, the levels of the precursor OPDA, jasmonic acid (JA), and the final product JA-Ile were compared in salt stressed cells with or without pretreatment with plant PeptoQ after 1 and 3 h of salt stress. While JA was not detectable in none of the samples, OPDA and JA-Ile accumulated to measurable amounts (Fig. 36). The steady-state levels of OPDA did not respond to NaCl (Fig. 36A). However, they were significantly increased in presence of the peptoid at 3 h, and this increase was constant independently of the respective concentration of NaCl. It was maximum at the control (0 mM NaCl) and decreased in a dose-dependent manner a 1 h. For JA-Ile, the levels were not significantly changed by the peptoid (Fig. 36B). Again, salt stress did not cause any significant change either. At both 1 and 3 h, at the control (0 mM NaCl), BY-2 cells with and without plant PeptoQ pretreatment attained similar value; however, at moderate (75 mM NaCl) and high (150 mM NaCl) salt stress, the latter attained relatively higher JA-Ile value as compared to the former. Since OPDA is not only a precursor of active jasmonate, but a signal by itself, the molar ratio between JA-Ile and OPDA was plotted, to see, whether salt stress or peptoid treatment repartitioned the balance between these two signalling molecules (Fig. 36C). Here, a significant shift of the biosynthetic pathway from JA-Ile towards OPDA was seen after peptoid treatment. This channeling of the pathway towards OPDA was significantly more accentuated for 75 mM NaCl, but faded, if the concentration of salt was raised further at 3 h. On the other hand, in the absence of the peptoid, more JA-Ile per OPDA was formed at both 1 and 3 h time points.

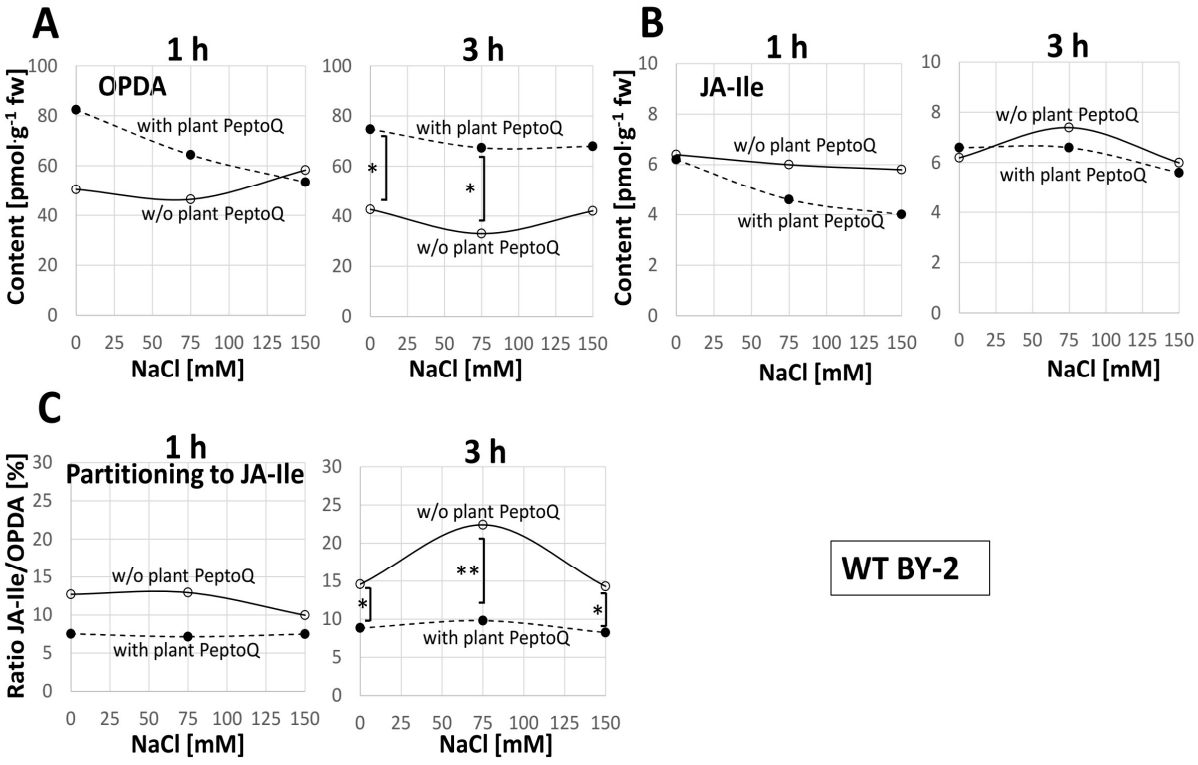

Figure 36: Effect of salt stress on 12-oxo-phytodienoic acid (12-OPDA) and jasmonyl-isoleucine (JA-Ile) levels as well as on the ratio between JA-Ile and OPDA (%). The level of 12-OPDA (**A**), JA-Ile (**B**) and JA-Ile/OPDA (%) (**C**) in salt stressed WT BY-2 cells with (broken curve) and without (black curve) plant PeptoQ pretreatment. Data represent mean values and standard errors of three independent experimental series. ** indicate differences significant at $P \leq 0.01$, *at $P \leq 0.05$ based on student's t-test.

3.9. Effect of OsOPR7 overexpression in WT tobacco BY-2 cells on salt tolerance

3.9.1. Localisation of OsOPR7 protein

To identify the subcellular localisation of the OsOPR7 protein (enzyme), WT suspension-cultured tobacco BY-2 cells were transformed with OsOPR7-GFP binary vector plasmid DNA and further co-transformed with agrobacterium containing PTS1-mCherry plasmid (for transient transformation of mCherry binary vector). Grown on solid Paul's medium for 3 days, and then examined microscopically (without proceeding to selection step) for the localisation of OsOPR7 protein. The result showed that the OsOPR7 protein was localised in peroxisomes of the stably OsOPR7 overexpressor (OE) BY-2 cells which is evident from the significant colocalisation (Fig. 37C) between the mCherry (Fig. 37A) and OsOPR7 bound GFP (Fig. 37B).

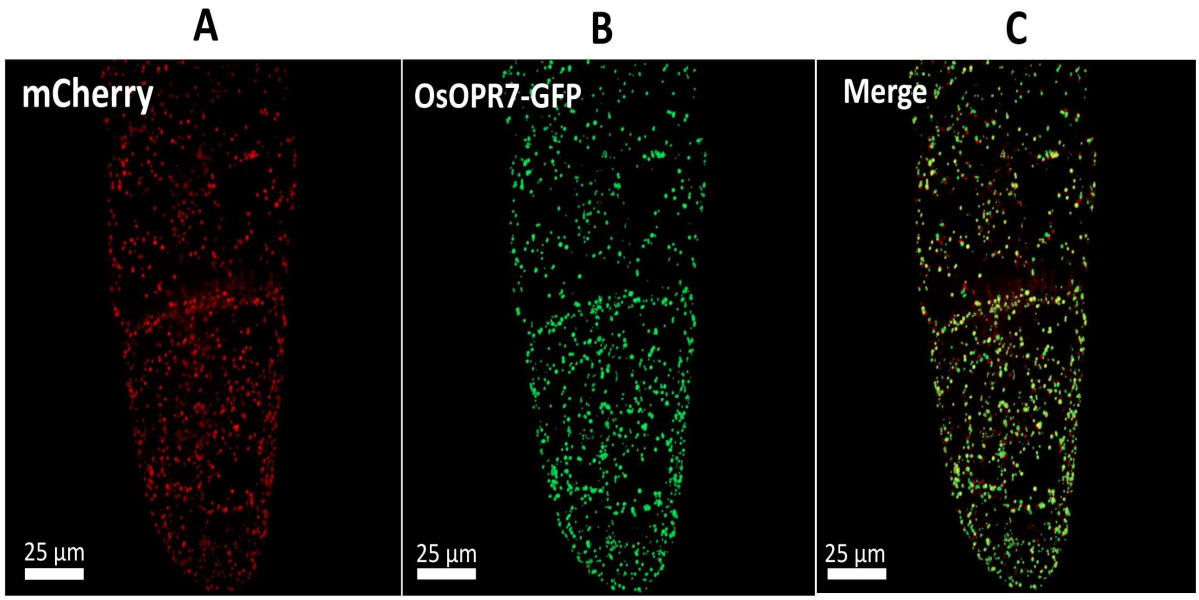

Figure 37: Peroxisomal localisation of OsOPR7 enzyme in the OE BY-2 cells. Agrobacterium containing PTS1-mCherry plasmid was co-transformed with WT BY-2 cells which were transformed with OsOPR7-GFP binary vector plasmid DNA and grown on solid Paul's medium. Eventually, followed by spinning disc confocal microscopy making use of the red fluorescent signal from mCherry **(A)**, and the green fluorescent signal from GFP(**B**). The merge of the two channels shown in (**C**) shows the close overlap of both signals. Confocal sections recorded in the mid-plane from representative cells recorded at constant laser power and exposure time are shown.

3.9.2. OsOPR7 overexpression improved cell proliferation, expansion and viability

In comparison to salt stressed WT BY-2 cells, cell density, mitotic index (MI), cell length and width, cell viability and doubling time were improved in salt stressed OE BY-2 cells.

3.9.2.1. Cell density

Salinity caused a drastic decline in cell proliferation activity, but this decline was ameliorated in the OE BY-2 cells as compared to the WT counterparts (Fig. 38). In WT BY-2 cells, cell number was decreased at moderate salt stress (75 mM NaCl) even at the initial incubation time, 24 h (29%) and it increased progressively in the subsequent incubation times: 48 h (44%), 72 h(60%) and 96 h(68%) (Fig. 38A). However, this decline in cell number was effectively mitigated in the OE BY-2 cells: 15% (24 h), 29% (48h), 37% (72h) and 38% (96h) (Fig. 38B). In WT BY-2 cells, for high salt stress (150 mM NaCl), at 96 h, cell proliferation activity was almost entirely inhibited, only 8% of cells were in proliferation activity as compared to the untreated control (Fig. 38A). At the same salinity level and incubation time, in the OE BY-2 cells, relatively better and reasonable cells were in proliferation phase, 17% (96 h) as compared to the untreated control (Fig. 38B). On the one hand, doubling time was estimated on the basis of an exponential growth model, from the time course of cells proliferation (Fig. 38C). In the absence of salt stress, cells were doubling each day irrespective of the cell types under consideration. However, doubling time was affected and delayed, in the presence of salt stress where in WT BY-

2 cells, at moderate salt stress (75 mM NaCl), doubling time was increased to 39 h whereas in the OE BY-2 cells, the increase was relatively low (28 h). For high salt stress (150 mM NaCl), in WT BY-2 cells, doubling time was extremely high (330 h) which implies doubling was practically arrested but in the OE BY-2 cells, even if, doubling time was quite delayed, it was significantly low (69 h) (Fig. 38C).

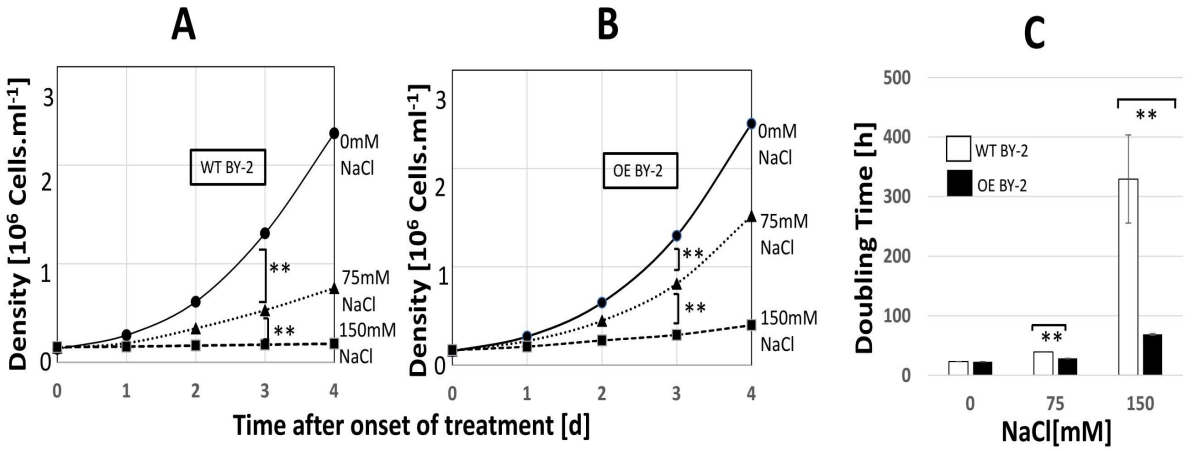

Figure 38: Effect of salt stress on cell proliferation in non-transformed WT and OE BY-2 cells. Time courses of cell density in the absence of salt stress (0 mM NaCl, black circles), under moderate (75 mM NaCl, black triangles), and under high (150 mM NaCl, black squares) salt stress in WT BY-2 cells (**A**) and OE BY-2 cells (**B**). Doubling time was estimated from the time constant of exponential growth over the concentration of NaCl in WT BY-2 cells (white bars) and OE BY-2 cells (black bars) (**C**). Data represent mean values and standard errors of three independent experimental series. ** indicate differences significant at $P \leq 0.01$ based on a student's t-test.

3.9.2.2. Cell length and cell width

Whether the salt stress mitigation observed with respect to cell proliferation in OE BY-2 cells has relationship with cell expansion phase or not was considered at day 3 and day 7 after subcultivation (during the expansion phase) as cells enlarge their central vacuole (Fig. 39A). In WT BY-2 cells, at moderate salt stress (75mM NaCl), relative growth rate was decreased profoundly where it attained less than 30% residual growth as compared to the untreated control (0mM NaCl). The value became even negative for high salt stress (150 mM NaCl) which implies the cells shrank perhaps due to the fact that the osmotic potential in the protoplast was less negative than that of the medium. However, in the OE BY-2 cells, the decrease in cell expansion (relative cell growth rate) was significantly compensated where at moderate salt stress (75 mM NaCl), similar (even slightly better) relative growth rate was observed as compared to the non-stressed control (0 mM NaCl). This implies that the negative osmotic potential of the medium was completely compensated by the OE BY-2 cells. Unlike the case in WT BY-2 cells, even, at high salt stress (150 mM NaCl), a residual expansion of about 24% was attained (i.e. a level slightly less than that seen for 75 mM NaCl in the WT BY-2 cells). Thus, in the OE BY-2 cells, the impact of moderate (75 mM NaCl) and high (150 mM NaCl) salt stress upon cell expansion was fully and partially mitigated respectively. As compared to the effects seen on cell proliferation under salt stress, cell expansion seemed to

be more responsive to the OsOPR7 overexpression. On the other hand, salt stress had no significant effect on cell width in both WT and OE BY-2 cells. However, cell length(L) to width(W) ratio (L: W) was significantly decreased both in the OE and WT BY-2 cells at day 3 and day 7. In the former time point, there was no significant difference in the two cell samples (Fig. 39 B) but in the latter, the OE and WT BY-2 cells attained significantly different L to W ratio, specifically at high salt stress (150 mM NaCl) (Fig. 39C). The OE BY-2 cells displayed better L to W ratio as compared to the WT BY-2 cells. Thus, this shows that OE BY-2 cells attained elongated and less broader cells as compared to the WT BY-2 cells under salt stress.

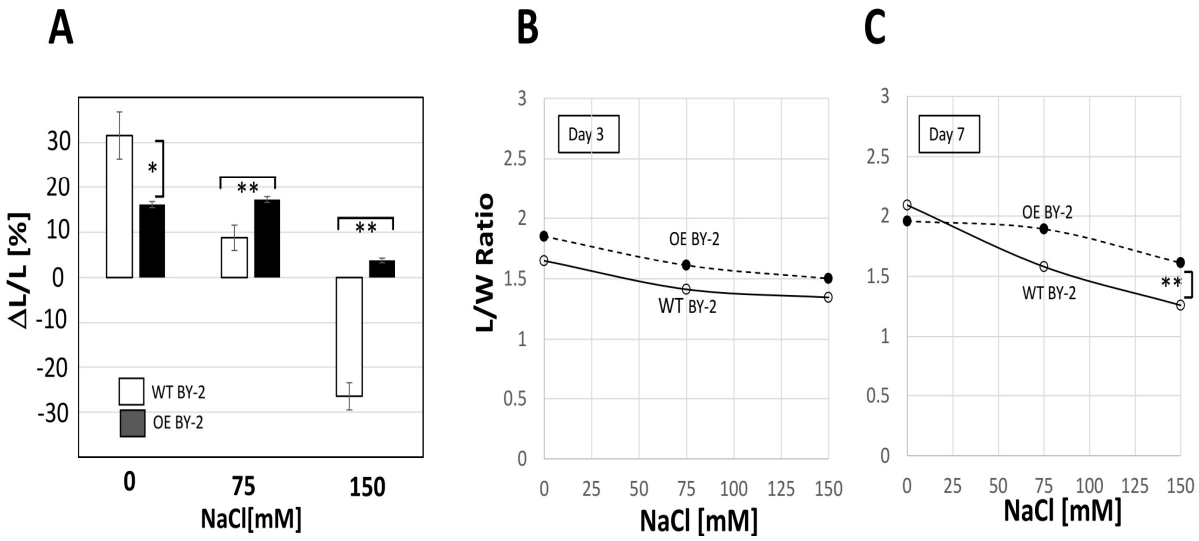

Figure 39: Effect of salt stress on cell expansion in WT (white bars) and OE (black bars) tobacco BY-2 cells. **A** relative elongation during the expansion phase (day 3 to 7 after subcultivation) in control (0 mM NaCl), under moderate (75 mM NaCl), and under high (150 mM NaCl) salt stress. Cell length to width (L/W) ratio at day 3(**B**) and day 7(**C**) in WT (black curve) and OE (broken curve) BY-2 cells at the control (0mM NaCl), moderate (75 mM NaCl) and high (150 mM NaCl) salt stress. Data represent mean values and standard errors of three independent experimental series. ** indicate differences significant at $P \leq 0.01$, *at $P \leq 0.05$ based on a student's t-test.

3.9.2.3. Cell viability

Cell death is the usual subsequent consequence of salt-induced arrest in cell proliferation. Thus, using the Evans Blue Dye Exclusion assay, cell mortality was followed in response to salt stress over 96 h incubation period. In WT BY-2 cells, at moderate salt stress (75 mM NaCl), cell mortality was sharply increased to more than 40% at initial incubation time (24 h) but it decreased during later incubation times and attained 20% at 96 h (Fig. 40B). This improvement in cell viability implies the continued proliferation of surviving cells unlike the dead ones which were incapable of doing so. Even if, this temporal pattern happened in the OE BY-2 cells, the amplitude of cell mortality was profoundly reduced. At moderate salt stress (75 mM NaCl), the maximum cell mortality at 24 h was 38% and it dropped to 15% at 96 h. This implies that more cells were able to return to viability through the elapse of time as compared to the case in salt stressed WT BY-2 cells. At high salt stress (150 mM NaCl), cells

were not able to recover to viability (at least not during the maximum incubation period considered, 96 h) (Fig. 40C). In the WT BY-2 cells, about 80% of cells were died during the initial incubation time (24 h) after salt treatment and the percent of mortality increased progressively in the subsequent incubation times, and it reached more than 90% at the final incubation time, 96 h. Whereas, in the OE BY-2 cells, even if, there was increased cell mortality (that increases upon increment in incubation time), the amplitude of death toll is relatively low. For example, at 96 h after the onset of salt stress, the cell mortality was only 81% (still about one fourth of the cells had remained alive).

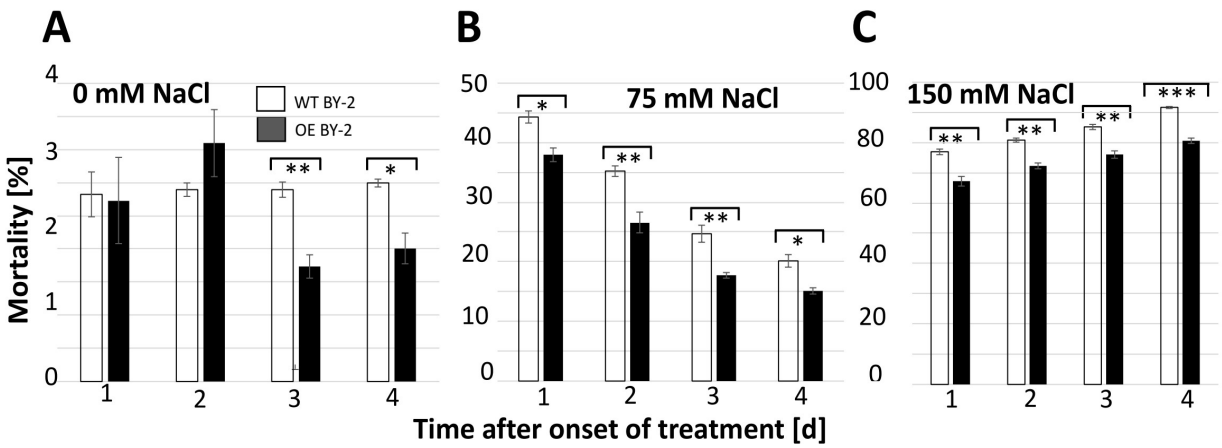

Fig. 40: Effect of salt stress on cell mortality of WT (white bars) and OE (black bars) tobacco BY-2 cells. Time courses of mortality at the control(**A**), moderate (**B**) and high (**C**) salt stress. Data represent mean values and standard errors of three independent experimental series. *** indicate differences significant at P ≤ 0.001, **at P ≤ 0.01, *at P ≤ 0.05 based on a student's t-test.

3.9.2.4. Mitotic Index (MI)

Mitotic index (MI) was measured just after subcultivation and continued until 96 h (day 4). In general, MI increased at the control (0 mM NaCl), moderate (75 mM NaCl) and high (150 mM NaCl) salt stress as it goes from day 0 to day 1 (24 h). However, it decreased as the incubation time proceeds from 24 (day 1) to 96 h (day 4) both at the control and the salt stress. Moreover, the percent decline in MI, at moderate and high salt stress as compared to the control was more prominent in the WT BY-2 cells as compared to the OE counterparts (Fig. 41).Thus, in WT BY-2 cells, it decreased from 62% (24 h) to 46% (96 h) at moderate salt stress (Fig. 41B) but it increased from 72% (24 h) to 79 %(96h) at high salt stress (Fig. 41C) exceptionally. On the other hand, in OE BY-2 cells, the percent decrease in MI dropped from 34% (24 h) to 13% (96 h) and from 57% (24 h) to 40% (96 h) at moderate (75mM NaCl) and high (150mM NaCl) salt stress respectively as compared to the control (Fig.41B,C). Except that the maximum decline in MI (compared to the control) in WT BY-2 cells, at high salt stress (150mM NaCl) was being at 96 h, in all the rest cases, the maximum declines in MI were observed at 24 h incubation time and high (150 mM NaCl) salt stress.

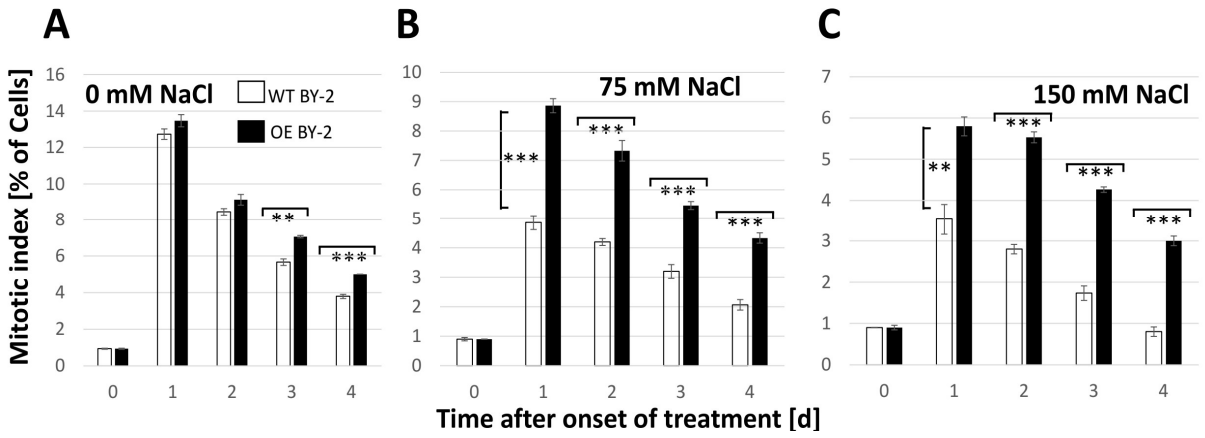

Figure 41: Effect of salt stress on mitotic index (MI) in WT (white bars) and OE (black bars) tobacco BY-2 cells. The value of MI at the control (0 mM NaCl) (**A**), moderate (75 mM NaCl) (**B**) and high (150 mM NaCl) (**C**) salt stress. Data represent mean values and standard errors of three independent experimental series. *** indicate differences significant at $P \leq 0.001$, **at $P \leq 0.01$ based on a student's t-test.

3.9.3. OsOPR7 overexpression ameliorated oxidative homeostasis under salt stress

3.9.3.1. Lipid Peroxidation

The level of lipid peroxidation is measured using the product malondialdehyde (MDA) and can be used as the readout for oxidative degradation of membranes (Heath and Packer, 1968). In order to investigate whether the OsOPR7 overexpression compensated the oxidative effect of salt stress in tobacco BY-2 cells, both WT and OE BY-2 cells were treated with moderate (75 mM NaCl) and high (150 mM NaCl) salt stress at day 4 after subcultivation (at the onset of cell expansion). Sampling for MDA determination was carried out at 1 and 4 h after salt treatment together with non-stressed (0 mM NaCl) negative control. In WT BY-2 cells, MDA content increased in a dose-and time-dependent manner at both moderate (75 mM NaCl) and high (150 mM NaCl) salt stress (Fig. 42). At the latter salt stress, it attained, MDA value of more than double of the negative control (0 mM NaCl) both at 1 and 4 h. In the OE BY-2 cells, at moderate salt stress (75 mM NaCl), the salt-induced increase of MDA steady-state levels were completely suppressed at both time points. Even at high salt stress (150 mM NaCl), the MDA level was similar to the MDA level of WT BY-2 at moderate salt stress (75 mM NaCl) (Fig. 42A, B).

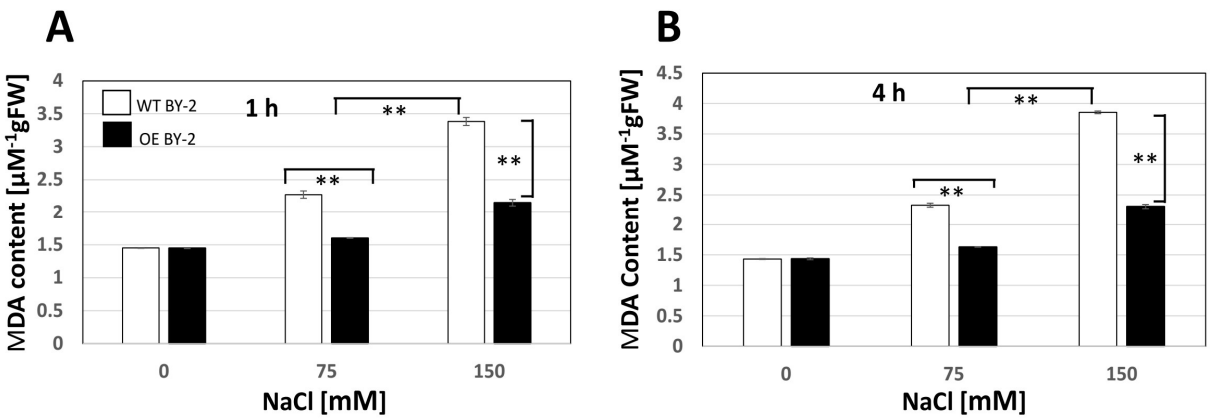

Figure 42: Effect of salt stress on lipid peroxidation. Content of malonedialdehyde (MDA) at the control (0mM NaCl), moderate (75 mM NaCl), and high (150 mM NaCl) salt stress in WT (white bars) and OE (black bars) tobacco BY-2 cells at 1(**A**) and 4 h (**B**). Data represent mean values and standard errors of three independent experimental series. ** indicate differences significant at $P \leq 0.01$ based on a student's t-test.

3.9.3.2. Apoplastic Reactive Oxygen Species (ROS)

To understand the relation of the observed lipid peroxidation (measured by MDA) with the reactive oxygen species (ROS), the steady-state levels of apoplastic ROS such as, hydrogen peroxide (using Ferrous Oxidation with Xylenol Orange Assay) and superoxide (using the Nitroblue Tetrazolium Assay) was determined at 1, 4 and 6 h after the onset of salt stress. In the WT BY-2 cells, the superoxide level increased (Fig. 43C) while hydrogen peroxide level decreased (Fig. 43A) in a dose-dependent manner. On the other hand, in the OE BY-2 cells, just the opposite effect had occurred; that is, the superoxide level decreased (Fig. 43D), and the hydrogen peroxide level increased (Fig. 43B) in a dose-dependent manner. In both the WT and OE BY-2 cells, the effect of incubation time was negligible with respect to superoxide content.

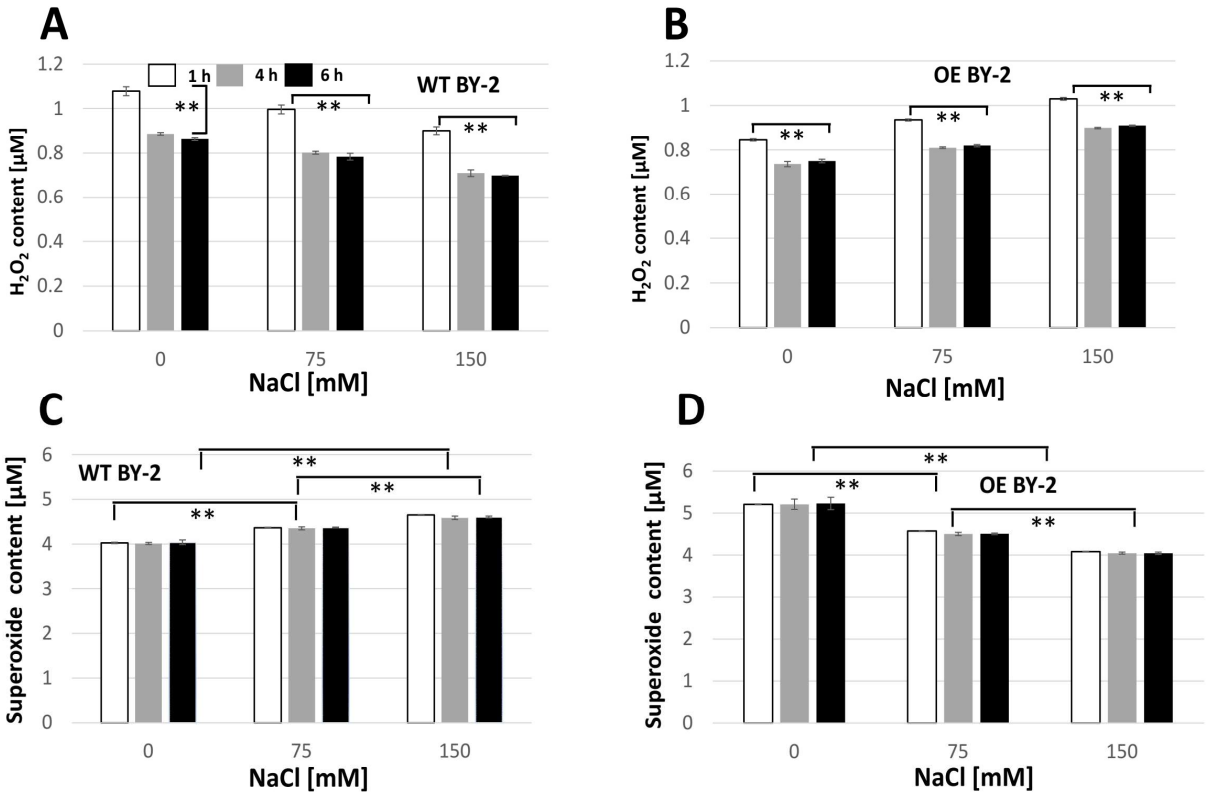

Figure 43: Effect of salt stress on oxidative balance. Accumulation of apoplastic Reactive Oxygen Species (ROS) in salt stressed WT and OE tobacco BY-2 cells at 1 (white bars), 4 (grey bars) and 6 h (black bars). Data represent mean values and standard errors of three independent experimental series. ** indicate differences significant at $P \leq 0.01$ based on a student's t-test.

3.9.4. OsOPR7 overexpression stimulated SOD activity and mitochondrial SOD expression

3.9.4.1. Antioxidant enzymes activity

The specific activities of superoxide dismutase (SOD) and catalase (CAT) were measured as central enzymatic components of intracellular oxidative homeostasis. This is in order to pinpoint and identify the mechanisms behind the better performance of the OE BY-2 cells under salt-induced oxidative stress. In WT BY-2 cells, SOD activity decreased significantly and attained less than third of the untreated control at high salt stress (150 mM NaCl). In the OE BY-2 cells, the SOD activity at moderate salt stress (75 mM NaCl) was more or less comparable to the SOD activity in the non-stressed control (0 mM NaCl) but at high salt stress (150 mM NaCl), SOD activity increased by 27%. On the other hand, in the OE BY-2 cells which were pretreated with plant PeptoQ, the SOD activity was increased both at moderate (75 mM NaCl) and high (150 mM NaCl) salt stress by 98% and 130% respectively as compared to salt free negative control (0 mM NaCl) (Fig. 44A). In the WT, OE and plant PeptoQ pretreated OE BY-2 cells, the activity of catalase (CAT) increased more or less, in a comparable manner (Fig. 44B). Unlike, the case in SOD activity, both OsOPR7 overexpression and plant PeptoQ pretreatment of OE BY-2 cells, had less prominent effect on CAT activity.

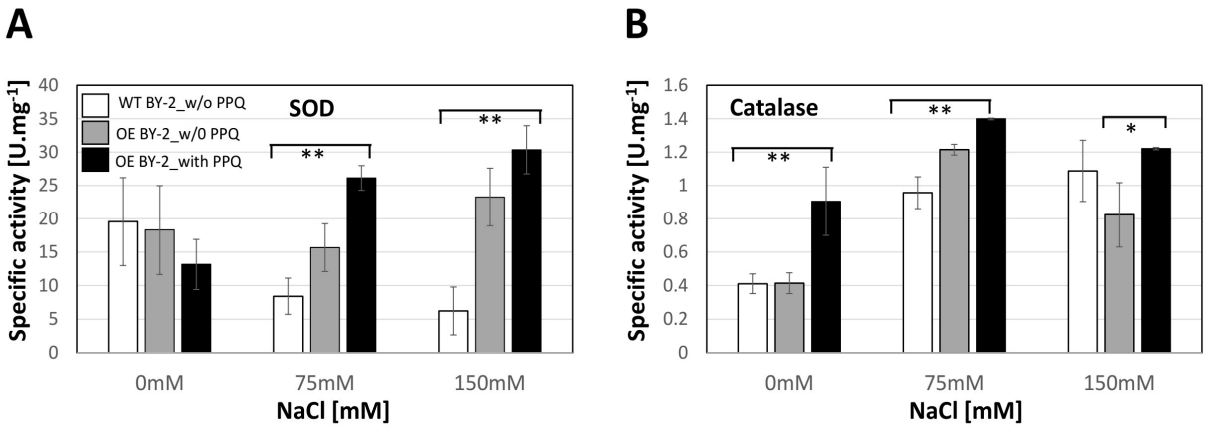

Figure 44: Effect of salt stress on antioxidant enzymes activity. Superoxide dismutase (Mn-SOD) (**A**) and catalase (CAT) (**B**) activities in WT (white bars), OE without peptoid (grey bars) and OE with peptoid (black bars) tobacco BY-2 cells. Data represent mean values and standard errors of three independent experimental series. ** indicate differences significant at $P \leq 0.01$, * at $P \leq 0.05$ based on a student's t-test.

3.9.4.2. Mitochondrial SOD gene expression

Under salt stress, in OE BY-2 cells, there were reduced lipid peroxidation level, and increased (strong and specific) SOD activity unlike the case in WT BY-2 cells; consequently, whether these effects are related with modulated SOD expression (Fig. 45) or not was investigated. Thus, the steady-state transcript levels of SOD after 1 (Fig. 45A) and 3 h (Fig. 45B) of salt treatment in WT and OE BY-2 cells were measured. To ensure comparability, the value at 1 h in the WT BY-2 cells, in absence of the peptoid was used as reference for all conditions (WT BY-2, 3 h, and OE BY-2, 1 and 3 h). At earlier time point (1 h), the Mn-SOD gene was significantly and stably induced at the control (0 mM NaCl), moderate (75 mM NaCl) and high (150 mM NaCl) salt stress in the OE BY-2 cells; however, in the WT BY-2 cells, at the control (0 mM NaCl), it was not induced whereas at moderate (75 mM NaCl) and high (150 mM NaCl) salt stress, it was induced significantly and attained the maximum induction at the former salinity level (Fig. 45A). On the other hand, at the later time point (3 h), the Mn-SOD gene was induced significantly at all salinity levels in both WT and OE BY-2 cells. At the control (0 mM NaCl), it stuck out and induced quite significantly in OE BY-2 cells but in WT BY-2 cells it was minimum. At moderate (75 mM NaCl) and high (150 mM NaCl) salt stress, the Mn-SOD gene was induced more or less similarly in WT and OE BY-2 cells (Fig. 45 B).

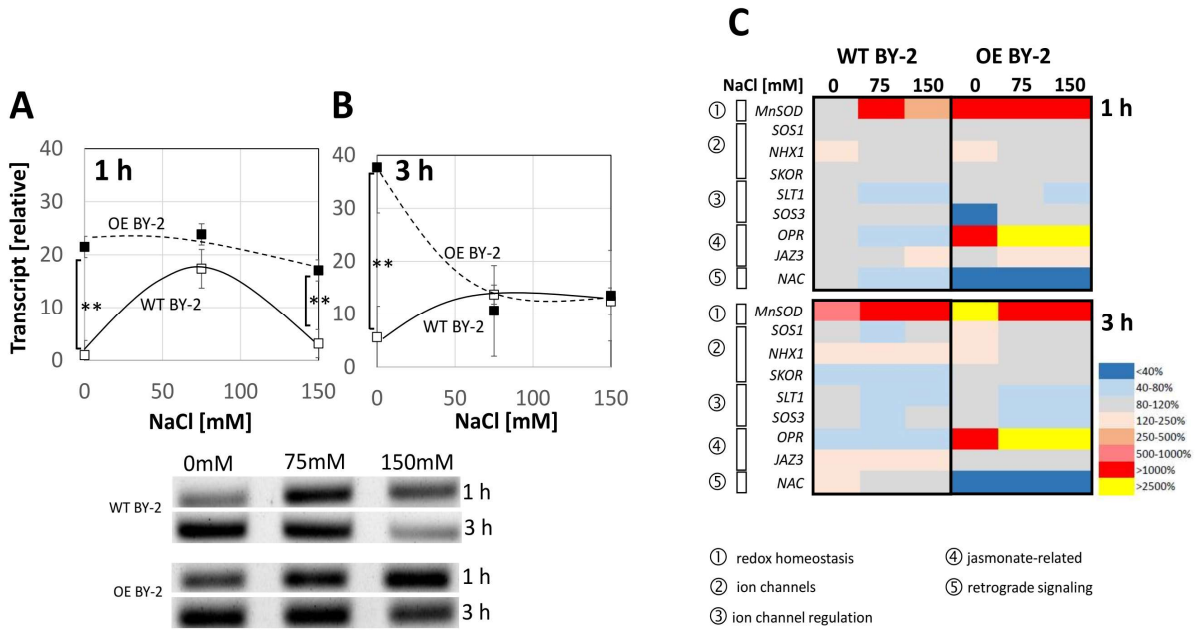

Figure 45: The relative expression of the mitochondrial gene, manganese superoxide dismutase (Mn-SOD), at earlier (1) (**A**) and later (3 h) (**B**) time points in salt stressed WT (black curve) and OE (broken curves) tobacco BY-2 cells. The expression of all the other salt-stress related genes in salt stressed WT and OE tobacco BY-2 cells (**C**). Agarose gel image of semiquantitative PCR (SQ-PCR) product of one representative example out of three independent experiments is shown. Data represent mean values and standard errors of three independent experimental series. ** indicate differences significant at $P \leq 0.01$ based on a student's t-test.

3.9.4.3. Other salt-related genes expression

On the other hand, the transcripts for relevant ion channels (SOS1 as channel extruding sodium through the plasma membrane, NHX1 as channel responsible for sequestration of sodium in the vacuole, and SKOR as channel involved in sodium-potassium homeostasis), regulators for ion channels (SOS3 as calcium-dependent regulator of SOS1, and STL1, a phosphate regulating sodium-potassium homeostasis), jasmonate-related genes (OPR as key enzyme for the peroxisomal synthesis of jasmonic acid, JAZ3 as salinity-related jasmonate-responsive regulator), and NAC as readout for retrograde signalling from mitochondria to the nucleus were measured (Fig.46 A-H). This is in order to identify, whether the strong modulations of steady-state transcript levels seen for Mn-SOD were specific for it, or a rather general feature of salinity related genes expression.

In order to ensure compatibility, the value at 1 h, in the WT BY-2, in absence of the peptoid was used as reference for all conditions (WT BY-2 w/o peptoid 3 h, and OE BY-2, 1 and 3 h). Generally, the transcripts of the two genes considered (SKOR and SLT1) were not induced at all both in response to salinity and OsOPR7 overexpression at both earlier and later time points (Fig. 46 C, D). Furthermore, the SOS1 and SOS3 genes were not induced in both the WT and OE BY-2 cells except that they were relatively upregulated at the control (0 mM NaCl) at 3 h (Fig. 46 A, E). Likewise, the transcript of the NHX1 gene was induced constantly irrespective of the salinity levels

in WT but was not induced in OE BY-2 cells at 1 h. At 3 h, in both WT and OE BY-2 cells, there was transcript induction at the control (0 mM NaCl) and high (150 mM NaCl) salt stress but it was downregulated at moderate (75 mM NaCl) salt stress in both cell types (Fig. 46 B). On the other hand, at 1 h, the transcript of JAZ3 gene was induced relatively in a dose-dependent manner under salt stress similarly both in the WT and OE BY-2 cells. At 3 h, in OE BY-2 cells, the JAZ3 transcript level was not induced and was the same irrespective of salinity level but in WT BY-2 cells it was induced slightly in a dose-dependent manner (Fig.46 H). Furthermore, the NAC (tobacco homologue of AtNAC13) gene, was downregulated at both moderate (75 mM NaCl) and high (150 mM NaCl) salt stress at 1 h both in WT and OE BY-2 cells. However, in the WT at 3 h, its transcripts were induced at the control (0 mM NaCl) but down regulated at moderate (75 mM NaCl) and high (150 mM NaCl) salt stress in both the WT and OE BY-2 cells (Fig. 46F). Based on a phylogeny constructed on Arabidopsis and tobacco NAC sequences, this gene seemed to be the closest homologue of ANAC013 (Fig. 33). Unlike all the rest genes, in the OE BY-2 cells, OPR7 gene was stuck out and modulated quite significantly at both time points. At 1 h, the induction was more or less constant irrespective of salinity level but at 3 h the induction was dose dependent. But in the WT BY-2 cells, this gene was not induced at all the three salinity levels and both time points (Fig. 46G).

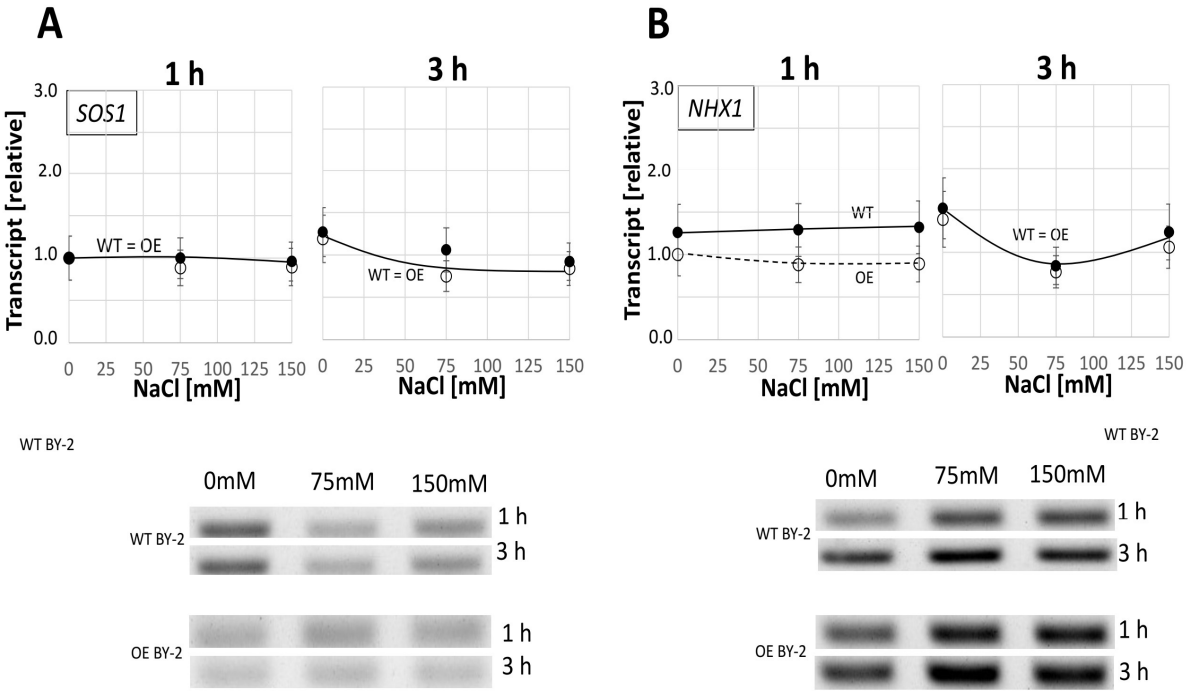

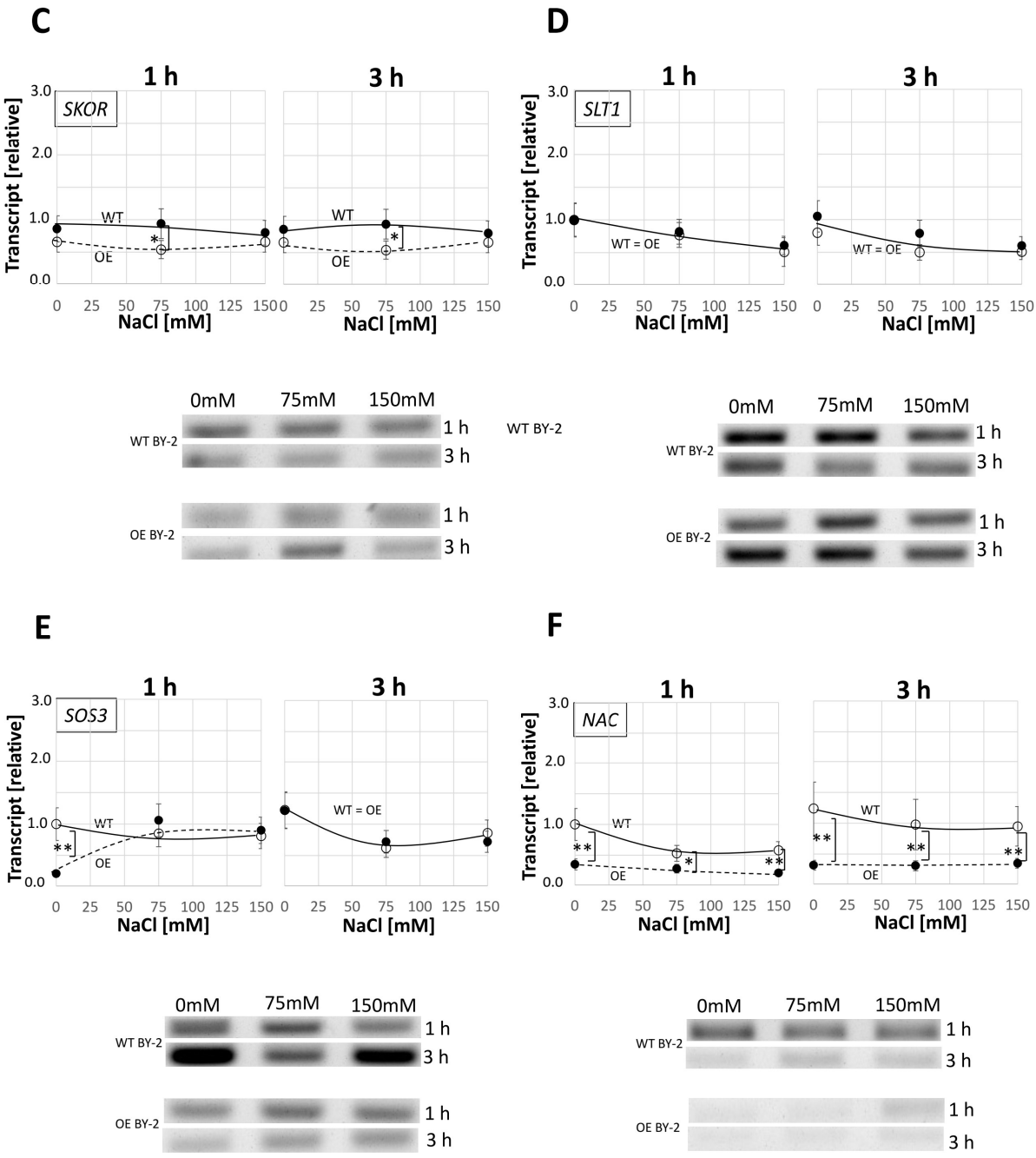
C
1 h
3 h
SKOR
Transcript [relative]
3.0
2.0
1.0
0.0
WT
OE
*
0 25 50 75 100 125 150
NaCl [mM]
D
SLT1
WT = OE
0mM
75mM
150mM
WT BY-2
OE BY-2
1 h
3 h
E
SOS3
**
F
NAC

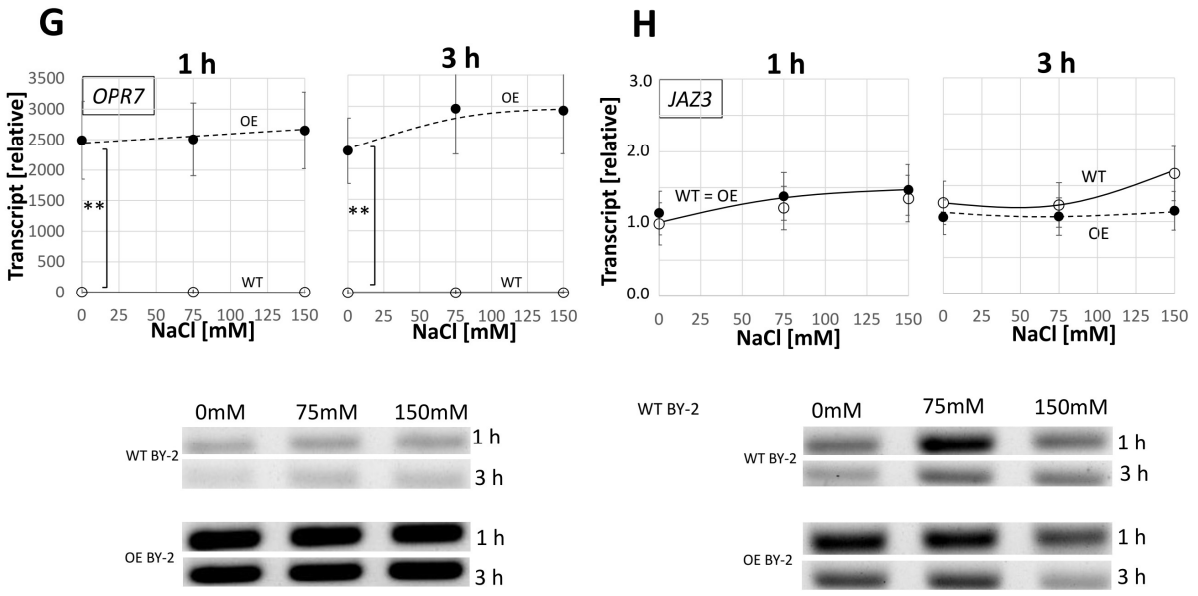

Figure. 46: Expression of different salt-related genes. Effect of salt stress on the expression of eight genes in WT (black curve) and OE (broken curve) tobacco BY-2 cells (**A-H**). In each case, agarose gel image of semiquantitative PCR (SQ-PCR) product of one representative example out of three independent experiments is shown. Data represent mean values and standard errors of three independent experimental series. **indicate differences significant at $P \leq 0.01$, *at $P \leq 0.05$ based on a student's t-test.

In addition to, the genes mentioned above, additional four salt-related genes; namely, JAZ1 and JAZ2 (salinity-related jasmonate-responsive regulators), and HKT1 and HAK1 (high-affinity K^+ transporters) had been investigated in preparatory studies (Fig. 47) using semiquantitative PCR (SQ-PCR) using the primers mentioned in (Table 5). However, since no significant responses were detected with respect to the expression of these genes, they were not studied further.

Figure 47. Agarose gel image of the semiquantitative PCR (SQ-PCR) product of four salt-related genes. In each case, one representative example out of three independent experiments is shown.

3.9.5. OsOPR7 overexpression did not improve ionic balance under salt stress

Ionic stress, such as elevated levels of sodium ions, accompanied by depletion of potassium is part of the causes of salt stress induced cellular damage. Therefore, the cellular contents for both ions after treatment with 0, 75 and 150 mM NaCl in WT and OE BY-2 cells were measured (Fig. 48). As expected, salt stress caused a dose-dependent increase in the content of sodium ions (Fig. 48A). The increase was quite strong and not alleviated by OsOPR7 overexpression. There was a significant decrease in potassium ions following the uptake of sodium ion (Fig. 48B). Despite the fact that sodium uptake was doubled at high salt stress (150 mM NaCl), as compared to moderate salt stress (75 mM NaCl), the decrease in potassium ion was already saturated at moderate salt stress (75 mM NaCl) and was not accentuated further at high salt stress (150 mM NaCl) (Fig. 48B). Similar to the case with sodium ion, OsOPR7 overexpression had no peculiar effect on potassium ion. Under salt stress, ionic balance was strongly perturbed, and it showed no sign of alleviation in OE BY-2 cells.

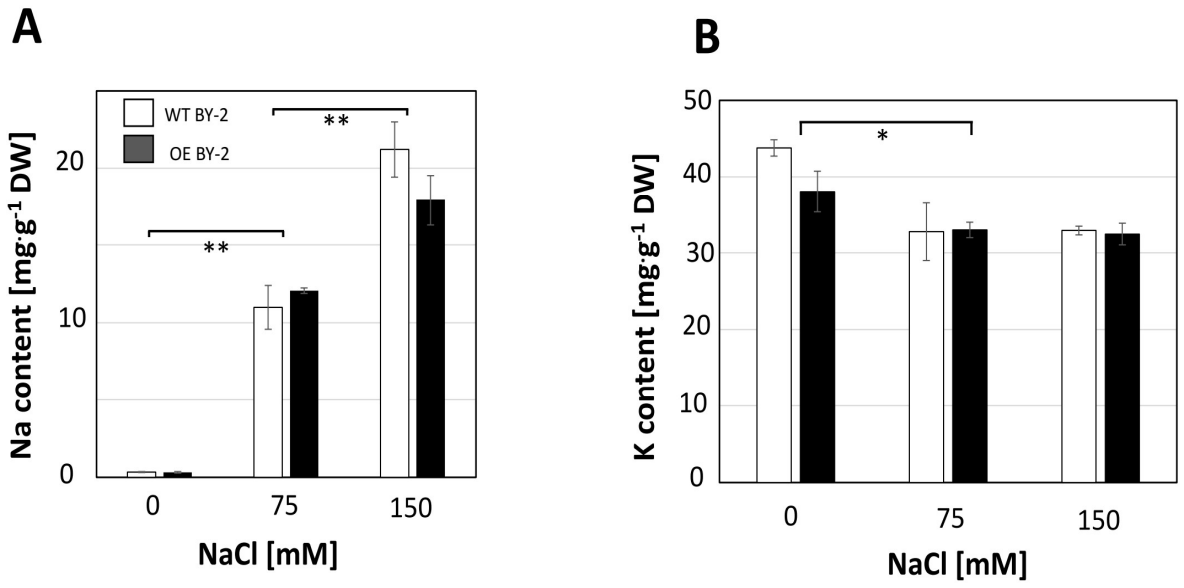

Figure 48: Effect of salt stress on the uptake of sodium (**A**) and potassium (**B**) at the control (0 mM NaCl), moderate (75 mM NaCl), and high (150 mM NaCl) salt stress in WT (white bars) and OE (black bars) tobacco BY-2 cells. Ion content is given relative to dry weight. Data represent mean values and standard errors of three independent experimental series. ** indicate differences significant at $P \leq 0.01$, *at $P \leq 0.05$ based on a student's t-test.

3.9.6. OsOPR7 overexpression and plant PeptoQ pretreatment partition jasmonate synthesis towards OPDA

Salt stress leads to activation of jasmonate synthesis and signalling, which improves adaptation, if appropriately down-modulated, but can initiate salinity-induced necrosis, if constitutively active (Ismail et al., 2014). Therefore, the levels of the precursor OPDA, jasmonic acid (JA), and the final product JA-Ile were compared in salt stressed WT and OE BY-2 cells after 1 and 3 h of salt stress. While JA was not detectable in none of the samples, OPDA and JA-Ile were accumulated to measurable amounts (Fig. 49). The steady-state levels of OPDA

did not respond to NaCl (Fig. 49A). However, they were significantly increased in the OE BY-2 cells at both 1 h [control (0 mM NaCl) and moderate (75 mM NaCl) salt stress], and 3 h [control (0 mM NaCl), moderate (75 mM NaCl) and high (150 mM NaCl) salt stress], and this increase was constant independently of the respective salt stress. At 1 h, at high salt stress (150 mM NaCl) both WT and OE BY-2 cells attained equal OPDA level (Fig. 49A). For JA-Ile, the levels were not significantly changed by the OsOPR7 overexpression, and again, salt stress did not cause any significant change either. At 1 h [moderate (75 mM NaCl) salt stress] and 3 h [control (0 mM NaCl) and moderate (75 mM NaCl) salt stress], the OE BY-2 cells attained relatively higher JA-Ile level as compared to the WT BY-2 cells. However, at 1 h [control (0 mM NaCl)] and 3 h [high salt stress (150 mM NaCl)], both OE and WT BY-2 cells secured more or less similar JA-Ile values (Fig. 49B). Since OPDA is not only a precursor of active jasmonate, but a signal by itself, the molar ratio between JA-Ile and OPDA was plotted, to see, whether salt stress or OsOPR7 overexpression repartitioned the balance between these two signalling molecules (Fig. 49C). Here, a significant shift of the biosynthetic pathway from JA-Ile towards OPDA was seen with regard to OsOPR7 overexpression. This channeling of the pathway towards OPDA was significantly more accentuated for 75 mM NaCl, but faded, if the concentration of salt was raised further especially at 3 h. On the other hand, in the WT BY-2 cells, more JA-Ile per OPDA was formed at both 1 and 3 h time points.

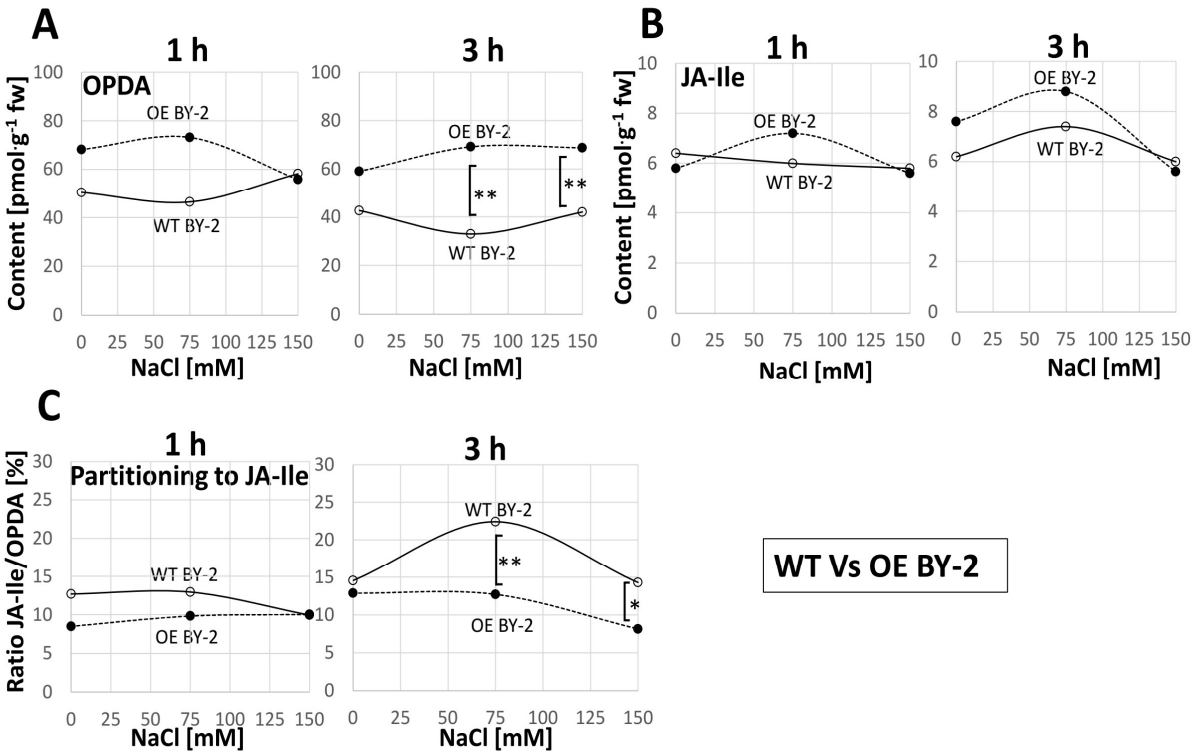

Figure 49: Effect of salt stress on 12-oxo-phytodienoic acid (12-OPDA) and jasmonyl-isoleucine (JA-Ile) levels as well as on the ratio between JA-Ile and OPDA (%). The level of 12-OPDA (**A**), JA-Ile (**B**) and JA-Ile/OPDA (%) (**C**) in salt stressed OE (broken curve) and WT (black curve) BY-2 cells. Data represent mean values and standard errors of three independent experimental series. ** indicate differences significant at $P \leq 0.01$, *at $P \leq 0.05$ based on a student's t-test.

On the other hand, the precursor OPDA, JA, and the final product JA-Ile levels, in OE BY-2 cells with and without plant PeptoQ pretreatment after 1 and 3 h salt stress were measured. While JA was detectable in none of the samples, OPDA and JA-Ile accumulated to measurable amounts (Fig. 50). In the OE BY-2 cells, both plant PeptoQ pretreatment and salt stress did not cause significant effect on OPDA level at both 1 and 3 h. At moderate (75 mM NaCl) and high (150 mM NaCl) salt stress, peptoid treatment had antagonistic effect on OPDA level where at 1 h it increased but at 3 h it decreased in a dose-dependent manner as compared to the OE BY-2 cells without peptoid pretreatment (Fig. 50A). With regard to JA-Ile level, at 1 h, OE BY-2 cells both in the presence and absence of plant PeptoQ pretreatment had more or less comparable value at the control (0 mM NaCl), moderate (75 mM NaCl) and high (150 mM NaCl) salt stress. At 3 h, the plant PeptoQ pretreated OE BY-2 cells attained lower JA-Ile value at the control (0 mM NaCl) and moderate (75 mM NaCl) salt stress as compared to the OE BY-2 cells without plant PeptoQ pretreatment but they secured the same value at high (150 mM NaCl) salt stress (Fig. 50B). On the other hand, since OPDA is not only a precursor of active jasmonate, but a signal by itself, the molar ratio between JA-Ile and OPDA was plotted to see, whether, salt stress, OsOPR7 overexpression or plant PeptoQ pretreatment repartitioned the balance between these two signalling molecules. At 1 h in the absence of salt stress, peptoid treatment caused the synthesis of more JA-Ile per OPDA; however, at moderate (75 mM NaCl) and high (150mM NaCl) salt stress, OE BY-2 cells with and without peptoid treatment, achieved similar JA-Ile/OPDA percentage. At 3 h, at the control (0 mM NaCl) and moderate (75 mM NaCl) salt stress, a significant and comparable shift of the biosynthetic pathway from JA-Ile towards OPDA was seen in peptoid treated OE BY-2 cells. However, this situation was reversed at high salt stress (150 mM NaCl) where the biosynthetic pathway generated more JA-Ile per OPDA as compared to the case in OE BY-2 cells without peptoid pretreament (Fig. 50C).

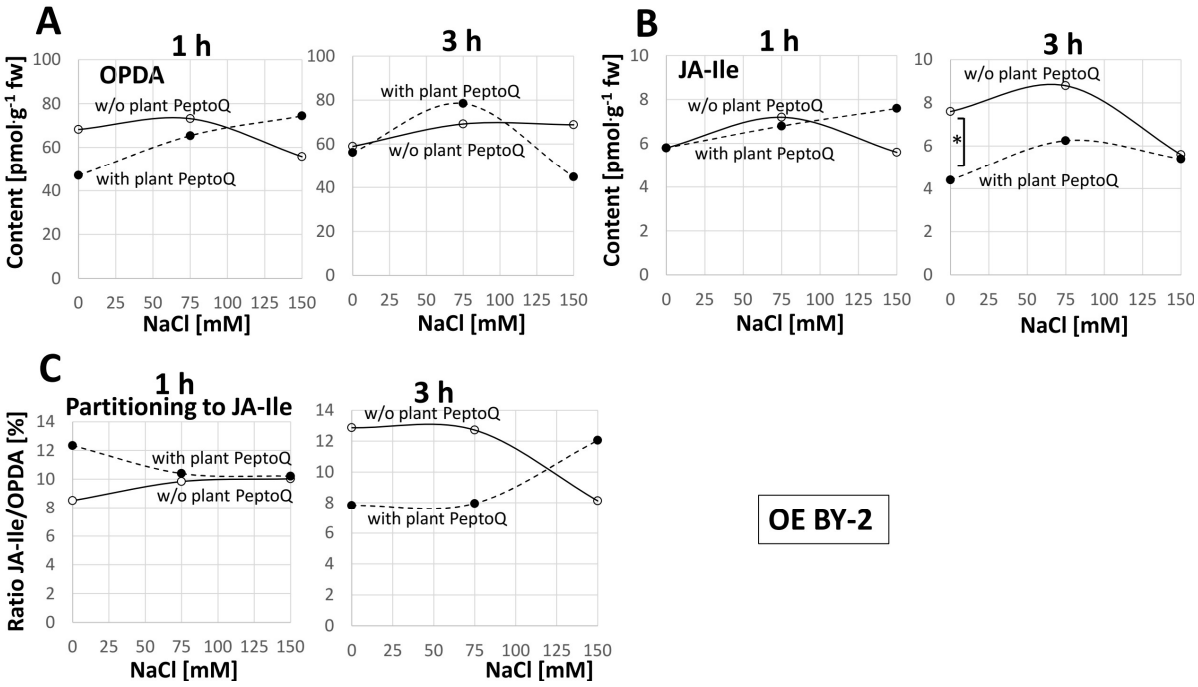

Figure 50: Effect of salt stress on 12-oxo-phytodienoic acid (12-OPDA) and jasmonyl-isoleucine (JA-Ile) levels as well as on the ratio between JA-Ile and OPDA (%). The level of 12-OPDA (**A**), JA-Ile (**B**) and JA-Ile/OPDA (%) (**C**) in salt stressed OE tobacco BY-2 cells without (black curve) and with (broken curve) plant PeptoQ pretreatment. Data represent mean values and standard errors of three independent experimental series. * indicate differences significant at $P \leq 0.05$ based on a student's t-test.

3.10. Summary of results

In this dissertation, we tried to impart salt tolerance to non-transformed WT tobacco BY-2 cells through plant PeptoQ pretreatment and OsOPR7 overexpression. Hence, the interaction of plant PeptoQ with the WT BY-2 cells was investigated and characterized. The dose-response and time-course experiments indicated that the uptake of plant PeptoQ proceeds in two stages where in the first step a pool in the endoplasmic reticulum (ER) is filled before the signal in the second slower step accumulates in the vermiform-vesicular final patterns. Upon subcellular localisation study of plant PeptoQ, these vermiform-vesicular patterns were interpreted as mitochondria. Thus, the final subcellular destinations of plant PeptoQ are mitochondria. To reach the mitochondria, plant PeptoQ passes through endosomes, trans-Golgi network (TGN), Golgi complex and the ER using both the clathrin-dependent and clathrin-independent endocytosis where actin filaments are actively involved whereas microtubules are dispensable. A tool for chemical manipulation like plant PeptoQ should not impose toxicity on the target cell. To this effect, the potential cytotoxicity of plant PeptoQ (2-50µM) on WT BY-2 cells was investigated, and the result showed no sign of toxicity at all. Instead, it improved the survival and adaptation of WT BY-2 cells to salt stress, and this mitigation effect of plant PeptoQ was not dependent on the conjugated rhodamine moiety. On the other hand, following the complete and effective internalisation of plant PeptoQ into the WT BY-2 cells, the fact that whether it is able to be internalised into the real plant cell system or not was scrutinised using rice root and root hairs. Consequently, the result depicted that plant PeptoQ was able to be internalised into both the rice root and root hairs effectively and efficiently. Like the case in WT BY-2 cells, its final subcellular destination was in the mitochondria.

Both pretreatment with plant PeptoQ and overexpression of OsOPR7 in WT BY-2 cells, mitigated salt stress induced detrimental effects more or less in a similar manner. Cell expansion and cell viability were fully and partially compensated at moderate (75 mM NaCl) and high (150 mM NaCl) salt stress respectively by both approaches. However, even if, the detrimental effects of salt stress on cell division (proliferation) were mitigated by both peptoid treatment and OsOPR7 overexpression, it was more sensitive as compared to cell expansion and cell viability. Both approaches significantly ameliorated doubling time, and strongly suppressed the salt stress induced increase in MDA and superoxide (ROS) levels in WT BY-2 cells. However, they had no effect on the level of hydrogen peroxide. Plant PeptoQ pretreatment and OsOPR7 overexpression lead to increased SOD activity but decreased Mn-SOD transcript induction under salt stress. However, both approaches had no effect on Catalase (CAT) activity. Except SOS1, NAC and OPR7 genes, other salt-related genes such as ion channels (NHX1 and SKOR), regulators for ion channels (SOS3 and SLT1) and jasmonate related gene (JAZ3) did not show strong transcript modulation in response to salinity, plant PeptoQ pretreatment and OsOPR7 overexpression. Similarly, even if, ionic balance was strongly perturbed by salt stress, both plant PeptoQ pretreatment and OsOPR7 overexpression had no mitigatory role at all. Pretreatment of salt stressed WT and OE BY-2 cells with plant PeptoQ caused increased OPDA level; however, it had no significant effect on JA-Ile level. On the other hand, it lead to a significant shift of the biosynthetic pathway from JA-Ile to OPDA, and this channeling of the pathway towards OPDA was significantly more accentuated for moderate salt stress (75 mM NaCl) but it faded as it proceeds to high salt stress (150 mM NaCl).

4. Discussion

Although powerful as approach, plant genetic engineering is limited by the need to introduce the foreign gene into the target cell and to regenerate an entire organism from this cell, which often turns out to be difficult, if one moves beyond *Arabidopsis thaliana* as model. Approaches, where functional cargo molecules are directly delivered into cell of interest by means of cell penetrating peptides have potential as alternative strategy of manipulation. Since peptides are prone to proteases, their stability *in vivo* might become limiting. To overcome this limitation, peptidomimetics are interesting alternatives. Consequently, in this dissertation, a particular strategy was used, where the cationic amino-acid side chains are linked to nitrogen instead of carbon, such that these molecules should not be accessible for proteolytic cleavage. As proof of concept for a functional cargo delivered to tobacco BY-2 cells as experimental model, a rhodamine-labelled semiquinone (plant PeptoQ) as mimetic of coenzyme Q10 was used to test the efficiency of cellular uptake, the mechanism for cellular internalisation, the route of subcellular targeting, and potential impacts on cellular physiology.

4.1. Characterization of the interaction between plant PeptoQ and non-transformed WT tobacco BY-2 cells

The cellular uptake of plant PeptoQ was both, dose and time dependent, impaired by inhibitors of endocytosis, and strongly depends on actin, while microtubules are dispensable. Furthermore, plant PeptoQ specifically targets to mitochondria, is not toxic, and even, if followed over several days; it ameliorates the adaptation of tobacco BY-2 cells to salt stress.

4.1.1. The plant PeptoQ targets to mitochondria in two steps involving passage through the ER membrane

To determine the molar concentrations to which the peptoid accumulates in mitochondria, it would be necessary to purify the mitochondria and quantify the plant PeptoQ by mass spectroscopy based analytical methods. However, even based on the relative quantification using the rhodamine fluorescence, it is evident that the plant PeptoQ is efficiently targeted to the mitochondria (Fig. 11). While the outer mitochondrial membrane probably does not represent a tight barrier due to the presence of porins with an exclusion size limit of 5 kDa (reviewed in Flowers et al., 2015), there must be one point, where the peptoid has to pass a membrane to reach the outer mitochondrial membrane. Principally, this membrane passage could occur at the plasma membrane. Alternatively, the peptoid might be taken up through endocytosis and exit into the cytoplasm from endosomes. Both mechanisms have been reported for the uptake of cell penetrating peptides into mammalian cells (reviewed in Madani et al., 2011; Gao et al.,2016) depending on the type of transporter and also depending on the type of cargo.

For the uptake of the plant PeptoQ, a working model was developed that describes a third scenario (Fig. 51): The plant PeptoQ is taken up by endocytosis (both clathrin-dependent and clathrin-independent), depending

on dynamic actin filaments. Then, it reaches the ER by retrograde transport passing early endosomes, trans-Golgi network, and the Golgi organelle, and arrives at its final destination, the mitochondrial intermembrane space at the contact sites between ER and mitochondria (Jaipargas et al., 2015). It is this final step, where the peptoid has to pass through a membrane-this membrane is neither the plasma membrane, nor the endosomal membrane, but the membrane of the ER. The evidences that lead to the working model are discussed below.

4.1.2. The uptake of the plant PeptoQ is saturable. Membrane passage of a cell penetrating peptide might involve interaction with a binding site. If this binding site is present with limited abundance, uptake should be saturable. Alternatively, the membrane passage could proceed at any point of the membrane, independently of a particular binding site, as it seems to be the case for the Tat and Tat_2 cell penetrating peptides, where the entry into triticale mesophyll protoplasts never became saturated (Chugh and Eudes, 2007). The uptake of the plant PeptoQ is clearly saturable, but this uptake seems to occur in two steps (Fig. 10): Since there was no detectable uptake below a threshold of 0.9 µM (a value derived from fitting the data by a two-phase Michaelis-Menten model, Fig. 10D), it seems that a first binding site has to be occupied, before the plant PeptoQ becomes available for the passage from the ER into the mitochondrion. This first binding site (which is predicted to be relatively abundant, in the range of 1 µM) might reside on the plasma membrane and defines, how much peptoid can enter clathrin-dependent endocytosis (Fig. 51, ①). The second bottleneck is the membrane passage itself, which occurs at the ER-mitochondrial contact points (Fig. 51, ④). The size-exclusion of the porins in the outer mitochondrial membrane would be large enough to allow for back-diffusion from the stroma to the cytoplasm, but the negative charge of the inner mitochondrial membrane supposedly sequesters the charged side-chains of the peptoid very efficiently. The reticulate patterns seen during early stages of uptake of a saturating pulse with plant PeptoQ (Fig. 9) can be explained by this two-step model-this ER pool of labelled peptoid should become manifest as intermediary state at early time points, when the second step (the passage through the ER membrane) becomes limiting. This is indeed the case, as to be concluded from the patterns observed for dual labelling of the plant PeptoQ along with DioC6 (Fig. 14), and Mitotracker Green FM (Fig. 15), support the existence of a transient pool in the ER. The second step, i.e. the transition from this ER pool into the final destination, the mitochondrial stroma, is much more constrained, with an estimated K_D of 0.2 µM, indicative of a presumed binding site that is a factor of 5 less abundant as compared to the binding site at the membrane. Due to this difference in the abundance of the two binding sites, feeding lower concentrations of plant PeptoQ should lead to a steady state, where more peptoid is delivered to the ER as can be exported in the second step, such that the signal should accumulate in the ER also for later time points. Also, this implication of the model is supported by the available data (Fig. 10). A third piece of evidence is the pronounced discontinuity in uptake seen for incubation with saturating (2 µM) concentrations of the plant PeptoQ (Fig. 9). The two waves of uptake can be interpreted by a situation, where the first step is saturated within 60 min, possibly because the recycling of the clathrin-dependent machinery towards the membrane becomes limiting, or because the

peptoids accumulating in the ER due to time-limiting membrane passage into the mitochondrion shift the equilibrium to the left side. It then takes some time to recover the capacity of uptake, such that the second wave can proceed. A similar threshold of uptake followed by time- and concentration dependent, saturable uptake was also seen in human cells for guanidinium- and amino-peptoids (Schröder et al., 2007; 2008) and might, thus, represent a feature of the uptake system that has been conserved during evolution.

Neither the molecular nature of both binding sites is known at this stage, nor the involvement of temperature-sensitive events, nor the potential mechanisms regulating membrane passage at the ER-mitochondrial contact points. From structure-function relationships (reviewed in Wender et al., 2000), positively charged side groups have been determined as central factor for efficient uptake, whereby arginine and guanidine residues were more effective than lysines. In case of the plant PeptoQ, the positive charges will not only promote membrane passage, but may also be a key factor for the strong partitioning to the mitochondria, because the cytosolic face of the inner membrane (where the "natural" ubiquinone, mimicked by this peptoid, is located as well) is negatively charged due to the proton gradient across this membrane.

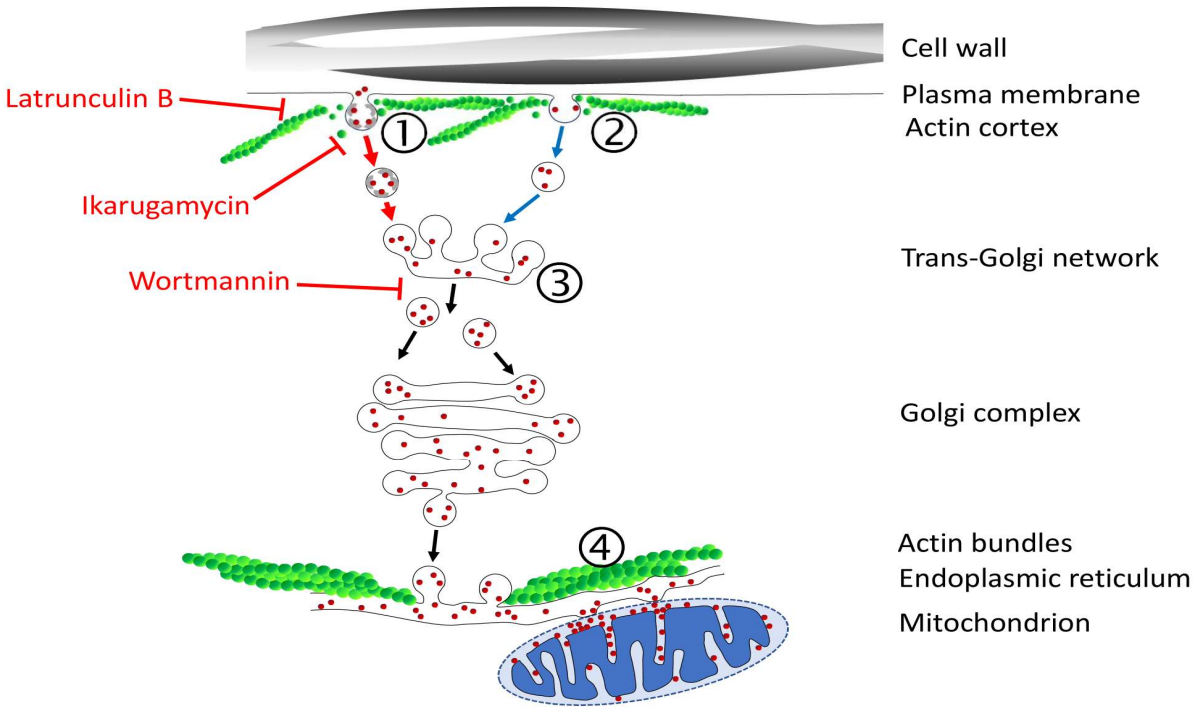

Figure 51: Working model for the cellular uptake of plant PeptoQ into non-transformed WT tobacco BY-2 cells. The majority of the plant PeptoQ (red dots) enters via clathrin-dependent endocytosis, following interaction with a binding site (①, red arrows). Alternatively, the plant PeptoQ can enter through pinocytotic, clathrin-independent, uptake (②, blue arrows). The invagination of the plasma membrane requires a dynamic subpopulation, which is subtending the membrane and can be eliminated by Latrunculin B. Both pathways of uptake converge at the trans-Golgi Network (TGN), which is the plant version

of the early endosome (③). The site of action of Ikarugamycin is assumed to be upstream in the clathrin-dependent pathway (①, red arrows), while Wortmannin is assumed to act more downstream, at the TGN. From the TGN, the plant PeptoQ reaches by retrograde transport via the Golgi complex to the ER (black arrows). The ER is structured by stable cables of actin that also is responsible for the movement of mitochondria. The membrane passage of the plant PeptoQ is proposed to occur at the mitochondria-associated ER membranes (④). Through the porins of the outer mitochondrial membrane, the plant PeptoQ readily enters the intermembrane space of the mitochondrion. Due to the negative charge of the cytoplasmic face of the inner mitochondrial membrane, the positively charged plant PeptoQ attaches to this membrane and is therefore removed from the equilibrium at the outer face of the ER membrane, such that the plant PeptoQ accumulates in the mitochondrion to levels that are much higher than those seen in the ER lumen. Note that the model is simplified and focused on the route of uptake, aspects of membrane trafficking that are not relevant here (such as the multivesicular body or the vacuole, microtubules) have been deliberately omitted for the sake of clarity. Adapted from Asfaw et al., 2019.

4.1.3. The plant PeptoQ enters the BY-2 cells via clathrin-dependent and clathrin-independent endocytosis

To understand, whether the plant PeptoQ undergoes a membrane passage at the plasma membrane, or whether it is first taken up through endocytosis, two inhibitors of endocytosis were used such as Wortmannin and Ikarugamycin (Fig. 10). While both inhibitors suppressed the uptake into mitochondria, the observed patterns were significantly different: After treatment with Wortmannin, only few residual signals could be seen at the cross walls, while with Ikarugamycin, the residual signals were significantly more abundant and also lining the lateral walls (Fig.12). Also, for FM4-64, which was used as control for the efficacy of the two inhibitors, the suppression of uptake after treatment with Wortmannin was more pronounced as that seen for Ikarugamycin. This is not the first time that such a difference in efficacy has been observed: Also, for the endocytotic uptake of nanobeads into tobacco BY-2 cells, the suppression by Wortmannin was more pronounced as compared to that achieved by Ikarugamycin (Bandmann et al., 2012). Unfortunately, the mode of action of the two inhibitors is far from clear, not even in mammalian cells, but the published record supports a scenario, where Ikarugamycin blocks internalisation of membrane receptors, while leaving intracellular trafficking untouched (Hasumi et al., 1992; Luo et al., 2001). Wortmannin blocks phosphatidyl-inositol 3-kinase. Phosphorylated phosphatidyl inositol 3 interacts with the proteins that build up the retromer. Wortmannin, therefore, seems to interfere with a step of clathrin-dependent endocytosis downstream of the early endosome (Kundra and Kornfeld, 1998). Consistent with this scenario, Wortmannin was found, for root cells of *Arabidopsis thaliana*, to cause rapid fusions of multivesicular bodies, a plant specific precursor of vacuoles (Wang et al., 2009). In addition to clathrin-dependent endocytosis, clathrin-independent pathways have been demonstrated also for plant cells. For instance, the uptake of a fluorescent derivative of glucose, 2-(N-(7-nitrobenz-2-oxa-1,3-diazol-4-yl) amino)-2-deoxyglucose, into tobacco BY-2 protoplasts still proceeds, when clathrin-dependent endocytosis (probed by the uptake of FM4-64) is suppressed by either Ikarugamycin, or by genetic interference by overexpression of a fragment of the clathrin heavy chain (Bandmann and Homann, 2012). Since the fluorescent glucose derivative was later seen in the trans-Golgi network, the two pathways seem to converge here (Fig. 51, ③), similar to their

mammalian counterparts (for review see Gruenberg, 2001). If this assumption holds true, the stronger inhibition by Wortmannin observed for the uptake of the plant PeptoQ (Fig. 12), would mean that both endocytotic pathways are intercepted, while for Ikarugamycin only the contribution from clathrin-dependent endocytosis is suppressed. Irrespective of the relative contribution of the two pathways, the plant PeptoQ should be detectable in both early and late endosomes. By using a strategy, where the plasma-membrane located auxin-influx carrier AUX1 was expressed in fusion with YFP under a estradiol-inducible promoter, we were able to see the plant PeptoQ small vesicles close to the plasma membrane that presumably represented early endosomes (Fig. 13), and were accompanied by larger vesicles deeper in the cytoplasm that might be late endosomes supporting the conclusion from the experiments with endocytotic inhibitors.

4.1.4. Membrane-associated actin is needed for endocytic uptake, microtubules are dispensable

Mitochondria were seen to be aligned with actin cables, and pretreatment with Latrunculin B eliminated uptake as efficiently as pretreatment with the endocytotic inhibitors, leaving only punctate signals lining the lateral cell membrane (Fig. 16). This leads to the question, whether the tethering of ER and mitochondrial by actin cables is required for mitochondrial targeting. This question is stimulated by three reasons: (i) The role of actin cables for ER structure and movement of the Golgi complex in plant cells has been addressed in classical work (Boevink et al., 1998). (ii) The close link between mitochondria and ER structure has been shown by live imaging (Jaipargas et al., 2015). (iii) Plant mitochondria move along actin cables (Van Gestel et al., 2002). However, if Latrunculin B would act by interrupting the actin-dependent association of ER and mitochondria, the signal is expected to remain trapped in the ER. This is not observed-the signal fails to enter the cell almost completely, only occasionally, fluorescent foci are seen at the nuclei that have been displaced to the cross wall (Fig. 16) in consequence of the breakdown of the perinuclear actin cage that usually tethers the nucleus (Durst et al., 2014). Our data indicate a different scenario linked to a different population of actin: Highly dynamic actin filaments subtend the cell membrane and participate in the sensing of membrane integrity (Eggenberger et al., 2017). Their proximity to the membrane is so close that it is possible to image fluorescently labelled actin filaments by Total Internal Reflection Fluorescence (TIRF) Microscopy in tobacco protoplasts (Hohenberger et al., 2011), indicative of a distance that must be well below 50 nm. We propose that Latrunculin B eliminates this membrane-associated, highly dynamic (and therefore also highly sensitive) population of actin filaments, which will intercept the formation of membrane invagination and, thus, block endocytotic uptake. In fact, the role of actin filaments for endocytotic uptake in mammalian and yeast cells is well established (for review, see Engqvist-Goldstein and Drubin, 2003), and has also been discovered in plants from experiments, where the internalisation of the auxin-transport facilitator PIN1 was blocked by cytochalasin D (Geldner et al., 2001). Since the anchoring of mitochondria has been linked with microtubules (Van Gestel et al., 2002), and since the microtubule +TIP protein CLASP was found to participate in endocytotic cycling of PIN2 (Ambrose et al., 2013), a role of microtubules for peptoid uptake is plausible. In fact, the uptake of polyguanidine peptoids (mimicking a

polyarginine peptide) into tobacco BY-2 cells was inhibited by Oryzalin, although only partially. Although we could see, using a fluorescent tubulin marker line, that some mitochondria colocalised with microtubules (Fig. 17), the orientation of the mitochondrion often deviated from the direction of the tethering microtubules indicative of a different lattice (actin cables) intersecting with the microtubules. Most importantly, when we eliminated microtubules using Oryzalin, the plant PeptoQ was still taken up in the same manner as in the controls, where microtubules were intact. Thus, in contrast to actin filaments, microtubules were not involved in the uptake and mitochondrial targeting of the plant PeptoQ.

4.1.5. The plant PeptoQ efficiently circumvented programmed cell death

The peptoid used in the current study represents a novel approach to deliver functional cargoes to the mitochondria. However, alternative strategies are possible and have been already employed in plants (Chuah et al., 2015; Yoshizumi et al., 2018): fusions of mitochondrial and plastid transit peptides with a charged domain binding DNA have been used to engineer the genomes of both organelles. By adding the cell penetrating BP100, the efficiency of delivery could be increased (Chuah et al., 2015) indicating that passage through the plasma membrane is limiting for these constructs. While the use of peptides as carrier is convenient and versatile, the need of the transit peptides to travel through the cytoplasm, might also have certain limitations: Even a transient perturbation of membrane integrity can activate a sensory circuit composed of the membrane-located NADPH oxidase RboH and membrane associated actin which acts as trigger for programmed cell death (Eggenberger et al., 2017). By hijacking the endosome-ER-mitochondria pathway, this problem can be circumvented. In fact, even for high concentrations of peptoid, we could not detect any indication of elevated mortality (Fig. 19), which is in stark contrast of the behaviour obtained by the cell-penetrating peptide BP100. For the purpose of organelle transformation, where most cells will be anyway eliminated by subsequent selection, this aspect may not be so relevant. For studies, where the response to altered mitochondrial physiology is to be studied, this aspect is crucial, though. Here, the peptoid strategy brings significant payoff that makes up to the somewhat more cumbersome synthesis (although modular strategies of peptoid synthesis have strongly reduced this challenge). A further benefit for long-term studies, is the inaccessibility of the peptoid bond to protease activity.

4.2. Role of plant PeptoQ on salt stress-induced deleterious effects in WT tobacco BY-2 cells

In our published work, we showed that the construct, plant PeptoQ (which is composed of a peptoid mediating mitochondrial import, and a functional cargo that mimics coenzyme Q10) was efficiently and specifically accumulating in mitochondria of walled tobacco BY-2 cells and improved their resilience against salinity stress (Asfaw et al., 2019). For cell expansion, this recovery was more pronounced, and, for moderate salt stress, even complete (Fig. 25), while cell proliferation was more sensitive and rescued only partially (Fig. 24). The mechanism, by which plant PeptoQ mitigates salt stress has been addressed and as a result, we found that plant PeptoQ improved oxidative balance under salt stress, evident from reduced steady-state levels of

malonedialdehyde and superoxide, which were correlated with increased activity of superoxide dismutase (Fig. 28, 29, 30). The improved resilience was not caused by a better ionic homeostasis, because intracellular sodium increased, and intracellular potassium decreased to the same extent as in the absence of the peptoid in response to salt stress (Fig. 35). However, the steady-state levels of Mn-SOD transcripts were rapidly and strongly upregulated in response to plant PeptoQ in the absence of salt stress (Fig. 31A). This pattern is considered as specific, because the majority of salt-stress related genes (with exception of mild effects seen for the sodium extruder SOS1, the retrograde-signalling factor NAC, and the jasmonate signalling factor JAZ3), did not show significant responses to salt stress. These surplus Mn-SOD transcripts were then consumed under salt stress, which, together with the high enzymatic activity of SOD indicate that the peptoid induces a higher pool of transcripts that are then efficiently converted to protein under challenge. In the absence of the peptoid, Mn-SOD transcript levels were low, but increased in response to salt stress. This increase was more efficient for moderate salt stress (75 mM NaCl) but developed more sluggishly under high salt stress (150 mM NaCl). In other words, the pretreatment with plant PeptoQ activated adaptive gene regulation in an anticipative manner. We pursued the working hypothesis that this "pre-adaptation" provides a time gain which is decisive for survival under salt stress and several implications of this working hypothesis are explored and discussed below.

4.2.1. Is plant PeptoQ modulating retrograde signalling?

Chloroplasts and mitochondria originated from independent prokaryotic organisms, but most of their genes have been either lost or transferred to the nucleus of their eukaryotic host. The proteins encoded by these transferred genes have to be imported by virtue of specific signal peptides. However, both organelles have still retained some genes, for instance, for components involved in electron transport across the inner membranes, or components involved in organelle gene expression (Gould et al., 2008; Blanco et al., 2014). The retention of a residual gene set in the organellar genome has attracted considerable attention. One of the most plausible explanations for this phenomenon has been given by the colocation for redox regulation of gene expression (CoRR) hypothesis (reviewed in Allen, 2015). Because, in both organelles, free electrons are transported across a membrane in the presence of oxygen, or partially reduced derivatives of oxygen, any disbalance would lead to fatal consequences, which means that there has been a strong selective pressure towards rapid and efficient redox homeostasis, which is not compatible with a regulatory system, where the organelle has first to launch retrograde signalling to the nucleus, transcriptional activation, and then posttranslational import of the respective gene product. Nevertheless, redox homeostasis in plant mitochondria is secured beyond the CoRR mechanism and involves retrograde signalling as well, conveyed by redox-active components, such as ATP, acetyl-CoA, NAD^+, and glutathione (reviewed in Hartl and Finkemeier, 2012), which shows, how vital it is for a plant cell to safeguard redox balance against perturbations by biotic or abiotic stress. While retrograde signalling from the plastids has been intensively studied from the 1970ies (a historical review is given in Börner, 2017; for a recent update on the molecular components see the comprehensive review by Kleine and Leister, 2016), plant mitochondrial retrograde signalling is far less understood. However, disruption of mitochondrial electron

transport and subsequent accumulation of ROS has been shown as triggers for retrograde signalling (Ho et al., 2008; Blanco et al., 2014). Still, the pathway that conveys the information about the perturbed functional status of mitochondria to the nucleus leading to a specific transcriptional response had remained enigmatic over years (reviewed in Ng et al., 2014). Based on mutant approaches, several members of the NAC family of transcription factors, such as NAC13 (De Clercq et al.,2013), for a recent review (see Hoang et al., 2017), or NAC17(Ng et al., 2013) had been identified as crucial component for mitochondrial retrograde signalling. These proteins are integrated in the ER, but can be cleaved by a Rhomboid type protease, such that the N-terminal domain can be imported into the nucleus. Since mitochondria are transported along actin and since actin (Gestel et al., 2002) also is important for ER (Flis and Daum, 2013) mitochondrial contact, leakage of ROS through the mitochondrial permeability pore is expected to initiate this signal.

At the moment, the molecular nature of the signal that transfers information from the disturbed mitochondria to the transcription factors through the ER remains unknown. However, several studies indicate that mitochondrial ROS (especially superoxide ions) are responsible in relaying such information from the dysfunctional mitochondria to the downstream transcription factors (Huang et al., 2016; Moller, 2016). Interestingly, retrograde signalling is not only deployed by excess of mitochondrial superoxide ($O_2^{\bullet -}$), but as well, when steady-state levels of superoxide drop below normal (for a recent review see Wagner et al., 2018). In this dissertation, salt stress caused increased ROS generation (Fig. 29), impaired SOD activity (Fig. 30), but increased Mn-SOD transcripts (Fig. 31). This correlation would be consistent with a model, where Mn-SOD upregulation is the consequence of disturbed redox balance in the mitochondria. In response to pretreatment with plant PeptoQ, steady-state levels of Mn-SOD transcripts were strongly upregulated (Fig. 31), while resting levels of superoxide were extremely low (Fig. 29), as it would be expected, if the elevated transcripts result in enhanced accumulation of protein. This effect is not seen for hydrogen peroxide (Fig. 29) supporting Mn-SOD as specific target for the peptoid effect. Interestingly, the specific activity of SOD is not altered by the peptoid pretreatment (Fig. 30), but increases during salt stress, while the steady-state transcript levels for the Mn-SOD transcript decrease strongly (Fig. 31). These data suggest that the peptoid pretreatment stimulates transcription of Mn-SOD, and that this elevated pool of transcripts is then mobilised, once the mitochondria are challenged by salt stress. This scenario would indicate that posttranscriptional regulation becomes active during salt stress, but also that transcriptional activation of Mn-SOD prior to salt stress contributes to the mitigating effect of plant PeptoQ. To achieve this transcriptional activation, a signal has to be conveyed from the mitochondria, where plant PeptoQ accumulates, towards the nucleus, where the Mn-SOD gene is encoded. When this retrograde signalling is mediated by specific NAC proteins that are proteolytically cleaved during the process(De Clercq et al., 2013; Ng et al., 2013), meaning that the signalling molecule is consumed during signalling, one would expect that the corresponding genes would be upregulated in the long term to replenish the pool of the consumed NAC protein. The finding that the putative tobacco homologue of AtNAC13 is upregulated after prolonged incubation

with plant PeptoQ (Fig. 32F) is consistent with this hypothesis. Thus, our data support a scenario, where this peptoid activates retrograde signalling from mitochondria to the nucleus and, thus, induces the accumulation of Mn-SOD transcripts. Upon salt stress, this elevated pool is recruited to fuel elevated SOD activity, mitigating the oxidative disbalance caused by the excess of sodium ions.

4.2.2. Beyond retrograde signalling-A role for post-transcriptional regulation of mitochondrial SOD

The strong upregulation of steady-state transcript levels seen for Mn-SOD after treatment with plant PeptoQ prior to the onset of salt stress (Fig. 31A) would be expected to lead to elevated SOD activity resulting in reduced superoxide levels and concomitantly increased hydrogen peroxide levels. These implications are definitely not observed. Neither does the peptoid cause any elevated SOD activity in the absence of salt (Fig. 30A, 0 mM points), nor are hydrogen peroxide levels increased (Fig. 30B, 0 mM points). The only implication, which is met by the experimental data, is a drastic (by 90%) reduction of superoxide levels in presence of the peptoid (Fig. 29A, 0 mM points). If superoxide levels are reduced, while SOD activity is not increased, there must be a non-enzymatic component involved. This non-enzymatic component might be plant PeptoQ itself since its hydroxylated ring confers a very strong superoxide-scavenging property (Gulaboski et al., 2013). What remains to be explained is, why the massive (already 15-fold after 1 h) increase of transcripts does not culminate in an increase of SOD activity. This discrepancy calls for a role of post-transcriptional and even post-translational regulation. In fact, several mechanisms such as phosphorylation, nitration, methylation, glutathionylation, acetylation and metal incorporation (reviewed in Candas and Li, 2014) are known that control mitochondrial SOD beyond retrograde signalling.

Using the mitochondrial Alternative Oxidase as paradigm, the role of local superoxide in activation of retrograde signalling was tested in rice (Li et al., 2013) by expressing SOD in different subcellular compartments before inducing superoxide by methyl viologen. Only when the SOD was overexpressed in the mitochondria, but not in other compartments, did this overexpression attenuate the effect of oxidative stress on Alternative Oxidase expression. Thus, Mn-SOD activity, mitochondrial homeostasis (functionality) and mitochondrial retrograde signalling seem to be intimately linked. As one mechanism, release of oxidised peptides has been proposed (reviewed in Moller and Sweetlove, 2010). Alternatively, peroxynitrite, resulting from the reaction of superoxide with mitochondrial nitric oxide, can inactivate SOD by specific nitration (Holzmeister et al., 2015).

A third mechanism runs through a miRNA shown to regulate the stability of SOD transcripts in cytoplasmic and plastidic SODs (Sunkar et al., 2006). The abundance of the responsible miR398 is decreased under oxidative stress, such that SOD transcripts can accumulate to higher levels. Whether this mechanism can also act on Mn-SOD, is not known. The strong induction of transcripts for Mn-SOD (Fig. 31) by the peptoid would be expected, when the peptoid can downmodulate the steady-state levels of miR398, a testable implication of this hypothesis. Still, none of the three mechanisms would explain, how plant PeptoQ by itself can induce SOD

transcripts, while these transcripts are not translating into elevated activity prior to the onset of salt stress (Figs. 29, 30).

A fourth regulatory mechanism might play a role here: the activity of SOD can unfold only in presence of the metal co-factor, in case of the mitochondrial SOD, a Mn. The association of this metal co-factor with the SOD apo-protein has been addressed in yeast mitochondria (Luk et al., 2005) (reviewed in Culotta et al., 2006) and shown to occur in the mitochondria themselves with the still unfolded imported apo-protein. The mitochondrial import of manganese would therefore turn into a regulator of SOD activity. If the peptoid would trigger SOD transcription, while not promote manganese import, a strong accumulation of transcripts would not translate into increased SOD activity, which is exactly what we observe (Figs. 29, 30). If manganese import is stimulated in response to salt stress, enzyme activity would increase, which is again consistent with our observations (Fig. 30).

Whether any of the four mechanisms is acting in the context of plant PeptoQ activity remains to be elucidated. As unifying principle, they would relay information on the enzymatic activity of mitochondrial SOD to the nucleus, which means that they employ retrograde signalling, albeit the cellular responses would be different: either activation of SOD transcription, down-regulation of a miRNA gene, or activation of Mn import. These mechanisms are not mutually exclusive, but are likely acting in concert, and they all lead to implications that are testable experimentally.

4.2.3. Does plant PeptoQ deploy anticipative signalling by triggering the hypoxia pathway?

The specific and multivariate response patterns seen on the level of transcripts, the level of enzyme activity, and on the level of ROS abundance (Figs. 28, 29, 30,31) can be explained by a model (Fig. 52A), where plant PeptoQ acts as scavenger of mitochondrial superoxide. Thus, steady-state levels of superoxide (originating from complex III of the mitochondrial electron transport chain, Fig. 52A, ①) dissipate not only by conversion to hydrogen peroxide, catalysed by Mn-SOD (Fig. 52A, ②), but also by direct reduction through plant PeptoQ (Fig. 52A, ③). Thus, under physiological conditions, this additional mechanism of elimination, will reduce superoxide to a level, as it would occur during hypoxia. This deploys hypoxia-related retrograde signalling (Wagner et al., 2018), possibly involving specific NAC transcription factors (Fig. 52A, ④). Since these NAC proteins would be consumed by proteolytic cleavage, they are expected to be replenished by induction of NAC transcripts, as we actually have observed in this dissertation (Fig. 31C, Fig. 32F). This retrograde signalling would culminate in the induction of Mn-SOD (Fig. 52A, ⑤). After translation, the SOD protein is imported into the mitochondria establishing a pool of SOD that would, however, remain inactive, since it is still void of Mn (Fig. 52A, ⑥). This pool of excess SOD is then gradually activated through ongoing Mn import and subsequent complexation into the active holoenzyme. When SOD becomes inactivated under salt stress, for instance by nitration, the additional pool of SOD can be recruited to compensate for this inactivation. Thus, excessive formation of superoxide as it would

normally occur under salinity, is prevented, which allows the cells to buffer, at least partially, the negative impact of salt stress.

The implications from this working model under the four combinations derived from two factors (plant PeptoQ, salt stress) and two cardinal states (absence, presence) are met in detail by our observations (Fig. 52B-E). For instance, this model can explain, why pretreatment with plant PeptoQ in the absence of salt stress (compare Fig. 52B and D) leads to the observed (Fig. 29) very low steady-state levels of superoxide, while, simultaneously, steady-state levels of Mn-SOD transcripts increase more than 20-fold (Fig. 31) without a concomitant increase of SOD activity (Fig. 30). Likewise, the model can explain, why salt stress, in the absence of the peptoid (Fig. 52C) can induce SOD transcripts (Fig. 31), while SOD activity decreases (Fig. 30), while, simultaneously, superoxide levels increase (Fig. 29). Moreover, it can explain, why under salt stress in presence of plant PeptoQ (Fig. 52E) SOD transcript levels drop back to the levels found in cells that neither are exposed to salt stress, nor to peptoid treatment (Fig. 31), while SOD activities increase (Fig. 30). As a result, the oxidative damage resulting from salinity stress, is efficiently quelled, as evident from the observed suppression of MDA-levels in presence of plant PeptoQ (Fig. 28). In summary, the mitigation of salt-induced stress by pretreatment with plant PeptoQ can be explained by triggering the hypoxia pathway leading to anticipative stress signalling.

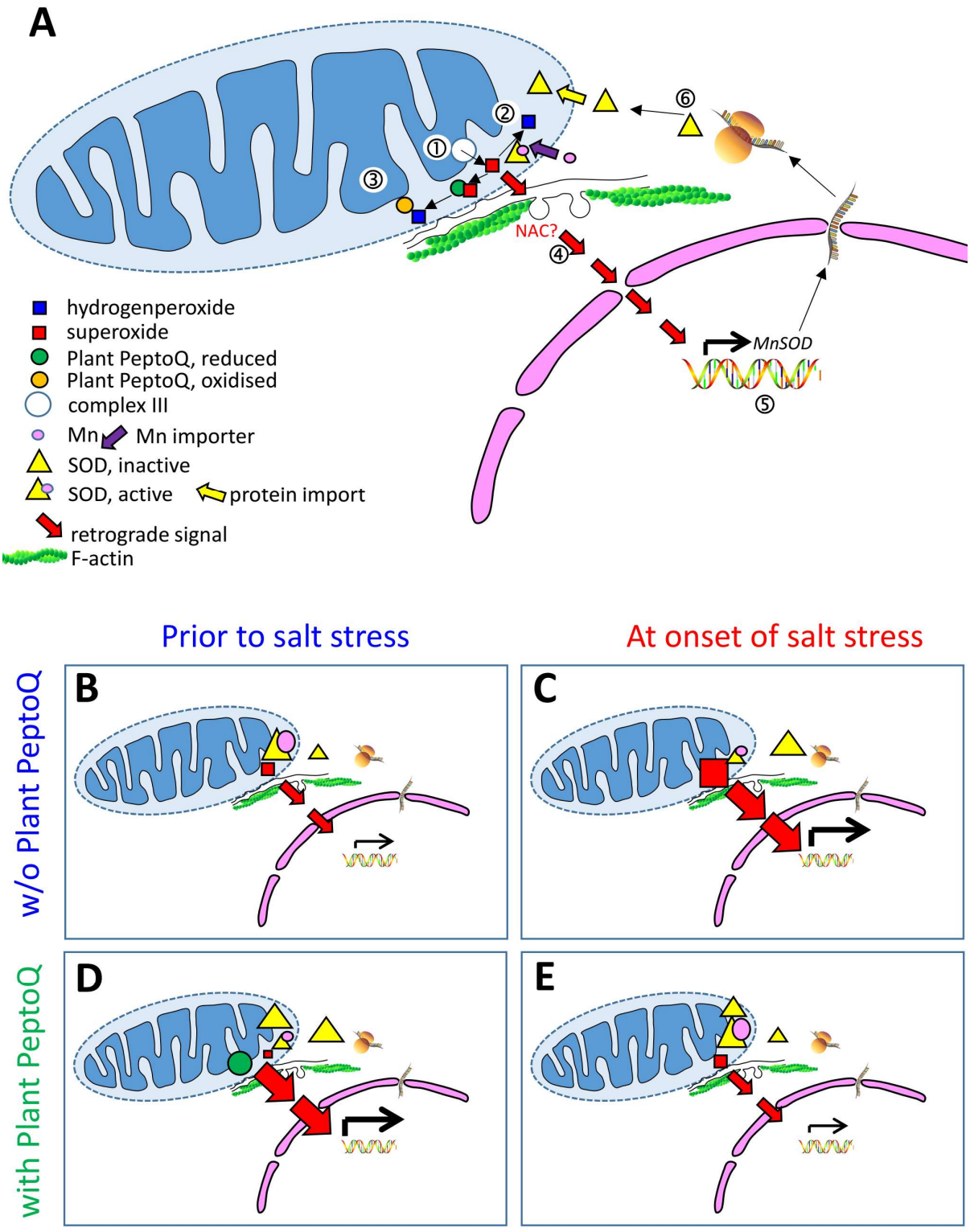

Figure 52: The steady-state levels of superoxide (originating from complex III of the mitochondrial electron transport chain A①) dissipate both by conversion to hydrogen peroxide, catalysed by Mn-SOD A② and by direct reduction through plant PeptoQ A③. Under physiological conditions, the additional mechanism of elimination (direct reduction through plant

PeptoQ), will reduce superoxide to a level, as it would occur during hypoxia. Thus, this deploys hypoxia-related retrograde signalling, that might involve specific NAC transcription factors A④. The NAC proteins would be consumed by proteolytic cleavage, they are expected to be replenished by induction of NAC transcripts. The retrograde signalling would culminate in the induction of Mn-SOD A⑤. After translation, the SOD protein is imported into the mitochondria establishing a pool of SOD that would, however, remain inactive, due to the lack of Mn A⑥. In the absence of plant PeptoQ pretreatment prior to salt stress (B) and in salt stressed plant PeptoQ pretreated non-transformed WT BY-2 cells (E) there was relatively limited retrograde signaling (due to low superoxide ion level) but active Mn-SOD due to Mn import and subsequent complexation into the active holoenzyme. However, in non-plant PeptoQ pretreated salt stressed (C) and plant PeptoQ pretreated non-salt stressed (D) non-transformed WT BY-2 cells there was high level retrograde signalling (due to the increased superoxide ion level) but inactive Mn-SOD due to the lack of (very limited) Mn import.

4.3. OsOPR7 overexpression mitigates salt stress-induced detrimental effects in OE BY-2 cells

Like in the case of plant PeptoQ pretreatment, the overexpression of OsOPR7 in the WT BY-2 cells mitigated the salt stress-induced growth deterioration and resulted in improved cell proliferation, expansion and viability, increased antioxidant enzymes activity, reduced ROS and MDA levels and certain salt-related genes transcripts induction.

4.3.1. Does OsOPR7 overexpression mitigate salinity induced mitodepressive effect in OE BY-2 cells?

In plants, early stages of developments are influenced by salinity (Hanif and Afshan, 2013), the rate at which an organ grows is a function of the rate of cell production (Yumurtaci et al., 2009), and the frequency of cellular division could be estimated reliably using mitotic index (Fernandes et al., 2007). Consequently, we measured the effect of salt stress on mitotic index (MI). Salinity caused both dose and time dependent reduction in MI in WT BY-2 cells with and without plant PeptoQ pretreatment and OE BY-2 cells. However, the decline was more pronounced and drastic in the WT BY-2 cells that lack plant PeptoQ pretreatment as compared to the case in the plant PeptoQ pretreated, and OE BY-2 counterparts (Figs.27 and 41). For instance, at 150mM NaCl salinity level at 96 h, the plant PeptoQ pretreated WT and OE BY-2 cells achieved MI of 2.4% and 3% respectively whereas at the same salt concentration and exposure time, WT BY-2 cells without plant PeptoQ pretreatment secured only 0.8% MI. Thus, salinity significantly affected mitotic activity and stimulated mitotic inhibition but the construct plant PeptoQ and OsOPR7 overexpression significantly mitigated the adverse effects of salinity on cell division. Our finding is in accordance with earlier reports in onion (*Allium cepa* L.) roots (Singh and Roy, 2015, Kietkowska, 2017), wheat (*Triticum aestivum* L.) genotypes (Hanif and Afshan, 2013) and Turkish durum and bread wheat genotypes (Yumurtaci et al., 2009). Studies revealed that cytotoxicity could be measured using changes in mitotic activities and the accompanying inhibition (Singh and Roy, 2015). Cells respond to salt stress through inhibition of cell production which is a result of salinity effect on S or G2/M phase, reduction in cyclin-dependent kinase (CDK) activity, inhibition of protein synthesis and DNA synthesis (Zhao et al., 2014) and

reduction in meristem size and inhibition of cell cycle (West et al., 2004). The remarkable reduction in mitotic index and mitotic activities under salt stress may be due to the decline in the number of dividing cells which is a result of the mitodepressive effect of the salt where it interferes in the normal process of mitosis (West et al., 2004; Singh and Roy, 2015). The mitodepressive effect may be due to the toxic effects of accumulated Na^+ and Cl^- which lead to the overproduction of reactive oxygen species (ROS). Consequently, the resulting ROS could affect nuclear dynamics, chromosome movement and anaphase chromosomes through the induction of significant delay in prophase to prometaphase transition (Foreman et al., 2003). Thus, in general, salt stress induced ion homeostasis imbalance (Zhu, 2002) and the production of excessive amounts of ROS which have a damaging effect on DNA and cellular structures that eventually results in cell death (Affenzeller et al., 2009).

4.3.2. OPDA induces retrograde signalling and reduces ROS levels through elevated antioxidant enzymes activity

The level of JA precursor, 12-oxo-phytodieonic acid (12-OPDA) increased in OE BY-2 cells both in the presence and absence of peptoid pretreatment (Fig.50A). Especially, in the latter, the OPDA level was constantly (stably) higher irrespective of the salinity levels whereas the jasmonic acid (JA) was undetectable but the jasmonyl-isoleucine (JA-Ile) accumulated to a measurable amount (Fig.50B). The increased OPDA level was accompanied by low MDA (Fig.42) and ROS levels (Fig.43), increased SOD activity (Fig.44A), and upregulation of Mn-SOD (Fig.45) and OsOPR7 (Fig.46G) genes. This result agrees with a recent report in variegated Epipremnum 'Marble Queen' plant leaves where increased OPDA level resulted in reducing the ROS levels by increasing glutathione (GSH) generation and scavenging activity through the upregulation of a group of glutathione-S-transferases (GSTs) (Sun et al., 2017). OPDA, JA and JA-Ile are known to be involved in responses to biotic and abiotic stresses as well as in plant growth and development (Dave and Graham, 2012). However, unlike JA-Ile, OPDA is not perceived by the SCF^{COI1}-JAZ-co-receptor complex (Thines et al., 2007) and genes involved in OPDA and JA signalling pathways are not identical (Taki et al., 2005; Park et al., 2013). It is known that OPDA is a signalling molecule by itself (Taki et al., 2005) and as a signalling molecule, it takes part in plastid retrograde signalling and induces the retrograde signalling upon binding to its plastid localized receptor cyclophilin 20-3 (CYP20-3) (Park et al., 2013). The OPDA-CYP20-3 complex forms the cysteine synthase complex (CSC) comprising serine acetyltransferase (SAT) for cysteine synthesis. Earlier reports show that the OPDA receptor, CYP20-3, binds with SAT, an enzyme that involves in sulfur assimilation (Dominguer-solis et al., 2008; Takahashi et al., 2011). This SAT binding with CYP20-3 increases its activity and results in elevated cysteine production (Blaszczyk et al., 1999). Moreover, the binding is considered to be important for plants abiotic stress tolerance (e.g. salt stress) (Dominguer-solis et al., 2008) and is facilitated by the binding of OPDA with its receptor CYP20-3 (Park et al., 2013). The cysteine generated in this way, could not take part directly in the regulation of gene expression as a signal or secondary messenger, but it is the change in redox potential caused by increased concentration of thiol groups that convey the message from the plastid to the nucleus. Thus, the mediator of OPDA induced retrograde signalling is the change in the redox status of the cells (Kopriva, 2013). More specifically, the increasingly and

newly synthesized cysteine can be metabolized into glutathione (GSH) to alter the redox state of the cells and to convey the redox signals that regulate expressions of OPDA-responsive genes (ORGs) through the activation of TGA transcription factors (Böttcher and Pollmann, 2009; Park et al., 2013; Sun et al., 2017). Thus, sulfur metabolites are necessary for OPDA-triggered retrograde signalling, and OPDA-induced retrograde signalling, sulfur metabolism and redox regulation are interconnected by the action of CYP20-3 (Kopriva, 2013). In general, the presence of increased OPDA level contributed for the reduced ROS level in two ways. First, under salt stress-induced oxidative stress, increased ROS level leads to lipid peroxidation in the plastids where the latter releases OPDA precursors. Thus, it contributes for the generation of OPDA and this OPDA generation consumes ROS indirectly and eventually decreased their level. On the other hand, the accumulated OPDA would induce the expression of salt-stress related genes through retrograde signalling, and further reduce the ROS level by increasing scavenging activity through the induction of a group glutathione-S-transferases (GSTs) (Taki et al., 2005; Sun et al., 2017).

4.3.3. Salt stress-induced superoxide triggers peroxynitrite generation which ends up in cell death

Mitochondrial genome contains bioenergetic (primary subset) and genetic system (secondary subset) genes (Allen, 2003b). The former actively involved in the mtETC (Allen, 2003a; Allen, 2017) and according to the CORR (co-location of genes and gene products for the redox regulation of gene expression) hypothesis, the expression of these mitochondrial bioenergetic genes is under the direct regulation of the redox state of respiratory electron carriers (gene products of bioenergetic genes or electron carriers with which the gene products interact) (Pfannschmidt et al., 1999, Allen, 2003b; Allen, 2015). In salt stressed WT BY-2 cells, the activity of Mn-SOD in scavenging superoxide ion is quite low or impaired (Fig.44A). This is due to the fact that in the presence of increased superoxide radical (Fig. 43C), the mitochondrial nitric oxide (NO) (which is generated through single electron leak from mtETC to nitrite) interacts with superoxide ion (Poyton et al., 2009; Gupta et al., 2011) and resulted in the formation of highly reactive peroxynitrite ($ONOO^-$) (Beckman et al., 1990). Then the produced peroxynitrite inactivates the Mn-SOD enzyme irreversibly through the nitration of a critical Tyr residue (Tyr 34) at its active site (MacMillan-Crow et al., 1998; Quijano et al., 2001; Redondo-Horcajo et al., 2010). Moreover, the peroxynitrite also causes mitochondrial dysfunction through lipid peroxidation, irreversible nitration of proteins and inactivation of enzymes other than Mn-SOD, mitochondrial DNA (mtDNA) damage and disruption of mitochondrial integrity. Thus, the irreversible nitration of proteins and inactivation of other enzymes that may take part in the post-translational regulation of Mn-SOD activity, would lead to the entire inactivation of Mn-SOD enzyme. Moreover, this Mn-SOD inactivation/nitration acts as a positive feedback loop where it triggers further generation of $ONOO^-$ that in turn leads to severe oxidative stress through superoxide ion ($O_2\bullet-$) accumulation (Fukai and Ushio-Fukai, 2011; Candas and Li, 2014). As a result, the regulation of mitochondrial bioenergetic genes failed. This in turn leads to the failure of mitochondrial genetic system genes that controls

the redox state-based regulation of bioenergetic genes expression (Allen, 2003b). Consequently, the whole system failed and resulted in the generation of quite huge amount of ROS in a vicious circle manner, and eventually, the cumulative effect of the entire process ends up in cell death (Fukai and Ushio-Fukai, 2011; Candas and Li, 2014). Therefore, the salt stressed WT BY-2 cells would not be able to tolerate the deleterious effects of salinity owing to the reasons discussed above. However, in salt stressed OE BY-2 cells, there would not be such defects due to the presence of very limited superoxide ion and increased SOD activity, consequently, the Mn-SOD scavenges the superoxide ion effectively and efficiently. This maintains the redox state of mtETC at normal and optimal situation which leads to effective regulation of mitochondrial bioenergetic genes (CORR hypothesis). Effective bioenergetic genes regulation enables the mtETC to proceed normally and sustainably which resulted in oxidants/antioxidants balance and consequently, the ROS level will be kept as low as possible. Thus, as a result, the salt stress induced mitochondrial ROS (mtROS) that might lead to cell death, would be significantly and effectively scavenged, and the cumulative effect conferred salt tolerance to the salt stressed OE BY-2 cells.

4.3.4. There is signalling from mitochondria to the plastids

When the plant PeptoQ pretreated WT and OE BY-2 cells were salt stressed, unlike the salt stressed counterparts without peptoid treatment, the OPDA level obviously increased. Thus, the fact that the mitochondria localized plant PeptoQ resulted in increased OPDA level (which is localized in the plastids), implies the presence of signalling from mitochondria to plastids. Published research reports show the existence of bidirectional communications between mitochondria and plastids besides their retrograde and anterograde interaction with the nucleus. There are several proposed routes with regard to mitochondria-plastids communications. However, here, we shall consider only three of them. Firstly, mitochondria to plastids and vice versa interaction (signalling) could occur through the modulation of nuclear gene expression by making use of the coordinated expression of nuclear encoding mitochondrial and plastidal proteins. In other words, there is a cross talk between mitochondrial and plastidal retrograde signalling (Blanco et al., 2014). For instance, impaired chloroplast development affects mitochondrial transcripts (Hedtke et al., 1999) and the expression of nuclear encoded photosynthetic genes were altered by changes in mitochondrial physiology and metabolism (Schwarzländer et al., 2012). Secondly, dual targeting of proteins could be a mechanism for mitochondria to plastids or vice versa signalling (Bobik and Burch-Smith, 2015). For example, in Arabidopsis, more than 100 proteins are targeted to both mitochondria and plastids (Carrie and Whelan, 2013). Thirdly, mitochondria and plastids may communicate making use of their physical interaction (contact). To this effect, in leaves, a close association between mitochondria, plastids and peroxisomes has been observed (Bobik and Burch-Smith, 2015). Thus, the signalling that we observed in this dissertation, could take place through one of the above-mentioned mechanisms (or else), and it might be induced and mediated by the plant PeptoQ. This is supported by earlier studies where plastoquinone, a plant CoQ analog, can act as a retrograde mediator from chloroplast-to-nucleus (Petrillo et al., 2014), and hence, the mitochondrial CoQ may play an analogous role, in mediating retrograde signalling from

mitochondria-to-nucleus (Stefely and Pagliarini, 2017). Since, the mitochondrial localized plant PeptoQ (a cell-penetrating peptoid) is endowed with a mitochondria-targeting motif and a semiquinone mimetic of coenzyme Q10, it might also play a similar signalling role as the mitochondrial CoQ.

4.3.5. OsOPR7 overexpression causes reduced ROS levels through increased antioxidant enzymes activity

The OE BY-2 cells attained significantly better cell proliferation (Fig.38B), expansion (Fig.39) and viability (Fig.40) under salt stress as compared to the WT counterparts. Moreover, the MDA (Fig.42) and the ROS (Fig.43C) (especially superoxide radical) levels were profoundly low as a result of increased superoxide dismutase (SOD) activity (Fig.44A) in the former as compared to the latter. This implies that the overexpression of OsOPR7 caused increased antioxidant activity of SOD which resulted in quite low mtROS level. The fact that OsOPR7 overexpression has alleviated ROS damage is inferred from the significantly low level of MDA (Fig.42). Because the reactive aldehyde MDA has been identified as an indicator of ROS-induced lipid peroxidation (Nankivell et al., 1994). Similar results were reported in wheat (*Triticum aestivum*) that overexpressed OPR1. The OPR1 overexpressor wheat (TaOPR1) resulted in large leaves size, increased shoot and root length, increased antioxidants activity and low MDA and ROS levels as compared to the wild type wheat. Salinity stress tolerance frequently has been associated with tolerance to oxidative stress and the latter is quite closely linked to the homeostasis between ROS production and scavenging. Thus, TaOPR1 promotes the antioxidant enzymes activity and consequently, effectively scavenged salt stress induced ROS and reduced it significantly. Thus, TaOPR1 promotes ROS scavenging in abscisic acid (ABA)-dependent manner to affect ROS removal but it does not directly protect cells from ROS-induced lipid peroxidation (Dong et al., 2013) that generates a number of toxic breakdown products such as α, ß-unsaturated aldehydes (Trotter et al., 2006). Even if, OsOPR7 gene is considered as it is involved in the biosynthesis of JA by encoding the enzyme that reduces (+)-cis-OPDA to (+)-cis-OPC-8:0 (Tani et al., 2008), in this dissertation, it does not affect the biosynthesis of JA. Consequently, the JA level was undetectable whereas there was a measurable amount of JA-Ile. The possible reasons for the amount of JA to be undetectable might be failure of the transport of OPDA from the plastid to the peroxisomes and/or the presence of defect in OsOPR7 enzyme in converting OPDA to JA. Thus, as a result of the above reasons (or else), OPDA would be accumulated in a reasonable level in the OE salt stressed BY-2 cells. Similarly, the TaOPR1 also does not disturb the JA biosynthesis and the signaling machinery. But here, it has been speculated that the TaOPR1 is not involved in the JA biosynthetic activity (Dong et al., 2013) unlike the case of OsOPR7.

5. Conclusion and Perspectives

5.1. The plant PeptoQ as tool to dissect spatial signatures of oxidative stress

Subcellular targeting to mitochondria has attracted considerable attention for biomedical applications, since mitochondria are not only crucial for energy acquisition, but also regulate numerous physiological and pathological processes (reviewed in Weissig, 2005). For plant cells as well, mitochondria have been intensively studied as central factors of oxidative balance and for the initiation of programmed cell death, for instance in the context of salt-stress (recently reviewed in Che-Othman et al., 2017). Sodium can enter the plasma membrane through non-selective cation channels and then activates oxidative signaling that either results in cellular adaptation, or in salt-induced necrosis, where the target cell undergoes self-sacrifice sequestering sodium from its neighbours. The decision on the respective response depends not only on the molecular nature of early signals, but mainly on their temporal and spatial pattern (reviewed in Ismail et al., 2014). Reactive oxygen species can convey a completely different signal, depending on the site of their occurrence (so called spatial signature). To experimentally address such a signature model requires to control oxidative balance differentially in different subcellular compartments. For instance, the sodium entering the cytoplasm, will accumulate at the cytoplasmic face of the inner mitochondrial membrane (reviewed in Flowers et al., 2015) and trigger the accumulation of superoxide. The same molecule, superoxide ($O_2\bullet-$), is also triggered at the plasma membrane by NADPH oxidase and seems to act as a signal, which has also been demonstrated for tobacco BY-2 cells (Monetti et al., 2014). It will be interesting to examine if the plant PeptoQ gets integrated into the electron transfer chain of the inner membrane and affects oxidative phosphorylation there. We already know that the plant PeptoQ does not induce any detectable toxicity by itself but is able to mitigate salt-stress dependent programmed cell death. Although salt stress is a serious problem in global agriculture with sharply rising impact, application of this peptoid in agriculture would not be economically feasible, and this is also not, what this dissertation is planning to develop. Rather we want to use this new tool to dissect the functional role of plasma membrane and mitochondria as important cellular sites of superoxide accumulation. In this context, synthetic CoQ variants are of interest, which harbour a potential that is more negative than that of native CoQs, which should allow for even more efficient elimination of superoxide and hydrogen peroxide. This strategy to tailor the functional cargo, can be accompanied by strategies to tailor the molecular vehicle: We have already launched a combinatorial approach, where different peptoids are synthetized from modular building blocks to get insight into the structural features that can be used to optimise the different steps of uptake. Goal of these endeavours is to obtain a tool to shape oxidative balance in mitochondria as a lever to control adaptive gene expression, for instance to promote salt tolerance in plant cells. It would be the genetic components identified by this approach that would then be the starting point for agricultural application, for instance, as targets in marker-assisted breeding for salt tolerance.

5.2. What is the role of plastids and OsOPR7 overexpression in salt stress?

Salt stress not only represents a challenge for mitochondrial redox homeostasis, but also impairs the performance of plastids. Even in non-photosynthetic cells as tobacco BY-2, plastids are present. Although their inner membranes are reduced, the plastids of suspension cells are metabolically active, and trigger, in response to salt stress, the synthesis of the plant stress hormone jasmonic acid (Ismail et al., 2012; Akaberi et al., 2018). Jasmonate signalling clearly responds to peptoid treatment. On the one hand, the transcripts of the jasmonate response factor JAZ3 are upregulated (by 50%) in response to plant PeptoQ in the absence of salt stress (Fig. 46H). On the other hand, the jasmonate biosynthesis pathway is partitioned towards the precursor 12-oxo-phytodieonic acid (OPDA), on cost of the final signal jasmonyl-isoleucine (JA-Ile) (Fig. 50C). This is interesting, because this precursor is normally exported from the plastids into peroxisomes, where it is converted to jasmonic acid. In the meantime, OPDA has been recognised as signal of its own virtue, triggering a separate signalling pathway (Park et al., 2013). One relevant target of OPDA is the induction of 3'-phosphoadenosine 5'-phosphate (PAP), which is one of the secondary metabolites involved in plastid retrograde signaling (Estavillo et al., 2011). Thus, modulation of redox homeostasis in the mitochondria through plant PeptoQ bears also on retrograde signalling of plastids, leading to the question, how the two organelles can communicate. An exciting possibility are the recently discovered peroxules, filamentous outgrowths of peroxisomes that are formed under stress and get into touch with mitochondria (Jaipargas et al., 2016). The peroxisomes as organelles that can interact with both, mitochondria and plastids, seem to be important players in this inter-organelle crosstalk. The partitioning between OPDA and jasmonic acid signalling depends on the enzyme OPDA-reductase. This peroxisomal protein converts OPDA imported from the plastid and represents the first committed step of the jasmonate branch of the pathway. Therefore, we have overexpressed the salinity-related rice gene OsOPR7 in wild type BY-2 cells and observed that these cells are significantly more tolerant to salt stress as compared to the non-transformed wild type. Analysis of this cell line with respect to its response to plant PeptoQ should provide new insights into mitochondria-plastid signalling.

Pretreatment of salt stressed WT and OE BY-2 cells with the construct plant PeptoQ resulted in an increased OPDA level through mitochondria to plastids signaling. Since plant PeptoQ confers a very strong antioxidant property through its hydroxylated ring (Gulaboski et al., 2013) and being a semiquinone mimetic of coenzyme Q10, it might activate the enzyme allen oxidase cyclase (AOC) which converts allene oxide to OPDA. Thus, this would result in the accumulation of OPDA, however, the exact mechanism by which plant PeptoQ contributes for the induction of OPDA level is far from clear. Thus, to have the clear picture, there should be future practical experimental investigations in relation to as how signaling between the two organelles would take place through plant PeptoQ mediation, and the precise effect of plant PeptoQ on AOC. On the other hand, in salt stressed, OE BY-2 cells, there was an increased OPDA level which is not completely expected. This is because of the fact that the peroxisome localised OsOPR7 enzyme is normally working in the reduction of OPDA level by converting it

into JA. But just contrary to this, in the OE BY-2 cells, accumulation of OPDA has been observed similar to the case in peptoid treated WT BY-2 cells. The two possible reasons might be: first, the transport of OPDA from the plastids to the peroxisomes, at least partly, through ATP binding-cassette (ABC) transporter called COMATOSE (CTS1) (Theodoulou et al., 2005) might fail and lead to the accumulation of OPDA in plastids. Second, the failure of the conversion of OPDA into JA which is evident from the undetectable JA level which might be due to a defect in the conversion machinery (e.g. inactivation OsOPR7 enzyme). However, since these might not be the only reasons, the exact reasons and mechanisms for the above antagonistic phenomenon with regard to OPDA level in the OE BY-2 cells, has to be investigated in detail by future practical endeavours.

6. References

Abbasi, H., Jamil, M., Haq, A., Ali, S., Ahmad, R., Malik, Z. & Parveen. (2016). Salt stress manifestation on plants, mechanism of salt tolerance and potassium role in alleviating it: a review. *Zemdirbyste-Agriculture* **103**(2), 229-238. DOI: 10.13080/z-a.2016.103.030.

Abogadallah, G. M. (2010). Antioxidative defense under salt stress. *Plant Signaling & Behavior* **5**(4), 369-374. DOI: 10.4161/psb.5.4.10873.

Abubakar, L.A. (2016). Effect of Salinity on the Growth Parameters of Halotolerant Microalgae, *Dunaliella spp*. *Nigerian Journal of Basic and Applied Science* **24**(2), 85-91. DOI: 10.4314/njbas. v24i2.12.

Adams, E. & Shin, R. (2014). Transport, signaling, and homeostasis of potassium and sodium in plants. *J. Integr. Plant Biol*. **56,** 231-249. DOI: 10.1111/jipb.12159.

Aebi, H. (1984). Catalase in vitro. *Methods in Enzymology* **105,** 121-126. DOI: 10.1016/S0076-6879(84)05016-3.

Affenzeller, J. M., Darehshouri, A., Andosch, A., Lütz, C. & Lütz-Meindl, U. (2009). Salt stress-induced cell death in the unicellular green alga Micrasterias denticulate. *Journal of Experimental Botany* **60**(3), 939-954. DOI: 10.1093/jxb/ern348.

Agati, G., Azzarello, E., Pollastri, S. & Tattini, M. (2012). Flavonoids as antioxidants in plants: Location and functional significance. *Plant Science* **196,** 67-76. DOI: 10.1016/j.plantsci.2012.07.014.

Ahmad, P., Ozturk, M., Sharma, S. & Gucel, S. (2014). Effect of sodium carbonate-induced salinity–alkalinity on some key osmoprotectants, protein profile, antioxidant enzymes, and lipid peroxidation in two mulberry (*Morus alba* L.) cultivars. *Journal of Plant Interactions* **9**(1), 460-467. DOI: 10.1080/17429145.2013.855271

Ahmad, P., Rasoo, S., Gul, A., Sheikh, S. A., Akram, N. A., Ashraf, M., Kazi, A. M. & Gucel, S. (2016). Jasmonates: Multifunctional roles in stress tolerance. *Frontiers in Plant Science* **7**(813), 1-15. DOI: 10.3389/fpls.2016.00813.

Akaberi, S., Wang, H., Claudel, P., Riemann, M., Hause, B., Hugueney, P. & Nick, P. (2018). Grapevine fatty acid hydroperoxide lyase generates actin-disrupting volatiles and promotes defence-related cell death. *Journal of Experimental Botany* **69**(12), 2883-2896 (2018). DOI: 10.1093/jxb/ery133.

Akhter, J., Mahmood, K., Malik, K.A., Ahmed, S. & Murray, R. (2003). Amelioration of a saline sodic soil through cultivation of a salt-tolerant grass *Leptochloa fusca. Environmental Conservation* **30**(2), 168-174. DOI:10.1017/S0376892903000158.

Allen, J. F. (2003a). Why chloroplasts and mitochondria contain genomes. *Comp Funct Genom* **4,** 31-36. DOI: 10.1002/cfg.245.

Allen, J. F. (2003b). The function of genomes in bioenergetic organelles. *Phil. Trans. R. Soc. Lond.* B **358,** 19-38. DOI: 10.1098/rstb.2002.1191.

Allen, J. F. (2015). Why chloroplasts and mitochondria retain their own genomes and genetic systems: Colocation for redox regulation of gene expression. *PNAS* **112** (33), 10231-10238. DOI: 10.1073/pnas.1500012112.

Allen, J. F. (2017). The CoRR hypothesis for genes in organelles. *Journal of Theoretical Biology* 1-8. DOI: 10.1016/j.jtbi.2017.04.008.

Almeida,D. M., Oliveira, M. M. & Saibo, N.J. M. (2017). Regulation of Na^+ and K^+ homeostasis in plants: towards improved salt stress tolerance in crop plants. *Genetics and Molecular Biology* **40**(1), 326-345. DOI: 10.1590/1678-4685-GMB-2016-0106.

Ambrose, C., Ruan, Y., Gardiner, J., Tamblyn, M. L., Catching, A., Kirik, V., Marc, J., Overal, R. and Wasteneys, O. G. (2013). CLASP Interacts with Sorting Nexin 1 to Link Microtubules and Auxin Transport via PIN2 Recycling in Arabidopsis thaliana. *Developmental Cell* **24,** 649-659. DOI: 10.1016/j.devcel.2013.02.007.

Apel, K. & Hirt, H. (2004). Reactive oxygen species: Metabolism, oxidative stress, and signal transduction. *Annu. Rev. Plant Biol.***55,** 373-99. DOI: 10.1146/annurev.arplant.55.031903.141701.

Arora, A., Byrem, T. M., Nair, M. G. & Strasburg, G. M. (2002). Modulation of liposomal membrane fluidity by flavonoids and isoflavonoids. *Archives of Biochemistry and Biophysics* **373**(1),102-109. DOI: 10.1006/abbi.1999.1525.

Arukuusk, P., Parnaste, L., Margus, H., Eriksson. K. J., Vasconcelos, L., Padari, K., Pooga, M., & Langel, Ü. (2013). Differential endosomal pathways for radically modified peptide vectors. *Bioconjugate Chem.* **24,** 1721-1732. DOI:10.1021/bc4002757.

Asada, K. (2000). The water-water cycle as alternative photon and electron sinks. *Phil. Trans. R. Soc. Lond. B*. **355,** 1419-1431.DOI: 10.1098/rstb.2000.0703.

Asfaw, K. G., Liu, Q., Maisch, J., Münch, S. W., Wehl, I., Bräse, S., Bogeski, I., schepers, U., & Nick, P. (2019). A peptoid Delivers CoQ-derivative to plant Mitochondria via endocytosis. *Sci. Rep.* **9,** 1-18. DOI: 10.1038/s41598-019-46182-z.

Ashraf, M., Athar, H.R., Harris, P.J.C. & Kwon, T.R. (2008). Some prospective strategies for improving crop salt tolerance. *Advances in Agronomy* **97,** 45-110. DOI: 10.1016/S0065-2113(07)00002-8.

Ashraf, M. & Foolad, M. R. (2007). Roles of glycine betaine and proline in improving plant abiotic stress resistance. *Environmental and Experimental Botany* **59,** 206-216. DOI: 10.1016/j.envexpbot.2005.12.006.

Ashrafijou, M., Sadat Noori, S. A., Darbandi, A. I. & Saghafi, S. (2010). Effect of salinity and radiation on proline accumulation in seeds of canola (*Brassica napus* L.). *Plant Soil Environ.* ***56,*** 312-317. DOI: 10.17221/2/2010-PSE.

Astle, J. M., Udugamasooriya, D. G., Smallshaw, J. E. & Kodadek, T. (2008). A VEGFR2 antagonist and other peptoids evade immune recognition. *Int. J. Pept. Res. Ther.* **14,** 223-227. DOI 10.1007/s10989-008-9136-1.

Avanci, N.C., Luche, D.D., Goldman, G. H. & Goldman, M. H. S. (2010). Jasmonates are phytohormones with multiple functions, including plant defense and reproduction. *Genetics and Molecular Research* **9**(1), 484-505. DOI:10.4238/vol9-1gmr754.

Balbi, V. & Devoto, A. (2007). Jasmonate signalling network in *Arabidopsis thaliana*: crucial regulatory nodes and new physiological scenarios. *New Phytologist* **177**, 301-318. DOI: 10.1111/j.1469-8137.2007. 02292.x.

Bandmann, V. and Homann, U. (2012). Clathrin-independent endocytosis contributes to uptake of glucose into BY-2 protoplasts. *The Plant Journal* **70,** 578-584. DOI:10.1111/j.1365-313X.2011. 04892.x.

Bandmann, V., Müller, D. J., Köhler, T. and Homann, U. (2012). Uptake of fluorescent nano beads into BY2-cells involves clathrin-dependent and clathrin-independent endocytosis. *FEBS Letters* **586,** 3626-3632. DOI: 10.1016/j.febslet.2012.08.008.

Barragan, V., Leidi, E. O., Andres, Z., Rubio, L., De Luca, A., Fernandez, J.A., Cubero, B. & Pardo, J. M. (2012). Ion exchangers NHX1 and NHX2 mediate active potassium uptake into vacuoles to regulate cell turgor and stomatal function in arabidopsis. *The Plant Cell* **24,** 1127-1142. DOI: 10.1105/tpc.111.095273.

Beauchamp, C. & Fridovich, I. (1971). Superoxide dismutase: Improved assays and an assay applicable to acrylamide gels. *Analytical Biochemistry* **44,** 276-287. DOI. 10.1016/0003-2697(71)90370-8.

Beckman, J. S., Beckman, T, W., Chen, J., Marshall, P. A. & Freeman, B.A. (1990). Apparent hydroxyl radical production by peroxynitrite: Implications for endothelial injury from nitric oxide and superoxide. *Proc. Nati. Acad. Sci. USA* **87,** 1620-1624. DOI:10.1073/pnas.87.4.1620.

Bellincampi, D., Dipierro, N., Salvi, G., Cervone, F. & De Lorenzo, G. (2000). Extracellular H_2O_2 induced by oligogalacturonides is not involved in the inhibition of the auxin-regulated rolB gene expression in tobacco leaf explants. *Plant Physiology* **122,** 1379-1385. DOI: 10.1104/pp.122.4.1379

Benschop, J. J., Mohammed, S., O'Flaherty, M., Heck, A, J. R., Slijper, M. & Menke, F. L. H. (2007). Quantitative phosphoproteomics of early elicitor signaling in *Arabidopsis. Molecular & Cellular Proteomics* ***6****(7), 1198-1214.* DOI: 10.1074/mcp.M600429-MCP200.

Bertani G. (1951). Studies on lysogenesis I. The mode of phage liberation by lysogenic *Escherichia coli. J. Bacteriol* **62,** 293-300.

Bhagavan, H. N. & Chopra, R. K. (2006). Coenzyme Q10: Absorption, tissue uptake, metabolism and pharmacokinetics. *Free Radical Research* **40**(5), 445-453. DOI: 10.1080/10715760600617843.

Bhattacharjee, S. (2005). Reactive oxygen species and oxidative burst: Roles in stress, senescence and signal transduction in plants. *Current Science* **89**(7), 1113-1121.

Bie, Z., Ito, T. & Shinohara, Y. (2004). Effects of sodium sulfate and sodium bicarbonate on the growth, gas exchange and mineral composition of lettuce. *Scientia Horticulturae* **99,** 215-224. DOI: 10.1016/S0304-4238(03)00106-7.

Birtalan, E., Rudat, B., Kömel, D. K., Fritz,D., Vollrath, S. B. L., Schepers, U. & Bräse, S. (2011). Investigating Rhodamine-B labeled Peptoids: Scopes and Limitations of its applications. *Peptide Science* **96**(5), 694-701. DOI 10.1002/bip.21617.

Blanco, N.E., Guinea-Dıaz, M., Whelan, J. & Strand, A. (2014). Interaction between plastid and mitochondrial retrograde signaling pathways during changes to plastid redox status. *Phil. Trans. R. Soc. B* **369,** 1-8. DOI: 10.1098/rstb.2013.0231.

Blaszczyk, A., Brodzik, R. & Sirko, A. (1999). Increased resistance to oxidative stress in transgenic tobacco plants overexpressing bacterial serine acetyltransferase. *The Plant Journal* **20**(2), 237-243. DOI: 10.1046/j.1365-313x.1999. 00596.x.

Blokhina, O. & Fagerstedt, K. V. (2010). Reactive oxygen species and nitric oxide in plant mitochondria: origin and redundant regulatory systems. *Physiologia Plantarum* **138,** 447-462. DOI: 10.1111/j.1399-3054.2009.01340.x.

Blokhina, O. Virolainen, E. & Fagerstedt, K. V. (2003). Antioxidants, oxidative damage and oxygen deprivation stress: a review. *Annals of Botany* **91,** 179-194. DOI:10.1093/aob/mcf118.

Blumwald, E., Aharon, G. S. & Apse, M. P. (2000). Sodium transport in plant cells. *Biochimica et Biophysica Acta* **1465,**140-151. DOI: 10.1016/S0005-2736(00)00135-8.

Bobik, K. & Burch-Smith, T, M. (2015). Chloroplast signaling within, between and beyond cells. *Frontiers in Plant science* **6**(781), 1-26. DOI: 10.3389/fpls.2015.00781.

Bockheim, J. G. & Gennadiyev, A.N. (2000). The role of soil-forming processes in the definition of taxa in soil taxonomy and the world soil reference base. *Geoderma* **95,** 53-72. DOI: 10.1016/S0016-7061(99)00083-X.

Boddapati, S. V., D'Souza, G. G. M., Erdogan, S., Torchilin,V. P. & Weissig, V. (2008). Organelle-targeted nanocarriers: Specific delivery of liposomal ceramide to mitochondria enhances its cytotoxicity in vitro and in vivo. *Nano Letters* **8**(8), 2559-2563. DOI: 10.1021/nl801908y.

Boevink, P., Oparka, K., Santa Cruz, S., Martin, B., Betteridge, A. and Hawes, C. (1998). Stacks on tracks: the plant Golgi apparatus traffics on an actin/ER network. *The Plant Journal* **15,** 441-447. DOI:10.1046/j.1365-313X.1998. 00208.x.

Bogeski, I., Gulaboski, R., Kappl, R., Mirceski, V., Stefova, M., Petreska, J. & Hoth, M. (2011). Calcium Binding and Transport by Coenzyme Q. *J. Am. Chem. Soc.* **133,** 9293-9303. DOI: 10.1021/ja110190t.

Bohnert, H. J., Nelson, D. E. & Jensen, R. G. (1995). Adaptations to environmental stresses. *The Plant Cell* **7,** 1099-1111. DOI: 10.2307/3870060.

Börner, T. (2017). The discovery of plastid-to-nucleus retrograde signaling-a personal perspective. *Protoplasma* **254,** 1845-1855. DOI: 10.1007/s00709-017-1104-1.

Böttcher, C. & Pollmann, S. (2009). Plant oxylipins: Plant responses to 12-oxo-phytodienoic acid are governed by its specific structural and functional properties. *FEBS Journal* **276,** 4693-4704. DOI: 10.1111/j.1742-4658.2009. 07195.x.

Boyer, J.S. (1982). Plant productivity and environment. *Science,* **218**(4571), 443-448. DOI : 10.1126/science.218.4571.443.

Browse, J. (2009). Jasmonate passes muster: A receptor and targets for the defense hormone. *Annu. Rev. Plant Biol.* **60,**183-205. DOI: 10.1146/annurev.arplant.043008.092007.

Cakmak, I. (2005). The role of potassium in alleviating detrimental effects of abiotic stresses in plants. *J. Plant Nutr. Soil Sci.**168,*** 521-530. DOI: 10.1002/jpln.200420485.

Candas, D. & Li, J. J. (2014). MnSOD in oxidative stress response-potential regulation via mitochondrial protein influx. *Antioxidants and Redox Signalling* **20**(10), 1599-1617. DOI: 10.1089/ars.2013.5305.

Carrie, C. & Whelan, J. (2013). Widespread dual targeting of proteins in land plants: when, where, how and why. *Plant Signal. Behav.* **8**(8), 1-13. DOI: 10.4161/psb.25034.

Cerrato, C. P., Künnapuu, K. & Langel, Ü. (2016). Cell-penetrating peptides with intracellular organelle targeting. *Expert Opinion on Drug Delivery* 1-11. DOI: 10.1080/17425247.2016.1213237.

Cerrato, C. P., Pirisinu, M., Vlachos, E. N. & Langel, U. (2015). Novel cell-penetrating peptide targeting mitochondria. *The FASEB Journal* 1-11. DOI: 10.1096/fj.14-269225.

Chaves, M. M. & Oliveira, M.M. (2004). Mechanisms underlying plant resilience to water deficits: prospects for water-saving agriculture. *Journal of Experimental Botany* **55**(407), 2365-2384.DOI: 10.1093/jxb/erh269.

Chen, H., Nelson, R.S. & Sherwood, J. L. (1994). Enhanced recovery of transformants of *Agrobacterium tumefaciens* after freeze-thaw transformation and drug selection. *Biotechniques* **16**, 664-670.

Chen, Z. & Gallie, D. R. (2006). Dehydroascorbate reductase affects leaf growth, development, and function. *Plant Physiology* **142,** 775-787. DOI: 10.1104/pp.106.085506.

Che-Othman, M. H., Millar, A. H. & Taylor, N.L. (2017). Connecting salt stress signalling pathways with salinity-induced changes in mitochondrial metabolic processes in C3 plants. *Plant Cell Environ.* **40,** 2875-2905. DOI: 10.1111/pce.13034.

Chinnusamy, V., Jagendorf, A. & Zhu, J-K. (2005). Understanding and improving salt tolerance in plants. *Crop Sci.* **45,** 437-448. DOI: 10.2135/cropsci2005.0437.

Choudhury, F. K., Rivero, R. M., Blumwald, E. & Mittler, R. (2017). Reactive oxygen species, abiotic stress and stress combination. *The Plant Journal* **90,** 856-867. DOI: 10.1111/tpj.13299.

Choudhury, S., Panda, P., Sahoo, L. & Panda, S. K. (2013). Reactive oxygen species signaling in plants under abiotic stress. *Plant Signaling & Behavior* **8,** 1-6. DOI: 10.4161/psb.23681.

Chuah, J., Yoshizumi, T., Kodama, Y. and Numata, K. (2015). Gene introduction into the mitochondria of Arabidopsis thaliana via peptide-based carriers. *Sci. Rep.* **5,** 1-7. DOI: 10.1038/srep07751.

Chugh, A., Amundsen, E. & Eudes, F. (2009). Translocation of cell-penetrating peptides and delivery of their cargoes in triticale microspores. *Plant Cell Rep.* **28,** 801-810. DOI: 10.1007/s00299-009-0692-4.

Chugh, A. & Eudes, F. (2007). Translocation and nuclear accumulation of monomer and dimer of HIV-1 Tat basic domain in triticale mesophyll protoplasts. *Biochimica et Biophysica Acta* **1768:** 419-426. DOI: 10.1016/j.bbamem.2006.11.012.

Chugh, A. & Eudes, F. (2008). Study of uptake of cell penetrating peptides and their cargoes in permeabilized wheat immature embryos. *FEBS Journal* **275,** 2403-2414. DOI:10.1111/j.1742-4658.2008.06384. x.

Collins, A. R. (2001). Carotenoids and genomic stability. *Mutation Research* **475,** 21-28. DOI:10.1016/S0027-5107(01)00071-9.

Crane, F. L. (2001). Biochemical functions of coenzyme Q10. *Journal of the American College of Nutrition* **20**(6), 591-598. DOI:10.1080/07315724.2001.10719063.

Cruz, C., Cairrao, E., Silvestre, S., Breitenfeld, L., Almeida, P. and Queiroz, J.A. (2011). Targeting of Mitochondria-Endoplasmic Reticulum by Fluorescent Macrocyclic Compounds. *PLoS ONE* **6,** e27078. DOI: 10.1371/journal.pone.0027078.

Culotta, V. C., Yang, M. & O'Halloranb, T. V. (2006). Activation of superoxide dismutases: Putting the metal to the pedal. *Biochim Biophys Acta* **1763**(7), 747-758. DOI: 10.1016/j.bbamcr.2006.05.003.

D'Autréaux, B. & Toledano, M. B. (2007). ROS as signalling molecules: mechanisms that generate specificity in ROS homeostasis. *Nature Reviews Molecular Cell Biology **8,** 813-824.* DOI: 10.1038/nrm2256.

Dar, T. A., Uddin, M., Khan, M. M. A., Hakeem, K. R. & Jaleel, H. (2015). Jasmonates counter plant stress: A Review. *Environmental and Experimental Botany* **115,** 49-57.DOI: 10.1016/j.envexpbot.2015.02.010.

Das, K. & Roychoudhury, A. (2014). Reactive oxygen species (ROS) and response of antioxidants as ROS scavengers during environmental stress in plants. *Frontiers in Environmental Science* **2**(53), 1-13. DOI : 10.3389/fenvs.2014.00053.

Dave, A. & Graham, I. A. (2012). Oxylipin signaling: a distinct role for the jasmonic acid precursor cis-(+)-12-oxo-phytodienoic acid (cis-OPDA). *Frontiers in Plant Science* **3**(42),1-6. DOI: 10.3389/fpls.2012.00042.

De Clercq, I.,Vermeirssen, V., Van Aken, O., Vandepoele, K., Murcha, M. W., Law, S. R., Inzé, A., Ng, S., Ivanova, A., Rombaut, D., van de Cotte, B., Jaspers, P., Van de Peer, Y., Kangasjärvi, J., Whelan, J. & Van Breusegema, F. (2013). The Membrane-Bound NAC transcription factor ANAC013 functions in mitochondrial retrograde regulation of the oxidative stress response in Arabidopsis. *The Plant Cell* **25,** 3472-3490. DOI: 10.1105/tpc.113.117168.

Demkura, P. V., Abdala, G., Baldwin, I. T. & Ballare, C. L. (2010). Jasmonate-dependent and -independent pathways mediate specific effects of solar ultraviolet B radiation on leaf phenolics and antiherbivore defense. *Plant Physiology* **152,** 1084-1095. DOI: 10.1104/pp.109.148999.

De Pinto, C. M., Paradiso, A., Leonetti, P. & de Gara, L. (2006). Hydrogen peroxide, nitric oxide and cytosolic ascorbate peroxidase at the crossroad between defence and cell death. *The Plant Journal* **48,** 784-795. DOI: 10.1111/j.1365-313X.2006. 02919.x.

Del Rio, L. A., Corpas, F. J., Sandalio, L.M., Palma, J.M., Gomez, M. & Barroso, J. B. (2002). Reactive oxygen species, antioxidant systems and nitric oxides in peroxisomes**.** *Journal of Experimental Botany* **53**(372), 1255-1272. DOI: 10.1093/jxb/53.372.1255.

Del Rio, L. A., Sandalio, L. M., Corpas, F. J., Palma, J. M. & Barroso, J. B. (2006). Reactive oxygen species and reactive nitrogen species in peroxisomes. Production, scavenging, and role in cell signaling. *Plant Physiology* **141,** 330-335. DOI: 10.1104/pp.106.078204.

De Souza Silva, C. M. M. & Fay, E. F. (2012). Effect of salinity on soil microorganisms. In: Soil Health and Land Use Management (Dr. Maria C. Hernandez Soriano Eds.). pp. 177-198.

D'Souza, G. G., Cheng, S-M., Boddapati, S. V., Horobin, R. W. & Weissig, V. (2008). Nanocarrier-assisted sub-cellular targeting to the site of mitochondria improves the pro-apoptotic activity of paclitaxel. *Journal of Drug Targeting* **16**(7-8), 578-585. DOI: 10.1080/10611860802228855.

Del Amor, F. M. & Cuadra-Crespo, P. (2011). Alleviation of salinity stress in broccoli using foliar urea or methyl-jasmonate: analysis of growth, gas exchange, and isotope composition. *Plant Growth Regul.* **63,** 55-62. DOI: 10.1007/s10725-010-9511-8.

Dietz, K.J., Tavakoli, N., Klunge, C., Mimura, T., Sharma, S. S., Harris, G.C., Chardonnens, A. N. & Golldack, D. (2001). Significance of the V-type ATPase for the adaptation to stressful growth conditions and its regulation on the molecular and biochemical level. *Journal of Experimental Botany* **52**(363), 1969-1980. DOI: 10.1093/jexbot/52.363.1969.

Dhakarey, R., Raorane, M.L., Treumann, A., Peethambaran, P. K., Schendel, R. R., Sahi, V. P., Hause, B., Bunzel, M., Henry, M., Kohli, A. & Riemann, M. (2017). Physiological and proteomic analysis of the rice mutant cpm2 suggests a negative regulatory role of jasmonic acid in drought tolerance. *Frontiers in Plant Science* **8**(1903), 1-17. DOI. 10.3389/fpls.2017.01903.

Dominguez-Solis, J. R., He, Z., Lima, A., Ting, J., Buchanan, B. B. & Luan, S. (2008). A cyclophilin links redox and light signals to cysteine biosynthesis and stress responses in chloroplasts. *PNAS* **105**(42), 16386-16391. DOI : 10.1073/pnas.0808204105.

Dong, W., Wang, M., Xu, F., Quan, T., Peng, K., Xiao, L. & Xia, G. (2013). Wheat oxophytodienoate reductase gene TaOPR1 confers salinity tolerance via enhancement of abscisic acid signaling and reactive oxygen species scavenging. *Plant Physiology* **161,** 1217-1228. DOI: 10.1104/pp.112.211854.

Dubiellaa, U., Seybolda, H., Duriana, G., Komandera, E., Lassiga, R., Wittea, C-P., Schulzeb, W. X. & Romeisa, T. (2013). Calcium-dependent protein kinase/NADPH oxidase activation circuit is required for rapid defense signal propagation. *PNAS* **110**(21), 8744-8749. DOI: 10.1073/pnas.1221294110.

Durst, S., Hedde, P.N., Brochhausen, L., Nick, P., Nienhaus, G.U. and Maisch, J. (2014). Organization of perinuclear actin in live tobacco cells observed by PALM with optical sectioning. *Journal of Plant Physiology* **141,** 97-108. DOI: 10.1016/j.jplph.2013.10.007.

Eggenberger, K., Birtalan, B., Schröder, T., Bräse, S. & Nick., P. (2009). Passage of Trojan Peptoids into Plant Cells. *ChemBioChem* **10,** 2504-2512. DOI: 10.1002/cbic.200900331.

Eggenberger, K., Sanyal, P., Hundt, S., Wadhwani, P., Ulrich, S.A. and Nick, P. (2017). Challenge Integrity: The Cell-Penetrating Peptide BP100 Interferes with the Auxin–Actin Oscillator. *Plant Cell Physiol.* **58,** 71-85. DOI: 10.1093/pcp/pcw161.

Elliott, G. & O'Hare, P. (1997). Intercellular trafficking and protein delivery by a herpesvirus structural protein. *Cell* **88,** 223-233. DOI: 10.1016/S0092-8674(00)81843-7.

Eltayeb, A. E., Kawano, N., Badawi, G.H., Kaminaka, H., Sanekata, T., Shibahara, T., Inanaga, S., & Tanaka, K. (2007). Overexpression of monodehydroascorbate reductase in transgenic tobacco confers enhanced tolerance to ozone, salt and polyethylene glycol stresses. *Planta* **225,** 1255-1264. DOI: 10.1007/s00425-006-0417-7.

Engqvist-Goldstein, Y. E. A. and Drubin, G. D. (2003). Actin assembly and Endocytosis: From Yeast to Mammals. *Annual Reviews of Cell and Developmental Biolology* **19,** 287-332. DOI: 10.1146/annurev.cellbio.19.111401.093127.

Ernster, L. & Dallner, G. (1995). Biochemical, physiological and medical aspects of ubiquinone function. *Biochimica et Biophysica Acta* **1271,** 195-204. DOI: 10.1016/0925-4439(95)00028-3.

Estavillo, G. M., Crisp, P. A., Pornsiriwong, W., Wirtz, M., Collinge, D., Carrie, C., Giraud, E., Whelan, J., David, P., Javot, H., Brearley, C., Hell, R., Marin, E. & Pogson, B. J. (2011). Evidence for a SAL1-PAP chloroplast retrograde pathway that functions in drought and high light signaling in Arabidopsis. *The Plant Cell* **23,** 3992-4012 (2011). DOI: 10.1105/tpc.111.091033.

Evans, M. D., Dizdaroglu, M. & Cooke, M.S. (2004). Oxidative DNA damage and disease: induction, repair and significance. *Mutation Research **567**, 1-61.* DOI: 10.1016/j.mrrev.2003.11.001.

Evans, N. H., McAinsh, M. R., Hetherington, A. M. & Knight, M. R. (2005). ROS perception in Arabidopsis thaliana: the ozone-induced calcium response. *The Plant Journal* **41,** 615-626. DOI: 10.1111/j.1365-313X.2004.02325. x.

FAO (1988). Salt-affected soils and their management. FAO soils bulletin 39. Rome, Italy. http://www.fao.org/3/x5871e/x5871e00.htm.

FAO (2008). FAO datasets on land use, land use change, agriculture and forestry and their applicability for national greenhouse gas reporting: A background paper for the IPCC expert meeting on guidance on greenhouse gas inventories of land uses such as agriculture and forestry. Helsinki, Finland, 13-15 May 2008.

FAO (2009). How to feed the world in 2050. pp. 35.

Fahad, S., Hussain, S., Bano, A., Saud, S., Hassan, S., Shan, D., Khan, F. A., Khan, F., Chen, Y., Wu, C., Tabassum, M. A., Chun, M. X., Afzal, M., Jan, A., Jan, M. T. and & Huang, J. (2015). Potential role of phytohormones and

plant growth-promoting rhizobacteria in abiotic stresses: consequences for changing environment. *Environ. Sci. Pollut. Res.* **22,** 4907-4921. DOI : 10.1007/s11356-014-3754-2.

Fato, R., Battino, M., Castelli, G. P. & Lenaz, G. (1985). Measurement of the lateral diffusion coefficients of ubiquinones in lipid vesicles by fluorescence quenching of 12-(9-anthroyl) stearate. *FEBS* **179**(2), 238-242. DOI:10.1016/0014-5793(85)80526-3.

Fernandes, C. C. T., Mazzeo, C.E. D. & Marin-Morales, A. M. (2007). Mechanism of micronuclei formation in polyploidizated cells of *Allium cepa* exposed to triXuralin herbicide. *Pesticide Biochemistry and Physiology* **88,** 252-259. DOI: 10.1016/j.pestbp.2006.12.003.

Finka, A., Cuendet, A. F. H., Maathuis, F. J. M. Saidi, Y. & Goloubinoff, P. (2012). Plasma membrane cyclic nucleotide gated calcium channels control land plant thermal sensing and acquired thermotolerance. *The Plant Cell* **24,** 3333-3348. DOI:10.1105/tpc.112.095844.

Fini, A., Brunetti, C., Di Ferdinando, M., Ferrini, F. & Tattini, M. (2011). Stress-induced flavonoid biosynthesis and the antioxidant machinery of plants. *Plant Signaling & Behavior* **6**(5), 709-711. DOI: 10.4161/psb.6.5.15069.

Fischer, G., Tubiello, F. N., van Velthuizen, H. & Wiberg, D. A. (2007). Climate change impacts on irrigation water requirements: Effects of mitigation, 1990–2080. *Technological Forecasting & Social Change* **74,** 1083-1107. DOI: 10.1016/j.techfore.2006.05.021.

Flis, V. V. & Daum, G. (2013). Lipid transport between the endoplasmic reticulum and mitochondria. *Cold Spring Harb Perspect Biol.* **5**(6), 1-22. DOI: 10.1101/cshperspect. a013235.

Flowers, T.J. (2004). Improving crop salt tolerance. *Journal of Experimental Botany,* **55**(396), 307-319. DOI: 10.1093/jxb/erh003.

Flowers, T.J., Munns, R. and Colmer, T.D. (2015). Sodium chloride toxicity and the cellular basis of salt tolerance in halophytes. *Annals of Botany* **115,** 419-431. DOI:10.1093/aob/mcu217.

Foreman, J., Demidchik, V., Bothwell, J. H. F., Mylona, P., Miedema, H., Torresk, M.A., Linstead, P., Costa, S., Brownlee, C., Jonesk, J. D. G. (2003). Reactive oxygen species produced by NADPH oxidase regulate plant cell growth. *Letters to Nature* **422,** 442-446. DOI:10.1038/nature01485.

Fowler, S. A. & Blackwell, H. E. (2009). Structure–function relationships in peptoids: Recent advances toward deciphering the structural requirements for biological function. *Org. Biomol. Chem.* **7,** 1508-1524. DOI: 10.1039/b817980h.

Foyer, C. H. & Noctor, G. (2005). Redox homeostasis and antioxidant signaling: A metabolic interface between stress perception and physiological responses. *The Plant Cell* **17,** 1866-1875. DOI: 10.1105/tpc.105.033589.

Frankel, A. O. & Pabo, C. O. (1988). Cellular Uptake of the Tat Protein from Human lmmunodeficiency Virus. *Cell* **55,** 1189-1193.

Fuchs, I., Stölzle, S., Ivashikina, N. & Hedrich, R. (2005). Rice K^+uptake channel OsAKT1 is sensitive to salt stress. *Planta* **221,** 212-221. DOI 10.1007/s00425-004-1437-9.

Fukai, T. & Ushio-Fukai, M. (2011). Superoxide Dismutases: Role in Redox Signaling, Vascular Function, and Diseases. *Antioxidants and Redox Signalling* **15**(6), 1-24. DOI: 10.1089/ars.2011.3999.

Fürniss, D., Mack, T., Hahn, F., Vollrath, S. B. L., Koroniak, K., Schepers, U. & Bräse, S. (2013). Peptoids and polyamines going sweet:Modular synthesis of glycosylated peptoids and polyamines using click chemistry. *Beilstein J. Org. Chem.* **9,** 56-63. DOI:10.3762/bjoc.9.7.

Gadallah, M. A. A. (1999). Effects of proline and glycinebetaine on *Vicia faba* responses to salt stress. *Biologia Plantarum* **42**(2), 249-257. DOI: 10.1023/A:1002164719609.

Gaff, F.D. & Okong'O-Ogola, O. (1971). The use of non-permeating pigments for testing the survival of cells. *Journal of Experimental Botany* **22,** 756-758. DOI: 10.1093/jxb/22.3.756.

Gao, N., Wadhwani, P., Mühlhäuser, P., Liu, Q., Riemann, M., Ulrich, S. A. and Nick, P. (2016). An antifungal protein from Ginkgo biloba binds actin and can trigger cell death. *Protoplasma* **253,** 1159-1174. DOI:10.1007/s00709-015-0876-4.

Geldner, N., Friml, J., Stierhof, Y-D., Jürgens, G. and Palme, K. (2001). Auxin transport inhibitors Block PIN1 cycling and vesicle trafficking. *Nature* **413,** 425-428. DOI: 10.1038/35096571.

Genova, M. L. & Lenaz, G. (2011). New developments on the functions of coenzyme Q in mitochondria. *International Union of Biochemistry and Molecular Biology* **37**(5), 330-354. DOI: 10.1002/biof.168.

Gestel, K.V., Köhler, R, H. & Verbelen,J-P. (2002). Plant mitochondria move on F-actin, but their positioning in the cortical cytoplasm depends on both F-actin and microtubules. *Journal of Experimental Botany* **53**(369), 659-667. DOI:10.1093/jexbot/53.369.659.

Gill, S. S. & Tuteja, N. (2010). Reactive oxygen species and antioxidant machinery in abiotic stress tolerance in crop plants. *Plant Physiology and Biochemistry* **48,** 909-930. DOI: 10.1016/j.plaphy.2010.08.016.

Gilroy, S., Suzuki, N., Miller, G., Choi, W-G., Toyota, M., Devireddy, A. R. & Mittler, R. (2014). A tidal wave of signals: calcium and ROS at the forefront of rapid systemic signaling. *Trends in Plant Science* **1202,** 1-8. DOI: 10.1016/j.tplants.2014.06.013.

Giri, B., Kapoor, R. & Mukerji, K.G. (2007). Improved tolerance of *Acacia nilotica* to salt stress by arbuscular mycorrhiza, *Glomus fasciculatum* may be partly related to elevated K/Na ratios in root and shoot tissues. *Microbial Ecology* **54,** 753-760. DOI: 10.1007/s00248-007-9239-9.

Golldack, D.,Li, C., Mohan, H. & Probst, N. (2014). Tolerance to drought and salt stress in plants: unraveling the signaling networs. *Frontiers in Plant Science* **5**(151), 1-10. DOI: 10.3389/fpls.2014.00151.

Gould, S. B., Waller, R.F. & McFadden, G. I. (2008). Plastid Evolution. *Annu. Rev. Plant Biol.* **59,** 491-517. DOI: 10.1146/annurev.arplant.59.032607.092915.

Green, M. & Loewenstein, P. M. (1988). Autonomous functional domains of chemically synthesized human immunodeficiency virus Tat trans-activator protein. *Cell* **55,** 1179-1188. DOI: 10.1016/0092-8674(88)90262-0.

Gruenberg, J. (2001). The endocytic pathway: a mosaic of domains. *Nature Reviews in Molecular Cell Biology* **2,** 721-730.DOI:10.1038/35096054.

Guan, X., Buchholz, G. & Nick, P. (2015). Tubulin marker line of grapevine suspension cells as a tool to follow early stress responses. *Journal of Plant Physiology* **176,** 118-128. DOI: 10.1016/j.jplph.2014.10.023.

Gulaboski, R., Bogeski, I., Kokoskarova, P., Haeri, H. H., Mitrev, S., Stefova, M., Stanoeva, J. P., Markovski, V., Mirčeski, V., Hoth, M. & Kappl, R. (2016). New insights into the chemistry of Coenzyme Q-0: A voltammetric and spectroscopic study. *Bioelectrochemistry* **111**, 100-108. DOI: 10.1016/j.bioelechem.2016.05.008.

Gulaboski, R., Bogeski, I., Mirceski, V., Saul, S., Pasieka, B., Haeri, H. H., Stefova, M., Stanoeva, J. P., Mitrev, S., Hoth, M. & Kappl, R. (2013). Hydroxylated derivatives of dimethoxy-1,4-benzoquinone as redox switchable earth-alkaline metal ligands and radical scavengers. *Sci. Rep.* **3** (1865), 1-8. DOI: 10.1038/srep01865.

Gupta, B. & Huang, B. (2014). Mechanism of salinity tolerance in plants: physiological, biochemical, and molecular characterization**.** *International Journal of Genomics* **2014,** 1-18. DOI:10.1155/2014/701596.

Gupta, K. J., Fernie, A, R., Kaiser, W. M. & van Dongen, J. T. (2011). On the origins of nitric oxide. *Trends in Plant Science* **16** (3), 160-168. DOI: 10.1016/j.tplants.2010.11.007.

Halliwell, B. (2006). Reactive species and antioxidants. Redox biology is a fundamental theme of aerobic Life. *Plant Physiology* **141,** 312-322. DOI: 10.1104/pp.106.077073.

Hanif, F. & Afshan, S. (2013). Evaluating the response of wheat genotypes to salinity stress. *Asian Journal of Agricultural Sciences* **5**(6), 126-129.

Hanin, M., Ebel, C., Ngom, M., Laplaze, L. & Masmoudi, K. (2016). New insights on plant salt tolerance mechanisms and their potential use for breeding. *Front. Plant Sci.* **7,** 1-17.DOI: 10.3389/fpls.2016.01787.

Harb, A., Krishnan, A., Ambavaram, M. M. R. & Pereira, A. (2010). Molecular and physiological analysis of drought stress in Arabidopsis reveals early responses leading to acclimation in plant growth. *Plant Physiology* **154,** 1254-1271. DOI: 10.1104/pp.110.161752.

Hartl, M. & Finkemeier, I. (2012). Plant mitochondrial retrograde signaling post-translational modifications enter the stage. *Frontiers in Plant science* **3**(253), 1-7. DOI: 10.3389/fpls.2012.00253.

Haruta, M., Burch, H. L., Nelson, R. B., Barrett-Wilt, G., Kline, K. G., Mohsin, S. B., Young, J. C., Otegui, M. S. & Sussman, M. R. (2010). Molecular characterization of mutant Arabidopsis plants with reduced plasma

membrane proton pump activity. *The Journal of Biological Chemistry* **285**(23), 17918-17929. DOI: 10.1074/jbc.M110.101733.

Hasan, M. I., Kibria, M. G., Jahiruddin, M., Murata, Y. & Hoque, M.A. (2015). Improvement of salt tolerance in maize by exogenous application of proline. *J. Environ. Sci. & Natural Resources,* **8**(1), 13-18. DOI: org/10.3329/jesnr. v8i1.24626.

Hasegawa, P.M., Bressan, R. A., Zhu, J-K. & Bohnert, H.J. (2000). Plant cellular and molecular responses to high salinity. *Annu. Rev. Plant Physiol. Plant Mol. Biol.* **51,** 463-499. DOI: 1040-2519/00/0601-0463$14.00.

Hashem Abeer, Abd_Allah, E.F., Alqarawi, A. A., El-Didamony, G., Alwhibi, M. S., Egamberdieva, D. & Ahmad, P. (2014). Alleviation of adverse impact of salinity on faba bean (Vicia faba L.) by arbuscular mycorrhizal fungi. *Pak. J. Bot.* **46**(6), 2003-2013.

Hasumi, K., Shinohara, C., Naganuma, S. and Endo, A. (1992). Inhibition of the uptake of oxidazed low-density lipoprotein in macrophage J774 by the antibiotic ikarugamycin. *European Journal of Biochemistry* **205**, 841-846. DOI: 10.1111/j.1432-1033. 1992.tb16848.x.

Hazman, M., Hause, B., Eiche, E., Nick, P. & Riemann, M. (2015). Increased tolerance to salt stress in OPDA-defcient rice *ALLENE OXIDE CYCLASE* mutants is linked to an increased ROS-scavenging activity. *Journal of Experimental Botany* **66**(11), 3339-3352. DOI:10.1093/jxb/erv142.

Heath, R. L. & Packer, L. (1968). Photoperoxidation in isolated chloroplasts: I. Kinetics and stoichiometry of fatty acid peroxidation. *Archives of Biochemistry and Biophysics* **125,** 189-198. DOI:10.1016/0003-9861(68)90654-1.

Hedtke, B., Wagner, I., Börner , T. & Hess, W. R. (1999). Inter-organellar crosstalk in higher plants: impaired chloroplast development affects mitochondrial gene and transcript levels. *The Plant Journal* **19**(6), 635-643. DOI:10.1046/j.1365-313x.1999. 00554.x.

Henderson, M. L. & Chappell, B. J. (1993). Dihydrorhodamine 123: a fluorescent probe for superoxide generation? *Eur. J. Biochem*. **217,** 973-980. DOI : 10.1111/j.1432-1033. 1993.tb18328.x.

Hernandez, J. A., Ferrer, M. A., Jimenez, A., Barcelo, A. R. & Sevilla, F. (2001). Antioxidant systems and $O_2^{\bullet -}/H_2O_2$ production in the apoplast of pea leaves. Its relation with salt-induced necrotic lesions in minor veins. *Plant Physiology*, **127,** 817-831. DOI :10.1104/pp.010188.

Hernandez, J. A., Jimenez, A., Mullineaux, P. & Sivilla, F. (2000). Tolerance of pea (*Pisum sativum L.*) to long-term salt stress is associated with induction of antioxidant defences. *Plant, Cell and Environment* **23**, 853-862. DOI: 10.1046/j.1365-3040.2000. 00602.x.

Hirsch, R. E., Lewis, B. D., Spalding, E. P. & Sussman, M. R. (1998). A role for the AKT1 potassium channel in plant nutrition. *Science* **280** (5365), 918-921. DOI: 10.1126/science.280.5365.918.

Ho, L. H. M., Giraud, E., Uggalla,V., Lister, R., Clifton, R., Glen, A., Thirkettle-Watts, D., Van Aken, O. & Whelan, J. (2008). Identification of regulatory pathways controlling gene expression of stress-responsive mitochondrial proteins in Arabidopsis. *Plant Physiology* **147**, 858-1873. DOI: 10.1104/pp.108.121384.

Hoang, X, L. T., Nhi, D. N. H., Thu, N.B.A., Thao, N. P. & Tran, L-S. P. (2017). Transcription factors and their roles in signal transduction in plants under abiotic stresses. *Current Genomics* **18,** 483-497. DOI: 10.2174/1389202918666170227150057.

Hodgson, J, A, R. & Raison, K, J. (1991). Lipid peroxidation and superoxide dismutase activity in relation to photoinhibition induced by chilling in moderate light. *Planta* **185,** 215-219. DOI: 10.1007/BF00194063.

Hohenberger, P., Eing, C., Straessner, R., Durst, S., Frey, W. & Nick, P. (2011). Plant actin controls membrane permeability. *Biochimica et Biophysica Acta* **1808,** 2304-2312. DOI: 10.1016/j.bbamem.2011.05.019.

Holzmeister, C., Gaupels, F., Geerlof, A., Sarioglu, H., Sattler, M., Durner, J. & Lindermayr, C. (2015). Differential inhibition of Arabidopsis superoxide dismutases by peroxynitrite-mediated tyrosine nitration. *Journal of Experimental Botany* **66**(3), 989-999. DOI:10.1093/jxb/eru458.

Holländer-Czytko, H., Grabowski, J., Sandorf, I., Weckermann, K. & Weiler, E. W. (2005). Tocopherol content and activities of tyrosine aminotransferase and cystine lyase in Arabidopsis under stress conditions. *Journal of Plant Physiology* **162,** 767-770. DOI: 10.1016/j.jplph.2005.04.019.

Hoque, M. A., Banu,M. N. A., Nakamura,Y., Shimoishi, Y. & Murata, Y. (2008). Proline and glycinebetaine enhance antioxidant defense and methylglyoxal detoxification systems and reduce NaCl-induced damage in cultured tobacco cells. *Journal of Plant Physiology* **165,** 813-824. DOI: 10.1016/j.jplph.2007.07.013.

Hoque, M. A., Banua, M. N. A., Okumaa, E., Amakob, K., Nakamuraa, Y., Shimoishia, Y. & Murata, Y. (2007). Exogenous proline and glycinebetaine increase NaCl-induced ascorbate–glutathione cycle enzyme activities, and proline improves salt tolerance more than glycinebetaine in tobacco Bright Yellow-2 suspension-cultured cells. *Journal of Plant Physiology* **164,** 1457-1468. DOI: 10.1016/j.jplph.2006.10.004.

Horemans, N., Foyer, C. H. & Asard, H. (2000). Transport and action of ascorbate at the plant plasma membrane. *Trends in Plant Science* **5**(6), 263-267. DOI:10.1016/S1360-1385(00)01649-6.

Horn, T., Lee,B-C., Dill, K. A. & Zuckermann, R. N. (2004). Incorporation of Chemoselective Functionalities into Peptoids via Solid-Phase Submonomer Synthesis. *Bioconjugate Chem.* **15,** 428-435. DOI: 10.1021/bc0341831.

Huang, B., DaCosta, M. & Jiang, Y. (2014). Research advances in mechanisms of turfgrass tolerance to abiotic stresses: From physiology to molecular biology. *Critical Reviews in Plant Sciences* **33,** 141-189. DOI: 10.1080/07352689.2014.870411.

Huang, S., Aken, V. O., Schwarzländer, M., Belt, K. & Millar, H. A. (2016). The Roles of mitochondrial reactive oxygen species in cellular signaling and stress response in plants. *Plant Physiol.***171**, 1551-1559. DOI: 10.1104/pp.16.00166.

Huang, X., Maisch, J. and Nick, P. (2017). Sensory role of actin in auxin-dependent responses of tobacco BY-2. *Journal of Plant Physiology* **218,** 6-15. DOI: 10.1016/j.jplph.2017.07.011.

Hu, G., Liu, Y., Zhang, X., Yao, F., Huang, Y., Ervin, E. H. & Zhao, B. (2015). Physiological evaluation of alkali-salt tolerance of thirty switchgrass (*Panicum virgatum*) lines. *PLoS ONE* **10**(7), 1-17. DOI: 10.1371/journal.pone.0125305.

Hu, L.,Huang, Z., Liu, S. & Fu, J. (2012). Growth response and gene expression in antioxidant-related enzymes in two bermudagrass genotypes differing in salt tolerance. *J. Amer. Soc. Hort. Sci.* **137**(3), 134-143. DOI: 10.21273/JASHS.137.3.134.

Igamberdiev, A. U., Manach, C.S. N. & Hill, R. D. (2004). NADH-dependent metabolism of nitric oxide in alfalfa root cultures expressing barley hemoglobin. *Planta* **219**, 95-102. DOI: 10.1007/s00425-003-1192-3.

Ippolito, A. J. & Barbarick, A, K. (2000). Modified nitric acid plant tissue digest method. Commun. *Soil Sci. Plant Anal.* **31**(15&16), 2473-2482. DOI: 10.1080/00103620009370602.

Ismail, A., Riemann, M. & Nick, P. (2012). The jasmonate pathway mediates salt tolerance in grapevines. *Journal of Experimental Botany* **63**(5), 2127-2139. DOI:10.1093/jxb/err426.

Ismail, A.,Takeda, S. and Nick, P. (2014). Life and death under salt stress: same players, different timing? *Journal of Experimental Botany* **65**(12), 2963-2979. DOI:10.1093/jxb/eru159.

Jaipargas, E.A., Barton, K.A., Mathur, N. and Mathur, J. (2015). Mitochondrial pleomorphy in plant cells is driven by contiguous ER dynamics. *Frontiers in Plant Science* **6,** 783. DOI:10.3389/fpls.2015.00783.

Jaipargas, E-A., Mathur, N., Daher, F. B., Wasteneys, G. O. & Mathur, J. (2016). High light intensity leads to increased peroxule-mitochondria interactions in plants. *Frontiers in Cell and Developmental Biology* **4**(6), 1-11. DOI: 10.3389/fcell.2016.00006.

Järver, P. & Langel, Ü. (2006). Cell-penetrating peptides-A brief introduction. *Biochimica et Biophysica Acta* **1758,** 260-263. DOI: 10.1016/j.bbamem.2006.02.012.

Jebara, S., Jebara, M., Limam, F. & Aouani, M. E. (2005). Changes in ascorbate peroxidase, catalase, guaiacol peroxidase and superoxide dismutase activities in common bean (Phaseolus vulgaris) nodules under salt stress. *Journal of Plant Physiology* **162,** 929-936. DOI: 10.1016/j.jplph.2004.10.005.

Joliot, A., Pernellet, C., Deagostint-Bazint, H. & Prochiantz, A. (1991). Antennapedia homeobox peptide regulates neural morphogenesis. *Proc. Natl. Acad. Sci.* **88,** 1864-1868. DOI: 10.1073/pnas.88.5.1864.

Jovanovic, A. M., Durst, S. & Nick, P. (2010). Plant cell division is specifically affected by nitrotyrosine. *Journal of Experimental Botany* **61**(3), 901-909. DOI: 10.1093/jxb/erp369.

Jung, J. K. H. & McCouch, S. (2013). Getting to the roots of it: genetic and hormonal control of root architecture. *Frontiers in Plant Science* **4**(186),1-32. DOI:10.3389/fpls.2013.00186.

Kalaji, M. H. & Pietkiewicz,s. (1993). Salinity effects on plant growth and other physiological processes. *ACTA Physiologiae Plantarum* **15**(2), 89-124.

Kang, D-J., Seo, Y-J., Lee, J-D., Ishii, R., Kim, K. U., Shin, D. H., Park, S. K., Jang, S. W. and Lee, I-J. (2005). Jasmonic acid differentially affects growth, ion uptake and abscisic acid concentration in salt-tolerant and salt-sensitive rice cultivars. *J. Agronomy & Crop Science* **191,** 273-282. DOI: 10.1111/j.1439-037X.2005. 00153.x.

Karuppanapandian, T. & Manoharan, K. (2008). Uptake and translocation of tri- and hexa-valent chromium and their effects on black gram *(Vigna mungo* L. Hepper cv. Co4) roots. *Journal of Plant Biology* **51**(3), 192-201.DOI: 10.1007/BF03030698.

Karuppanapandian, T., Moon, J-C., Kim, C., Manoharan, K. & Kim, W. (2011). Reactive oxygen species in plants: their generation, signal transduction, and scavenging mechanisms. *AJCS* **5**(6), 709-725.

Karuppanapandian T., Sinha, P. B., Haniya, K. & Manoharan, K. (2009). Chromium-induced accumulation of peroxide content, stimulation of antioxidative enzymes and lipid peroxidation in green gram (*Vigna radiata* L. cv. Wilczek) leaves. *African Journal of Biotechnology* **8**(3), 475-479.

Kauffman, W. B., Fuselier, T., He,J., & Wimley, W. C. (2015). Mechanism matters: A taxonomy of cell penetrating peptides. *Trends in Biochemical Sciences* **40**(12), 749-764. DOI: 10.1016/j.tibs.2015.10.004.

Kelso, M.J., Hoang, H. N., Appleton, T. G. & Fairlie, D. P. (2000). The first solution structure of a single α-helical turn. A pentapeptide α-helix stabilized by a metal clip. *J. Am. Chem. Soc.* **122,** 10488-10489. DOI: 10.1021/ja002416i.

Khan, M. N., Siddiqui, M. H., Mohammad, F. & Naeem, M. (2012). Interactive role of nitric oxide and calcium chloride in enhancing tolerance to salt stress. *Nitric Oxide* **27,** 210-218. DOI: 10.1016/j.niox.2012.07.005.

Khan, M. S. (2011). Role of sodium and hydrogen (Na^+/H^+) antiporters in salt tolerance of plants: Present and future challenges. *African Journal of Biotechnology* **10**(63), 13693-13704. DOI: 10.5897/AJB11.1630.

Kiełkowska, A. (2017). *Allium cepa* root meristem cells under osmotic (sorbitol) and salt (NaCl) stress *in vitro. Acta Bot. Croat.* **76** (2), 146-153. DOI: 10.1515/botcro-2017-0009.

Kleine, T. & Dario Leister, D.(2016). Retrograde signaling: Organelles go networking. *Biochimica et Biophysica Acta* **1857,** 1313-1325. DOI: 10.1016/j.bbabio.2016.03.017.

Knight, H., Trewavas, A. J. & Knight, M.R. (1997). Calcium signaling in *Arabidopsis thaliana* responding to drought and salinity. *The Plant Journal* **12**(5), 1067-1078. DOI: 10.1046/j.1365-313X.1997.12051067. x.

Kölmel, D. K., Fürniss, D., Susanto, S., Lauer, A., Grabher, C., Bräse, S. & Schepers, U. (2012). Cell Penetrating Peptoids (CPPos): Synthesis of a Small Combinatorial Library by Using IRORI MiniKans. *Pharmaceuticals* **5,** 1265-1281. DOI:10.3390/ph5121265.

Kopriva, S. (2013). 12-oxo-phytodienoic acid interaction with cyclophilin CYP20-3 is a benchmark for understanding retrograde signaling in plants. *PNAS* **110**(23), 9197-9198. DOI: 10.1073/pnas.1307482110.

Koren, E. & Torchilin, V. P. (2012). Cell-penetrating peptides: breaking through to the other side. *Trends in Molecular Medicine* **18**(7), 385-393. DOI: 10.1016/j.molmed.2012.04.012.

Kotera, A., Sakamoto, T., Nguyen, D. K. & Yokozawa, M. (2008). Regional consequences of seawater intrusion on rice productivity and land use in coastal area of the Mekong river delta. *JARQ* **42**(4), 267-274. DOI: 10.6090/jarq.42.267.

Kromdijk, J. & Long, S.P. (2016). One crop breeding cycle from starvation? How engineering crop photosynthesis for rising CO2 and temperature could be one important route to alleviation. *Proc. R. Soc. B.* **283,** 1-8. DOI: org/10.1098/rspb.2015.2578

Kronzucker, H, J. & Britto, D. T. (2011). Sodium transport in plants: a critical review. *New Phytologist* **189,** 54-81. DOI: 10.1111/j.1469-8137.2010.03540. x.

Ksenzhek, O.S., Petrova, S.A. & Kolodyazhny, M.V. (1982). 452-redox properties of ubiquinones in aqueous solutions. *Bioelectrochemistry and Bioenergetics* **9,** 167-174. DOI: 10.1016/0302-4598(82)80173-6.

Kundra, R. and Kornfeld, S. (1998). Wortmannin retards the movement of the mannose 6-phosphate/insulin-like growth factor II receptor and its ligand out of endosomes. *Journal of Biological Chemistry* **273,** 3848-3853. DOI: 10.1074/jbc.273.7.3848.

Kwon, Y-U. & Kodadek, T. (2007). Quantitative evaluation of the relative cell permeability of peptoids and peptides. *J. Am. Chem. Soc.***129,** 1508-1509. DOI:10.1021/ja0668623.

Lankova, M., Smith, R. S., Pesek, B., Kubes, M., Zazimalova, E., Petrasek, J. & Hoyerova, K. (2010). Auxin influx inhibitors 1-NOA, 2-NOA, and CHPAA interfere with membrane dynamics in tobacco cells. *Journal of Experimental Botany* **61,** 3589-3598. DOI:10.1093/jxb/erq172.

Lata, C., Jha, S., Dixit, V., Sreenivasulu, N. & Prasad, M. (2011). Differential antioxidative responses to dehydration-induced oxidative stress in core set of foxtail millet cultivars [Setaria italica (L.)]. *Protoplasma* **248,** 817-828. DOI: 10.1007/s00709-010-0257-y.

Ledford, H. K. & Niyogi, K. K. (2005). Singlet oxygen and photo-oxidative stress management in plants and algae. *Plant, Cell and Environment* **28,** 1037-1045. DOI: 10.1111/j.1365-3040.2005. 01374.x.

Li, C., Fang, B., Yang, C., Shi, D. & Wang, D. (2009). Effects of various salt–alkaline mixed stresses on the state of mineral elements in nutrient solutions and the growth of alkali resistant halophyte *Chloris Virgata*. *Journal of Plant Nutrition* **32,** 1137-1147. DOI : 10.1080/01904160902943163.

Li, C-R., Liang, D-D., Li, J., Duan, Y-B., Li, H., Yang, Y-C., Qin, R-Y., Wei, P-C. & Yang, J-B. (2013). Unravelling mitochondrial retrograde regulation in the abiotic stress induction of rice *ALTERNATIVE OXIDASE1* genes. *Plant, Cell and Environment* **36,** 775-788 (2013). DOI: 10.1111/pce.12013.

Lindgren, M., Hällbrink,M., Prochiantz, A. & Langel, Ü. (2000). Cell-penetrating peptides. *TiPS* **21,** 99-103. DOI: 10.1016/S0165-6147(00)01447-4.

Livak, J, K. Schmittgen, D, T. (2001). Analysis of relative gene expression data using real-time quantitative PCR and the $2^{\Delta\Delta Ct}$ method. *Methods* **25,** 402-408. DOI : 10.1006/meth.2001.1262.

Lopez-Lluch, G., Rodriguez-Aguilera, J. C., Santos-Ocana, C. & Navas, P. (2010). Is coenzyme Q a key factor in aging? *Mechanisms of Ageing and Development* **131,** 225-235. DOI: 10.1016/j.mad.2010.02.003.

Lu, Z., Liu, D. & Liu, S. (2007). Two rice cytosolic ascorbate peroxidases differentially improve salt tolerance in transgenic Arabidopsis. *Plant Cell Rep.***26,** 1909-1917. DOI: 10.1007/s00299-007-0395-7.

Luk, E., Yang, M., Jensen, L. T., Bourbonnais, Y. & Culot, V. C. (2005). Manganese activation of superoxide dismutase 2 in the mitochondria of *saccharomyces cerevisiae*. *The Journal of Biological Chemistry* **280**(24), 22715-22720. DOI: 10.1074/jbc.M504257200.

Luo, T., Fredericksen,L.B., Hasumi, K., Endo, A. and Garcia, V. J. (2001). Human Immunodeficiency Virus Type 1 Nef-Induced CD4 Cell Surface Downregulation Is Inhibited by Ikarugamycin. *Journal of Virology* **75,** 2488-2492. DOI:10.1128/JVI.75.5.2488-2492.2001.

Maathuis, F. J. M., Ahmad, I. & Patishtan, J. (2014). Regulation of Na^+ fluxes in plants. *Frontiers in Plant Science* **5**(467), 1-9. DOI: 10.3389/fpls.2014.00467.

MacMillan-Crow, L. A. Crow, J. P. & Thompson, J. A. (1998). Peroxynitrite-Mediated Inactivation of Manganese Superoxide Dismutase Involves Nitration and Oxidation of Critical Tyrosine Residues. *Biochemistry **37,*** 1613-1622. DOI: 10.1021/bi971894b.

Madani, F., Lindberg, S., Langel, Ü., Futaki, S. and Gräslund, A. (2011). Mechanisms of Cellular Uptake of Cell-Penetrating Peptides. *Journal of Biophysics* **2011,** 1-10. DOI:10.1155/2011/414729.

Mäe, M., Myrberg, H., Jiang, Y., Paves, H., Valkna, A., Langel, Ü. (2005). Internalisation of cell-penetrating peptides into tobacco protoplasts. *Biochimica et Biophysica Acta* **1669,** 101-107. DOI: 10.1016/j.bbamem.2005.01.006.

Mahajan, S., Sopory, S. K. & Tuteja, N. (2006). CBL-CIPK paradigm: Role in calcium and stress signaling in plants. *CBL-CIPK pathways Proc Indian Natn Sci Acad* **72(**2), 63-78.

Mahajan, S. & Tuteja, N. (2005). Cold, salinity and drought stresses: An overview. *Archives of Biochemistry and Biophysics* **444,** 139-158. DOI: 10.1016/j.abb.2005.10.018.

Maisch, J. & Nick, P. (2007). Actin Is Involved in Auxin-Dependent Patterning. *Plant Physiology* **143,** 1695-1704. DOI:10.1104/pp.106.094052.

Manchanda, G. & Garg, N. (2008). Salinity and its effects on the functional biology of legumes. *Acta Physiol Plant* **30,** 595-618. DOI 10.1007/s11738-008-0173-3.

Martinez-Atienza, J., Jiang, X., Garciadeblas, B., Mendoza, I., Zhu, J-K., Pardo, J. M. & Quintero, F. J. (2007). Conservation of the salt overly sensitive pathway in rice. *Plant Physiology* **143,** 1001-1012. DOI: 10.1104/pp.106.092635.

Matzke, M.A. and Matzke, J.M. (1986). Visualization of mitochondria and nuclei in living plant cells by the use of a potential-sensitive fluorescent dye. *Plant, Cell and Environment* **9,** 73-77. DOI: 10.1111/j.1365-3040. 1986.tb01725.x.

Mhamdi, A., Queval, G., Chaouch, S., Vanderauwera, S., Van Breusegem, F. & Noctor, G. (2010). Catalase function in plants: a focus on Arabidopsis mutants as stress-mimic models. *Journal of Experimental Botany* **61**(15), 4197-4220. DOI:10.1093/jxb/erq282.

Miller, G., Shulaev, V. & Mittler, R. (2008). Reactive oxygen signaling and abiotic stress. *Physiologia Plantarum* **133,** 481-489. DOI: 10.1111/j.1399-3054.2008.01090. x.

Miller, G., Suzuki, N., Ciftcl-Yilmaz, S. & Mittler, R. (2010). Reactive oxygen species homeostasis and signaling during drought and salinity stresses. *Plant, Cell and Environment* **33**, 453-467. DOI: 10.1111/j.1365-3040.2009.02041. x.

Miller, S. M., Simon, R. J., Ng, S., Zuckermann, R. N., Kerr, J. M. & Moos, W. H. (1994). Proteolytic studies of homologous peptide and N-substituted glycine peptoid oligomers. *Bioorganic & Medicinal Chemistry Letters,* **4**(22), 2657-2662. DOI:10.1016/S0960-894X(01)80691-0.

Miller, S. M., Simon, R. J., Ng, S., Zuckermann, R. N., Kerr, J. M. & Moos, W. H. (1995). Comparison of the proteolytic susceptibilities of homologous L-amino acid, D-amino acid, and N-substituted clycine peptide and peptoid oligomers. *Drug Development Research* **35,** 20-32. DOI: 10.1002/ddr.430350105.

Milletti, F. (2012). Cell-penetrating peptides: Classes, origin and current landscape. *Drug Discovery Today* **17**(15/16), 850-860. DOI: 10.1016/j.drudis.2012.03.002.

Mittler, R. (2002). Oxidative stress, antioxidants and stress tolerance. *TRENDS in Plant Science* **7**(9), 405-410. DOI: 10.1016/S1360-1385(02)02312-9.

Mittler, R. (2017). ROS are good. *Trends in Plant Science* **22**(1), 11-19. DOI: 10.1016/j.tplants.2016.08.002.

Mittler, R., Vanderauwera, S., Gollery, M., & Breusegem, F. V. (2004). Reactive oxygen gene network of plants. *TRENDS in Plant Science* **9**(10), 490-498. DOI: 10.1016/j.tplants.2004.08.009.

Mittler, R., Vanderauwera, S., Suzuki, N. Miller5, G., Tognetti,V. B., Vandepoele, K., Gollery, M., Shulaev, V. & Van Breusegem, F. (2011). ROS signaling: the new wave? *Trends in Plant Science* **16**(6), 300-309. DOI: 10.1016/j.tplants.2011.03.007.

Møller, I. M., Jensen, P.E. & Hansson, A. (2007). Oxidative modifications to cellular components in plants. *Annu. Rev. Plant Biol.* **58,** 459-481. DOI: 10.1146/annurev.arplant.58.032806.103946.

Møller, I. M. & Sweetlove, L. J. (2010). ROS signalling – specificity is required. *Trends in Plant Science* **15,** 370-374. i.org/10.1016/j.tplants.2010.04.008.

Moller, M. I. (2016). What is hot in plant mitochondria? *Physiologia Plantarum* **157,** 256-263. DOI :10.1111/ppl.12456.

Monetti, E., Kadono, T., Tran,D., Azzarello, E., Arbelet-Bonnin, D., Biligui, B., Briand, J., Kewano, T., Mancuso, S. and Bouteau, F. (2014). Deciphering early events involved in hyperosmotic stress-induced programmed cell death in tobacco BY-2 cells. *Journal of Experimental Botany* **65,** 1361-1375. DOI: 10.1093/jxb/ert460.

Moradas-Ferreira, P., Costa, V. Piper, P. & Mager, W. (1996). The molecular defences against reactive oxygen species in yeast. *Molecular Microbiology* **19**(4), 651-658. DOI: 10.1046/j.1365-2958.1996.403940. x.

Moreira-Nordemann, L. M. (1984). Salinity and weathering rate of rocks in a semi-arid region. *Journal of hydrology* **71,** 131-147. DOI: 10.1016/0022-1694(84)90074-X.

Movahedi, A., Moth-Poulsen, K., Eklöf, J., Nydén, M. & Kann, N. (2014). One-pot synthesis of TBTA-functionalized coordinating polymers. *Reactive and Functional Polymers* **82,** 1-8. DOI: 10.1016/j.reactfunctpolym.2014.05.008.

Muchate, N. S., Nikalje, G. C., Rajurkar, N. S., Suprasanna, P. & Nikam, T. D. (2016). Plant salt stress: Adaptive responses, tolerance mechanism and bioengineering for salt tolerance. *Bot. Rev.* **82,** 371-406. DOI: 10.1007/s12229-016-9173-y.

Mueller, J., Kretzschmar, I., Volkmer, R. & Boisguerin, P. (2008). Comparison of cellular uptake using 22 CPPs in 4 different cell lines. *Bioconjugate Chem.* **19,** 2363-2374. DOI: 10.1021/bc800194e.

Munns, R. (2002). Comparative physiology of salt and water stress. *Plant, Cell and Environment* **25,** 239-250. DOI: 10.1046/j.0016-8025.2001. 00808.x.

Munns, R. (2005). Genes and salt tolerance: bringing them together. *New Phytologist* **167**, 645-663. DOI: 10.1111/j.1469-8137.2005.01487. x.

Munns, R. & Tester, M. (2008). Mechanisms of salinity tolerance. *Annu. Rev. Plant Biol.* **59,** 651-681. DOI: 10.1146/annurev.arplant.59.032607.092911.

Murphy, M. T., Vu, H. & Nguyen, T. (1998). The superoxide synthases of rose cells: comparison of assays. *Plant Physiol.* **117,** 1301-1305. DOI: 10.1104/pp.117.4.1301.

Nabati, J., Kafi, M., Nezami, A., Moghaddam, P. R., Masoumi, A. & Mehrjerdi, M. Z. (2011). Effect of salinity on biomass production and activities of some key enzymatic antioxidants in kochia (*Kochia scoparia*). *Pak. J. Bot*. **43**(1), 539-548.

Nagata,T., Nemoto, Y. & Hasezaw, S. (1992). Tobacco BY-2 Cell Line as the "HeLa" Cell in the Cell Biology of Higher Plants. *International Review of Cytology* **132,** 1-30. DOI: 10.1016/S0074-7696(08)62452-3.

Nam, H. Y., Hong, J-A., Choi, J., Shin, S., Cho, S. K., Seo, J. & Lee, J. (2018). Mitochondria-targeting peptoids. *Bioconjugate Chem.* **29,** 1669-1676. DOI: 10.1021/acs.bioconjchem.8b00148.

Nankivell, B.J., Chen, J. & Harris, D.C.H. (1994). The role of tubulr iron accumulation in the remnant kidney. *J. Am. Soc. Nephrol.* **4,** 1598-1607.

Nathan, C. (2003). Specificity of a third kind: reactive oxygen and nitrogen intermediates in cell signaling. *The Journal of Clinical Investigation* **111**(6), 769-778. DOI : 10.1172/JCI200318174.

Navrot, N., Rouhier, N., Gelhaye, E. & Jean-Pierre Jacquot, J-P. (2007). Reactive oxygen species generation and antioxidant systems in plant mitochondria. *Physiologia Plantarum* **129,** 185-195. DOI: 10.1111/j.1399-3054.2006. 00777.x

Neill, S. J., Desikan, R. & Hancock, J. T. (2003). Nitric oxide signalling in plants. *New Phytologist* **159**, 11-35. DOI: 10.1046/j.1469-8137.2003.00804. x.

Nagesh, R. B. & Devaraj, V. R. (2008). High temperature and salt stress response in French bean (*Phaseolus vulgaris*). *Australian Journal of Crop Science* **2**(2), 40-48.

Ng, S., De Clercq, I., Van Aken, O., Law, S. R., Ivanova, A., Willems, P., Giraud, E., Van Breusegem, F. & Whelan, J. (2014). Anterograde and retrograde regulation of nuclear genes encoding mitochondrial proteins during growth, development, and stress. *Molecular Plant* **7,** 1075-1093. DOI:10.1093/mp/ssu037.

Ng, S., Ivanova, A., Duncan, O., Law, S. R.,Van Aken, O., De Clercq, I., Wang, Y., Carrie, C., Xu, L., Kmiec, B., Walker, H., Van Breusegem, F., Whelan, J. & Giraud, E. (2013). A membrane-bound NAC transcription factor, ANAC017, mediates mitochondrial retrograde signaling in Arabidopsis. *The Plant Cell* **25,** 3450-3471. DOI: 10.1105/tpc.113.113985.

Nick, P., Heuing, A. & Ehmann, B. (2000). Plant chaperonins: a role in microtubule-dependent wall formation? *Protoplasma* **211,** 234-244. DOI: 10.1007/BF01304491.

Nieves-Cordones, M., Aleman, F., Martinez, V. & Rubio, F. (2010). The *Arabidopsis thaliana* HAK5 K^+ transporter is required for plant growth and K^+ acquisition from Low K^+ solutions under saline conditions. *Molecular Plant* **3**(2), 326-333. DOI : 10.1093/mp/ssp102.

Noctor, G., De Paepe, R., & Foyer, C. H. (2007). Mitochondrial redox biology and homeostasis in plants. *TRENDS in Plant Science* **12**(3), 125-134. DOI: 10.1016/j.tplants.2007.01.005.

Noctor, G. & Foyer, C.H. (1998). Ascorbate and Glutathione: keeping active oxygen under control. *Annu. Rev. Plant Physiol. Plant Mol. Biol.* **49,** 249-279. DOI:10.1146/annurev.arplant.49.1.249.

Nongpiur, R. C., Singla-Pareek, S. L. & Pareek, A. (2016). Genomics approaches for improving salinity stress tolerance in crop plants. *Current Genomics* **17,** 343-357. DOI:10.2174/1389202917666160331202517.

Olivos, H. J., Alluri, P.G., Reddy, M. M., Salony, D. & Kodadek, T. (2002). Microwave-Assisted Solid-Phase Synthesis of Peptoids. *Org. Lett.* **4**(23), 4057-4059. DOI: 10.1021/ol0267578.

Oren, A. (1999). Bioenergetic aspects of halophilism. *Microbiology and Molecular Biology Review* **63**(2), 334-348.

Overmyer, K., Brosche, M. & Kangasjärvi, J. (2003). Reactive oxygen species and hormonal control of cell death. *TRENDS in Plant Science* **8**(7), 335-342**.** DOI: 10.1016/S1360-1385(03)00135-3.

Pardo, A., Amato, M. & Chiaranda, F. Q. (2000). Relationships between soil structure, root distribution and water uptake of chickpea (*Cicer arietinum* L.). plant growth and water distribution. *European Journal of Agronomy* **13,** 39-45.DOI: PII: S1161-0301(00)00056-3.

Park, S-W., Li, W., Viehhauser, A., He, B., Kim, S., Nilsson, A. K., Andersson, M. X., Kittle, J. D., Ambavaram, M. M. R., Luan, S., Esker, A. R., Tholl, D., Cimini, D., Ellerström, M., Coaker, G., Mitchell, T. K., Pereira, A., Dietz, K-J. & Lawrence, C. B. (2013). Cyclophilin 20-3 relays a 12-oxo-phytodienoic acid signal during stress responsive regulation of cellular redox homeostasis. *PNAS* **110**(23), 9559-9564. DOI :10.1073/pnas.1218872110.

Pastore, D., Trono, D., Laus, M. N., Di Fonzo, N. & Flagella, Z. (2007). Possible plant mitochondria involvement in cell adaptation to drought stress. A case study: durum wheat mitochondria. *Journal of Experimental Botany* **58**(2), 195-210. DOI:10.1093/jxb/erl273.

Paulsen, C. E. & Carroll, K. S. (2010). Orchestrating redox signaling networks through regulatory cysteine switches. *ACS Chem Biol*. **5**(1), 47-62. DOI: 10.1021/cb900258z.

Pauwels, L., Inze, D. & Goossens, A. (2009). Jasmonate-inducible gene: what does it mean? *Trends in Plant Science* **14**(2), 87-91. DOI: 10.1016/j.tplants.2008.11.005.

Petrillo, E., Herz, M. A. G., Fuchs, A., Reifer, D., Fuller, J., Yanovsky, M. J., Simpson, C., Brown, J. W. S., Barta, A., Kalyna, M. & Kornblihtt, A. R. (2014). A chloroplast retrograde signal regulates nuclear alternative splicing. *Science* **344**(6182), 427-430. DOI: 10.1126/science.1250322.

Pfannschmidt, T., Nilsson, A. & Allen, J. F. (1999). Photosynthetic control of chloroplast gene expression. *Nature* **397,** 625-628. DOI: 10.1038/17624.

Platten, J. D., Cotsaftis, O., Berthomieu, P., Bohnert, H., Davenport, R. J., Fairbairn, D. J., Horie, T., Leigh, R. A., Lin, H-X., Luan, S., Mäser, P., Pantoja, O., Rodriguez-Navarro, A., Schachtman, D. P., Schroeder, J. I., Sentenac, H., Uozumi, N., Very, A-A., Zhu, J-K., Dennis, E. S. & Tester, M. (2006). Nomenclature for HKT transporters, key determinants of plant salinity tolerance. *TRENDS in Plant Science* **11**(8), 372-374. DOI: 10.1016/j.tplants.2006.06.001.

Plaut, Z., Edelstein, M. & Ben-Hur, M. (2013). Overcoming salinity barriers to crop production using traditional methods. *Critical Reviews in Plant Sciences* **32** (4), 250-291. DOI**:**10.1080/07352689.2012.752236.

Poyton, R. O., Ball, K. A. & Castello, P.R. (2009). Mitochondrial generation of free radicals and hypoxic signaling. *Trends in Endocrinology and Metabolism* **20** (7), 332-340. DOI: 10.1016/j.tem.2009.04.001.

PPI (1998). Potassium: An essential plant food nutrient. *Better Crops* **82**(3),1-39.

Prakash, S., Sunitha, J. & Hans, M. (2010). Role of coenzyme Q10 as an antioxidant and bioenergizer in periodontal diseases. *Indian Journal of Pharmacology* **42**(6), 334-337. DOI: 10.4103/0253-7613.71884.

Price, A. H., Taylor, A., Ripley, S. J., Griffiths, A., Ttewavas, A. J. & Knight, M. R. (1994). Oxidative signals in tobacco increase cytosolic calcium. *The Plant Cell* **6,**1301-1310. DOI : 10.2307/3869827.

Qiu,Q-S., Barkla, B. J., Vera-Estrella, R., Zhu,J-K. & Schumaker, K.S. (2003). Na^+/H^+ exchange activity in the plasma membrane of Arabidopsis. *Plant Physiology* **132,** 1041-1052.DOI: 10.1104/pp.102.010421.

Qiu, Q-S., Guo, Y., Quintero, F. J., Pardo, J. M., Schumaker, K. S. & Zhu, J-K. (2004). Regulation of vacuolar Na^+/H^+ exchange in *Arabidopsis thaliana* by the salt-overly-sensitive (SOS) pathway. *The Journal of Biological Chemistry* **279**(1), 207-2015. DOI: 10.1074/jbc.M307982200.

Quijano, C., Hernandez-Saavedra, D., Castro, L., McCord, J. M., Freeman, B. A. & Radi, R. (2001). Reaction of Peroxynitrite with Mn-Superoxide Dismutase. *The Journal of Biological Chemistry* **276**(15), 11631-11638. DOI : 10.1074/jbc.M009429200.

Rahnama, A., James, R. A., Poustini, K. & Munns, R. (2010). Stomatal conductance as a screen for osmotic stress tolerance in durum wheat growing in saline soil. *Functional Plant Biology* **37**, 255-263. DOI: 10.1071/FP09148.

Rasmusson, A. G., Geisler, D. A. & Møller, I. M. (2008). The multiplicity of dehydrogenases in the electron transport chain of plant mitochondria. *Mitochondrion* **8,** 47-60. DOI: 10.1016/j.mito.2007.10.004.

Redondo-Horcajo, M., Romero, N., Martinez-Acedo, P., Martinez-Ruiz, A., Quijano, C., Lourenc, C. F., Movilla, N., Enriquez, J. A., Rodriguez-Pascual, F., Rial, E., Radi, R., Vazquez, J. & Lamas, S. (2010). Cyclosporine A-induced nitration of tyrosine 34 MnSOD in endothelial cells: role of mitochondrial superoxide. *Cardiovascular Research* **87,** 356-365. DOI:10.1093/cvr/cvq028.

Rengasamy, P. (2006). World salinization with emphasis on Australia. *Journal of Experimental Botany* **57**(5), 1017-1023. DOI: 10.1093/jxb/erj108.

Rhoads, D. M., Umbach, A. L., Subbaiah, C. C. & Siedow, J. N. (2006). Mitochondrial reactive oxygen species. contribution to oxidative stress and interorganellar signaling. *Plant Physiology* **141,** 357-366. DOI: 10.1104/pp.106.079129.

Riemann, M., Dhakarey, R.,Hazman, M., Miro, B., Kohli, A. & Nick, P. (2015). Exploring jasmonates in the hormonal network of drought and salinity responses. *Frontiers in Plant Science* **6**(1077), 1-16. DOI: 10.3389/fpls.2015.01077

Riemann, M., Haga, K., Shimizu, T., Okada, K., Ando, S., Mochizuki, S., Nishizawa, Y., Yamanouchi, U., Nick, P., Yano, M., Minami, E., Takano, M., Yamane, H., & Iino, M. (2013). Identification of rice Allene Oxide Cyclase mutants and the function of jasmonate for defence against *Magnaporthe oryzae. The Plant Journal* **74,** 226-238. DOI: 10.1111/tpj.12115.

Riemann, M., Müller, A., Korte,A., Furuya, M., Weiler, E. W. & Nick, P. (2003). Impaired induction of the jasmonate pathway in the rice mutant *hebiba. Plant Physiology* **133,** 1820-1830. DOI. 10.1104/pp.103.027490

Rolland, A. (2006). Nuclear gene delivery: the Trojan horse approach. *Expert Opin. Drug Deliv.* **3**(1), 1-10. DOI: 10.1517/17425247.3.1.1.

Rothbard, J. B., Jessop, T. C. & Wender, P. A. (2005). Adaptive translocation: the role of hydrogen bonding and membrane potential in the uptake of guanidinium-rich transporters into cells. *Advanced Drug Delivery Reviews* **57,** 495-504. DOI: 10.1016/j.addr.2004.10.003.

Roy, S. J., Negrao, S. &Teste, M. (2014). Salt resistant crop plants. *Current Opinion in Biotechnology* **26,** 115-124. DOI: 10.1016/j.copbio.2013.12.004.

Rudat, B., Birtalan, E., Thome, I., Kölmel, D. K., Horhoiu, V. L., Wissert, M. D., Lemmer, U., Eisler, H-J., Balaban, T. S. & Bräse, S. (2010). Novel pyridinium dyes that enable investigations of peptoids at the single-molecule level. *J. Phys. Chem. B.* **114,** 13473-13480. DOI: 10.1021/jp103308s.

Rydström, A., Deshayes, S., Kojate, K., Crombez, L., Padari, K., Boukhaddaoui, H., Aldrian, G., Pooga, M. & Divita, G. (2011). Direct translocation as major cellular uptake for CADY self-assembling peptide-based nanoparticles. *PLoSE ONE* **6**(10), 1-9. DOI: 10.1371/journal.pone.0025924.

Sairam, R. K & Tyagi, A. (2004). Physiology and molecular biology of salinity stress tolerance in plants. *Current Science* **86** (3), 407-421.

Samota, M. K., Bhatt, L., Garg, N. & Geat, N. (2017). Defense Induced by Jasmonic Acid: A Review. *Int.J.Curr.Microbiol.App.Sci* ***6***(5), 2467-2474.DOI: 10.20546/ijcmas.2017.605.276.

Sano, T., Higaki, T., Oda, Y., Hayashi, T. & Hasezawa, S. (2005). Appearance of actin microfilament 'twin peaks' in mitosis and their function in cell plate formation, as visualized in tobacco BY-2 cells expressing GFP-fimbrin. *Plant J.* **44,** 595-605. DOI: 10.1111/j.1365-313X.2005. 02558.x.

Schaller, F., Biesgen, C., Müssig, C., Altmann, T. & Weiler, E. W. (2000). 12-Oxophytodienoate reductase 3 (OPR3) is the isoenzyme involved in jasmonate biosynthesis. *Planta* **210,** 979-984. DOI: 10.1007/s004250050706.

Schaller, F., Hennig, P. & Weiler, E. W. (1998). 12-Oxophytodienoate-10,11-Reductase: Occurrence of Two Isoenzymes of Different Specificity against Stereoisomers of 12-Oxophytodienoic Acid. *Plant Physiol.* **118,** 1345-1351. DOI: 10.1104/pp.118.4.1345.

Schaller, F. & Weiler, E. W. (1997). Molecular Cloning and Characterization of 12-Oxophytodienoate Reductase, an Enzyme of the Octadecanoid Signaling Pathway from *Arabidopsis thaliana. The Journal of Biological Chemistry* **272**(44), 28066-28072. DOI: 10.1074/jbc.272.44.28066.

Schröder, T., Niemeier, N., Afonin, S., Ulrich, A. S., Krug, H. F. & Bräse: S. (2008). Peptoidic amino- and guanidinium-carrier systems: Targeted drug delivery into the cell cytosol or the nucleus. *J. Med. Chem.* **51,** 376-379. DOI: 10.1021/jm070603m.

Schröder, T., Schmitz, K., Niemeier, N., Balaban, T. S., Krug, H. F., Schepers, U. & Bräse, S. (2007). Solid-phase synthesis, bioconjugation, and toxicology of novel cationic oligopeptoids for cellular drug delivery. *Bioconjugate Chem.***18,** 342-354. DOI: 10.1021/bc0602073.

Schwarzländer, M., König, A-C., Sweetlove, L.J. & Hinkemeyer, I. (2012). The impact of impaired mitochondrial function on retrograde signalling: a meta-analysis of transcriptomic responses. *Journal of Experimental Botany* **63**(4), 1735-1750. DOI:10.1093/jxb/err374.

Seo, J-S., Joo, J., Kim, M-J., Kim, Y-K., Nahm, B. H., Song, S. I., Cheong, J-J., Jong Seob Lee, J. S., Kim, J-K. & Choi, Y. D. (2011). OsbHLH148, a basic helix-loop-helix protein, interacts with OsJAZ proteins in a jasmonate signaling pathway leading to drought tolerance in rice. *The Plant Journal* **65,** 907-921. DOI: 10.1111/j.1365-313X.2010.04477. x.

Sewelam, N., Jaspert, N., Van Der Kelen, K., Tognetti, V. B., Schmitz, J., Frerigmann, H., Stahl E., Zeier, J., Van Breusegem , F. & Maurino, V. G. (2014). Spatial H_2O_2 signaling specificity: H_2O_2 from chloroplasts and peroxisomes modulates the plant transcriptome differentially. *Molecular Plant* **7,** 1191-1210. DOI:10.1093/mp/ssu070.

Sharma, M. & Laxmi, A. (2016). Jasmonates: Emerging players in controlling temperature stress tolerance. *Frontiers in Plant Science* **6**(1129), 1-10. DOI: 10.3389/fpls.2015.01129.

Sharma, P., Jha, A. B., Dubey, R. S. & Pessarakli, M. (2012). Reactive oxygen species, oxidative damage, and antioxidative defense mechanism in plants under stressful conditions. *Journal of Botany* **2012,** 1-26. DOI:10.1155/2012/217037.

Shi, H., Ishitani,M., Kim, C. & Zhu, J-K. (2000). The Arabidopsis thaliana salt tolerance gene SOS1 encodes a putative Na^+/H^+ antiporter. *PNAS* **97**(12), 6896-6901. DOI: 10.1073/pnas.120170197.

Simon, R. J., Kania, R. S., Zuckermann, R. N., Huebner, V. D., Jewell, D. A., Banville, S., Ng., S., Wang, L., Rosenberg., S., Marlowe, C., Spellmeyer, D. C., Tans, R., Frankel, A. D., Santi, D. V., Cohen, F. E. and Bartletts, P. A. (1992). Peptoids: A modular approach to drug discovery. *Proc. Nad. Acad. Sci. USA* **89,** 9367-9371. DOI : 10.1073/pnas.89.20.9367.

Simpson, L. S., Burdine, L., Dutta, A. K., Feranchak, A. P. & Kodadek, T. (2009). Selective Toxin Sequestrants for the Treatment of Bacterial Infections. *J. Am. Chem. Soc.* **131,** 5760-5762. DOI: 10.1021/ja900852k.

Singh, D. & Roy, K. B. (2015). Salt stress affects mitotic activity and modulates antioxidant systems in onion roots. *Braz. J. Bot* 1-10. DOI: 10.1007/s40415-015-0216-0.

Singh, T., Murthy, A. S. N., Yang, H-J. & Im, J. (2018). Versatility of cell-penetrating peptides for intracellular delivery of siRNA. *Drug Delivery* **25**(1), 2005-2015. DOI:10.1080/10717544.2018.1543366

Smirnoff, N. (2000). Ascorbic acid: metabolism and functions of a multi-facetted molecule. *Current Opinion in Plant Biology* **3,** 229-235. DOI:10.1016/S1369-5266(00)00069-8.

Sreenivasulu, N., Harshavardhan, V. T., Govind, G., Seiler, C. & Kohli, A. (2012). Contrapuntal role of ABA: Does it mediate stress tolerance or plant growth retardation under long-term drought stress? *Gene* **506,** 265-273. DOI: 10.1016/j.gene.2012.06.076.

Stefely, J.A. & Pagliarini, D. J. (2017). Biochemistry of Mitochondrial Coenzyme Q Biosynthesis. *Trends Biochem Sci.* **42**(10), 824-843. DOI: 10.1016/j.tibs.2017.06.008.

Straßner, J., Fürholz, A., Macheroux, P., Amrhein, N. & Schaller, A. (1999). A homolog of old yellow enzyme in tomato. *The Journal of Biological Chemistry* **274**(49), 35067-35073. DOI: 10.1074/jbc.274.49.35067.

Sun, J., Dai, S., Wang, R., Chen, S., Li, N., Zhou, X., Lu, C., Shen, X., Zheng, X., Hu, Z., Zhang, Z., Song, J. & Xu, Y. (2009). Calcium mediates root K^+/Na^+ homeostasis in poplar species differing in salt tolerance. *Tree Physiology* **29,** 1175-1186. DOI:10.1093/treephys/tpp048.

Sun,Y-H., Hung, C-Y., Qiu, J., Chen, J., Kittur., F. S., Oldham, C. E., Henny, R.J., Burkey, K. O., Fan, L. & Xie,J. (2017). Accumulation of high OPDA level correlates with reduced ROS and elevated GSH benefiting white cell survival in variegated leaves. *Sci. Rep.* **7,** 1-16. DOI: 10.1038/srep44158.

Sunkar, R., Kapoor, A. & Zhu, J-K. (2006). Posttranscriptional induction of two Cu/Zn superoxide dismutase genes in Arabidopsis is mediated by downregulation of miR398 and important for oxidative stress tolerance. *The Plant Cell* **18,** 2051-2065. DOI: 10.1105/tpc.106.041673.

Suzuki, K., Okada, K., Kamiya, Y., Zhu, X. F., Nakagawa, T., Kawamukai, M. & Matsuda, H. (1997). Analysis of the decaprenyl diphosphate synthase (dps) gene in fission yeast suggests a role of ubiquinone as antioxidant. *J. Biochem.* **121,** 496-505. DOI: 10.1093/oxfordjournals.jbchem.a021614.

Szeto, H. H. (2006). Cell-permeable, mitochondrial-targeted, peptide antioxidants. *The AAPS Journal **8***(2), E277-E283. DOI:10.1007/BF02854898.

Takahashi, H., Kopriva, S., Giordano, M., Saito, K. & Hell, R. (2011). Sulfur assimilation in photosynthetic organisms: molecular functions and regulations of transporters and assimilatory enzymes. *Annu. Rev. Plant Biol.* **62,** 157-184. DOI:10.1146/annurev-arplant-042110-103921.

Takahashi, S., Ogiyama, Y., Kusano, H., Shimada, H., Kawamukai, M. & Kadowaki, K-I. (2006). Metabolic engineering of coenzyme Q by modification of isoprenoid side chain in plant. *FEBS Letters* **580,** 955-959. DOI: 10.1016/j.febslet.2006.01.023.

Taki, N., Sasaki-Sekimoto, Y., Obayashi, T., Kikuta, A., Kobayashi, K., Ainai, T., Yagi, K., Sakurai, N., Suzuki, H., Masuda, T., Takamiya, K-I., Shibata, D., Kobayashi, Y. & Ohta, H. (2005). 12-oxo-phytodienoic acid triggers expression of a distinct set of genes and plays a role in wound-induced gene expression in Arabidopsis. *Plant Physiology* **139,** 1268-1283. DOI: 10.1104/pp.105.067058.

Tan, N. C., Yu, P., Kwon, Y-U. & Kodadek, T. (2008). High-throughput evaluation of relative cell permeability between peptoids and peptides. *Bioorganic & Medicinal Chemistry* **16**, 5853-5861. DOI: 10.1016/j.bmc.2008.04.074.

Tani, T., Sobajima, H., Okada, K., Chujo, T., Arimura, S-I., Tsutsumi, N., Nishimura, M., Seto, H., Nojiri, H. & Yamane, H. (2008). IdentiWcation of the *OsOPR7* gene encoding 12-oxophytodienoate reductase involved in the biosynthesis of jasmonic acid in rice. *Planta* **227**, 517-526. DOI: 10.1007/s00425-007-0635-7.

Teh, S.Y. & Koh, H. L. (2016). Climate change and soil salinization: Impact on agriculture, water and food security. *International Journal of Agriculture, Forestry and Plantation* **2,** 1-9.

Teixeira de Mattos, M. J. & Neijssel, O. M. (1997). Bioenergetic consequences of microbial adaptation to low-nutrient environments. *Journal of Biotechnology* **59,** 117-126. DOI: 10.1016/S0168-1656(97)00174-0.

Theodoulou, F. L., Job, K., Slocombe, S. P., Footitt, S., Holdsworth, M., Baker, A., Larson, T. R. & Graham, I. A. (2005). Jasmonic acid levels are reduced in COMATOSE ATP-Binding Cassette transporter mutants. Implications for transport of jasmonate precursors into peroxisomes. *Plant Physiology* **137,** 835-840. DOI: 10.1104/pp.105.059352.

Thines, B., Katsir, L., Melotto, M., Niu, Y., Mandaokar, A., Liu, G., Nomura, K., He, S. Y., Howe, G. A. & Browse, J. (2007). JAZ repressor proteins are targets of the SCFCOI1 complex during jasmonate signaling. *Nature* **448,** 661-666. DOI: 10.1038/nature05960.

Toda, Y., Tanaka, M., Ogawa, D., Kurata, K., Kurotani, K-I., Habu, Y., Ando, T., Sugimoto, K., Mitsuda, N., Katoh, E., Abe, K., Miyao, A., Hirochika, H., Hattori, T., & Takeda, S. (2013). RICE SALT SENSITIVE3 forms a ternary complex with JAZ and class-C bHLH factors and regulates jasmonate-induced gene expression and root cell elongation. *The Plant Cell* **25,** 1709-1725. DOI: 10.1105/tpc.113.112052.

Tomemori, H., Hamamura, K. & Tanabe, K. (2002). Interactive Effects of Sodium and Potassillm on. the Growth and Photosynthesis of Spinach and Konnatsuna. *Plant Prod. Sci.* **5**(4), 281-285. DOI: 10.1626/pps.5.281.

Torchilin, V. P. (2007). Tatp-mediated intracellular delivery of pharmaceutical nanocarriers. *Biochemical Society Transactions* **35**(4), 816-820. DOI: 10.1042/BST0350816.

Trotter, E. W., Collinson, E. J. Dawes, I. W. & Grant, C. M. (2006). Old yellow enzymes protect against acrolein toxicity in the yeast *Saccharomyces cerevisiae*. *Applied and Environmental Microbiology* **72**(7), 4885-4892. DOI: 10.1128/AEM.00526-06.

Turrens, J. F. (2003). Mitochondrial formation of reactive oxygen species. *J Physiol* **552**(2), *335*-344. DOI: 10.1113/jphysiol.2003.049478.

Turunen, M., Olsson, J. & Dallner, G. (2004). Metabolism and function of coenzyme Q. *Biochimica et Biophysica Acta* **1660,** 171-199. DOI: 10.1016/j.bbamem.2003.11.012.

Tuteja, N. (2007). Mechanisms of high salinity tolerance in plants. *Methods in Enzymology* **428,** 419-438. DOI: 10.1016/S0076-6879(07)28024-3.

Udugamasooriya, D. G., Dineen, S. P., Brekken, R. A. & Kodadek, T. (2008). A Peptoid "Antibody surrogate" that antagonizes VEGF receptor 2 activity. *J. Am. Chem. Soc.* **130,** 5744-5752. DOI: 10.1021/ja711193x.

Udugamasooriya, G. (2013). Peptoids: An emerging class of peptidomimetics for cancer therapy and diagnostics. *J. Biomol. Res. Ther.* **3,** 1-3. DOI: 10.4172/2167-7956.1000e121.

Ueda, J., Miyamoto, K. & Aoki, M. (1994). Jasmonic acid inhibits the IAA-induced elongation of oat coleoptile segments: A possible mechanism involving the metabolism of cell wall polysaccharides. *Plant Cell Physiol.* **35**(7), 1065-1070.

Van Gestel, K., Köhler, R.H. and Verbelen, J.P. (2002). Plant mitochondria move on F-actin, but their positioning in the cortical cytoplasm depends on both F-actin and microtubules. *Journal of Experimental Botany* **53,** 659-667. DOI: 10.1093/jexbot/53.369.659.

Varela-López A., Bullón, P., Giampieri, F. & Quiles, J. L. (2015). Non-nutrient, naturally occurring phenolic compounds with antioxidant activity for the prevention and treatment of periodontal diseases. *Antioxidants* **4,** 447-481. DOI :10.3390/antiox4030447.

Varela-López, A., Giampieri, F., Battino, M. & Quiles, J. L. (2016). Coenzyme Q and Its Role in the Dietary Therapy against Aging. *Molecules* **21 (**373), 1-26. DOI:10.3390/molecules21030373.

Velitchkova, M. & Fedina, I. (1998). Response of photosynthesis of *Pisum sativum* to salt stress as affected by methyl jasmonate. *Photosynthetica* **35**(1), 89-97. DOI: 10.1023/A:1006878016556.

Verbruggen, N. & Hermans, C. (2008). Proline accumulation in plants: a review. *Amino Acids* **35,**753-759. DOI: 10.1007/s00726-008-0061-6.

Wadia, J. S., Stan, R. V. & Dowdy, S. F. (2004). Transducible TAT-HA fusogenic peptide enhances escape of TAT-fusion proteins after lipid raft micropinocytosis. *Nature Medicine* **10**(3), 310-315. DOI:10.1038/nm996.

Wagner, S., Aken O, V., Elsässer, M.& Schwarzländer, M. (2018). Mitochondrial energy signaling and its role in the low-oxygen stress response of plants. *Plant Physiol* **176**, 1156-1170. DOI:10.1104/pp.17.01387.

Wagstaff, K. M. & Jans, D. A. (2006). Protein transduction: Cell penetrating peptides and their therapeutic application. *Current Medicinal Chemistry* **13,** 1371-1387. DOI: 10.2174/092986706776872871

Walia, H., Wilson, C., Condamine, P., Liu, X., Ismail, A. M. & Close, T. J. (2007). Large-scale expression profiling and physiological characterization of jasmonic acid-mediated adaptation of barley to salinity stress. *Plant, Cell and Environment* **30**, 410-421. DOI: 10.1111/j.1365-3040.2006.01628. x.

Wang, B., Lüttge, U., Ratajczak, R. (2001). Effects of salt treatment and osmotic stress on V-ATPase and V-PPase in leaves of the halophyte Suaeda salsa. *Journal of Experimental Botany* **52**(365), 2355-2365. DOI: 10.1093/jexbot/52.365.2355.

Wang, H., Wu, Z., Chen, Y., Yang, C. & Shi, D. (2011). Effects of salt and alkali stresses on growth and ion balance in rice (Oryza sativa L.). *Plant Soil Environ.* **57**(6), 286-294. DOI :10.17221/36/2011-PSE.

Wang, J., Zuo, K., Wu, W., Song, J., Sun, X., Lin, J., Li, X. & Tang, K. (2004). Expression of a novel antiporter gene from *Brassica napus* resulted in enhanced salt tolerance in transgenic tobacco plants. *Biologia Plantarum* **48**(4), 509-515. DOI:10.1023/B: BIOP.0000047145. 18014.a3.

Wang, J.Q., Cai, Y., Miao, Y.S., Lam, Sh.K., Jiang, L.W. (2009). Wortmannin induces homotypic fusion of plant prevacuolar compartments. *Journal of Experimental Botany* **60,** 3075-3083. DOI:10.1093/jxb/erp136.

Wang, Y. R., Kang, S. Z., Li, F. S., Zhang, L. & Zhang, J. H. (2007). Saline water irrigation scheduling through a crop-water-salinity production function and a soil-water-salinity dynamic model. *Pedosphere* **17**(3), 303-317. DOI: 10.1016/S1002-0160(07)60037-X.

Wani, S. H., Kumar, V., Shriram, V. & Sah, S. K. (2016). Phytohormones and their metabolic engineering for abiotic stress tolerance in crop plants. *The Crop Journal* 162-176. DOI: 10.1016/j.cj.2016.01.010.

Wasternack, C. (2007). Jasmonates: An update on biosynthesis, signal transduction and action in plant stress response, growth and development. *Annals of Botany* **100,** 681-697. DOI:10.1093/aob/mcm079.

Webster, A. M. & Cobb, S. L. (2018). Recent advances in the synthesis of peptoid macrocycles. *Chem. Eur. J.* **24,** 7560-7573. DOI: 10.1002/chem.201705340.

Weissig, V. (2005). Targeted drug delivery to mammalian mitochondria in living cells. *Expert Opin. Drug Deliv.* **2**(1), 89-102. DOI: 10.1517/17425247.2.1.89.

Wender, A. P., Mitchell, J. D., Pattabiraman, K., Pelkey, T. E., Steinman, L. and Rothbard, B.J. (2000). The design, synthesis, and evaluation of molecules that enable or enhance cellular uptake: Peptoid molecular transporters. *PNAS* **97,** 13003-13008. DOI:10.1073/pnas.97.24.13003.

West, G., Inze, D. & Beemster, S. T. G. (2004). Cell cycle modulation in the response of the primary root of arabidopsis to salt stress. *Plant Physiology* **135,** 1050-1058. DOI:10.1104/pp.104.040022.

Weydert, J. C. & Cullen, J.J. (2010). Measurement of superoxide dismutase, catalase and glutathione peroxidase in cultured cells and tissue. *Nature Protocols* **5,** 51-66. DOI:10.1038/nprot.2009.197.

Winkel-Shirley, B. (2002). Biosynthesis of flavonoids and effects of stress. *Current Opinion in Plant Biology* **5,**218-223. DOI: 10.1016/S1369-5266(02)00256-X.

Wong, V. N. L., Greene, R.S. B., Murphy, B. W., Dalal, R. & Mann, S. (2005). Decomposition of added organic material in salt affected soils. *In: Regolith 2005 – Ten Years of CRC LEME (*Roach I.C. ed*),* pp. 333-337.

Wong, V. N. L., Greene, R. S. B., Murphy, B.W., Dalal, R., Mann, S. & Farquhar, G. (2006). The effects of salinity and sodicity on soil organic carbon stocks and fluxes: An overview. *REGOLITH 2006 Proceedings: Consolidation and Dispersion of Ideas, 367-371.*

Wu, C. W., Sanborn, T. J., Huang, K., Zuckermann, R. N. & Barron, A. E. (2001). Peptoid oligomers with R-chiral, aromatic side chains: Sequence requirements for the formation of stable peptoid helices. *J. Am. Chem. Soc.* **123***,* 6778-6784. DOI: 10.1021/ja003154n.

Yan, N., Marschner, P., Cao, W., Zuo, C. & Qin, W. (2015). Influence of salinity and water content on soil microorganisms. *International Soil and Water Conservation Research* **3,** 316-323. DOI: 10.1016/j.iswcr.2015.11.003.

Yano, T., Aydin, M. & Haraguchi, T. (2007). Impact of climate change on irrigation demand and crop growth in a mediterranean environment of Turkey. *Sensors* **7,** 2297-2315. DOI : 10.3390/s7102297.

Ye, H., Du, H., Tang, N., Li, X. & Xiong, L. (2009). Identification and expression profiling analysis of TIFY family genes involved in stress and phytohormone responses in rice. *Plant Mol. Biol.* **71,** 291-305. DOI: 10.1007/s11103-009-9524-8.

Yeo, A. R., Yeo, M. E. & Flowers, T. J. (1987). The contribution of an apoplastic pathway to sodium uptake by rice roots in saline conditions. *Journal of Experimental Botany* **38**(192), 1141-1153. DOI: 10.1093/jxb/38.7.1141.

Yoon, J. Y., Hamayun, M., Lee, S-K. & Lee, I-J. (2009). Methyl jasmonate alleviated salinity stress in soybean. *J. Crop Sci. Biotech.* **12**(2), 63-68. DOI: 10.1007/s12892-009-0060-5.

Yoshizumi, T., Oikawa, K., Chuah, J., Kodama, Y. and Numata, K. (2018). Selective Gene Delivery for Integrating Exogenous DNA into Plastid and Mitochondrial Genomes Using Peptide-DNA Complexes. *Biomacromolecules* **19**, 1582-1591. DOI : 10.1021/acs.biomac.8b00323.

Yu, L., Yang, F-D. & Yu, C-A. (1985). Interaction and identification of ubiquinone-binding proteins in ubiquinol-cytochrome **c** reductase by azido-ubiquinone derivatives. *The Journal of Biological Chemistry* **260**(2), 963-973.

Yu, P., Liu, B., & Kodadek, T. (2005). A high-throughput assay for assessing the cell permeability of combinatorial libraries. *Nature Biotechnology* **23**(6), 746-751. DOI:10.1038/nbt1099.

Yumurtaci, A., Aydin, Y., Uncuoglu, A.A. (2009). Cytological changes in Turkish durum and bread wheat genotypes in response to salt stress. *Acta Biologica Hungarica* **60** (2), 221-232. DOI:10.1556/ABiol.60.2009.2.9.

Ziegler, A. (2008). Thermodynamic studies and binding mechanisms of cell-penetrating peptides with lipids and glycosaminoglycans. *Advanced Drug Delivery Reviews* **60,** 580-597. DOI: 10.1016/j.addr.2007.10.005.

Zhang, H., Zhang, Q., Zhai, H., Li, Y., Wang, X., Liu, Q. & He, S. (2017). Transcript profle analysis reveals important roles of jasmonic acid signalling pathway in the response of sweet potato to salt stress. *Sci. Rep.* **7,** 1-12. DOI: 10.1038/srep40819.

Zhang, H-X., Hodson, J. N., Williams, J. P. & Blumwald, E. (2001). Engineering salt-tolerant Brassica plants: Characterization of yield and seed oil quality in transgenic plants with increased vacuolar sodium accumulation. *PNAS* **98**(22), 12832-12836. DOI:10.1073/pnas.231476498.

Zhao, K., Luo, G., Zhao, G-M., Schiller, P. W. & Szeto, H. H. (2003). Transcellular transport of a highly polar 3+ net charge opioid tetrapeptide. *JPET* **304** (1), 425-432. DOI: 10.1124/jpet.102.040147.

Zhao, Y., Dong, W., Zhang, N., Ai, X., Wang, M., Huang, Z., Xiao, L. & Xia, G. (2014). A wheat allene oxide cyclase gene enhances salinity tolerance via jasmonate signaling. *Plant Physiology* **164,** 1068-1076. DOI: 10.1104/pp.113.227595.

Zheng,Y., Jia, A., Ning, T., Xu, J., Li, Z. & Jiang, G. (2008). Potassium nitrate application alleviates sodium chloride stress in winter wheat cultivars differing in salt tolerance. *Journal of Plant Physiology* **165,** 1455-1465. DOI: 10.1016/j.jplph.2008.01.001.

Zhu, J-K. (2001). Plant salt tolerance. *TRENDS in Plant Science* **6(**2), 66-71. DOI: PII: S1360-1385(00)01838-0.

Zhu, J-K. (2002). Salt and drought stress signal transduction in plants. *Annu. Rev. Plant Biol.* **53,** 247-273. DOI: 10.1146/annurev.arplant.53.091401.143329.

Zhu, J-K. (2003). Regulation of ion homeostasis under salt stress. *Current Opinion in Plant Biology* **6,** 441-445. DOI:10.1016/S1369-5266(03)00085-2.

Zuckermann, R. N., Kerr, J. M., Kent, S. B. H. & Moos, W. H. (1992). Efficient method for the preparation of peptoids [Oligo (N-substituted glycines)] by submonomer solid-phase synthesis. *J. Am. Chem. SOC.* **114,** 10646-10647. DOI:10.1021/ja00052a076.

7. Appendix

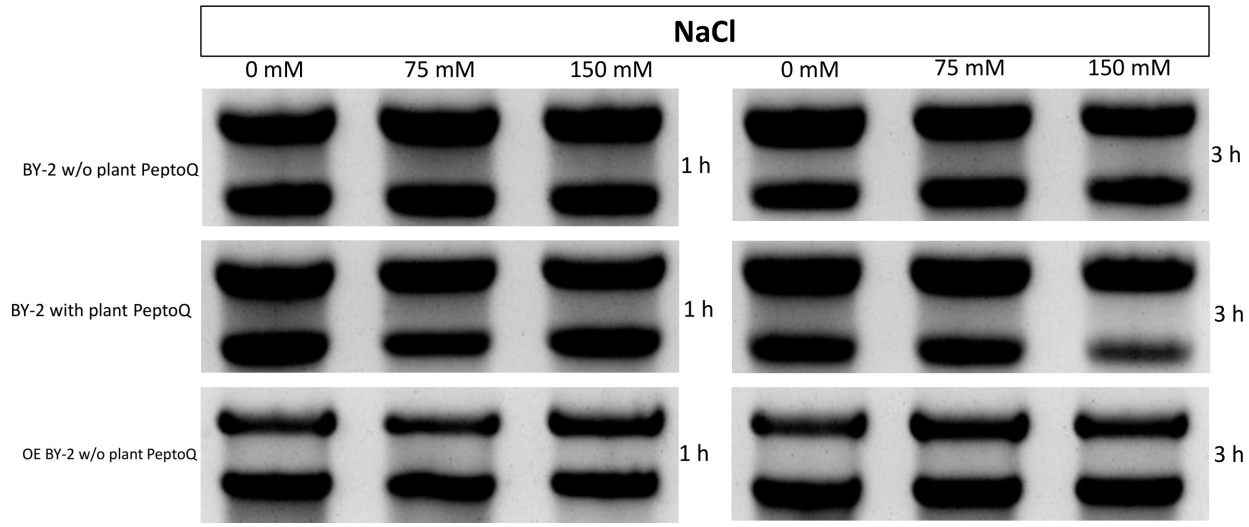

Supplementary Figure S1: Agarose gel images of total RNA extracted from salt stressed (0, 75 and 150 mM NaCl) non-transformed WT with and without plant PeptoQ pretreatment, and OE BY-2 cells without plant PeptoQ pretreatment. In each case, one representative example out of three independent experiments is shown.

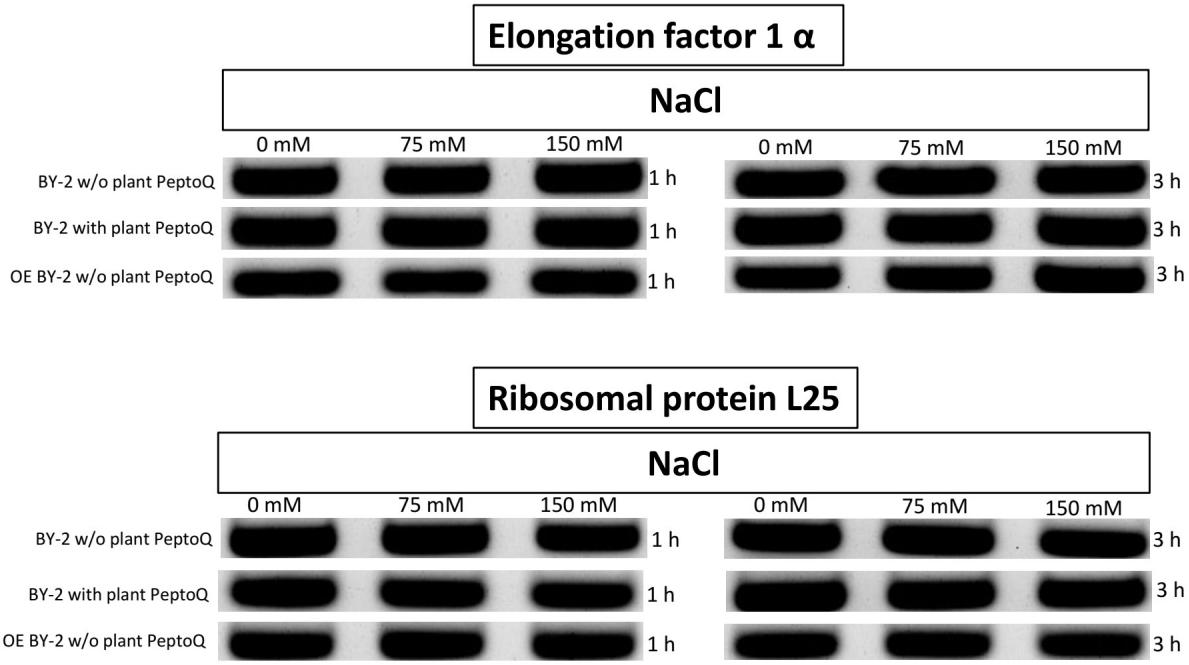

Supplementary Figure S2: Agarose gel images of the semiquantitative PCR (SQ-PCR) products of the two reference genes such as elongation factor 1 α (EF-1α) and ribosomal protein L25 from salt stressed (0, 75 and 150 mM NaCl) non-transformed WT with and without plant PeptoQ pretreatment, and OE BY-2 cells without plant PeptoQ pretreatment. In each case, one representative example out of three independent experiments is shown.